ANÁLISES FISIOLÓGICAS E BIOQUÍMICAS APLICADAS AOS ESTUDOS DE PROPAGAÇÃO *in vitro* E CONSERVAÇÃO DE SEMENTES DE *Cariniana legalis* (MARTIUS) O. KUNTZE

JOVIANA LERIN

UNIVERSIDADE ESTADUAL DO NORTE FLUMINENSE DARCY RIBEIRO - UENF

CAMPOS DOS GOYTACAZES - RJ
FEVEREIRO - 2020

ANÁLISES FISIOLÓGICAS E BIOQUÍMICAS APLICADAS AOS ESTUDOS DE PROPAGAÇÃO *in vitro* E CONSERVAÇÃO DE SEMENTES DE *Cariniana legalis* (MARTIUS) O. KUNTZE

JOVIANA LERIN

"Tese apresentada ao Centro de Ciências e Tecnologias Agropecuárias da Universidade Estadual do Norte Fluminense Darcy Ribeiro, como parte das exigências para obtenção do título de Doutor em Produção Vegetal".

Orientadora: Profª. Drª. Claudete Santa Catarina

CAMPOS DOS GOYTACAZES - RJ
FEVEREIRO – 2020

FICHA CATALOGRÁFICA

UENF - Bibliotecas

Elaborada com os dados fornecidos pela autora.

L61 Lerin, Joviana.

Análises fisiológicas e bioquímicas aplicadas aos estudos de propagação *in vitro* e conservação de sementes de *Cariniana legalis* (Martius) O. Kuntze / Joviana Lerin. - Campos dos Goytacazes, RJ, 2020.

161 f. : il.

Bibliografia: 111 - 124.

Tese (Doutorado em Produção Vegetal) - Universidade Estadual do Norte Fluminense Darcy Ribeiro, Centro de Ciências e Tecnologias Agropecuárias, 2020.

Orientadora: Claudete Santa Catarina.

1. Micropropagação. 2. Armazenamento de sementes. 3. Proteômica. 4. Jequitibá rosa. I. Universidade Estadual do Norte Fluminense Darcy Ribeiro. II. Título.

CDD -

ANÁLISES FISIOLÓGICAS E BIOQUÍMICAS APLICADAS AOS ESTUDOS DE PROPAGAÇÃO *in vitro* E CONSERVAÇÃO DE SEMENTES DE *Cariniana legalis* (MARTIUS) O. KUNTZE

JOVIANA LERIN

"Tese apresentada ao Centro de Ciências e Tecnologias Agropecuárias da Universidade Estadual do Norte Fluminense Darcy Ribeiro, como parte das exigências para obtenção do título de Doutor em Produção Vegetal".

Aprovada em 19 de fevereiro de 2020.

Comissão Examinadora:

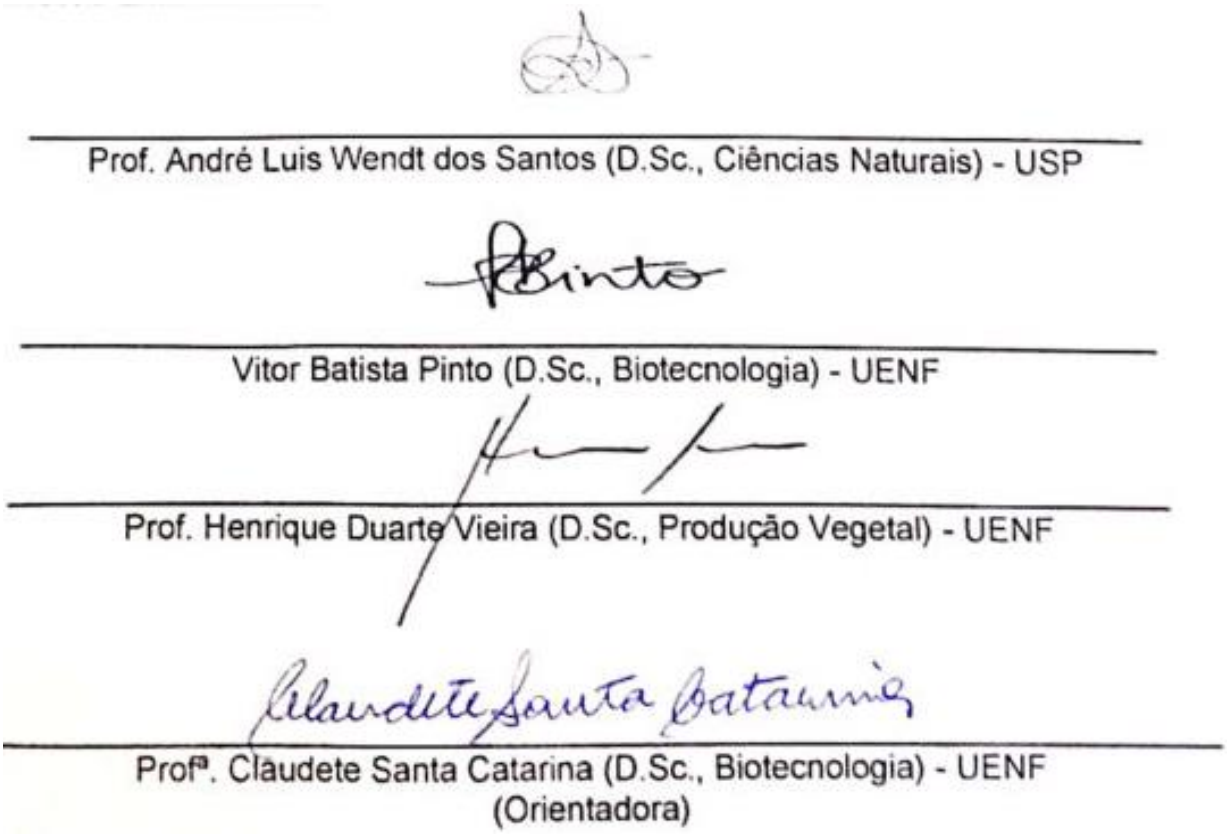

Prof. André Luis Wendt dos Santos (D.Sc., Ciências Naturais) - USP

Vitor Batista Pinto (D.Sc., Biotecnologia) - UENF

Prof. Henrique Duarte Vieira (D.Sc., Produção Vegetal) - UENF

Profª. Claudete Santa Catarina (D.Sc., Biotecnologia) - UENF
(Orientadora)

À minha amada e saudosa mãe Delma.

Dedico

AGRADECIMENTOS

Ao meu pai Darci, meu porto seguro, às minhas irmãs Eliete e Jociane e ao meu irmão Eder agradeço pela compreensão, confiança, amor e dedicação de uma vida inteira;
Ao meu estimado Rafael L. F. Rocha pelo carinho, apoio, dedicação e bons momentos vividos;
À minha orientadora Claudete Santa Catarina, pela orientação, confiança e ensinamentos ao longo deste tempo;
Aos amigos do grupo de pesquisa do Laboratório de Biologia Celular e Tecidual, Victor, Kariane, Yrexam, Lídia, Rosana, Renan, Tadeu, Laíse e Jackellinne, pela parceria, confiança e ajuda durante este percurso;
Ao professor Vanildo Silveira e aos amigos do Laboratório de Biotecnologia, Ricardo e Ellen, pela contribuição e apoio ao desenvolvimento deste trabalho;
Ao professor Henrique D. Vieira e colegas do Laboratório de sementes, pelo suporte aos trabalhos e disposição em todos os momentos;
Aos colegas e amigos que ao longo destes quatro anos contribuíram para a elaboração e conclusão deste trabalho, meu respeito e admiração a todos;
À UENF, pela oportunidade de acesso à pós-graduação;
O presente trabalho foi realizado com apoio da Coordenação de Aperfeiçoamento de Pessoal de Nível Superior - Brasil (CAPES) - Código de Financiamento 001;

Aos amigos, Kariane, Victor, Jackellinne, Rosana, Renan e Erika, agradeço pelo companheirismo e momentos de alegria dentro e fora da UENF;
Às minhas amigas, Vivian, Lígia e Beatriz, pela amizade, apoio e compreensão;
A Deus que nunca me desampara, eu agradeço.

SUMÁRIO

RESUMO

LERIN, Joviana; D.Sc.; Universidade Estadual do Norte Fluminense Darcy Ribeiro. Fevereiro de 2020. Análises fisiológicas e bioquímicas aplicadas aos estudos de propagação *in vitro* e conservação de sementes de *Cariniana legalis* (Martius) O. Kuntze. Professora orientadora: Claudete Santa Catarina.

Esta tese teve como objetivo estabelecer estudos de conservação de sementes e propagação *in vitro* de *Cariniana legalis* (jequitibá-rosa), uma espécie de relevância ecológica e econômica, ameaçada de extinção. Os estudos realizados e os resultados obtidos estão apresentados na forma de três capítulos. No primeiro capítulo, o objetivo foi avaliar o efeito do ácido indol-3-butírico (AIB) e do floroglucinol (PG) no enraizamento *in vitro* e no perfil proteômico das microestacas de *C. legalis*. As microestacas foram incubadas em meio de cultura MS (Murashige e Skoog) (¼ da concentração), suplementado com combinações de AIB (0, 50 e 100 µM) e PG (0 e 30 µM). Após 30 dias, foram analisados o desenvolvimento das raízes, as alterações histomorfológicas e o perfil proteômico. O AIB foi necessário para indução radicular e no tratamento AIB 50 µM + PG 30 µM, aos 12 dias de incubação foram observadas células meristemáticas entre as células do calo induzido na base das microestacas, as quais permitiram o desenvolvimento de primórdios radiculares e o enraizamento.
Proteínas de metabolismo secundário, como a chalcona sintase, foram identificadas e

relacionadas ao não-enraizamento, enquanto proteínas de homeostase celular foram associadas ao enraizamento das microestacas. O segundo capítulo teve como objetivo avaliar a influência da temperatura e do tempo de armazenamento na viabilidade e no perfil proteômico de sementes de *C. legalis*. As sementes foram armazenadas a 6 e 25°C em embalagem de papel trifoliado durante 24 meses. Foram avaliados germinação, comprimento das plântulas, grau de umidade, condutividade elétrica e perfil proteômico durante o armazenamento. Aos 8 meses a 25°C, as sementes apresentaram ausência de germinação, maior grau de umidade e de condutividade elétrica. A 6°C, as sementes mantiveram maior viabilidade embora, com redução significativa na germinação de 36% e 63%, aos 8 e 20 meses, respectivamente. A temperatura e o tempo de armazenamento modificaram o perfil proteômico aumentando o acúmulo de proteínas de resposta a estresse, como o álcool desidrogenase e diminuindo o acúmulo de proteínas de choque térmico associadas à viabilidade de sementes. Esses estudos forneceram informações inéditas e relevantes sobre eventos fisiológicos e bioquímicos, possibilitando otimizar as condições tanto para a propagação *in vitro*, quanto para a conservação de sementes em *C. legalis*.

ABSTRACT

LERIN, Joviana; D.Sc.; Universidade Estadual do Norte Fluminense Darcy Ribeiro. February of 2020. Physiological and biochemical analyzes applied to the studies of *in vitro* propagation and seed conservation of *Cariniana legalis* (Martius) O. Kuntze. Professor advisor: Claudete Santa Catarina.

This thesis aimed to establish studies for seed conservation and *in vitro* propagation of *Cariniana legalis* (jequitibá-rosa), an endangered specie of ecological and economic relevance. The studies carried out and the results obtained are presented in the form of three chapters. The first chapter aimed to evaluate the effect of different light sources on the *in vitro* development of *C. legalis* shoots. Cotyledonary and apical nodal explants were kept under light emitting diode (LED) lamps with different spectral combinations and fluorescent lamp (control). After 60 days, shoots growth, polyamine content and proteomic profile were analyzed. The LED lamp W/$_{l}$B/$_{d}$R composed of white, low blue and deep red spectra increased the shoots elongation and the content of putrescine, spermidine and total polyamines. The higher accumulation of homeostasis and cellular organization proteins and the reduction of stress response proteins accumulation were related to the higher elongation of *C. legalis* shoots under this LED lamp compared to fluorescent. In the second chapter, the objective was to evaluate the effect of indole-3-butyric acid (IBA) and phloroglucinol (PG) on *in vitro* rooting and on the proteomic

profile of *C. legalis* microcuttings. The microcuttings were incubated in MS culture medium (Murashige and Skoog) (¼ of the concentration), supplemented with combinations of IBA (0, 50 and 100 µM) and PG (0 and 30 µM). After 30 days, the root development, histomorphological changes and proteomic profile were analyzed. AIB was necessary for roots induction and in the treatment IBA 50 µM + PG 30 µM at 12 days of incubation meristematic cells were observed among the cells of the callus induced at the base of these microcutting, which allowed the development of root primordium, and the rooting. Secondary metabolism proteins such as chalcone synthase were identified and related to non-rooting, while cellular homeostasis proteins were associated to rooting of the microcuttings. The third chapter aimed to evaluate the influence of temperature and time storage on viability and alteration of the proteomic profile of *C. legalis* seeds. The seeds were stored at 6 and 25°C in trifoliate paper packaging for 24 months. Germination, seedling length, moisture content, electrical conductivity and proteomic profile were evaluated during storage. At 8 months at 25°C, the seeds showed no germination, a higher degree of humidity and electrical conductivity. At 6°C the seeds maintained higher viability, although with a significant reduction on germination of 36% and 63% at 8 and 20 months of storage, respectively. Temperature and time storage modified the proteomic profile, increasing the accumulation of stress response proteins, such as alcohol dehydrogenase and decreasing the accumulation of heat shock proteins associated to seed viability. These studies provided unpublished and relevant information on physiological and biochemical events, making it possible to optimize conditions for both *in vitro* propagation and for the conservation of seeds in *C. legalis*.

1. INTRODUÇÃO

Cariniana legalis (Martius) O. Kuntze (Lecythidaceae), conhecida como jequitibá-rosa, é uma espécie ameaçada de extinção do bioma brasileiro Mata Atlântica (IUCN, 2019). Essa espécie tem sido explorada ao longo dos anos devido ao valor econômico de sua madeira, utilizada pelas indústrias moveleiras e de construção civil (Rêgo, 2002; Carvalho, 2005). Com isso, o reduzido número de indivíduos de ocorrência natural e a baixa disponibilidade de sementes limitam a sua propagação. Portanto, práticas de propagação *ex situ* podem ser importantes aliadas na busca pela preservação dessa espécie.

Nesse sentido, o armazenamento de sementes é uma prática fundamental a fim de manter disponibilidade contínua de sementes viáveis. Os principais fatores que afetam o armazenamento são temperatura e umidade do ar (Roberts, 1973), estando diretamente relacionados à deterioração das sementes. A deterioração é observada por alterações fisiológicas que levam à perda do poder germinativo, bem como, alterações bioquímicas que culminam com a perda da viabilidade das sementes (Sousa et al., 2016). Para *C. legalis,* as sementes podem apresentar germinação inicial superior a 70%, mas essa porcentagem tende a diminuir para 20% em 12 meses, dependendo das condições de armazenamento (Sousa et al., 2016). Portanto, estudos para definir condições adequadas de armazenamento são essenciais para prolongar a viabilidade das sementes desta espécie.

Adicionalmente, uma alternativa para propagação de *C. legalis* é o cultivo *in vitro*, como um método rápido de multiplicação, considerando a ausência de respostas morfogênicas às técnicas convencionais, como estaquia (Oliveira et al., 2013). Estudos iniciais para estabelecer a regeneração *in vitro* foram realizados para *C. legalis* (Aragão et al., 2017a), porém, o desenvolvimento de brotações e posterior enraizamento destas são etapas que precisam ser aprimoradas. Para o desenvolvimento de brotações, a luz parece ser fator chave, visto que *C. legalis* apresenta sensibilidade à luminosidade no início do desenvolvimento (Vieira et al., 2012). Assim, o controle espectral da luz, com o uso de lâmpadas com a tecnologia diodo emissor de luz (LED), pode ser eficiente para melhorar essa etapa.

Além disso, essa espécie mostrou dificuldade para induzir raízes adventícias nas brotações micropropagadas (Aragão et al., 2017a). O enraizamento *in vitro* é influenciado por fatores como reguladores de crescimento e compostos fenólicos (De Klerk et al., 2011; Dewir et al., 2016). A auxina ácido indol-3-butírico (AIB) tem apresentado bons resultados no enraizamento de espécies, como *Cassia siamea* (Parveen et al., 2010) e *Juglans nigra* (Stevens e Pijut, 2018). Adicionalmente, compostos fenólicos, como o floroglucinol, têm sido utilizados para melhorar os efeitos da auxina no enraizamento *in vitro* (da Silva, 2013). Portanto, a combinação de AIB com floroglucinol pode ser uma alternativa para aumentar o enraizamento das brotações em *C. legalis.*

Fatores endógenos podem ser alterados pelos tratamentos aos quais explantes e sementes são submetidos. Nesse sentido, as poliaminas atuam como substâncias reguladoras de crescimento e alterações nos seus níveis estão relacionadas às respostas de crescimento e desenvolvimento e estresses em plantas (Alcázar et al., 2010; Aragão et al., 2016). Em adição, a proteômica comparativa tem sido utilizada para compreender alterações no acúmulo de proteínas envolvidas com germinação e envelhecimento de semente (Trindade et al., 2018; Aragão et al., 2019) e desenvolvimento da organogênese em plantas (Tang et al., 2016). Assim, os estudos destes compostos podem esclarecer eventos que ocorrem no armazenamento de sementes e na propagação *in vitro* de plantas. Portanto, o presente trabalho teve como objetivo estabelecer estudos para a conservação de sementes e de propagação *in vitro*, aliado ao conhecimento de alterações fisiológicas e bioquímicas em *C. legalis*.

2. REVISÃO DE LITERATURA

2.1. A Mata Atlântica

O Brasil possui a maior cobertura de florestas tropicais do mundo. Devido à sua extensão territorial e às diferenças geográficas e climáticas, a diversidade florestal brasileira se destaca no número absoluto de espécies (Forzza et al., 2010). Dentre as formações vegetais encontradas ao longo da extensão territorial do Brasil, pode-se destacar uma variedade de biomas como: Cerrado, Pantanal, Mata Atlântica, Campos Sulinos, Caatinga, Amazônia e Ecossistemas Costeiros e Marinhos, cada um com suas particularidades de clima, relevo, fauna e flora, que os tornam, por sua grande biodiversidade, vulneráveis à exploração desordenada para fins econômicos (Brandon et al., 2005).

A Mata Atlântica é composta por diferentes ecossistemas que se encontram até hoje, sob forte pressão antrópica. Originalmente, sua extensão cobria total e/ou parcialmente 17 estados brasileiros, abrangendo a costa litorânea leste desde o Rio Grande do Norte até o Rio Grande do Sul. Nos últimos anos, a Mata Atlântica tem sido reduzida a 12,4% da área original, somados os remanescentes florestais preservados e os fragmentos naturais acima de 3 hectares (SOSMA, 2018). Essa situação se deu devido à exploração predatória dos recursos naturais, práticas não sustentáveis da

agropecuária e aumento da industrialização e expansão urbana (Almeida, 2006). Em virtude da sua grande biodiversidade e dos níveis de ameaça, esse bioma foi indicado em um estudo coordenado pela *Conservation International*, como um dos 25 *hotspots* mundiais, ou seja, uma das prioridades para a conservação da biodiversidade, ao lado do Cerrado brasileiro e outras 23 regiões localizadas em diferentes partes do planeta (Myers et al., 2000; Brandon et al., 2005).

As regiões de áreas de remanescentes da Mata Atlântica estão geralmente associadas às unidades de conservação de proteção integral e possuem área menor ou igual a 100 hectares. Somadas, essas áreas representam apenas 8% da extensão territorial total protegida do Brasil. No entanto, em uma paisagem dominada por interferências antrópicas, esses pequenos fragmentos assumem grande importância na busca pela conscientização e recuperação do bioma (Pinto et al., 2006). Diante do atual quadro de desmatamento da Mata Atlântica, algumas ações vêm sendo realizadas em prol da conversação e recuperação da biodiversidade desse bioma.

Nesse sentido, uma das estratégias é a implementação dos chamados corredores ecológicos ou corredores de conservação da biodiversidade (Sanderson et al., 2003; Pinto et al., 2006). Esses corredores referem-se às faixas de vegetação que ligam blocos de remanescentes naturais, compreendidos como unidades de planejamento regional, contemplam grandes unidades de paisagem e envolvem áreas protegidas e outras áreas sujeitas aos diversos tipos de manejo que devem fazer parte das estratégias de conservação. Por finalidade, é esperado que esses corredores possam diminuir o isolamento de áreas naturais da mata. Para possibilitar o sucesso da sua implementação, um planejamento baseado em informações biológicas, sociais e econômicas da área é essencial (Sanderson et al., 2003; Pinto et al., 2006).

Segundo o relatório anual de 2018 da Fundação SOS Mata Atlântica (SOSMA, 2018), no ano de 2017 foram desmatados 125 Km² de área da Mata Atlântica, no entanto, esse foi o menor número registrado desde 1985, quando o monitoramento foi iniciado. Assim, é necessário dar continuidade e aprimorar o monitoramento do desmatamento, bem como intensificar o processo de restauração florestal para que mais resultados positivos de proteção e recuperação sejam alcançados.

Em se tratando das espécies arbóreas do bioma, a grande maioria apresenta dificuldade de propagação. Entre as características dessas espécies estão: o longo

período de desenvolvimento até atingirem a fase de reprodução, dificultando a sua propagação e perpetuação; a floração esporádica entre anos, influenciada por variações climáticas; e a baixa viabilidade das sementes de algumas espécies que pode dificultar a regeneração natural e a disponibilidade de mudas para programas de reflorestamento (Sebbenn et al., 2000; Carvalho, 2003; Shimizu, 2007). Além disso, os programas de conservação ainda são poucos perto da sua necessidade e têm sido estabelecidos para um número reduzido de espécies, comprovando a importância da existência e continuidade de estudos relacionados à propagação e conservação de espécies que se encontram em risco de extinção.

2.2. Espécie alvo: *Cariniana legalis*

Dentre as diversas espécies encontradas na Mata Atlântica, a *Cariniana legalis* (Mart.) Kuntze (Lecythidaceae), popularmente conhecida como jequitibá rosa, é considerada uma espécie nativa do bioma e endêmica do Brasil (Ribeiro et al., 2017). Encontrada na Floresta Ombrófila Densa, ocupa regiões de clima quente, úmido e fortemente chuvoso, com temperatura média de 25°C. Suas árvores chegam a atingir até 60 m de altura, com 4 m de diâmetro de tronco na idade adulta (Corrêa, 1996; Carvalho, 2005). A madeira da *C. legalis* tem alto valor econômico, sendo muito utilizada nas indústrias de construção civil, celulose e moveleiras, entre outros (Rêgo, 2002; Carvalho, 2005). A exploração desordenada tem diminuído a quantidade de indivíduos dessa espécie restando apenas um reduzido número em ocorrência natural. Essa situação levou a inclusão desta espécie na lista vermelha de espécies ameaçadas de extinção, segundo a *International Union for Conservation of Nature* (IUCN), sendo classificada como vulnerável, em uma escala de 7 grupos que variam entre a categoria pouco preocupante, sendo a de risco mais baixo de extinção até a categoria extinta, quando não há qualquer dúvida que o último indivíduo de uma determinada espécie morreu (IUCN, 2019).

A *C. legalis* apresenta característica de espécie secundária tardia, ou seja, necessita de luz solar direta apenas em parte da sua vida, sendo que na sua fase juvenil é totalmente tolerante à sombra, portanto, a luz pode ser um fator regulador do

seu desenvolvimento (Carvalho, 2005; Vieira et al., 2012). A propagação dessa espécie se faz por sementes e a produção de frutos inicia-se quando a planta está próxima dos 20 anos de idade. As sementes não apresentam dormência e estão prontas para germinar assim que se desprendem da planta, podendo germinar à sombra de outras plantas, porém, elas tendem a perder a viabilidade rapidamente, o que dificulta sua propagação e o seu armazenamento por períodos prolongados (Rêgo, 2002; Sousa et al., 2016).

Para a propagação, seja por via seminífera ou vegetativa, há uma escassez de resultados referentes a *C. legalis*. Técnicas de cultivo *in vitro* têm sido testadas e um protocolo inicial já foi desenvolvido (Aragão et al., 2017a). Apesar da necessidade de melhorias no protocolo para desenvolvimento e enraizamento de brotações, a regeneração *in vitro* representa uma possibilidade de propagação e conservação para a espécie. Trabalhos têm mostrado a dificuldade na manutenção da viabilidade das sementes durante o armazenamento e necessidade de aprimoramento das práticas para conservação de sementes (Sousa et al., 2016; Aragão et al., 2019). Juntamente com os resultados fisiológicos e morfológicos, esses trabalhos fornecem informações valiosas sobre aspectos bioquímicos, como as alterações no conteúdo de carboidratos, poliaminas e aminoácidos que ocorrem durante um período de 12 meses de armazenamento das sementes (Sousa et al., 2016). Ademais, uma mudança no perfil de proteínas acumuladas nas sementes de *C. legalis* armazenadas também já foi identificada (Aragão et al., 2019). Esses estudos ressaltam a importância da busca de novas alternativas para melhorar as formas de propagação dessa espécie, uma vez que a baixa disponibilidade de sementes, juntamente com a extração desordenada, dificulta a produção de mudas em viveiros para reflorestamento e o processo de recuperação natural nas áreas de ocorrências.

2.3. Armazenamento de sementes

As espécies nativas apresentam alternância de produção de sementes caracterizadas por um ano de alta produção, seguido de um ou dois anos de baixa produção, por isso necessitam ser armazenadas para utilização futura, uma vez que

nem sempre são utilizadas logo após a coleta (Fowler e Martins, 2001). Além disso, algumas espécies tendem a perder a viabilidade rapidamente em decorrência de alterações físicas, fisiológicas e bioquímicas que levam à deterioração das sementes (Fowler e Martins, 2001; Jyoti e Malik, 2013; Sousa et al., 2016).

O processo de deterioração das sementes é contínuo, inevitável e irreversível, tendo início logo após a maturidade fisiológica. A velocidade com que ocorre a deterioração durante o armazenamento depende da capacidade da semente para resistir às alterações metabólicas de degradação e aos seus mecanismos de proteção. Essas características podem variar entre espécie, lote ou mesmo entre sementes de um mesmo lote (Kapoor et al., 2010; Carvalho e Nakagawa, 2012; Jyoti e Malik, 2013). Em espécies como *Sesamum indicum*, *Albizia hasslerii* e *Piptadenia moniliformis*, o uso de tecnologias de conservação adequadas pôde manter a viabilidade das sementes por um período maior por diminuir a sua velocidade de deterioração (Azevedo et al., 2003; Kissmann et al., 2009; Benedito et al., 2011). As técnicas empregadas procuram controlar os dois principais fatores que afetam a conservação das sementes durante o armazenamento, a temperatura e a umidade relativa do ar (Roberts, 1973). Além das condições do ambiente, o teor de água das sementes também influencia na manutenção da sua viabilidade (Rosa et al., 2005) e a tolerância à dessecação pode aumentar o período de armazenamento suportado (Hong e Ellis, 1996; Villela e Peres, 2004). Considerando-se a capacidade de tolerar à dessecação, as sementes foram classificadas em dois grupos distintos: ortodoxas (tolerantes à dessecação) e recalcitrantes (não tolerantes) (Roberts, 1973).

As sementes consideradas ortodoxas mantêm-se viáveis após desidratação até um grau de umidade em torno de 5% (Roberts, 1973). Em condições de baixa umidade relativa do ar e de baixa temperatura, essas sementes podem ficar armazenadas por muitos anos sem que ocorra perda significativa em sua viabilidade (Medeiros e Eira, 2006). Nestas sementes, a tolerância à dessecação é adquirida no final do desenvolvimento, quando ocorre o acúmulo de reservas, redução do volume vacuolar e diminuição do metabolismo (Barbedo e Filho, 1998).

As sementes recalcitrantes apresentam sensibilidade à desidratação e maior grau de umidade ao serem dispersas da planta-mãe no final da maturação. Não toleram níveis de umidade inferiores a 12 e 30%, dependendo da espécie, e não

suportam armazenamento em temperaturas de congelamento, o que impede o seu armazenamento a longo prazo (Roberts, 1973; Medeiros e Eira, 2006). Além desses grupos, há um terceiro no qual as sementes apresentam um comportamento de armazenamento intermediário ao ortodoxo e ao recalcitrante (Ellis et al., 1990). Essas podem tolerar dessecação até 10 a 12% de umidade, semelhante às sementes ortodoxas, porém, não toleram temperaturas de congelamento semelhantes às recalcitrantes (Hong e Ellis, 1996). Sendo assim, as sementes que toleram a dessecação, seja ela natural ou artificial, tendem a manter a viabilidade, podendo ser armazenadas por longos períodos, enquanto aquelas que não suportam a perda de água necessitam de técnicas alternativas de armazenamento para a manutenção da viabilidade (Medeiros e Eira, 2006).

Nesse sentido, a perda da viabilidade das sementes envolve um conjunto de atividades metabólicas. A primeira modificação degenerativa decorrente do processo de deterioração ocorre nas membranas celulares com consequente perda da permeabilidade seletiva (Popinigis, 1985). Em seguida, várias outras transformações podem ocorrer como a redução das reservas, alteração da composição química, degradação do DNA (Kibinza et al., 2006), perda de exsudados essenciais à germinação e redução da atividade respiratória e biossintética (Marcos Filho, 2005). Em decorrência disso, ocorre uma redução do potencial de conservação, fisiologicamente caracterizada por germinação, crescimento e desenvolvimento das plântulas mais lentos, resultando em desuniformidade na formação das plântulas, aumento no percentual de plântulas anormais e a perda total do poder de germinação (Marcos Filho, 2005; Carvalho e Nakagawa, 2012; Abbade e Takaki, 2014).

A composição química das sementes tem influência direta no potencial de armazenamento. Substâncias de reserva como carboidratos, lipídios e proteínas desempenham papel importante na tolerância à desidratação atuando como protetores celulares e impedindo a ruptura da membrana plasmática (Kermode e Finch-Savage, 2002). Portanto, estudos direcionados para as alterações bioquímicas podem ser úteis para esclarecer alterações que ocorrem no metabolismo de sementes durante o armazenamento e que levam à perda da sua capacidade germinativa.

2.4. Propagação *in vitro*

A cultura *in vitro* de células e tecidos vegetais é uma importante ferramenta biotecnológica em diversas áreas de estudo como agricultura, silvicultura e melhoramento de plantas. Refere-se ao cultivo asséptico de células, tecidos ou órgãos isolados de um organismo, mantidos em um ambiente *in vitro* sob condições físicas e químicas controladas (Thorpe, 2007). O conceito de totipotência proposta por Gottlieb Haberlandt em 1902, na qual, uma célula vegetal possui todas as informações genéticas necessárias para se dividir e diferenciar, formando um organismo completo, estabeleceu o uso da técnica de cultivo de células *in vitro* de plantas em solução nutritiva, permitindo a investigação de importantes problemas relacionados ao desenvolvimento e a multiplicação de espécies vegetais (Giri et al., 2004; Thorpe, 2007).

Dentre as aplicações da cultura de tecidos vegetais, a micropropagação é uma das mais usadas por permitir a manutenção das características genotípicas e fenotípicas das mudas, possibilitar a produção em larga escala de mudas sadias em curto espaço de tempo, utilizando uma área relativamente pequena quando comparada ao sistema convencional e por manter o controle das condições ambientais durante o processo de propagação (Giri et al., 2004; Cruz et al., 2009). Essa técnica tem sido usada com sucesso na propagação de espécies ameaçadas de extinção (Giri et al., 2004; Oseni et al., 2018).

O sucesso da regeneração *in vitro* depende do controle de fatores como tipo do explante, meio de cultura e seus componentes nutricionais, reguladores de crescimento vegetal e fatores ambientais, como luz e temperatura (Floh et al., 2007; Xavier e Otoni, 2009). A morfogênese nas plantas é consequência da integração dos processos de divisão e diferenciação celular entre o explante e sinais fornecidos a ele pelo meio de cultura e ambiente, os quais conduzem a formação de uma estrutura organizada e característica. Dentro da micropropagação, a propagação vegetal pode ser obtida através do desenvolvimento de gemas axilares pré-existentes (Floh et al., 2007; Xavier e Otoni, 2009).

A propagação *in vitro* pelo desenvolvimento de gemas axilares compreende as fases de multiplicação e alongamento das brotações, após a iniciação e

estabelecimento da cultura. A regeneração a partir de gemas pré-existentes nos explantes oriundos de plântulas ou material adulto é o método mais utilizado para várias espécies lenhosas. Seu sucesso também depende da concentração de reguladores de crescimento e de fatores ambientes (Xavier e Otoni, 2009; Oliveira et al., 2013). Para algumas espécies como *Daphne gnidium* e *Cedrela fissilis* foi demonstrado que o balanço entre auxinas e citocininas é importante na promoção do desenvolvimento de brotações *in vitro* (Gavidia et al., 1996; Nunes et al., 2002; Aragão et al., 2016). No entanto, em *C. legalis*, o uso de diferentes concentrações de poliaminas e o balanço entre os reguladores de crescimento auxina, giberelina e citocininas não influenciou no desenvolvimento de brotações *in vitro* (Aragão et al., 2017a). Neste sentido, outros fatores que influenciam a propagação *in vitro* precisam ser testados, como por exemplo, a qualidade e quantidade de luz, podendo melhorar a regeneração de brotações.

2.5. Influência da luz na propagação de brotações *in vitro*

A luz é o ponto de partida do desenvolvimento vegetal que gera uma sinalização inicial na planta. Este sinal é transmitido através de moléculas e caminhos metabólicos até finalmente modificar algum aspecto na planta, seja ele morfológico ou metabólico (Möglich et al., 2010). A luz que irá participar de tais modificações é diretamente absorvida por moléculas proteicas conhecidas como fotorreceptores. As plantas possuem várias famílias de fotorreceptores que podem perceber a direção, duração, qualidade e quantidade da luz, usando-a para regular as etapas de crescimento e desenvolvimento, desde a germinação das sementes até a senescência (Chen et al., 2004; Möglich et al., 2010; Deng et al., 2014).

A grande diversidade de respostas influenciadas pela luz requer um conjunto igualmente diverso de fotorreceptores para controlá-las. Estes fotorreceptores incluem os fitocromos que absorvem vermelho e vermelho distante, os criptocromos que absorvem azul e UV-A e fototropinas, receptores de luz azul (Devlin et al., 2007; Deng et al., 2014; Demotes-Mainard et al., 2016). Algumas das respostas fisiológicas intermediadas pelos fitocromos são germinação de sementes, estiolamento de

plântulas e evitação à sombra. Os criptocromos têm ação na indução à floração e ritmo circadiano, enquanto as fototropinas são essenciais em respostas como movimento de cloroplastos e abertura e fechamento estomático (Somers et al., 1998; Christie, 2007; Deng et al., 2014; Demotes-Mainard et al., 2016).

Na micropropagação, a luz exerce grande influência no desenvolvimento das culturas *in vitro*. O uso de luz artificial fornecida por lâmpadas fluorescentes é comumente realizado, uma vez que essas lâmpadas emitem fótons em ampla faixa espectral. No entanto, lâmpadas fluorescentes apresentam algumas desvantagens como o elevado consumo de energia elétrica e produção de calor que limita a radiação disponibilizada pela lâmpada (Bula et al., 1991). Uma alternativa para a otimização de protocolo de morfogênese tem sido o uso de lâmpadas com a tecnologia “Diodo Emissor de Luz” (LED) que permite o controle da composição espectral compensada pelos fotorreceptores das plantas (Yeh e Chung, 2009; Singh et al., 2015). Dentre as vantagens no uso das lâmpadas LED sobre a fluorescente destaca-se o maior tempo de vida útil, alta eficiência, visto que a maior parte da energia elétrica é convertida em radiação, reduzida emissão de calor e a capacidade de selecionar diferentes espectros de forma isolada (Massa et al., 2008; Gupta e Jatothu, 2013).

Em diversas espécies, o efeito positivo do uso de lâmpadas LED no cultivo *in vitro* vem sendo evidenciado como na embriogênese de *Saccharum spp* (Heringer et al., 2017), *Pinus densiflora* (Kim e Moon, 2014) e *Phalaenopsis* (Park et al., 2010), na organogênese em *Curculigo orchioides* (Gupta e Sahoo, 2015) e no desenvolvimento de gemas axilares de *Gossypium herbaceum* (Li et al., 2010) e *Lippia gracilis* (Lazzarini et al., 2018). Entretanto, este tipo de abordagem para espécies arbóreas é pouco expressivo, abrindo um novo cenário de pesquisa que pode contribuir para a propagação *in vitro* de espécies florestais, como a *C. legalis*.

2.6. Enraizamento de brotações propagadas *in vitro*

As respostas das plantas à regeneração *in vitro* são variáveis e dependentes da espécie ou cultivar, época de coleta, tipo de explante e das condições de cultivo *in vitro* (Floh et al., 2007; Oliveira et al., 2013). Visando a obtenção de plantas completas,

o enraizamento das brotações micropropagadas se faz necessário, sendo a última fase do processo de micropropagação. Esta etapa caracteriza-se pela formação de raízes adventícias a partir de células do caule da brotação ou a partir do calo formado na base das brotações (Oseni et al., 2018).

O enraizamento pode ocorrer *in vitro* ou ex vitro. No caso de enraizamento *in vitro*, as raízes são induzidas em meio de cultura, onde há melhor controle das condições ambientais. Posteriormente ao desenvolvimento das raízes *in vitro*, as micromudas são transferidas para substratos e levadas para a aclimatização. No enraizamento ex vitro, as brotações alongadas são enraizadas diretamente em substrato, ocorrendo concomitantemente a aclimatização das mudas (Leitzke et al., 2009; Oliveira et al., 2013).

Para o enraizamento de espécies florestais, geralmente se faz necessário o uso de reguladores de crescimento, como a auxina (Oliveira et al., 2013). Dentre as auxinas, o AIB tem sido muito utilizado em razão da baixa fitotoxicidade aos explantes e pela possibilidade de autoclavagem juntamente com o meio de cultura (Oinam et al., 2011), proporcionando resultados positivos, como já reportado para as espécies *Cordia trichotoma* (Mantovani et al., 2001) e *Ocotea porosa* (Pelegrini et al., 2011). Para *C. legalis*, o enraizamento dentro de um sistema de propagação *in vitro* ainda é uma limitação e precisa ser melhor estudado.

Alguns estudos apontam a necessidade de redução da concentração salina do meio de cultura para o sucesso do enraizamento, como observado para *Cassia siamea* (Parveen et al., 2010) e *Juglans regia* (Vahdati et al., 2004), uma vez que a composição nutricional, especialmente a concentração de nitrogênio (amônio) do meio de cultura pode ser prejudicial, dificultando o enraizamento (Grimaldi et al., 2008).

Recentemente, o composto floroglucinol, um composto fenólico com propriedades reguladoras de crescimento, também tem sido usado para a promoção do enraizamento *in vitro*, isoladamente ou combinado com auxinas, como AIB e ANA. Nessa situação, ele pode apresentar um efeito sinérgico com esse regulador de crescimento, na qual, o floroglucinol assumiria um papel protetor, evitando a oxidação da auxina adicionada ao meio de cultura e promovendo melhores resultados no enraizamento (da Silva et al., 2013). Essas estratégias devem ser avaliadas e podem ser incorporadas ao protocolo de propagação *in vitro* para *C. legalis*.

2.7. Alterações bioquímicas envolvidas no armazenamento de sementes e na propagação *in vitro*

A composição bioquímica tem influência direta no potencial de armazenamento das sementes e no desenvolvimento de órgãos vegetais durante a propagação *in vitro*. Entre as substâncias envolvidas estão as poliaminas, moléculas capazes de interferir em diversas vias metabólicas relacionadas ao processo de germinação, desenvolvimento e senescência de sementes e plantas (Santa-Catarina et al., 2006; Alcázar et al., 2010; Pieruzzi et al., 2011; Sousa et al., 2016; Aragão et al., 2017b). Além delas, as proteínas têm recebido enfoque a partir do uso da análise de alteração no perfil de proteínas acumuladas, com o objetivo de identificar conjuntos de proteínas envolvidas em eventos fisiológicos de células, tecidos e órgãos (Di Palma et al., 2012; Aragão et al., 2019; Passamani et al., 2019). Assim, elas podem ser úteis para esclarecer eventos que ocorrem durante o armazenamento de sementes e o desenvolvimento *in vitro* de plantas.

2.7.1. Poliaminas

As poliaminas são compostos nitrogenados de baixo peso molecular, presentes em todos os organismos vivos. Devido à sua carga positiva, estes compostos podem se ligar por interações eletrostáticas a várias macromoléculas, incluindo DNA, RNA, cromatina, fosfolipídios, proteínas e componentes da parede celular (Baron e Stasolla, 2008; Kusano et al., 2008). Considerada uma classe de reguladores de crescimento, a putrescina (Put), a espermidina (Spd) e a espermina (Spm) são as principais poliaminas encontradas em plantas (Kaur-Sawhney et al., 2003; Baron e Stasolla, 2008; Kusano et al., 2008). As poliaminas têm sido relacionadas a vários processos de controle de divisão e diferenciação celular, essenciais para o crescimento e desenvolvimento da planta (Santa-Catarina et al., 2006; Alcázar et al., 2010; Aragão et al., 2016; Reis et al., 2016).

Em arbóreas, o papel das poliaminas tem sido relatado em estudos com embriogênese zigótica e somática (Santa Catarina et al., 2004; Santa-Catarina et al.,

2006; Dutra et al., 2013) e germinação de sementes (Silveira et al., 2004; Dias et al., 2009; Pieruzzi et al., 2011). Avaliações do conteúdo de poliaminas livres durante embriogênese zigótica e germinação de sementes de *Ocotea catharinensis* comprovaram o aumento no nível de Put no início do desenvolvimento embrionário e germinação. Esses resultados enfatizam a importância desta poliamina nas fases inicias destes dois processos, quando a taxa de divisão celular é mais elevada. Já os níveis de Spm e Spd diminuíram durante o período de germinação, enquanto na embriogênese zigótica desta espécie houve um considerável aumento no nível de Spm no período final, quando ocorre principalmente alongamento celular (Santa-Catarina et al., 2006; Dias et al., 2009). Em adição, o papel das poliaminas foi relatado também à organogênese *in vitro*. Na espécie *C. fissilis,* a adição da citocinina 6-benzyladenine (BA) resultou no aumento da concentração de Put endógena e foi relacionado com o aumento no número de brotações (Aragão et al., 2016), além disso, a adição de Put no meio de cultura promoveu maior alongamento das brotações de *C. fissilis* (Aragão et al., 2017b).

Além disso, estudos mostraram a relação das poliaminas com a perda de viabilidade em sementes de *C. legalis* (Sousa et al., 2016). Os autores mostraram que o nível de poliaminas livres em sementes armazenadas durante 12 meses foi mais elevado em *C. legalis* comparativamente com *C. fissilis*, especialmente de Put, o qual foi relacionado com a perda da viabilidade das sementes. Esses resultados sugerem que, em níveis mais elevados, as poliaminas podem atuar em processos de deterioração da semente (Sousa et al., 2016). Dada a importância das poliaminas para o crescimento e desenvolvimento de plantas, destaca-se a necessidade de estudos para maior compreensão da influência destas moléculas nestes processos.

2.7.2. Perfil proteômico

As proteínas são os componentes básicos de toda célula viva, sua estrutura e conformação são modificadas por diversos fatores externos e internos (Dias et al., 2007). Essas modificações geram alterações físico-químicas que levam as proteínas a interagirem de forma diferente com outras moléculas (Chen e Harmon, 2006). O

estudo do proteoma, pela identificação de proteínas, possibilita encontrar alterações no perfil proteômico e associar proteínas específicas relacionadas a diferentes respostas que ocorrem em um determinado processo de desenvolvimento ou evento fisiológico, sob uma condição específica (Chen e Harmon, 2006; Kormuták et al., 2006). O objetivo inicial da proteômica foi a identificação em larga escala de todos os grupos de proteínas em células ou tecidos. Atualmente, diversas são as aplicações da proteômica em análises dos aspectos funcionais, análises das atividades e estruturas das proteínas e de interações entre proteínas (Park, 2004).

Nos processos morfogênicos *in vitro*, a proteômica comparativa apresenta-se como uma importante ferramenta para monitorar e compreender o perfil de proteínas em diferentes fases do desenvolvimento da planta. Essa técnica já vem sendo amplamente utilizada para identificar proteínas diferencialmente acumuladas durante o processo de embriogênese somática e em estudos comparativos para competência embriogênica (Heringer et al., 2015; Reis et al., 2016; Passamani et al., 2019).

Na propagação *in vitro* de espécies florestais, a alteração do perfil proteômico em brotações da espécie *C. fissilis* cultivadas com e sem putrescina mostrou que a adição de putrescina pode alterar o acúmulo de proteínas associadas com respostas a estresse e processos como a divisão celular das brotações em desenvolvimento (Aragão et al., 2017b).

Avaliações proteômicas têm sido utilizadas em estudos relacionados ao desenvolvimento e germinação de semente como em *Glycine max* (Hajduch et al., 2005), *Araucaria angustifolia* (Balbuena et al., 2011) e *Arabidopsis thaliana* (Gallardo et al., 2001). Para *C. legalis*, análises foram realizadas usando eletroforese em gel bidimensional (2-DE) e foram identificadas proteínas que desempenham papel importante no processo germinativo, como as globulinas, que são fonte de energia para a germinação (Trindade et al., 2018). Além disso, durante armazenamento, a análise proteômica por 2-DE mostrou diminuição de proteínas relacionadas à proteção das plantas contra estresse oxidativo e danos aos componentes celulares, como as ferritinas e superóxido dismutase (Aragão et al., 2019).

No entanto, análise proteômica por *shotgun*, sem uso de gel (gel-*free*), ainda não foi realizada em *C. legalis*. Essas abordagens permitem a identificação de proteínas de baixa abundância que muitas vezes não são identificadas pelas

abordagens proteômicas baseadas em gel (Heringer et al., 2018). Neste sentido, a análise proteômica comparativa é importante para o conhecimento de processos bioquímicos complexos associados com a competência para propagação *in vitro* e com a perda da viabilidade de sementes durante o armazenamento.

3. TRABALHOS

3.1. PROTEOMIC PROFILE AND POLYAMINE CONTENTS ARE MODULATED BY LIGHT SOURCE TO PROMOTE in vitro SHOOT DEVELOPMENT IN Cariniana legalis (MARTIUS) O. KUNTZE (LECYTHIDACEAE)*

RESUMO

O efeito de diferentes fontes de luz no desenvolvimento *in vitro* de brotações de *Cariniana legalis*, uma espécie ameaçada de extinção da Mata Atlântica, foi avaliada. Explantes nodais cotiledonares e apicais foram submetidos a lâmpadas de diodo emissor de luz (LED) com diferentes combinações espectrais e lâmpada fluorescente (controle). Aos 60 dias foram analisados o crescimento de brotações, conteúdo endógeno de poliaminas livres (PAs) e perfil proteômico. Os tratamentos consistindo dos espectros branco, azul baixo e vermelho profundo, com ($W/_lB/_dR/_fR$) e sem ($W/_lB/_dR$), vermelho distante resultaram em maior alongamento das brotações em explantes a partir de segmentos nodais cotiledonares e a combinação espectral de

* Os dados deste capítulo foram publicados:
Lerin, J; Aragão VPM; Reis, RS; Silveira, V; Santa-Catarina, C. (2019). Plant Cell, Tissue and Organ Culture.

baixo azul e vermelho profundo pareceu ser um fator positivo que estimula as respostas de evitação a sombra. As brotações cultivadas sob o LED W/$_{l}$B/$_{d}$R exibiram maior alongamento e maior conteúdo de putrescina, espermidina e PAs totais livres em comparação com as brotações cultivadas sob a lâmpada fluorescente. A análise da proteômica comparativa revelou 15 proteínas up- e 41 down-reguladas em brotações cultivadas sob a lâmpada LED W/$_{l}$B/$_{d}$R quando comparadas as cultivadas no controle. As proteínas diferencialmente reguladas em brotações cultivadas sob a lâmpada LED foram relacionadas à organização e composição celular, bem como processos de regulação biológica, enquanto as proteínas relacionadas ao processo de estresse foram down-reguladas. A lâmpada LED consistindo de espectros branco, azul baixo e vermelho profundo, aumentou o alongamento das brotações em *C. legalis*, em associação com diferencial acúmulo de proteínas e PAs, sugerindo a relevância da fonte de luz no desenvolvimento de brotações *in vitro* nessa espécie.

Palavras-chave: Proteômica comparativa, organogênese i*n vitro*, lâmpadas LED, fotomorfogênese

ABSTRACT

The effect of different light sources on *in vitro* shoot development in *Cariniana legalis*, an endangered species from the Atlantic Forest, was evaluated. Cotyledonary and apical nodal explants were subjected to light-emitting diode (LED) lamps with different spectral combinations and fluorescent lamps (control). Shoot growth, endogenous contents of free polyamines (PAs) and proteomic profiles were analyzed at 60 days of development. Treatments consisting of white, low-blue and deep red, with (W/$_{l}$B/$_{d}$R/$_{f}$R) and without (W/$_{l}$B/$_{d}$R) far-red spectra, resulted in greater elongation of shoots from cotyledonary nodal explants, and the low-blue and deep-red spectral combination appeared to be a positive factor stimulating shade-avoidance responses. Shoots grown under the W/$_{l}$B/$_{d}$R LED exhibited greater elongation and higher contents of free putrescine, spermidine and total free PAs compared to those grown under the

fluorescent lamp. Comparative proteomic analysis revealed 15 up- and 41 down-regulated proteins in shoots grown under the W/$_{l}$B/$_{d}$R LED lamp when compared to the control. The differentially up-regulated proteins in shoots grown under the LED lamp are related to cell organization and composition, as well as biological regulation processes, whereas proteins related to stress processes were down-regulated. The LED lamp consisting of white, low-blue and deep-red spectra increased shoot elongation in *C. legalis*, in association with differential accumulation of proteins and PAs, suggesting the relevance of source light on *in vitro* shoot development in this species.

Keywords: Comparative proteomics, *In vitro* organogenesis, LED lamps, photomorphogenesis

INTRODUCTION

Cariniana legalis (Martius) O. Kuntze (Lecythidaceae), known popularly as jequitibá-rosa, is a native tree species from the Atlantic Forest (Matta e Scudeller, 2012) and is currently included on the red list of endangered species by the International Union for Conservation of Nature (IUCN), being classified as vulnerable (IUCN, 2018). This species has been exploited because of the high economic value of its wood, which is widely used for the furniture and construction industries (Carvalho, 1994; Rêgo, 2002). In addition, this species exhibits propagation difficulty due to the rapid loss of seed viability (Sousa et al., 2016) and the absence of a morphogenic response to common propagation techniques, such as cuttings. These are common features for some forest species (Oliveira et al., 2013), and as a method of rapid mass multiplication, *in vitro* propagation appears to be an alternative for the conservation of this species (Bunn et al., 2011). Although initial studies to establish *in vitro* regeneration for *C. legalis* have been carried out (Aragão et al., 2017a), shoot growth remains a problem and needs to be improved.

Light quantity and quality appear to be key factors for the development of this species, as *C. legalis*, considered a late secondary growth species, presenting sensitivity to high light intensity and direct incidence, especially in the early stages of development (Rego e Possamai, 2006; Vieira et al., 2012). These characteristics of *C. legalis* emphasize the need to understand the effect of this environmental factor on its *in vitro* development. Among the different light triggered responses in plants is shade avoidance, which is signaled by a condition of low light, inducing an increase in the length of the internodes of young plants to provide a greater leaf exposure to light (Smith, 1982). To promote such responses under *in vitro* propagation conditions, lamps with specific combinations of light spectra can be applied, imitating natural conditions and stimulating shoot elongation.

Accordingly, light-emitting diode (LED) lamps have been used in *in vitro* plant propagation (Gupta e Sahoo, 2015; Singh et al., 2015), and multiple studies have shown the importance of LED lamps on *in vitro* induction, elongation and number of shoots in different species, such as *Anthurium andreanum*, *Curculigo orchioides* and *Lippia gracilis* (Budiarto, 2010; Gupta e Sahoo, 2015; Lazzarini et al., 2018). Compared to fluorescent lamps, LED lamps have the advantages of lower energy consumption, higher durability, lower heat emission and higher spectral composition control, which are important variables for *in vitro* tissue culture (Massa et al., 2008; Gupta e Jatothu, 2013). The relevance of light source for *in vitro* propagation is known, but the effects of different combinations of light spectra on morphogenic responses related to endogenous metabolism of polyamines (PAs) and protein profiles are not clear.

PAs are small aliphatic amines that play important roles in regulating plant growth (Kusano et al., 2008; Alcázar et al., 2010). The most common PAs found in higher plants, spermidine (Spd), spermine (Spm) and putrescine (Put) are involved in physiological events such as cell division and differentiation during organogenesis (Parimalan et al., 2011; Aragão et al., 2017b) and the concentrations of endogenous PAs can be altered during development by environmental factors including light spectra, leading to different morphological responses (Hunter e Burritt, 2005). Thus, understanding this interaction is fundamental, and LED systems with different combinations of spectra can be applied to examine the effects of light on the endogenous content of PAs in *in vitro* shoot development.

In addition, proteins are essential for plant development, and proteomic analysis is an important tool used in identifying abundant proteins to help understand events during *in vitro* morphogenesis (Reis et al., 2016; Heringer et al., 2017; Aragão et al., 2017b). Nonetheless, the effects of different light spectra provided by LEDs on proteomic profiles during *in vitro* shoot development are uncertain. It is, however, known that the content of some proteins may be changed by different light spectra (Muneer et al., 2014). Furthermore, different light spectra can increase the level of oxidative stress enzymes, and a blue light LED reportedly increased antioxidant enzyme activity improving organogenesis responses (Gupta e Sahoo, 2015). These findings show that light spectra function in plant morphogenesis by altering protein activity. However, studies related to alterations in proteomic profiles induced by the use of combinations of different LED light spectra during *in vitro* shoot development are lacking, especially for tree species such as *C. legalis*.

Therefore, in this work, we evaluated the effect of different light spectral combinations of LED and fluorescent lamps on *in vitro* shoot development in *C. legalis* as well as its effects on alterations in the endogenous content of PAs and in the profile of differentially abundant proteins.

MATERIALS AND METHODS

Plant material

Mature *C. legalis* seeds were commercially obtained from the Sementes Caiçara nursery located in Brejo Alegre, SP, Brazil (21°10′S and 50°10′W) and germinated *in vitro*. For *in vitro* organogenesis experiments, *in vitro*-germinated 90-days-old seedlings were used as the explant source to obtain apical and cotyledonary nodal segments (± 1.5 cm), as suggested Aragão et al. (2017a).

In vitro seed germination

Prior to inoculation, seeds were surface-disinfected according to Aragão et al. (2016), following *in vitro* germination in culture tubes (150 × 25 mm) containing 10 mL of woody plant medium (WPM) culture medium (Lloyd e McCown, 1981)

(Phytotechnology Lab; Lenexa, KS, USA) supplemented with 20 gL^{-1}sucrose (Synth; São Paulo, Brazil) and 7 gL^{-1}agar (Sigma-Aldrich; Saint Louis, USA). The pH was adjusted to 5.7 before autoclaving at 121 °C for 15 min. The seeds were then incubated for 90 days in a growth room under a photoperiod of 16 h, with a light intensity of 55 µmol m2 s^{-1} and at 25 ± 2°C, to obtain seedlings used as the explant source.

The effect of light spectra on shoot development in *C. legalis*

Apical and cotyledonary nodal segments (± 1.5 cm) were inoculated in WPM culture medium supplemented with 20 g L^{-1}sucrose and 2 g L^{-1}Phytagel® (Sigma). The pH of the culture medium was adjusted to 5.7, Phytagel was added; 30 mL medium was distributed into culture vessels (150 mL) (Aapace; São Paulo, Brazil) and autoclaved at 121 °C for 15 min. After inoculation, the explants were maintained in a growth room at 25 ± 2 °C under a photoperiod of 16 h and fluorescent or four different Green Power TLED (Koninklijke Philips Electronics NV, Amsterdam, Netherlands) lamps, according to Heringer et al. (2017). The following LED lamp treatments were performed: white, low blue and deep red ($W/_lB/_dR$ LED); white, low blue, deep red and far red ($W/_lB/_dR/_fR$ LED); white, medium blue and deep red ($W/_mB/_dR$ LED); white, medium blue, deep red and far red ($W/_mB/_dR/_fR$ LED). The fluorescent lamp, usually used for *in vitro* propagation, was used as a control treatment.

Eight replicates were performed for each treatment, with each replicate composed of one culture vessel containing five explants, for a total of 40 explants per treatment. After 60 days, the length (cm) and number of shoots per explant and shoot induction (%) were evaluated. In addition, samples (three biological replicates) of shoots from cotyledonary nodal segments at 60 days of culture under the fluorescent lamp (control) and the LED lamp treatment with the best result for shoot development were obtained for endogenous PAs content and proteomic profile analysis.

Free PAs determination

PAs contents were determined according to Santa-Catarina et al. (2006). Samples (200 mg fresh matter-FM-each, in triplicate) of shoots were macerated with 1.2 mL of 5% perchloric acid (PCA) (Merck Millipore; Darmstadt, Germany), incubated

at 4°C for 1 h and centrifuged for 20 min at 16,000 ×g and 4 °C. The supernatant was collected, and free PAs in the supernatant were analyzed directly by derivatization with dansyl chloride (Merck Millipore) and identified by high-performance liquid chromatography (HPLC) (Shimadzu; Kyoto, Japan) using a 5-µm C18 reverse-phase column (Shin-pack CLC ODS, Shimadzu). The HPLC column gradient was achieved by adding increasing volumes of absolute acetonitrile Merck Millipore to a 10% aqueous acetonitrile solution with the pH adjusted to 3.5 with hydrochloric acid (Merck Millipore). The absolute acetonitrile concentration was maintained at 65% for the first 10 min, increased from 65 to 100% between 10 and 13 min, and maintained at 100% between 13 and 21 min; at a flow rate of 1 mL min^{-1} and 40 °C. The PAs concentration was determined using a fluorescence detector at 340 nm (excitation) and 510 nm (emission). The peak areas and retention times of the samples were measured through comparisons with PAs standards Put, Spd and Spm (Sigma-Aldrich).

Comparative proteomic analysis

Protein extraction and digestion

Total protein extraction was performed according to Damerval et al. (1986), with modifications. Samples (300 mg FM each, in three biological replicates) were first macerated to a fine powder with liquid nitrogen, resuspended in 1 mL of extraction buffer containing 10% (w/v) trichloroacetic acid (TCA; Sigma-Aldrich) in acetone (Merck) with 20 mM dithiothreitol (DTT; GE Healthcare; Piscataway, USA), vortexed for 5 min at 4°C, and kept at − 20°C for 1 h. The samples were then centrifuged at 16,000 ×g for 20 min at 4°C, and the resulting pellets were washed three times with cold acetone containing 20 mM DTT. The pellets were resuspended in 1 mL of lysis buffer containing 7 M urea (GE Healthcare), 2 M thiourea (GE Healthcare), 2% Triton X-100 (GE Healthcare), 1% DTT (GE Healthcare), and 1 mM phenylmethanesulfonyl fluoride (PMSF; Sigma-Aldrich), vortexed, incubated on ice for 30 min and centrifuged at 16,000 ×g for 20 min at 4°C. The supernatants were collected, and the protein concentration was measured using a 2-D Quant Kit (GE Healthcare).

For protein digestion, 100 µg of protein from each biological replicate was used. Before digestion, proteins were precipitated with methanol:chloroform to remove any detergent from the samples (Nanjo et al., 2012). Then, the samples were resuspended

in 7 M urea (GE Healthcare) and 2 M thiourea (GE Healthcare) buffer and desalted Amicon Ultra-0.5 3 kDa centrifugal filters (Merck). The filters were filled to maximum capacity with buffers and centrifuged at 15,000 ×g for 10 min at 20°C. The samples were washed twice with 8 M urea and then twice with 50 mM ammonium bicarbonate (Sigma-Aldrich) pH 8.5, leaving approximately 50 µL per sample after the last wash. Protein digestion was performed according to the methodology described by Calderan-Rodrigues et al. (2014), with modifications. For each sample, 25 µL of 0.2% (v/v) RapiGest® (Waters, Milford, USA) was added, and the samples were briefly vortexed and incubated in an Eppendorf Thermomixer® (Eppendorf, Hamburg, Germany) at 80°C for 15 min. Then, 2.5 µL of 100 mM DTT was added, and the samples were vortexed and incubated at 60°C for 30 min under agitation (350 rpm). Next, 2.5 µL of 300 mM iodoacetamide (GE Healthcare) was added, and the samples were vortexed and incubated in the dark for 30 min at room temperature, after which 5 µL of 100 mM DTT was added to quench excess iodoacetamide. For protein digestion, 20 µL of trypsin solution (50 ng μL^{-1}; V5111, Promega, Madison, USA) prepared in 50 mM ammonium bicarbonate was added, and the mixture was incubated at 37 °C for 15 h. For RapiGest® precipitation and trypsin activity inhibition, 10 µL of 5% (v/v) trifluoroacetic acid (TFA; Sigma-Aldrich) was added, and the mixture was incubated at 37°C for 30 min and then centrifuged for 20 min at 16,000 ×g. The samples were transferred to Total Recovery Vials (Waters) for mass spectrometry analysis.

Mass spectrometry analysis

A nanoAcquity UPLC connected to a Synapt G2-Si HDMS mass spectrometer (Waters) was used for electrospray-liquid chromatography-tandem mass spectrometry analysis (nanoESI-LC–MS/MS analysis). During separation, 1 µg of digested proteins from each sample was loaded onto a nanoAcquity UPLC 5 µm C18 trap column (180 µm × 20 mm; Waters) at 5 µL min^{-1} for 3 min and then onto a nanoAcquity HSS T3 1.8 µm analytical reverse phase column (75 µm × 150 mm; Waters) at 400 nL min^{-1}, with a column temperature of 45°C. A binary gradient was used for peptide elution: mobile phase A consisted of water (Tedia, Fairfield, USA) and 0.1% formic acid (Sigma-Aldrich), and mobile phase B consisted of acetonitrile (Sigma-Aldrich) and 0.1% formic acid. Gradient elution was performed sequentially as follows: 7% B, ramping from 7 to

40% B until 91.12 min, from 40 to 99.9% B until 92.72 min, maintained at 99.9% B until 106 min, decreased to 7% B until 106.1 min and maintained at 7% B until the end of the run at 120 min. Mass spectrometry was performed in positive and resolution mode (V mode), 35,000 full width at half maximum, with ion mobility separation (IMS) and in data-independent acquisition (DIA) mode (HDMSE). IMS was performed using a wave velocity of 600 m s^{-1} and a helium and IMS gas flow of 180 and 90 mL min^{-1}, respectively. The transfer collision energy ramped from 19 to 55 V in high-energy mode, with cone and capillary voltages of 30 and 2750 V, respectively, and a source temperature of 70°C. Regarding time of flight (TOF) parameters, the scan time was set to 0.5 s in continuum mode with a mass range of 50 to 2000 Da. Human [Glu1]-fibrinopeptide B (Sigma-Aldrich) at 100 fmol μL^{-1} was used as an external standard, and lock mass acquisition was performed every 30 s. Mass spectral acquisition was carried out for 90 min using MassLynx v4.0 software.

Proteomics data analysis

Spectral processing and database search conditions were performed using ProteinLynx Global SERVER (PLGS) software v.3.02 (Waters). Apex3D parameters were set to a low-energy threshold of 150 counts, an elevated-energy threshold of 50 counts, and an intensity threshold of 750 counts. In addition, the analysis used one missed cleavage, minimum fragment ions per peptide equal to 3, minimum fragment ions per protein equal to 7, minimum peptides per protein equal to 2, automatic peptide and fragment tolerance, and fixed modifications of carbamidomethyl and variable modifications of oxidation and phosphoryl. The false discovery rate (FDR) was set to a maximum of 1%. The *Helianthus annuus* protein databank from UniProtKB (http://www.uniprot.org) was used for protein identification, as it is the largest databank with proximity to *C. legalis*.

Comparative label-free quantification analyses were performed using ISOQuant software v.1.7 (Distler et al., 2014). Briefly, the following parameters were used: FDR 1% for peptide and protein identification, sequence length of at least six amino acid residues, and minimum peptide score equal to 6. The analysis included retention time alignment, exact mass retention time, ion-mobility spectrometry clustering, data normalization and protein homology filtering. Samples were normalized

by a multidimensional normalization process, which corrects peak intensities based on intensity and retention time domains. The software performed the relative protein quantification according to the TOP3 method. Based on the relative abundances of uniquely assigned peptides, the abundances of shared peptides were redistributed to the respective source proteins, followed by TOP3-based quantification (Distler et al., 2014).

To ensure the quality of the results after data processing, only proteins present or absent (for unique proteins) in all three biological replicates were considered for differential abundance analysis. Protein data were analyzed using student's t test (two-tailed). Proteins with P values of $P < 0.05$ were deemed up-regulated if the log2 value of the fold change (FC) was greater than 0.58 and down-regulated if the log2 value of the FC was less than − 0.58. Functional annotations were performed using Blast2Go software v.5.0 (Conesa et al., 2005) and UniProtKB (http:// www.uniprot.org).

Statistical analysis

The experimental design was completely randomized. Data were analyzed using analysis of variance ($P < 0.05$), and means were compared using a Student–Newman–Keuls(SNK) test (Sokal e Rohlf, 1995) in the R program (R Foundation for Statistical Computing, version 3.4.4, 2018, Vienna, Austria).

RESULTS

Effect of light spectra on shoot development in *C. legalis*

Among the LED and fluorescent lamp treatments, the $W/_lB/_dR$ LED, consisting of white, low-blue (8–10%) and deep-red (30–50%) spectra, showed the best results for shoot length (3.54 cm), which did not differ significantly from the result for the $W/_lB/_dR/_fR$ LED (3.21 cm) comprising the same light spectra plus far red (12%) in shoots obtained from cotyledonary nodal explants (Fig. 1a). For shoots obtained from apical nodal explants, there was no significant difference in length among light

treatments. In addition, the growth of shoots was significantly higher in cotyledonary compared to those from apical nodal explants (Fig. 1a).

The number of shoots was statistically higher for those obtained from cotyledonary nodal compared to apical nodal explants (Fig. 1b). For the former, the number of shoots in the fluorescent lamp (control) and W/$_{l}$B/$_{d}$R LED treatments was statistically equal, which were significantly higher than those in the other light treatments (Fig. 1b). In addition, no significant difference was observed between light treatments for shoot number from apical nodal explants (Fig. 1b).

Moreover, the different treatments of light tested did not significantly influence shoot induction from both types of explants (Fig. 1c).

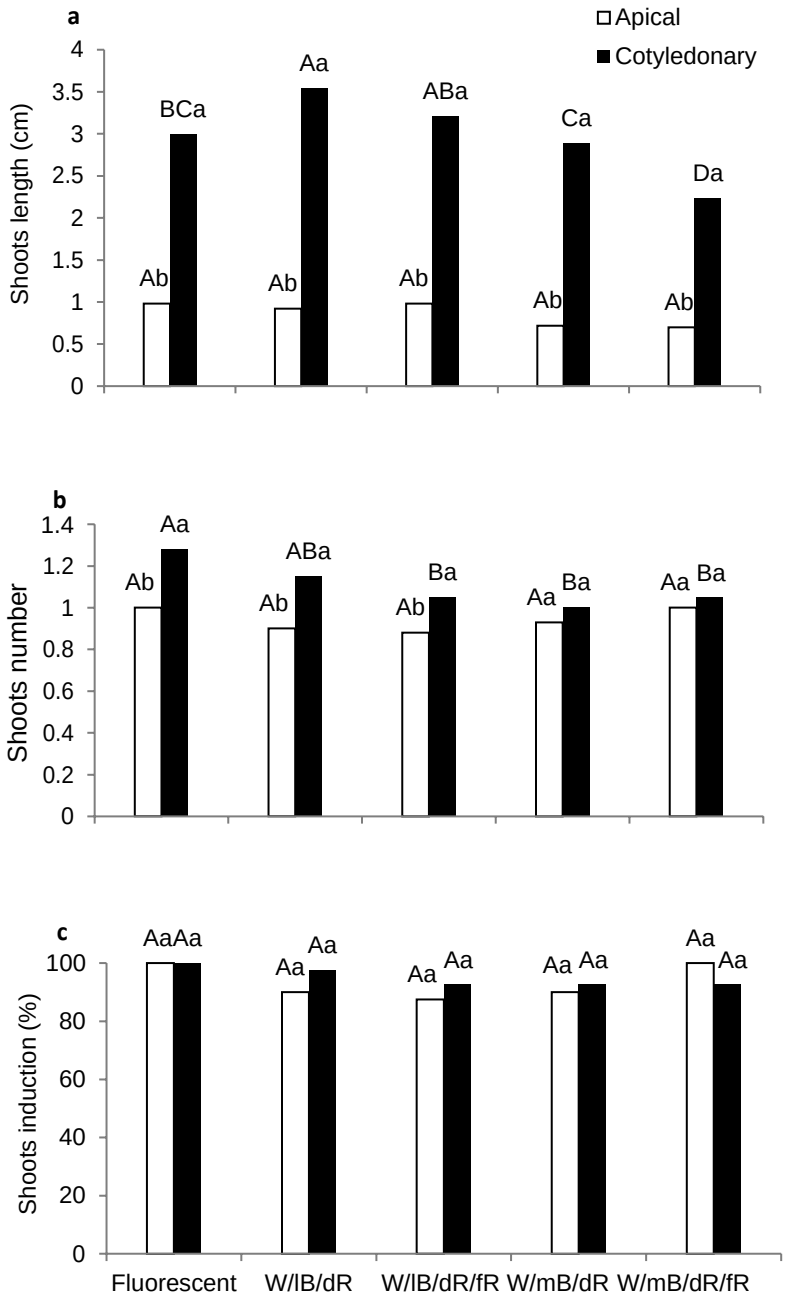

Fig. 1 Effect of different combinations of LED light spectra and fluorescent lamp in length (a), number (b) and induction (c) of shoots from apical and cotyledonary nodal explants of *C. legalis* at 60 days of *in vitro* growth. Means followed by the same letter do not differ statistically between them, according to SNK test ($P < 0.05$). Lowercase letters denote significant differences between explant types for each lamp source treatment tested. Uppercase letters denote significant differences among each lamp source treatment tested within each type of explant. W/$_h$B: white and high blue, W/$_m$B: white and medium blue, W/$_l$B/$_d$R: white, low blue and deep red, W/$_m$B/$_d$R: white, medium blue and deep red, W/$_l$B/$_d$R/$_f$R: white, low blue, deep red and far red, W/$_m$B/$_d$R/$_f$R: white, medium blue, deep red and far red. CV coefficient of variation. (n = 40, CV shoot length = 23.49%; CV shoot number = 13.11%; CV shoot induction = 11.12%).

Effect of light spectra on free PAs content in shoots from cotyledonary nodal explants

As the shoots from cotyledonary nodal explants grown under the W/$_l$B/$_d$R LED treatment at 60 days of culture showed a significant increase in elongation compared to those from apical nodal explants, comparison of free PAs contents between W/$_l$B/$_d$R LED and fluorescent lamp treatments was performed using shoots from the best type of explant comparing both, W/$_l$B/$_d$R LED and fluorescent lamp treatments. Compared to the fluorescent treatment, shoots cultivated under the W/$_l$B/$_d$R LED treatment exhibited a significantly higher content of free Put (Fig. 2a) and free Spd (Fig. 2b). In contrast, free Spm contents were not significantly affected by the treatments (Fig. 2c). Moreover, the light spectra of the W/$_l$B/$_d$R LED treatment significantly increased the endogenous content of total free PAs (Fig. 2d).

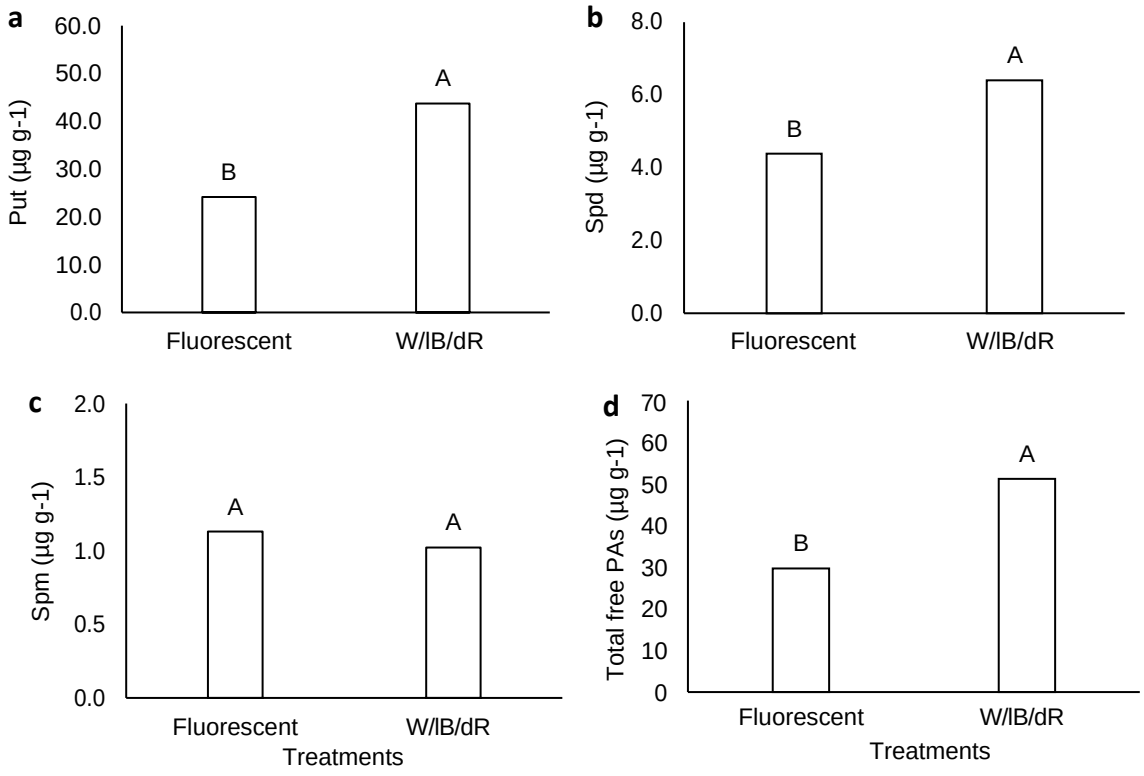

Fig. 2 Endogenous content (µg g^{-1} FM) of Put (a), Spd (b), Spm (c) and total free PAs (d) in shoots from cotyledonary nodal explants of *C. legalis* at 60 days of *in vitro* growth in W/$_l$B/$_d$R LED and fluorescent lamps. Means followed by the same letter do not differ statistically according to SNK test ($P < 0.05$). FM = Fresh matter; CV = coefficient of variation (n = 3, CV Put = 18.64%, CV Spd = 13.40%, CV Spm = 19.13%, CV total free PAs = 16.38%).

Effect of light spectra on the proteomic profile of shoots from cotyledonary nodal explants

Proteomic analysis was performed using samples of shoots from cotyledonary nodal explants incubated under a W/$_l$B/$_d$R LED or a fluorescent lamp. A total of 342 proteins were identified (Supplementary Table 1), 67 of which were differentially accumulated and 275 unchanged. Among the 67 differentially accumulated proteins, 15 and 41 were up- and down-regulated, respectively. Moreover, three proteins were unique in shoots grown under the W/$_l$B/$_d$R LED treatment, and eight were unique in shoots under the fluorescent treatment. The 67 regulated protein were classified according to biological process by Blast2Go and grouped into five classes. The majority of regulated proteins are involved in metabolic processes, followed by biological regulation processes, cellular organization and composition processes, photosynthetic processes, and stress response processes (Fig. 3).

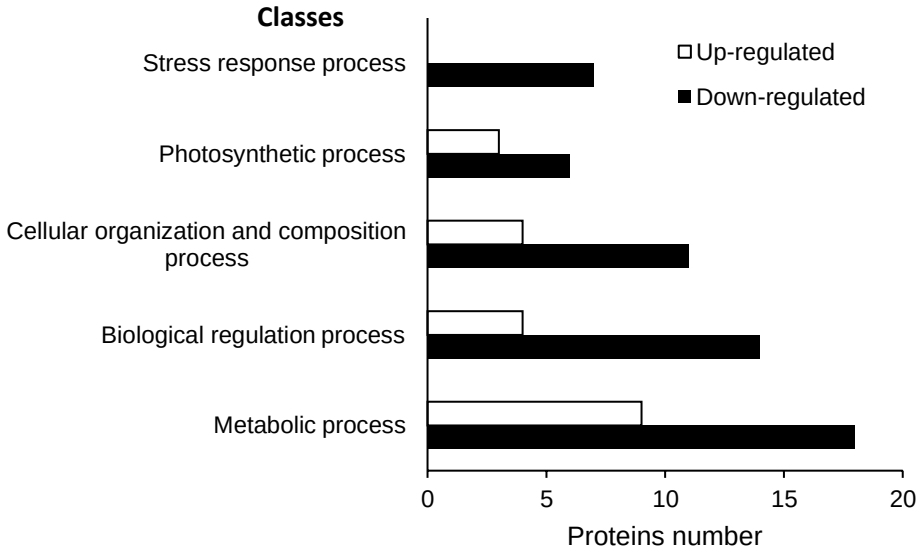

Fig. 3 Functional classification in the biological process of the 67 differentially abundant proteins identified in shoots of the *C. legalis.*

Among the proteins related to metabolic processes, cystathionine-β-synthase (CBS) domain-containing protein (A0A251VNA4) and cobalamin-independent methionine synthase (MetE) (A0A251UD42) were down-regulated in shoots grown under W/$_{l}$B/$_{d}$R light compared to those grown under fluorescent lamp (Table 1). In addition, ten proteins related to the function of carbohydrate metabolic processes in the class of metabolic processes were also identified (Table 1), four of which, triosephosphate isomerase (A0A251U316) glyceraldehyde-3-phosphate dehydrogenase (I3RXT3 and A0A251RRT4), phosphoglycerate kinase (A0A251TAV7), alpha-mannosidase (A0A251S9S9) and beta-glucosidase (A0A251VAJ5), were down-regulated in shoots grown under the W/$_{l}$B/$_{d}$R LED compared to those grown under the fluorescent lamp. Moreover, two proteins, aldehyde dehydrogenase (A0A251SJQ7) and alcohol dehydrogenase (A0A251UUW2), were unique in shoots grown under the fluorescent lamp (Table 1).

Regarding the class of biological regulation processes, four chaperonin proteins (A0A251VBK3, A0A251TPX4, A0A251VPP7 and A0A251VPF5) related to protein folding were up-regulated I shoots maintained under the W/$_{l}$B/$_{d}$R LED treatment compared to the fluorescent lamp (Table 1). However, ATP-dependent Clp protease proteolytic (A0A251TJP2) related to protein degradation was downregulated in shoots grown under W/$_{l}$B/$_{d}$R compared to those grown under fluorescent.

For the cellular organization and composition process class, some proteins, such as tubulins, were identified. Among them, the tubulin beta chain-like (A0A251RL41) was unique under the W/$_{l}$B/$_{d}$R LED lamp, and tubulin alpha chain (A0A251TD80) was up-regulated in shoots grown under the W/$_{l}$B/$_{d}$R LED lamp, with the highest fold change among regulated proteins (Supplementary Table 1).

Furthermore, nine proteins related to the photosynthesis process class were identified, six of which were down-regulated in shoots grown under the W/$_{l}$B/$_{d}$R LED lamp compared to the fluorescent lamp. These six proteins were ribulose bisphosphate carboxylase/oxygenase activase (A0A251TQ78), oxygen evolving enhancer protein (A0A251UDZ3), carbonic anhydrase (A0A251RUV1), photosystem I reaction center subunit V (A0A251T0E7), photosynthesis system II assembly factor Ycf48/Hcf136- like domain protein (A0A251TQ58) and oxygen-dependent coproporphyrinogen-III oxidase (A0A251VAW4) (Table 1).

Moreover, proteins related to the stress response process class, such as calreticulin isoform X1 (CRT) (A0A251TU95) and plastid lipid-associated protein/fibrillin (A0A251SF43), were downregulated in shoots grown under the W/$_l$B/$_d$R LED compared to those grown under the fluorescent lamp (Table 1). The proteins above mentioned or biologic processes in which they are involved are discussed below.

Table 1 Differentially abundant proteins identified in comparative proteomic analysis of the shoots at 60 days of culture from cotyledonary nodal explants of *Cariniana legalis* cultured in W/$_l$B/$_d$RLED and fluorescent treatments.

Accession	Peptide count	Score	Description	Biological Process	Differential abundance regulation LED / Fluorescent
A0A251TQ78	22	12844.37	Ribulose bisphosphate carboxylase/oxygenase activase 2	Positive regulation of catalytic activity; photosynthesis	Down
A0A251TDI1	21	5804.79	Cell division cycle protein 48 homolog	Cellcycle; cell division	Down
A0A251VI84	2	870.92	Heat shock protein 70 family	Stress response; protein folding	Down
A0A251VCX7	2	350.19	Purple acid phosphatase	Phosphorus metabolic process; Nitrogen compound metabolic process	Down
A0A251U9Y1	21	17788.95	Tubulin beta chain	Organelle organization	Down
A0A251UKC4	3	5318.89	Peptidyl-prolyl cis-trans isomerase	Protein folding; Cellular protein modification process	Down
A0A251TCD2	5	4498.06	Aldo/keto reductase/potassium channel subunit beta	Oxidation-reduction process	Down
A0A251RU22	3	679.67	UV excision repair protein Rad23, UBA-like, Ubiquilin, Ubiquitin-related domain protein	DNA repair; Proteolysis	Down
A0A251VIV4	13	3708.39	Elongation factor 1-alpha	Translation; Biological regulation	Down
A0A251SRB9	5	9112.62	Ribosomal protein S7 domain protein	Translation; Organelle organization; Ribosome biogenesis	Down

Table 1 (continued)

A0A251U316	8	4931.58	Triosephosphate isomerase	Carbohydrate metabolic process; Generation of precursor metabolites and energy;	Down
I3RXT3	9	16971.10	Glyceraldehyde-3-phosphate dehydrogenase (Fragment)	Carbohydrate metabolic process; Generation of precursor metabolites and energy	Down
A0A251UDZ3	5	8096.83	Oxygen-evolving enhancer protein 1 protein	Photosynthesis; Biological regulation	Down
A0A251TQ58	2	922.64	Photosynthesis system II assembly factor Ycf48/Hcf136-like domain protein	Generation of precursor metabolites and energy; Photosynthesis	Down
A0A251TJP2	3	1456.60	ATP-dependent Clp protease proteolytic subunit	Biological regulation; Response to stimulus	Down
A0A251RUV1	4	5045.40	Carbonic anhydrase	Carbon metabolic process; Photosynthesis	Down
A0A251TAV7	12	8306.11	Phosphoglycerate kinase	Carbohydrate metabolic process; Generation of precursor metabolites and energy	Down
A0A251TPA8	8	2070.75	Regulatory particle triple-A 1A	RNA metabolic process; Response to stimulus; Biological regulation	Down
O65352	9	3219.31	14-3-3-like protein	Biological process regulation	Down
A0A251T0E7	2	4665.66	Photosystem I PsaH, reaction center subunit VI	Photosynthesis; Metabolic process	Down
A0A251SRU1	6	2153.59	Phenylalanine ammonia-lyase	Nitrogen compound metabolic process; Secondary metabolic process; Primary metabolic process	Down
A0A251SL53	23	13772.62	Actin family	Cell constitution; Cellular cytoskeletal formation	Down
A0A251RNJ4	5	2258.27	Eukaryotic translation initiation factor 5A	Translation; Biological regulation	Down
A0A251TU95	10	2866.14	Calreticulin	Protein folding; Response to stimulus	Down
A0A251S9S9	2	204.81	Alpha-mannosidase	Carbohydrate metabolic process; Cellular protein modification process	Down
A0A251RY75	3	609.99	Proteasome endopeptidase complex	Cellular metabolic process	Down

Table 1 (continued)

A0A251S6A3	16	4548.28	Chaperonin Cpn60/TCP-1 family	Protein folding; cellular homeostasis; Response to stimulus; Biological regulation	Down
A0A251UD42	8	2755.18	Cobalamin-independent methionine synthase	Organic acid metabolic process; Primary metabolic process	Down
A0A251VAJ5	2	721.55	B-S glucosidase 44	Carbohydrate metabolic process;	Down
A0A251VAW4	3	1425.87	Oxygen-dependent coproporphyrinogen-III oxidase protein	Nitrogen compound metabolic process; Photosynthetic process	Down
A0A251SF43	3	2966.52	Plastid lipid-associated protein/fibrillin conserved domain-containing protein	Chloroplast organization; Response to stimulus	Down
A0A251U157	6	1962.24	Elongation factor 1-delta	Translation; Biological regulation	Down
A0A251RV88	3	1323.91	Nucleoside diphosphate kinase	Nucleoside metabolic process	Down
A0A251S5H6	4	892.17	Regulatory particle AAA-ATPase 2A	Cellular metabolic process; Protein degradation	Down
A0A251RRT4	15	15281.42	Glyceraldehyde-3-phosphate dehydrogenase	Carbohydrate metabolic process	Down
A0A251SMP9	4	1776.65	Outer plastidial membrane protein porin	Ion transport	Down
A0A251VS82	15	13578.90	Tubulin alpha chain	Organelle organization	Down
A0A251TCM9	3	2200.04	NAD(P)-linked oxidoreductase superfamily protein	Oxidation-reduction process	Down
A0A251TDZ2	19	4373.76	Cell division cycle protein	Cell division	Down
A0A251VNA4	6	6635.17	CBS domain-containing protein	Cellular process; Response to stimulus; Biological regulation	Down
A0A251SX18	11	11010.45	Malate dehydrogenase	Carbohydrate metabolic process; Organic acid metabolic process; Cellular respiration	Up

Table 1 (continued)

A0A251V667	6	1304.85	NADP-dependent glyceraldehyde-3-phosphate dehydrogenase	Carbohydrate metabolic process; Generation of precursor metabolites and energy	Up
Q9M504	6	2231.62	Catalase	Organic acid metabolic process; Cellular aromatic compound metabolic process; Primary metabolic process	Up
A0A251VPF5	6	2186.83	Chaperonin-60alpha	Protein folding; cellular homeostasis; Response to stimulus; Biological regulation	Up
A0A251RV70	3	969.03	Biotin carboxylase 2, chloroplastic	Organic acid metabolic process; Cellular lipid metabolic process	Up
A0A251RND2	3	530.94	Hydroxypyruvate reductase	Nitrogen compound metabolic process; Primary metabolic process; Photosynthetic process	Up
A0A251VPP7	2	1236.32	Chaperonin 20	Protein folding; cellular homeostasis; Response to stimulus; Biological regulation	Up
A0A251TPX4	15	4692.02	Chaperonin 60 beta	Protein folding; cellular homeostasis; Response to stimulus; Biological regulation	Up
A0A251TTN4	21	14467.90	Ribulose bisphosphate carboxylase/oxygenase activase 1 protein	Positive regulation of catalytic activity; Photosynthetic process	Up
A0A251V3J4	5	262.50	Ferredoxin-dependent Glutamate synthase	Developmental process; Primary metabolic process; Photosynthetic process	Up
A0A251VIG0	3	377.88	Lipoxygenase	Organic acid metabolic process; Cellular lipid metabolic process;	Up
A0A251TN12	3	712.20	Polyadenylate-binding protein	Regulation of translation; Response to cadmium ion; viral process	Up
A0A251VBK3	12	3275.08	Chaperonin Cpn60	Protein folding; cellular homeostasis; Response to stimulus; Biological regulation	Up
A0A251SKJ6	20	4363.94	Cell division cycle protein	Organelle organization; Cell division	Up
A0A251TD80	15	7482.28	Tubulin alpha chain	Organelle organization;	Up
A0A251RL41	11	10869.76	Tubulin beta chain	Organelle organization;	Unique LED lamp

Table 1 (continued)

A0A251SHB7	**3**	1798.64	Pyridoxal phosphate-dependent decarboxylase, Pyridoxal phosphate-dependent transferase	Organic acid metabolic process; Primary metabolic process	Unique LED lamp
A0A251U6F5	14	10186.94	Alcohol dehydrogenase superfamily, zinc-type	Oxidation-reduction process	Unique LED lamp
A0A251S412	6	1981.89	Succinate dehydrogenase [ubiquinone] flavoprotein subunit, mitochondrial	Organic acid metabolic process; Oxidative phosphorylation; Cellular respiration	Unique fluorescent lamp
A0A251SJQ7	4	1397.48	Aldehyde/histidinol dehydrogenase	Carbohydrate metabolic process; Organic acid metabolic process; Cellular lipid metabolic process	Unique fluorescent lamp
A0A251SZA2	3	1538.46	AAA-type ATPase family protein	RNA metabolic process; Response to stimulus; Biological regulation	Unique fluorescent lamp
A0A251UC35	3	5200.04	Glutamine synthetase	Nitrogen compound metabolic process; Primary metabolic process; Response to stimulus	Unique fluorescent lamp
A0A251UP18	6	4763.81	Histone H4	DNA packaging; Cellular protein-containing complex assembly; Response to stimulus	Unique fluorescent lamp
A0A251UUW2	14	10204.29	Alcohol dehydrogenase superfamily, zinc-type	oxidation-reduction process	Unique fluorescent lamp
A0A251V7Z7	7	2960.25	Heat Shock Protein 89.1	Protein folding; Response to stimulus	Unique fluorescent lamp
A0A251VIL2	19	11394.47	Tubulin alpha chain	Organelle organization	Unique fluorescent lamp

DISCUSSION

Plant development is influenced by light, and different spectra may alter *in vitro* organogenesis, highlighting the relevance of blue and red light combinations (Cybularz-Urban et al., 2007; Mengxi et al., 2011; Gupta e Sahoo, 2015). In this work, the use of different light spectral combinations by LEDs and fluorescent lamps, as well as two types of explants, revealed significant effects on *in vitro* shoot development in *C. legalis* (Fig. 1). Indeed, the results showed the importance of low-blue spectra combined with deep-red ($W/_lB/_dR$) or deep red plus far-red ($W/_lB/_dR/_fR$) spectra for shoot elongation in *C. legalis* cotyledonary nodal explants. This is highly relevant for this species, as an initial investigation performed by Aragão et al. (2017a) showed no significant increase in *in vitro* shoot growth of *C. legalis* using variable concentrations and combinations of plant growth regulator (PGRs) and PAs. The response obtained with the $W/_lB/_dR$ and $W/_lB/_dR/_fR$ LED treatments, without using PGRs, is a significant result and may be used to improve *in vitro* propagation in this species.

Among the spectra, it is known that blue light causes significant improvements in plant development, including in the number of shoots in *in vitro* culture (Budiarto, 2010; Gupta e Sahoo, 2015). Additionally, red light is known to be involved in plant elongation ((Mengxi et al., 2011; Demotes-Mainard et al., 2016). Under natural environmental conditions, *C. legalis* is considered a species of late secondary growth, i.e., seedlings can grow under forest shade, responding easily to incident low-blue and red spectra and high far-red light (Swaine e Whitmore, 1988), with longer stem elongation. This morphological response is known as shade avoidance (Smith, 1982), and the low red:far-red (R:FR) ratio has long been associated with all shade avoidance responses. However, low-blue light can also act in this process (Keller et al., 2011; Pedmale et al., 2016). In this case, the same response is mediated not only by phytochrome but also by cryptochrome photoreceptors, which perceive diminished blue light early and can phenocopy shade-avoidance responses in the absence of genes mediating the response to a low R:FR ratio. Nonetheless, the mechanisms by which the low-blue light signal regulates this response are not clear; in contrast to the response to a low R:FR ratio, it does not appear to involve regulation of auxin synthesis,

but brassinosteroids may be necessary (Keller et al., 2011; Pedmale et al., 2016). According to our results, the signal mediated by the combination of low-blue and deep-red (W/$_{l}$B/$_{d}$R) and low-blue and deep-red plus far-red (W/$_{l}$B/$_{d}$R/$_{f}$R) LED treatments may be related to shade-avoidance responses, resulting in increased elongation of *in vitro* shoots in *C. legalis*.

In addition to the increase in shoot elongation, the W/$_{l}$B/$_{d}$R LED treatment positively affected the endogenous PAs content in shoots from cotyledonary nodal segments, with a higher content of free Put, Spd and total free PAs compared to shoots grown under a fluorescent lamp (Fig. 2). Similar to our results, the highest content of Put, compared to other PAs, during *in vitro* organogenesis has been observed in other species, such as *Bixa orellana* (Parimalan et al., 2011) and *Cedrela fissilis* (Aragão et al., 2016). In general, accumulation of Put is related to intense cellular division activity, whereas Spd and Spm are positively correlated to higher rates of cell differentiation and plant development (Niemi et al., 2002; Santa-Catarina et al., 2006; Aragão et al., 2017b). It has also been shown that PAs act directly in cell cycle progression at the G1/S transition, stimulating synthesis of protein such as tubulins, which contribute to cell growth (Yamashita et al., 2013). In this sense, change in PAs metabolism might be an important aspect of a mechanism to regulate the organogenesis process (Paschalidis e Roubelakis-Angelakis, 2005). Moreover, PAs biosynthesis can be controlled by light, specifically under conditions of low light (Andreadakis e Kotzabasis, 1996; Kotzabasis et al., 1999; Ioannidis e Kotzabasis, 2007). Therefore, the combination of a low quantity of blue with deep-red light in the W/$_{l}$B/$_{d}$R LED treatment may have influenced shoot elongation, possibly by inducing an increase in Put and Spd contents compared to the fluorescent treatment (Fig. 2). These results suggest that PAs and specific light spectra can together play a fundamental role in *in vitro* shoot development, including that in *C. legalis*.

Furthermore, the proteomic profile of *in vitro* propagated *C. legalis* shoots was altered by the light spectral combination provided by the W$_{l}$B/$_{d}$R LED lamp compared to the fluorescent lamp (Fig. 3; Table 1). Among the identified proteins, chaperonins (A0A251VBK3, A0A251TPX4, A0A251VPP7 and A0A251VPF5) were up-regulated in shoots grown under the W/$_{l}$B/$_{d}$R LED treatment compared to those grown under the fluorescent lamp treatment (Table 1). Chaperonins are involved in protein folding and

cellular homeostasis (Lee e Tsai, 2005; Saibil, 2013; Zhang et al., 2016), and proteins targeted by chaperonins include actin, tubulins and other cytosolic proteins, which are strongly up-regulated during the cell cycle, especially from the G1/S transition (Yokota et al., 1999). In our analysis, tubulin alpha chain (A0A251TD80) was up-regulated in shoots grown under the W/$_{l}$B/$_{d}$R LED compared to the fluorescent lamp (Table 1), with the highest fold change among all regulated proteins. At the same time, a higher content of endogenous PAs, especially Put (Fig. 2), was observed in shoots grown under the W/$_{l}$B/$_{d}$R LED treatment. Thus, the light spectral combination of W/$_{l}$B/$_{d}$R LED treatment may have promoted higher contents of free Put and Spd and higher abundance of tubulin, as well as chaperonin proteins, which may have acted together to stimulate the G1/S transition of the cell cycle, leading to the observed greater shoot elongation.

Proteins related to metabolic processes were also identified. One cobalamin-independent methionine synthase (MetE) (A0A251UD42) was down-regulated in shoots grown under W/$_{l}$B/$_{d}$R compared to fluorescent lamp (Table 1). MetE is the enzyme that catalyzes the final step in methionine biosynthesis, which involves transfer of a methyl group to homocysteine (Ravanel et al., 1998). In this context, s-adenosylmethionine (SAM), synthetized from methionine, is a substrate for ethylene biosynthesis. CBS domain-containing (A0A251VNA4) protein (Table 1) was also down-regulated in shoots grown under the W/$_{l}$B/$_{d}$R compared to fluorescent lamp. Proteins containing the CBS domain participate in the cysteine biosynthesis pathway by catalyzing serine and homocysteine condensation to form cystathionine and provide a regulatory point for SAM catalysis (Ignoul e Eggermont, 2005). The lowest abundance of these two proteins in shoots grown under the W/$_{l}$B/$_{d}$R LED lamp suggest lower levels of methionine compared to shoots grown under the fluorescent lamp. However, the possible increase of methionine in shoots under the fluorescent treatment may have led to an increase in the level of ethylene, which has been related to a low capacity of shoot growth (Pua e Lee, 1995; Park et al., 2016; Sarropoulou e Maloupa, 2017). Overall, compared to those grown under the W/$_{l}$B/$_{d}$R LED lamp, the highest abundance of CBS and MetE in shoots grown under the fluorescent lamp may be related to lower elongation observed.

Furthermore, a small group of proteins involved in the response to stress was identified; among them, plastid lipid associated proteins (A0A251SF43), referred to as plant fibrillins (FIBs), was down-regulated in shoots grown under the W/$_{l}$B/$_{d}$R LED compared to fluorescent lamp (Table 1). FIBs are thylakoid-associated proteins that can accumulate under biotic and abiotic stress conditions (Gillet et al., 1998; Leitner-Dagan et al., 2006). In Arabidopsis, a lack of FIB protein leads to inefficient protection against light damage of the photosynthetic apparatus, as well as to photosystem II photoinhibition (Yang et al., 2006; Youssef et al., 2010). Thus, the highest abundance of this protein in shoots grown under the fluorescent treatment suggests a low efficiency of this lamp as a light source for shoot development compared to the LED lamp, likely due to the broad light spectral composition of this the former. The use of LED lamps allows for the adjustment of specific spectra necessary for the optimal morphogenic responses (Kim et al., 2004; Gupta e Jatothu, 2013), which is not possible when using fluorescent lamps and may limit the development of shoots. In addition, an ATP-dependent caseinolytic protease proteolytic (A0A251TJP2) was down-regulated in shoots grown under the W/$_{l}$B/$_{d}$R LED compared to the fluorescent lamp (Table 1). This protein is an essential housekeeping enzyme in chloroplasts (Olinares et al., 2011), and although the specific roles of this protein are unclear, one well-reported function is the removal of unwanted or damaged proteins, such as the D1 protein (protein of photosystem II), after lightinduced damage (Olinares et al., 2011). Accordingly, the highest abundance of FIB proteins and caseinolytic protease in shoots grown under the fluorescent treatment highlights a negative response to this lamp as a light source for shoot development in *C. legalis*.

Calreticulin isoform X1 (CRT) (A0A251TU95), a multifunctional protein that can act as a stress-inducible chaperone and a Ca^{2+}-buffering and signaling protein (Persson et al., 2001; Jia et al., 2009), was also down-regulated in shoots grown under the W/$_{l}$B/$_{d}$R LED lamp compared to the fluorescent lamp (Table 1). This protein has been related to *in vitro* organogenesis, with a possible role in cell division (Jin et al., 2007). In addition, higher abundance of CRT has been related to abiotic stress responses, such as high-temperature stress in *Solanum lycopersicum* leaves (Sang et al. 2017). Thus, the higher abundance of this protein in shoots grown under fluorescent lamp suggests possible stress related to unsatisfactory characteristics, such as higher

heat emission and lower control of spectral composition compared to LEDs (Massa et al., 2008; Gupta e Jatothu, 2013), which affected the growth of *C. legalis* shoots.

Proteins related to the photosynthesis process were identified, mostly as being down-regulated, in shoots grown under the W/$_{l}$B/$_{d}$R LED lamp compared to those under the fluorescent lamp (Fig. 3). Among them, oxygen-dependent coproporphyrinogen-III oxidase (A0A251VAW4) (Table 1) is an enzyme related to chlorophyll biosynthesis (Von Wettstein et al., 1995; Beale, 1999), and an increase in this protein was observed in *S. lycopersicum* leaves subjected to high-temperature stress (Sang et al., 2017). The highest abundance of this protein in shoots grown under the fluorescent lamp may have occurred in response to the stress promoted by the features of this type of lamp. In addition, photosynthetic activity is minimized during *in vitro* propagation, and the enzymes responsible for photosynthesis may be inactive (Hazarika, 2006). Thus, changes in photosynthesis-related proteins may not be directly associated with the results of shoot development in *C. legalis*, which might well be explained by the regulation of proteins related to cell composition and regulation.

Moreover, proteins related to carbohydrate metabolic processes were observed as being altered in abundance, being mostly down-regulated, in shoots grown under the W/$_{l}$B/$_{d}$R LED. Two unique proteins in shoots grown under the fluorescent lamp were also observed (Table 1). Among them, triosephosphate isomerase (A0A251U316), glyceraldehyde- 3-phosphate dehydrogenase (I3RXT3 and A0A251RRT4), and phosphoglycerate kinase (A0A251TAV7) (Table 1) participate directly in glycolysis (Plaxton, 1996). In addition, aldehyde dehydrogenase (A0A251SJQ7) and alcohol dehydrogenase (A0A251UUW2), which were unique in the shoots grown under the fluorescent lamp (Table 1), are involved in carbohydrate metabolism in plants under stress (Matton et al., 1990; Kirch et al., 2004). Thus, the highest abundance of proteins related to both photosynthesis and carbohydrate metabolism in shoots grown under fluorescent lamps compared to those grown under the W/$_{l}$B/$_{d}$R LED may be associated with an investment in energy accumulation induced by abiotic stress associated with the light source more than to an investment in the growth of shoots.

CONCLUSION

Our results showed the positive influence of the combination of low-blue with red and far-red light spectra on shoot elongation, likely as a shade-avoidance response, in *C. legalis*. The W/$_{l}$B/$_{d}$R LED lamp affected the endogenous contents of PAs Put and Spd in shoots, highlighting the importance of these PAs on shoot elongation due to their activity in cell cycle progression. Moreover, an increase in the abundance of proteins related to protein folding, homeostasis and cell organization, such as chaperonin and tubulins, along with a reduction in the abundance of proteins related to stress, may be related to the enhanced growth of *C. legalis* shoots under the LED lamp compared to the fluorescent lamp. This work provides relevant data regarding the effects of light source as a positive factor in *C. legalis* shoot elongation through responses of PAs content and protein profile modulation.

REFERENCES

Alcázar R, Altabella T, Marco F, Bortolotti C, Reymond M, Koncz C, Carrasco P, Tiburcio AF (2010) Polyamines: molecules with regulatory functions in plant abiotic stress tolerance. Planta 231:1237-1249

Andreadakis A, Kotzabasis K (1996) Changes in the biosynthesis and catabolism of polyamines in isolated plastids during chloroplast photodevelopment. J Photochem Photobiol B: Biol 33:16-170

Aragão VPM, Reis RS, Silveira V, Santa-Catarina C (2017b) Putrescine promotes changes in the endogenous polyamine levels and proteomic profiles to regulate organogenesis in *Cedrela fissilis* Vellozo (Meliaceae). Plant Cell Tiss Org Cult 130:495–505

Aragão VPM, Ribeiro YRdS, Reis RS, Macedo AF, Floh EIS, Silveira V, Santa-Catarina C (2016) *In vitro* organogenesis of *Cedrela fissilis* Vell. (Meliaceae): the involvement of endogenous polyamines and carbohydrates on shoot development. Plant Cell Tiss Org Cult 124:611-620

Aragão VPM, Silveira V, Santa Catarina C (2017a) Micropropagation of *Cariniana legalis* (Martius) O. Kuntze, an endangered hardwood tree from the brazilian Atlantic Forest. Plant Cell Cult Micro 13:41-50

Beale SI (1999) Enzymes of chlorophyll biosynthesis. Photosynt Res 60:43-73

Budiarto K (2010) Spectral quality affects morphogenesis on *Anthurium* plantlet during *in vitro* culture. Agrivita 32:234-240

Bunn E, Turner SR, Dixon KW (2011) Biotechnology for saving rare and threatened flora in a biodiversity hotspot. In Vitro Cell Dev Biol Plant 47:188-200

Calderan-Rodrigues MJ, Jamet E, Bonassi MBCR, Guidetti-Gonzalez S, Begossi AC, Setem LV, Franceschini LM, Fonseca JG, Labate CA (2014) Cell wall proteomics of sugarcane cell suspension cultures. Proteomics 14:738-749

Carvalho PER (1994) Espécies florestais brasileiras: recomendações silviculturais, potencialidades e uso da madeira. Colombo: Embrapa/CNPF edn. Embrapa/SPI, Brasília

Conesa A, Götz S, García-Gómez JM, Terol J, Talón M, Robles M (2005) Blast2GO: a universal tool for annotation, visualization and analysis in functional genomics research. Bioinformatics 21:3674-3676

Cybularz-Urban T, Hanus-Fajerska E, Swiderski A (2007) Effect of light wavelength on *in vitro* organogenesis of a *Cattleya* hybrid. Acta Biol Cracov 49:113-118

Damerval C, De Vienne D, Zivy M, Thiellement H (1986) Technical improvements in two-dimensional electrophoresis increase the level of genetic variation detected in wheat-seedling proteins. Electrophoresis 7:52-54

Demotes-Mainard S, Péron T, Corot A, Bertheloot J, Le Gourrierec J, Pelleschi-Travier S, Crespel L, Morel P, Huché-Thélier L, Boumaza R (2016) Plant responses to red and far-red lights, applications in horticulture. Environ Exp Bot 121:4-21

Distler U, Kuharev J, Navarro P, Levin Y, Schild H, Tenzer S (2014) Drift time-specific collision energies enable deep-coverage data-independent acquisition proteomics. Nat Methods 11:167-170

Gillet B, Beyly A, Peltier G, Rey P (1998) Molecular characterization of CDSP 34, a chloroplastic protein induced by water deficit in *Solanum tuberosum* L. plants, and regulation of CDSP 34 expression by ABA and high illumination. The Plant J 16:257-262

Gupta SD, Jatothu B (2013) Fundamentals and applications of light-emitting diodes (LEDs) in *in vitro* plant growth and morphogenesis. Plant Biotechnol Rep 7:211-220

Gupta SD, Sahoo T (2015) Light emitting diode (LED)-induced alteration of oxidative events during *in vitro* shoot organogenesis of *Curculigo orchioides* Gaertn. Acta Physiol Plant 37:233

Hazarika B (2006) Morpho-physiological disorders in *in vitro* culture of plants. Sci Hortic 108:105-120

Heringer AS, Reis RS, Passamani LZ, de Souza-Filho GA, Santa-Catarina C, Silveira V (2017) Comparative proteomics analysis of the effect of combined red and blue lights on sugarcane somatic embryogenesis. Acta Physiol Plant 39:52

Hunter DC, Burritt DJ (2005) Light quality influences the polyamine content of lettuce (*Lactuca sativa* L.) cotyledon explants during shoot production *in vitro*. Plant growth regul 45:53-61

Ignoul S, Eggermont J (2005) CBS domains: structure, function, and pathology in human proteins. Am J Physiol Cell Physiol 289:C1369-C1378

Ioannidis NE, Kotzabasis K (2007) Effects of polyamines on the functionality of photosynthetic membrane *in vivo* and *in vitro*. Biochim Biophy Acta 1767:1372-1382

IUCN (2018) International Union for Conservation of Nature.The Red List of Threatened species. http://www.iucnredlist.org/about. Accessed 8th july 2018

Jia XY, He LH, Jing RL, Li RZ (2009) Calreticulin: conserved protein and diverse functions in plants. Physiol Plant 136:127-138

Jin ZL, Ryu SH, Hong JK, Song CE, Lim CJ, Choi YJ, Lee KO, Chung WS, Lee SY, Lim CO (2007) Over-expression of Chinese cabbage calreticulin 1b, BrCRT1b, induces initiation of organogenesis in *Arabidopsis*. Genes Genom 29:409-418

Keller MM, Jaillais Y, Pedmale UV, Moreno JE, Chory J, Ballaré CL (2011) Cryptochrome 1 and phytochrome B control shade-avoidance responses in *Arabidopsis* via partially independent hormonal cascades. The Plant J 67:195-207

Kim S-J, Hahn E-J, Heo J-W, Paek K-Y (2004) Effects of LEDs on net photosynthetic rate, growth and leaf stomata of *chrysanthemum* plantlets *in vitro*. Sci Horti 101:143-151

Kirch H-H, Bartels D, Wei Y, Schnable PS, Wood AJ (2004) The ALDH gene superfamily of *Arabidopsis*. Trends Plant Sci 9:371-377

Kotzabasis K, Strasser B, Navakoudis E, Senger H, Dörnemann D (1999) The regulatory role of polyamines in structure and functioning of the photosynthetic apparatus during photoadaptation. J Photochem Photobiol B: Biol 50:45-52

Kusano T, Berberich T, Tateda C, Takahashi Y (2008) Polyamines: essential factors for growth and survival. Planta 228:367-381

Lazzarini LES, Bertolucci SKV, Pacheco FV, dos Santos J, Silva ST, de Carvalho AA, Pinto JEBP (2018) Quality and intensity of light affect *Lippia gracilis* Schauer plant growth and volatile compounds *in vitro*. Plant Cell Tiss Org Cult 135:367–379

Lee S, Tsai F (2005) Molecular chaperones in protein quality control. J Biochem Mol Biol 38:259-265

Leitner-Dagan Y, Ovadis M, Shklarman E, Elad Y, David DR, Vainstein A (2006) Expression and functional analyses of the plastid lipid-associated protein CHRC suggest its role in chromoplastogenesis and stress. Plant Physiol 142:233-244

Lloyd G, McCown B (1981) Commercially-feasible micropropagation of mountain laurel, *Kalmia latifolia*, by use of shoot-tip culture. Int Plant Propag Societ 30:421-427

Massa GD, Kim H-H, Wheeler RM, Mitchell CA (2008) Plant productivity in response to LED lighting. HortSci 43:1951-1956

Matta LBV, Scudeller VV (2012) Lecythidaceae Poit. in the Tupé Sustainable Development Reserve, Manaus, Brazil. Braz J Bot 35:195-217

Matton DP, Constabel P, Brisson N (1990) Alcohol dehydrogenase gene expression in potato following elicitor and stress treatment. Plant Mol Biol 14:775-783

Mengxi L, Zhigang X, Yang Y, Yijie F (2011) Effects of different spectral lights on *Oncidium* PLBs induction, proliferation, and plant regeneration. Plant Cell Tiss Org Cult 106:1-10

Muneer S, Kim EJ, Park JS, Lee JH (2014) Influence of green, red and blue light emitting diodes on multiprotein complex proteins and photosynthetic activity under different light intensities in lettuce leaves (*Lactuca sativa* L.). Int J Mol Sci 15:4657-4670

Nanjo Y, Skultety L, Uváčková Lu, Klubicová Kn, Hajduch M, Komatsu S (2012) Mass spectrometry-based analysis of proteomic changes in the root tips of flooded soybean seedlings. J Prot Res 11:372-385

Niemi K, Sarjala T, Chen X, Häggman H (2002) Spermidine and methylglyoxal bis (guanylhydrazone) affect maturation and endogenous polyamine content of Scots pine embryogenic cultures. J Plant Physiol 159:1155-1158

Olinares PDB, Kim J, Van Wijk KJ (2011) The Clp protease system; a central component of the chloroplast protease network. Biochim Biophys Acta Bioenerg 1807:999-1011

Oliveira LSd, Dias PC, Brondani GE (2013) Micropropagação de espécies florestais brasileiras. Pes Florest Bras 33:439-453

Parimalan R, Giridhar P, Ravishankar G (2011) Enhanced shoot organogenesis in *Bixa orellana* L. in the presence of putrescine and silver nitrate. Plant Cell Tiss Org Cult 105:285-290

Park JS, Naing AH, Kim CK (2016) Effects of ethylene on shoot initiation, leaf yellowing, and shoot tip necrosis in roses. Plant Cell Tiss Org Cult 127:425-431

Paschalidis KA, Roubelakis-Angelakis KA (2005) Spatial and temporal distribution of polyamine levels and polyamine anabolism in different organs/tissues of the tobacco plant. Correlations with age, cell division/expansion, and differentiation. Plant Physiol 138:142-152

Pedmale UV, Huang S-sC, Zander M, Cole BJ, Hetzel J, Ljung K, Reis PA, Sridevi P, Nito K, Nery JR (2016) Cryptochromes interact directly with PIFs to control plant growth in limiting blue light. Cell 164:233-245

Persson S, Wyatt SE, Love J, Thompson WF, Robertson D, Boss WF (2001) The Ca2+ status of the endoplasmic reticulum is altered by induction of calreticulin expression in transgenic plants. Plant Physiol 126:1092-1104

Plaxton WC (1996) The organization and regulation of plant glycolysis. Annu Rev Plant biol 47:185-214

Pua E-C, Lee JE (1995) Enhanced de novo shoot morphogenesis *in vitro* by expression of antisense 1-aminocyclopropane-1-carboxylate oxidase gene in transgenic mustard plants. Planta 196:69-76

Ravanel S, Gakière B, Job D, Douce R (1998) The specific features of methionine biosynthesis and metabolism in plants. Proc Natl Acad Sci 95:7805-7812

Rêgo GM (2002) Jequitibá-rosa (*Cariniana legalis*): espécie em extinção da floresta Atlântica. Circular técnico edn. Embrapa Tabuleiros Costeiros, Aracaju

Rego GM, Possamai E (2006) Efeito do Sombreamento sobre o Teor de Clorofila e Crescimento Inicial do Jequitibá-rosa. Pesq Fl Bras:179-194

Reis RS, Vale EM, Heringer AS, Santa-Catarina C, Silveira V (2016) Putrescine induces somatic embryo development and proteomic changes in embryogenic callus of sugarcane. J Proteomics 130:170-179

Saibil H (2013) Chaperone machines for protein folding, unfolding and disaggregation. Nat Rev Mol Cell Biol 14:630–642

Sang Q, Shan X, An Y, Shu S, Sun J, Guo S (2017) Proteomic analysis reveals the positive effect of exogenous spermidine in tomato seedlings' response to high-temperature stress. Front Plant Sci 8:120

Santa-Catarina C, Silveira V, Balbuena TS, Viana AM, Estelita MEM, Handro W, Floh ELS (2006) IAA, ABA, polyamines and free amino acids associated with zygotic embryo development of *Ocotea catharinensis*. Plant Growth Regul 49:237-247

Sarropoulou V, Maloupa E (2017) Effect of the NO donor "sodium nitroprusside"(SNP), the ethylene inhibitor "cobalt chloride"(CoCl 2) and the antioxidant vitamin E "α-tocopherol" on *in vitro* shoot proliferation of *Sideritis raeseri* Boiss. & Heldr. subsp. *raeseri*. Plant Cell Tiss Org Cult 128:619-629

Singh D, Basu C, Meinhardt-Wollweber M, Roth B (2015) LEDs for energy efficient greenhouse lighting. Renewable and Sustainable Energy Reviews 49:139-147

Smith H (1982) Light quality, photoperception, and plant strategy. Annual Rew Plant Physiol 33:481-518

Sokal RR, Rohlf FJ (1995) *Biometry* vol 3ª ed., edn. WH Freeman and Co, NY

Sousa KR, Aragão VPM, Reis RS, Macedo AF, Vieira HD, de Souza CLM, Floh EIS, Silveira V, Santa-Catarina C (2016) Polyamine, amino acid, and carbohydrate profiles during seed storage of threatened woody species of the Brazilian Atlantic Forest may be associated with seed viability maintenance. Braz J Bot 39:985-995

Swaine MD, Whitmore T (1988) On the definition of ecological species groups in tropical rain forests. Vegetatio 75:81-86

Vieira TO, Lage-Pinto F, Ribeiro DR, Alencar TdS, Vitória AP (2012) Estresse luminoso em plântulas de jequitibá-rosa *(Cariniana legalis*, Lecythidaceae): monitoramento da capacidade de aclimatação fotossintética sob duas intensidades de luz. Vértices 13:129-142

Von Wettstein D, Gough S, Kannangara CG (1995) Chlorophyll biosynthesis. The Plant Cell 7:1039-1057

Yamashita T, Nishimura K, Saiki R, Okudaira H, Tome M, Higashi K, Nakamura M, Terui Y, Fujiwara K, Kashiwagi K, Igarashi K (2013) Role of polyamines at the G1/S boundary and G2/M phase of the cell cycle. The Int J Biochem Cell Biol 45:1042-1050

Yang Y, Sulpice R, Himmelbach A, Meinhard M, Christmann A, Grill E (2006) Fibrillin expression is regulated by abscisic acid response regulators and is involved in abscisic acid-mediated photoprotection. Proc Nat Acad Sci 103:6061-6066

Yokota S-i, Yanagi H, Yura T, Kubota H (1999) Cytosolic Chaperonin Is Up-regulated during Cell Growth: preferential expression and binding to tubulin at g1/s transition through early s phase. J Biol Chemis 274:37070-37078

Youssef A, Laizet Yh, Block MA, Maréchal E, Alcaraz JP, Larson TR, Pontier D, Gaffé J, Kuntz M (2010) Plant lipid-associated fibrillin proteins condition jasmonate production under photosynthetic stress. The Plant J 61:436-445

Zhang S, Zhou H, Yu F, Bai C, Zhao Q, He J, Liu C (2016) Structural insight into the cooperation of chloroplast chaperonin subunits. BMC Biol 14:29

3.2. DIFFERENTIALLY REGULATED PROTEINS COULD BE RELATED TO DIFFICULTIES FOR in vitro ROOTING OF MICROPROPAGATED SHOOTS IN Cariniana legalis (MARTIUS) O. KUNTZE*

RESUMO

O enraizamento é um passo importante na propagação *in vitro*, sendo a auxina necessária para sinalizar a indução em algumas espécies. O objetivo deste trabalho foi avaliar os efeitos do ácido indol-3-butírico (AIB) e do floroglucinol (PG) no enraizamento *in vitro* e no perfil proteômico em microestacas de *Cariniana legalis*. Microestacas obtidas de brotações cultivadas *in vitro* foram incubadas em meio de cultura ¼ MS (Murashige e Skoog), suplementado com conbinações de AIB (0, 50 e 100 µM) e PG (0 e 30 µM). O desenvolvimento radicular, o perfil histomorfológico e proteômico foram analisados. O AIB foi necessário para o enraizamento, sem diferença entre 50 e 100 µM. Aos 12 dias de incubação, a análise histomorfológica no tratamento com AIB 50 µM mais PG 30 µM mostrou células meristemáticas em calos, induzidas nas microestacas permitindo enraizamento. O perfil proteômico das microestacas aos 12 dias deste tratamento foi comparado com microestacas no tempo inicial (0 dias) e microestacas aos 12 dias não tratadas com AIB e PG. Proteínas relacionadas aos processos metabólicos de carboidratos e aminoácidos foram up-

* Os dados deste capítulo serão submetidos para publicação:
Lerin, J; Ribeiro, YRS; Oliveira, TR; Silveira, V; Santa-Catarina, C. (2020). Plant Growth Regulation.

reguladas na comparação microestacas 12 dias tratadas / 0 dias, sendo associadas ao enraizamento. Na comparação microestacas 12 dias tratadas / 12 dias não tratadas, proteínas do processo metabólico secundário foram *down*-reguladas e relacionadas ao não enraizamento, enquanto proteínas de homeostase celular foram *up*-reguladas, sendo relacionadas ao enraizamento nas microestacas tratadas. Portanto, o AIB exógeno foi necessário para o enraizamento *in vitro*, alterando o proteoma da microestaca enraizada, como observado no tratamento AIB 50 µM mais PG 30 µM em comparação ao tratamento controle.

Palavras-chave: Auxina, enraizamento *in vitro,* proteômica comparativa, morfogênese de raiz

ABSTRACT

Rooting is important step on *in vitro* propagation, being the auxin necessary to signaling the induction in some wood species. The aim of this work was to evaluated the effects of indole-3-butyric acid (IBA) and phloroglucinol (PG) on *in vitro* rooting and proteomic profile in *Cariniana legalis* microcutting. Microcuttings obtained from shoots grown *in vitro* were incubated in ¼ MS (Murashige and Skoog) culture medium, supplemented with conbinations of IBA (0, 50 and 100 µM) and PG (0 and 30 µM). Root development, histomorphological and proteomic profile were analyzed. IBA was necessary for root induction and at 12 days of incubation in the treatment with IBA 50 µM plus PG 30 µM meristematic cells observed in callus induced in the microcuttings allowed rooting. The proteomic profile of microcutting at 12 days treated with IBA 50 µM plus PG 30 µM was compared to microcutting at the initial time (0 days) and microcutting at 12 days non-treated with IBA and PG. Proteins related to carbohydrates and amino acids metabolic processes were up-regulated in the comparison microcutting 12 days treated/0 days, being associated with rooting. In the comparison microcutting 12 days treated/12 non-treated days, proteins related to the secondary metabolic process were down-regulated and related to non-rooting, while proteins

related to cellular homeostasis were up-regulated being related to rooting in treated microcuttings. Therefore, IBA was effective for rooting and in the IBA 50 µM plus PG 30 µM treatment were identified proteins involved with rooting.

Keywords: Auxin, *In vitro* rooting, Comparative proteomics, Root morphogenesis.

INTRODUCTION

The *Cariniana legalis* (Martius) O. Kuntze (Lecythidaceae), commonly known as jequitibá-rosa (Rêgo, 2002), is a forest species native from Brazil (Ribeiro et al., 2017). Because of the intense exploration for the high economic value of its wood for furniture and construction industry (Rêgo, 2002; Carvalho, 2005), in addition to the difficulty of propagation by conventional methods, this species is nowadays added in the red list of threatened species by the International Union for Conservation of Nature (IUCN), being classified as vulnerable (IUCN, 2019). The difficulty of propagation occur due to the rapid loss of seed viability (Sousa et al., 2016), and absence of morphogenic response to conventional propagation techniques, such as cuttings, commons feature for some forest species (Oliveira et al., 2013).

In this sense, *in vitro* propagation appears as an alternative for preservation of wood tree species, especially those endangered (Bunn et al., 2011). For *C. legalis*, initial studies has been carried out to establish the *in vitro* regeneration (Aragão et al., 2017), and the shoot development was improved by the use of different spectra of light-emitting diode (LED) lamps (Lerin et al., 2019). However, *C. legalis* showed difficult to induce roots from the micropropagated shoots, being the rooting an important step to overcome a micropropagation system.

The *in vitro* rooting, an important phase for plants propagation, is influenced by several factors, including the culture medium and the use of auxins (De Klerk et al., 2011; Dewir et al., 2016). For some species, the reduction in the salts level of Murashige and Skoog (MS) culture medium (Murashige e Skoog, 1962) to a half ($^1/_2$) or quarter ($^1/_4$) was essential and increased the root induction (Vahdati et al., 2004;

Parveen e Shahzad, 2010; Parveen et al., 2010). This response is mainly due to the reduction in nitrogen content of the culture medium (Dewir et al., 2016).

The auxin found naturally in plants is involved with root formation process and its exogenous application has been considered effective for rooting (Da Costa et al., 2013; Dewir et al., 2016). Among the auxin, the indole-3-butyric acid (IBA) showed higher performance for shoot rooting in several species, such as *Cassia siamea* (Parveen et al., 2010), *Parkia timoriana* (Thangjam e Sahoo, 2012) and *Juglans nigra* (Stevens e Pijut, 2018). During adventitious root development, the auxin have an important role in the root induction phase more than in the following initiation and expression phases (Da Costa et al., 2013; Pacurar et al., 2014).

Phenolic compounds also have been seen in higher level during the root induction phase, suggesting their involvement in adventitious rooting (Da Costa et al., 2013). One of the effects attributed to phenolic compound is the protective action from auxin oxidation, allowing greater auxin availability during root induction (De Klerk et al., 2011; da Silva et al., 2013). An already studied phenolic compound for *in vitro* rooting is the phloroglucinol (PG), which can serve to enhance the auxin effects on root induction (da Silva et al., 2013). The PG addition into the rooting medium have shown efficiency in the root induction, as well increasing the number and length of adventitious root in some species, such as *Pterocarpus marsupium* (Husain et al., 2008), *Malus* 'Jork 9' (De Klerk et al., 2011) and *Carica papaya* (Pérez et al., 2016).

The histological analysis is an interesting approach to be carried out in order to demonstrate the morphological differences between rooted and unrooted microcuttings, allowing to characterize the phases of rooting in species with difficulties to rooting. In addition, among the biochemical changes that may occur is the alteration in proteins involved in the *de novo* root formation. Studies have shown the identification of proteins related to phenylpropanoid pathway (Vander Mijnsbrugge et al., 2000), glycolysis and tricarboxylic acid cycle (Ahkami et al., 2009; Tang et al., 2016) and hormone-related proteins (Sukumar et al., 2013; Tang et al., 2016), which are linked to promotion of adventitious roots. In this way, the proteomic analysis is an important tool to understand the protein profile related to the formation of adventitious roots, as well analyze the relationship of specific proteins to root induction in species that show difficulty in rooting, as the case of *C. legalis*. Therefore, this work aimed to analyze the

effect of IBA and PG on *in vitro* rooting and proteomic profiles in microcuttings of *C. legalis*.

MATERIAL AND METHODS

Plant material

Mature *C. legalis* seeds were obtained from the Sementes Caiçara nursery, being collected from trees of a natural area located in Brejo Alegre, SP, Brazil (21º10'S and 50º10'W). Seeds were germinated *in vitro* and 90-day-old seedlings served as source of explants for shoot induction. Shoots from cotyledonary nodal explants were *in vitro* developed under 16h of photoperiod and light intensity of 45 μmol m^2 s^{1} from LED lamps (Koninklijke Philips Electronics NV, Amsterdam, Netherlands) with white, low blue and deep red spectra at 25 ± 2 °C, according to Lerin et al. (2019).

Effect of IBA and PG on microcutting rooting

Sixty-day-old shoots (Fig. 1a) were used as microcuttings (2.0 cm length) explants (Fig. 1b) for rooting. The microcuttings were inoculated into culture medium MS (Murashige e Skoog, 1962) (Phytotechnology Lab, Overland Park, KS, USA) with ¼ of salt and vitamins ($^1/_4$ MS), supplemented with 20 g L^{-1} sucrose (Synth; São Paulo, SP, Brazil) and 2 g L^{-1} Phytagel (Sigma-Aldrich; Saint Louis, MO, USA) (Fig. 1c).

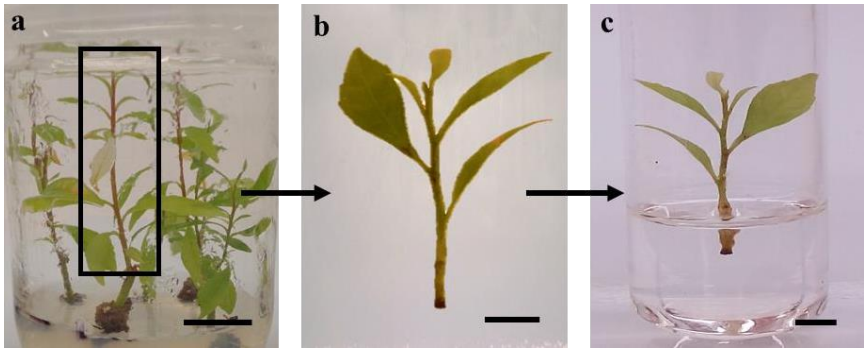

Fig. 1 Morphological aspects of sixty-day-old shoots of *C. legalis* developed *in vitro* (a) used for microcutting obtention (b), which were inoculated in culture medium for rooting (c). Bars = 0.5 cm.

Different concentrations (0, 50 and 100 µM) of IBA (Sigma-Aldrich) combined to different concentrations (0 and 30 µM) of PG (Sigma-Aldrich) were added into the culture medium to analyze the *in vitro* rooting. The pH of the culture medium was adjusted to 5.7 and distributed into culture tubes (10 mL per tube), followed by autoclaving for 15 min at 121 °C. Following inoculation, the microcuttings were incubated in a growth room with 16h of photoperiod and a light intensity of 45 µmol m^2 s^{1} from LED lamps with white, low blue and deep red spectra, at 25 ± 2 °C. The microcuttings were maintained in these conditions over 7 days for root induction. After, the microcuttings were transferred for a new $^1/_4$ MS culture medium supplemented with 20 g L^{-1} sucrose, 2 g L^{-1} Phytagel but without IBA or PG addition. After a total of 30 days of incubation, the root induction (%), number of roots per microcuttings and root length (cm) were analyzed. Six treatments were performed, each treatment consisted of eight replicates, and each replicate comprised five microcutting with a total of forty microcuttings per treatment.

For histomorphological and proteomic analysis, samples were compared among microcutting before incubation (0-day), microcutting in period of incubation in which IBA plus PG treatment induced rooting and microcutting of treatment without IBA plus PG (as a control). The sample was composed by base (0.5 cm) of microcuttings, where the root induction and formation occur. For proteomic analysis, samples (triplicate, 300 mg fresh matter each) were keep at -80 °C until the analysis being performed.

Statistical analysis

The experiment was performed using a completely randomized design. The data were submitted to analysis of variance (ANOVA) (P <0.05) followed by a Tukey test in program R core team (2018) (R Foundation for Statistical Computing, version 3.4.4, 2018, Vienna, Austria).

Histomorphological analysis

For the histomorphological analysis, the samples (0.5 cm of the base of microcutting) were fixed in fixative solution containing 2.5% gluteraldehyde (Sigma-Aldrich) and 4% formaldehyde (Sigma-Aldrich) in 0.1 M phosphate buffer (Sigma-Aldrich) pH ~ 7.2, at room temperature for 24 h. After, the samples were submitted to dehydration with increasing ethanolic series (30, 50, 70, 90 and 100%) twice, for 6 h each. Subsequently, the samples were infiltrated in 1:1 (v/v) Historesin® (Leica, Heidelberger, Germany) and 100% ethanol (Merck, Darmstadt, Germany) for 12 h, followed by 100% Historesin for 24 h and embed in 100% Historesin. Sections (5 µm) were obtained on a Leica microtome, mounted on slides (Sail Brand, Zhejiang, China) and then stained with 1% aqueous toluidine blue solution (Synth). The sections were observed in an AxioImager M2 microscope (Zeiss®, Jena, Germany), with AxioVision 4.8 program (Zeiss), and photographed with the aid of an AxioCam MR3 camera (Zeiss) coupled to the equipment.

Comparative proteomic analysis

Protein extraction and digestion

Protein extracts were prepared using biological triplicate (300 mg fresh matter each). Proteins were extracted using the trichloroacetic acid (TCA)/acetone precipitation method developed by Damerval et al. (1986), with modifications. Initially, the sample was frozen in liquid nitrogen and ground to a fine powder using a ceramic mortar and pestle. The resulting powder was resuspended in 1 mL of chilled extraction buffer containing 10% (w/v) TCA (Sigma Chemical Co., St. Louis, USA) in acetone with 20 mM dithiothreitol (DTT; GE Healthcare, Piscataway, NJ, USA) and vortexed for 5 min at 8 °C. Following, the samples were kept at −20 °C for 1 h before centrifugation

at 16,000 x *g* for 30 min at 4 °C. The resulting pellets were washed three times with cold acetone plus 20 mM DTT and centrifuged for 5 min each time. The pellets were air dried, and resuspended in buffer containing 7 M urea (GE Healthcare), 2 M thiourea (GE Healthcare), 2% Triton X-100 (GE Healthcare), 1% DTT, 1 mM phenylmethylsulfonyl fluoride (PMSF; Sigma-Aldrich), and complete protease inhibitor cocktail (Roche Diagnostics, Mannheim, Germany), being vortexed for 30 min at 8 °C, and centrifuged for 20 min at 16,000 x *g*. The supernatants were collected, and the protein concentrations were determined using 2-D Quant Kit (GE Healthcare).

Before the trypsin digestion step, protein samples were precipitated using the methanol/chloroform methodology to remove any interferent from samples (Nanjo et al., 2012). After protein precipitation, samples were resuspended in urea 7M/thiourea 2M solution for proper resuspension. Protein digestion was performed using the filter-aided sample preparation (FASP) methodology (Burrieza et al., 2019), with modifications. Before starting the digestion procedure, an integrity test was made to check for damaged filter units (Hernandez-Valladares et al., 2016), thus only the working units were used. After that, 100 µg of protein, from each sample, were added to the Microcon-30 kDa filter units (Millipore) (Lipecka et al., 2016), washed with 200 µL 50 mM ammonium bicarbonate and centrifuged at 12,000 x *g* for 15 min at 25 °C (otherwise stated, all centrifugation steps were performed at this condition). This step was repeated once for complete removal of urea before reduction of proteins. Next, 100 µL of 50 mM DTT freshly made in 50 mM ammonium bicarbonate were added, gently vortexed and incubated for 20 min at 60 °C (1 min agitation and 4 min stopped, 650 rpm). Then, 200 µL of 8 M Urea in 50 mM ammonium bicarbonate were added and centrifuged for 15 min. For protein alkylation, 100 µL of 50 mM iodoacetamide (GE Healthcare) freshly prepared in 8 M Urea in 50 mM ammonium bicarbonate were added, gently vortexed and incubated for 20 min at 25 °C in the dark (1 min agitation at 650 rpm and 19 min stopped). Next, 200 µL of 8 M urea in 50 mM ammonium bicarbonate were added and centrifuged for 15 min. This step was repeated once. Then, 200 µL of 50 mM ammonium bicarbonate were added and centrifuged for 15 min. This step was repeated twice. In the last washing, it should remain approximately 50 µL of sample. For protein digestion, 25 µL of 0.2% (v/v) RapiGest (Waters, Milford, CT, USA) and 20 µL of trypsin solution (50 $ng.\mu L^{-1}$, V5111, Promega, Madison, WI,

USA) were added, gently vortexed and incubated for 16 h at 37 °C (1 min agitation at 650 rpm and 4 min stopped). For peptide elution, the filter units were transferred for new microtubes and centrifuged for 10 min at 12,000 x *g*. Then, 50 µL of 50 mM ammonium bicarbonate were added and centrifuged for 15 min at 12,000 x *g*. This step was repeated once. For RapiGest precipitation and trypsin inhibition, 5 µL of 15% trifluoroacetic acid (TFA, Sigma-Aldrich) were added, gently vortexed and incubated for 30 min at 37 °C. Then, samples were centrifuged for 15 min, the supernatants collected and vacuum dried. Peptides were resuspended in 100 µL solution of 95% 50 mM ammonium bicarbonate in 5% acetonitrile and 0.1% formic acid.

Mass spectrometry analysis

Mass spectrometry was performed using a nanoAcquity UPLC connected to a Q-TOF SYNAPT G2-Si instrument (Waters, Manchester, UK). For proper sample normalization, an MSE scouting run approach was used, which consisted of previous MSE runs processed based on the summed intensities of TOP3 matched peptides of all identified proteins for each run. Thus, stoichiometrically injections were performed for HDMSE analysis. Runs consisted of three biological replicates of 1 µg of peptide samples. During separation, samples were loaded onto the nanoAcquity UPLC M-Class Symmetry C18 5 µm trap column (180 µm × 20 mm) at 5 $\mu L.min^{-1}$ during 3 min and then onto the nanoAcquity M-Class HSS T3 1.8 µm analytical reversed phase column (75 µm × 150 mm) at 400 $nL.min^{-1}$, with a column temperature of 45 °C. For peptide elution, a binary gradient was used, with mobile phase A consisting of water (Tedia, Fairfield, Ohio, USA) and 0.1% formic acid (Sigma-Aldrich) and mobile phase B consisting of acetonitrile (SigmaAldrich) and 0.1% formic acid. Gradient elution started at 5% B, then ramped from 5 B to 40% B up to 91.12 min, and from 40 B to 99% B until 95.12 min, being maintained at 99% until 99.12 min, then decreasing to 5% B until 101.12 min and kept 5% B until the end of experiment at 117.00 min. The instrument settings were based on that described by Distler et al. (2016) for IMS-enhanced data-independent acquisition (DIA). Briefly, mass spectrometry was performed in positive and resolution mode (V mode), 35,000 FWHM, with ion mobility, and in DIA mode; ion mobility separation (HDMSE) used an IMS wave velocity ramp starting with 800 m/s and ending with 500 m/s, helium and IMS gas flow of 180 and 90

mL.min^{-1}, respectively; the transfer collision energy ramped from 25 V to 55 V in high-energy mode; cone and capillary voltages of 30 V and 3000 V, respectively; nano flow gas of 0.5 Bar and purge gas of 150 L.h^{-1}; and a source temperature of 100 °C. In TOF parameters, the scan time was set to 0.6 s in continuum mode with a mass range of 50 to 2000 Da. The human [Glu1]-fibrinopeptide B (Sigma-Aldrich) at 100 fmol.µL^{-1} was used as an external calibrant and lock mass acquisition was performed every 30 s. Mass spectra acquisition was performed by MassLynx v4.0 software.

Bioinformatics

Spectra processing and database search conditions were performed using ProteinLynx Global SERVER (PLGS) software v.3.02 (Waters). The HDMSE analysis utilized the following parameters: Apex3D of 150 counts for low-energy threshold, 50 counts for elevated-energy threshold, and 750 counts for intensity threshold; one missed cleavage; minimum fragment ions per peptide equal to three; minimum fragment ions per protein equal to seven; minimum peptides per protein equal to two; fixed modifications of carbamidomethyl (C) and variable modifications of oxidation (M) and phosphoryl (STY); default false discovery rate (FDR) of 1%; automatic peptide and fragment tolerance. For protein identification, we used the *Helianthus annuus* protein databank (ID: UP000215914), which was selected based on the PhyloT phylogenetic tree proximity (Letunic e Bork, 2016) generated from all plant species (http://itol.embl.de), being the database available at UniProtKB (www.uniprot.org). Label-free quantification analyses were performed using ISOQuant software v.1.7 (Distler et al., 2014). Briefly, the following parameters were used: peptide and protein FDR 1%, sequence length of at least six amino acid residues, and minimum peptide score equal six. Samples were normalized by a multidimensional normalization process, which corrects peak intensities based on the intensity and retention time domains. The software performed the relative protein quantification based on the TOP3 method. Based on relative abundances of uniquely assigned peptides, the abundances of shared peptides were redistributed to the respective source proteins, followed by the TOP3-based quantification (Distler et al., 2014). To ensure the quality of the results after data processing, only proteins present in the three runs were accepted for differential abundance analysis. Proteins with ANOVA ($P< 0.05$) were deemed up-

regulated if the $\log_2$ value of the fold change (FC) was greater than 0.60 and down-regulated if the $\log_2$ value of the FC was less than − 0.60. Functional annotations were performed using OmicsBox software 1.0.34 and UniProtKB (http://www.unipr ot.org).

RESULTS

Effect of IBA and PG on microcutting rooting

The treatments supplemented with 50 and 100 µM IBA affected significantly the roots induction comparatively to control treatment and to treatment only with PG. The IBA concentrations, combined or not with PG, did not differ statistically from each other (Fig. 2a). The use of IBA was necessary to root induction in *C. legalis* and the treatments without IBA had few or none roots induction.

For the number of roots, the treatment 50 µM IBA plus 30 µM PG showed the best results, not differing significantly from 50 µM IBA and 100 µM IBA plus 30 µM PG (Fig. 2b).

In addition, for root length, the concentrations 50 µM IBA combined or not with 30 µM PG showed the best results, being statistically higher than the other treatments (Fig. 2c).

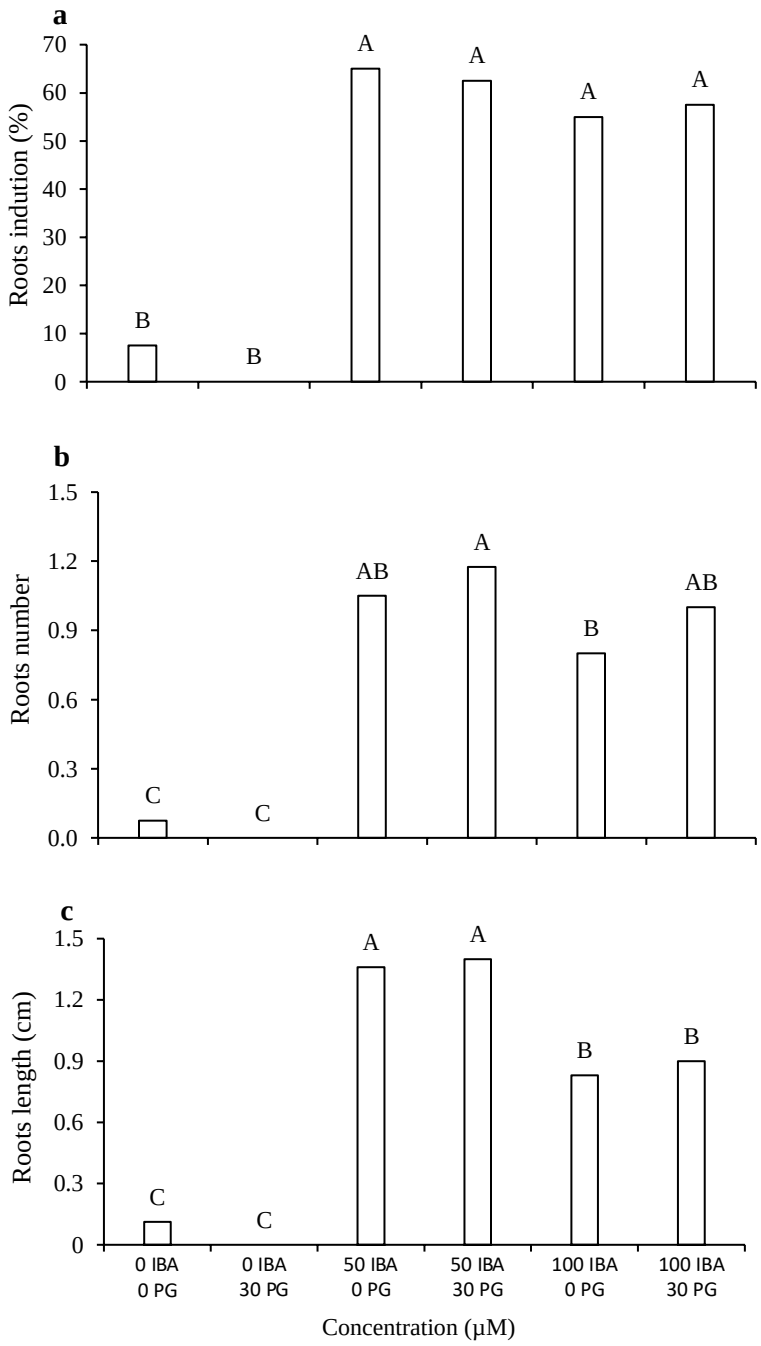

Fig. 2 Root induction (a), number (b) and length of roots (c) in microcuttings from cotyledonary nodal explants of *C. legalis* after 7 days of incubation in different concentrations of indole-3-butyric acid (IBA; 0, 50 and 100 µM) and phloroglucinol (PG; 0 and 30 µM), following the incubation in $^{1}/_{4}$MS culture medium without IBA and PG, in a total of 30 days *in vitro* incubation. Means followed by the same letter do not differ statistically between them, according to Tukey test ($P < 0.05$). CV: coefficient of variation. (n = 40, CV root induction = 22.58%; CV root number = 25.47%; CV root length = 15.93%).

In all treatments it was observed the callus formation at the basis of the microcuttings, including in those incubated without IBA (Fig. 3). In addition, all microcuttings with root formation showed also the callus formation. The development of callus at the base of microcuttings was visible from 7th days after incubation.

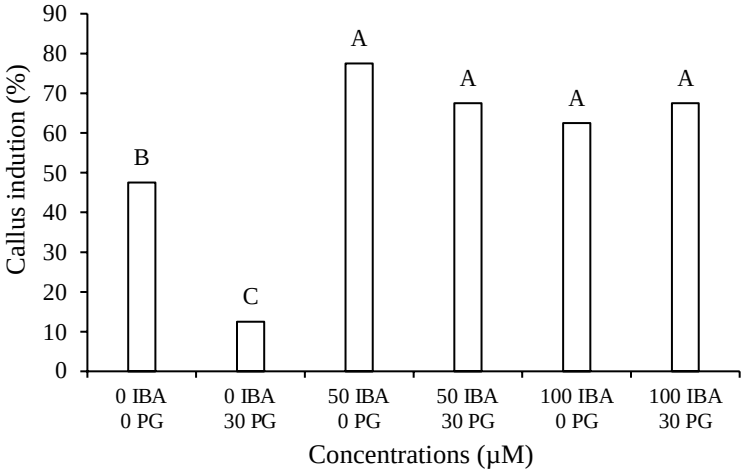

Fig. 3 Callus formation (%) at the base of microcutting from cotyledonary nodal explants of *C. legalis* after 7 days of incubation in different concentrations of indole-3-butyric acid (IBA; 0, 50 and 100 µM) and phloroglucinol (PG; 0 and 30 µM), following of incubation in $^{1}/_{4}$MS culture medium without IBA and PG, totaling 30 days *in vitro*. Means followed by the same letter do not differ statistically between them, according to Tukey test ($P < 0.05$). CV: coefficient of variation. (n = 40, CV = 26.29%).

30 days after treatment, the rooted microcuttings showed well-developed roots, highlighting the response in the treatment with 50 µM IBA plus 30 µM PG, while in the control treatment without IBA and PG, there was no roots development (Fig. 4).

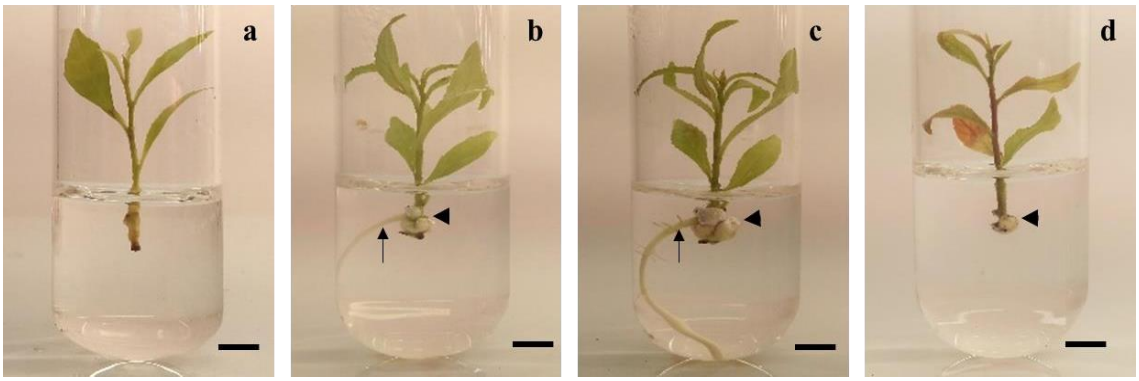

Fig. 4 Morphological aspects of the *in vitro* rooting of *C. legalis,* showing microcutting treated during 7 days with 50 µM IBA plus 30 µM PG, following of incubation in $^{1}/_{4}$ MS culture medium without IBA and PG at 1th-day (a), 18th-days (b) and 30th-days (c). Microcutting of control treatment incubated in ¼ MS culture medium without IBA and PG at 30th-days (d). The arrows indicate roots formation. The arrow-head indicated the callus formation at the base of explant. Bars = 0.5 cm.

Histomorphological analysis of microcuttings

The microcuttings before the incubation (0-days) (Fig. 5a-b) and at 12-days non-treated (without IBA and PG) (Figs. 5c-d) showed no organization to root formation. On the other hand, 12-days treated microcuttings with 50 µM IBA plus 30 µM PG showed the progression of adventitious root induction and development (Fig. 6).

The microcutting before the incubation *in vitro* (0-day) presented a large area of medullary cells, well developed vascular bundles and some layers of parenchyma cells (Figs. 5a-b). At 12-days incubation, the non-treated (without IBA and PG) microcuttings showed the presence of dividing cells, with dense cytoplasm and large nucleus originated from cells closed to the vascular bundles, in the region of the vascular cambium (Figs. 5c-d). These cells in division led to the formation of a callus containing undifferentiated cells, without meristematic characteristics, therefore, without the ability to form roots.

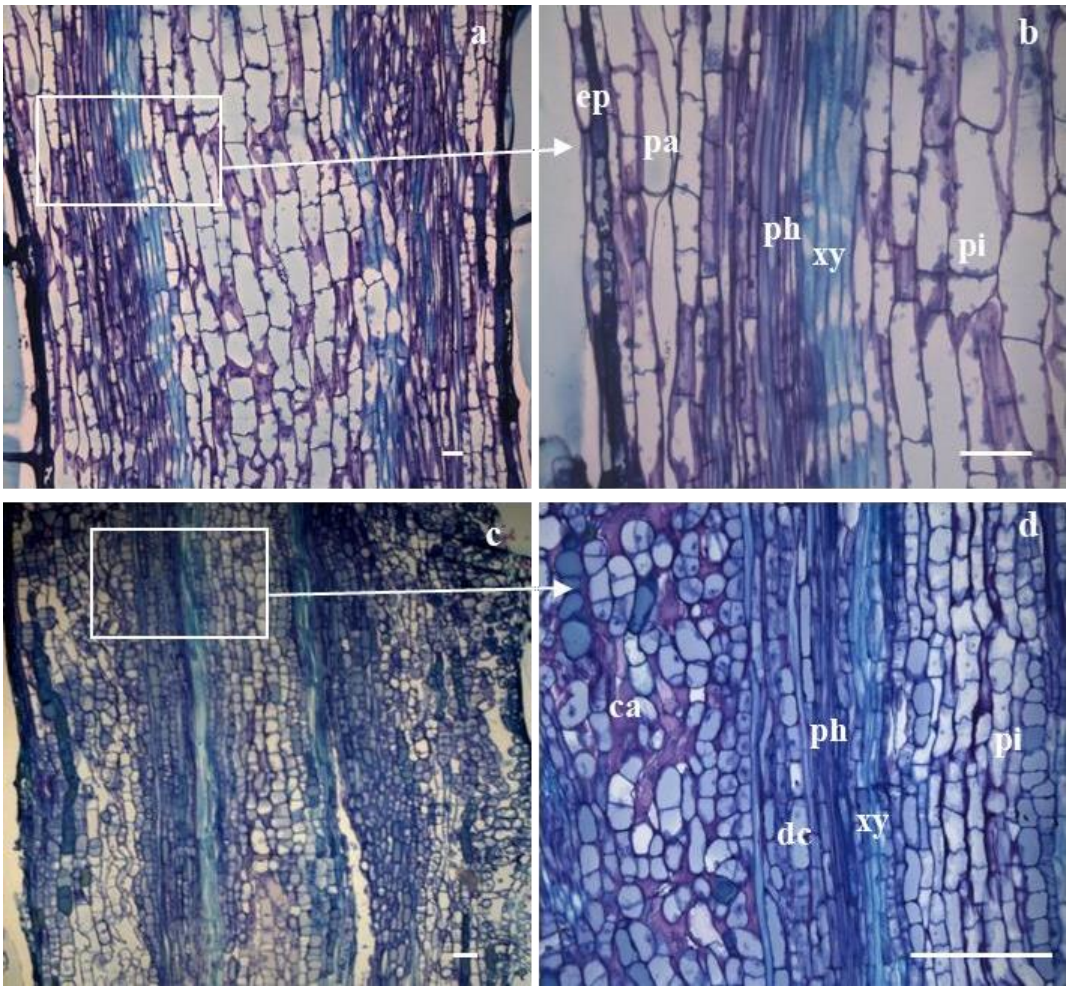

Fig. 5 Histomorphological aspects (longitudinal sections) from the base of *C. legalis* in microcuttings before incubation (0-day) (a-b) and after 12-days incubation without IBA and PG (c-d). The sections were stained with Toluidine Blue 1%. ep = epidermis, pa = parenchyma, ph = phloem, xy = xylem, pi = pith, ca = callus, dc = division cells. Bars = 100 µm.

Microcuttings 12-days treated with 50 µM IBA plus 30 µM PG presented dividing cells, which followed to callus formation. From the callus, it was observed the formation of root meristems (Fig. 6a) and root primordia development (Fig. 6b). At 15th day after incubation in rooting culture medium, the induced adventitious roots were already emerged from the base of microcutting through the callus and were visible in culture medium (Fig. 6c). The 12-days non-treated microcuttings showed callus formation, but it does not occur the formation of root primordia (Fig. 6d).

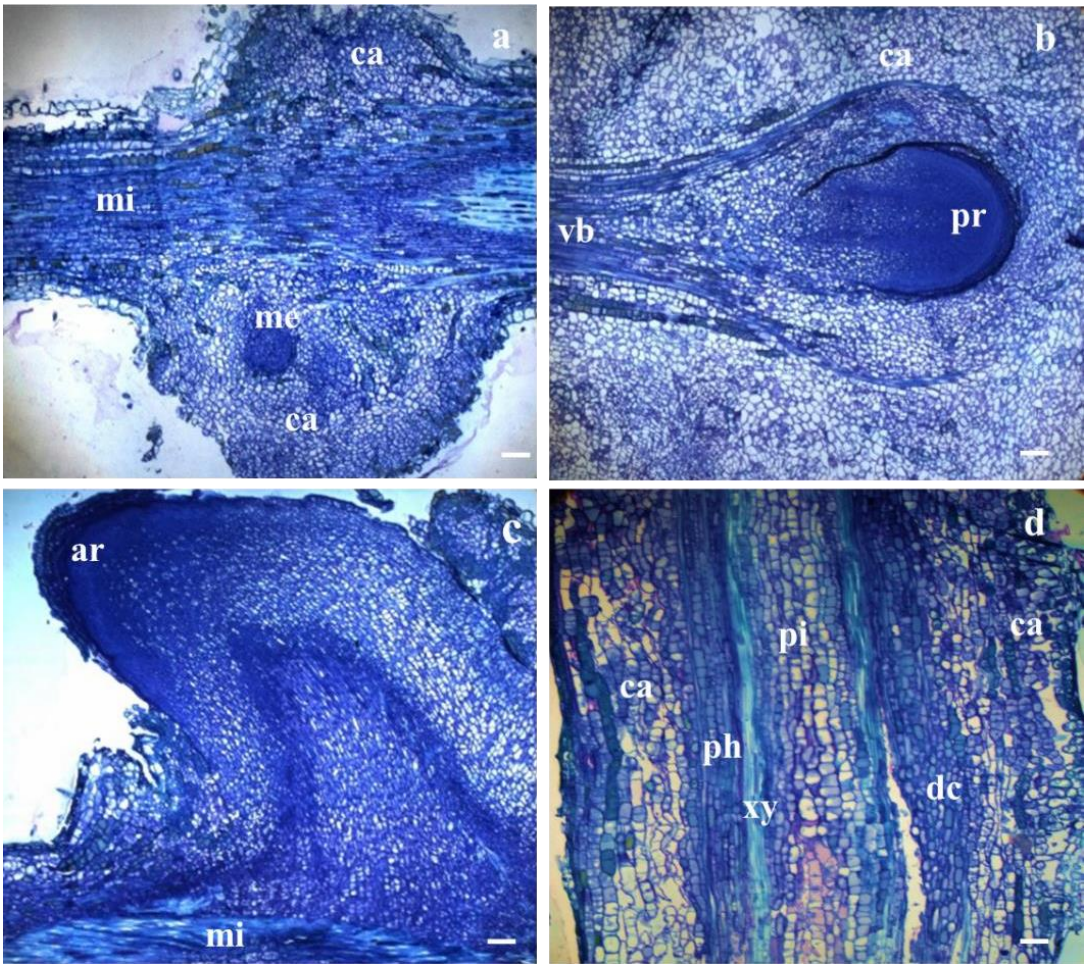

Fig. 6 Histomorphological aspects (longitudinal sections) from the base of *C. legalis* microcuttings 12-days treated with 50 µM IBA plus 30 µM PG, showing a group of meristematic-type cells which will allows the development the root primordia (a); the root primordia formation (b); 12-days treated microcuttings with the root emergence through the callus (c) and 12-days non-treated microcuttings without root formation (d). me = root meristem, ca = callus, mi = microcutting, vb = vascular bundle, pr = root primordia, ar = adventitious root, ph = phloem, xy = xylem, pi = pith, dc = division cells; Bars = 200 µm.

Effects of IBA and PG on proteomic profile

The proteomic analysis was performed using the bases of microcuttings before incubation (0-day microcuttings), treated microcutting with 50 µM IBA plus 30 µM PG at 12-day (when root primordia were observed) and non-treated microcuttings at 12-days which had no roots. Two different comparisons were performed: 12-days

treated/12-days non-treated microcuttings; and 12-days treated/0-day (initial time) microcuttings.

A total of 334 proteins were identified in this analysis, in the comparison 12-day treated/12-day non-treated microcuttings 120 proteins were regulated and 214 unchanged. Among the 120 regulated proteins, 41 were up- and 64 were down-regulated. Still, 6 proteins were unique in 12-days treated microcuttings, and 9 were unique in 12-days non-treated (Supplementary table 1). In the comparison 12-days treated/0-day microcuttings, 210 proteins were regulated and 121 unchanged. Among the 210 regulated proteins, 121 were up- and 76 were down-regulated, 7 proteins were unique in 12-days treated microcuttings and 6 were unique in 0-day microcutting (Supplementary table 1).

The identified proteins were classified according to their biologic processes into several groups, such as: photosynthesis, nucleobase-containing compound metabolic process, cellular component organization, translation signal, protein folding / homeostasis cellular, carbohydrate metabolic process, generation of precursor metabolites and energy, secondary metabolic process, amino-acid metabolic process, protein metabolic process, stress response and the group others composed of transporter, lipid metabolic process and nitrogen compound metabolic process (Figs. 7a-b).

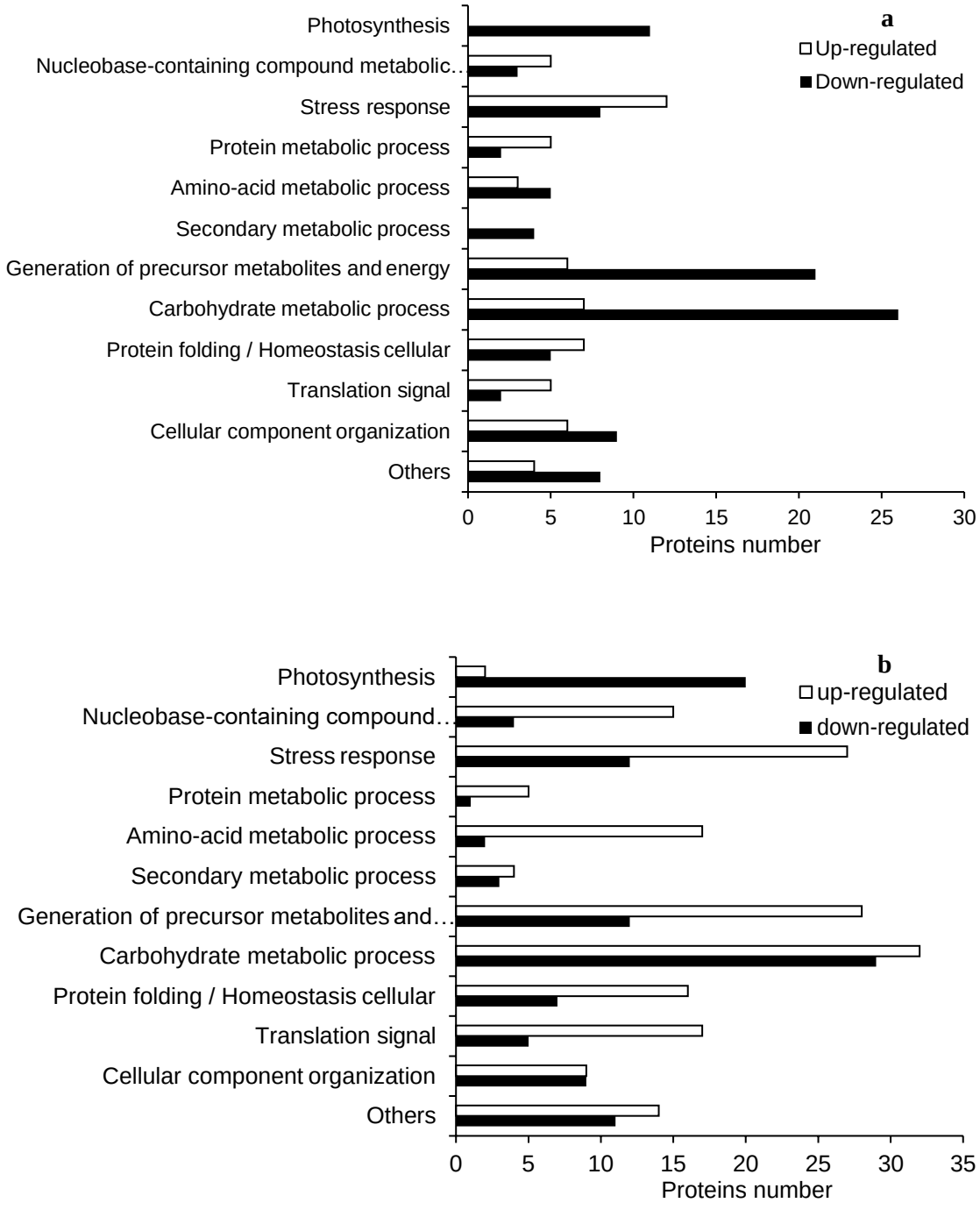

Fig. 7 Number of protein according to the biological process of differentially regulated proteins identified in *C. legalis* microcuttings in the comparisons 12-days treated/12-days non-treated microcuttings (a) and in the comparison 12-days treated/0-day microcuttings (b).

Among the regulated proteins, some of them were highlighted according their involvement to root induction and development processes (Table 1).

From the highlighted proteins, some were identified in the group of stress response. The glutamate-cysteine ligase (A0A251RL14) protein was up-regulated in both comparisons, being the accumulation higher in the 12-days treated microcutting compared to 12-days non-treated and 0-day microcutting (Table1). In addition, the time of incubation induced the accumulation of nine heat shock proteins (HSPs) (A0A251UN61, A0A251TI04, A0A251UZB2, A0A251U6R5, A0A251TNS0, A0A251VHZ2, A0A251SKI7, and A0A251UM84), which were up-regulated and one (A0A251S3K3) was unique in 12-days treated/0-day microcuttings comparison. The peroxidase (A0A251TG61 and A0A251U4X4) and catalase (A0A251U688) proteins were up-regulated in 12-days treated/12-days non-treated comparison, being the accumulation higher in the 12-days treated microcutting (Table 1).

The 10 kDa chaperonin (A0A251U2Z0), belonging to the group of protein folding/homeostasis cellular, was up-regulated in the two comparison, being the higher accumulation induced by IBA plus PG treatment and time of incubation (Table 1).

Proteins from the group of translation signal were identified, being the eukaryotic translation initiation factor (A0A251RNJ4) and ribosomal protein S28e (A0A251TVC8) up-regulated in the comparison 12-days treated/12-days non-treated microcuttings. The leucine aminopeptidase (A0A251V5D0), from protein metabolic process, was up-regulated in 12-days treated/0-day microcutting comparison and unique in 12-day treated microcutting (Table 1).

In the generation of precursor metabolites and energy groups, the citrate synthase (A0A251VRK6 and A0A251T189), ATP-citrate synthase beta chain protein 1 (A0A251SQ34), succinate dehydrogenase [ubiquinone] flavoprotein subunit (A0A251TWM3 and A0A251S412) and cysteine synthase (A0A251RZ67 and A0A251TIT5) proteins were up-regulated in 12-days treated/0-day microcuttings comparison (Table 1).

In amino-acid metabolic process, aconitate hydratase (A0A251UMF and A0A251VA91) were up-regulated in the two comparison, being the accumulation higher in the 12-days treated microcutting. The serine hydroxymethyltransferase

(A0A251SFI7) was up-regulated in the 12-days treated/0-day microcuttings comparison (Table 1).

In group of the carbohydrate metabolic process, the proteins starch synthase (A0A251V0T5) and fructokinase-6 (A0A251SGT6) were down-regulated in two comparison, while the proteins pyruvate kinase (A0A251TDM5, A0A251TJC8 and A0A251SC35), malate dehydrogenase (A0A251SX18, A0A251TLI1 and A0A251VCJ8) and glyceraldehyde-3-phosphate dehydrogenase (A0A251RMC4, A0A251RUY3 and A0A251T816) were up-regulated in 12-days treated/0-day microcuttings comparison (Table 1).

Among the proteins identified in the photosynthetic process are the oxygen-evolving enhancer protein (P85189, A0A251TE28 and P85194), chlorophyll a-b binding protein (A0A251S8L8 and A0A251V9V2) and ribulose bisphosphate carboxylase large chain (P45738), which were down-regulated in the microcuttings from the two comparison (Table 1).

In addition, in the secondary metabolic process, the phenylalanine ammonia-lyase (A0A251TUG3), caffeoyl-CoA O-methyltransferase (A0A251TLQ4) and chalcone synthase (B5KUB7 and A0A0S1M144) proteins were down-regulated in 12-days treated/12-days non-treated microcuttings comparison (Table 1).

Table 1 Differentially regulated proteins identified highlighted in microcuttings of *C. legalis* in the comparisons 12-days treated/12-days non-treated and 12-days treated/0-day (initial time) microcuttings.

Accession	Reported Peptide	Description	Biological Process	Comparison 12-days treated/12-days non-treated[a]	Comparison 12-days treated/0-day initial time[a]
A0A251TG61	5	Peroxidase	Response to stress	Up	Up
A0A251U4X4	3	Peroxidase	Response to stress	Up	-
A0A251U688	3	Catalase	Response to stress	Up	-
A0A251UN61	11	Heat shock 70 kDa protein	Response to stress; Protein folding	Down	Up
A0A251TI04	11	Heat shock protein 70 family	Response to stress; Protein folding	-	Up

Table 1 (continued)

A0A251UZB2	32	Heat shock protein 70 family	Response to stress; Protein folding	-	Up
A0A251U6R5	7	Heat shock protein Hsp90 family	Response to stress; Protein folding	-	Up
A0A251TNS0	3	Heat shock protein 70 family	Response to stress; Protein folding	-	Up
A0A251VHZ2	37	Heat shock protein 70 family	Response to stress; Protein folding	Up	Up
A0A251SKI7	4	Heat shock protein 70 family	Response to stress; Protein folding	Up	Up
A0A251UM84	3	Heat shock protein 70 family	Response to stress; Protein folding	Up	Up
A0A251S3K3	7	Heat shock protein Hsp90 family	Response to stress; Protein folding	Up	Unique 12-day-IBA
A0A251RL14	5	Glutamate--cysteine ligase protein	Plant defense; Response to stress	Up	Up
A0A251U2Z0	4	10 kDa chaperonin, mitochondrial-like	Cellular process; Protein folding	Up	Up
A0A251TVC8	4	Ribosomal protein S28e	Translation	Up	-
A0A251RNJ4	4	Eukaryotic translation initiation factor 5A	Translation; cellular component organization	Up	-
A0A251V5D0	3	Leucine aminopeptidase 2	Protein metabolic process	Unique 12-day-IBA	Up
A0A251TUG3	6	Phenylalanine ammonia-lyase	Secondary metabolic process	Down	Down
A0A251TLQ4	5	Caffeoyl-CoA O-methyltransferase	Secondary metabolic process; lignin biosynthesis	Down	Down
B5KUB7	6	Chalcone synthase	Secondary metabolic process; Flavonoid biosynthesis	Down	-
A0A0S1M144	7	Chalcone synthase	Secondary metabolic process; Flavonoid biosynthesis	Down	-

Table 1 (continued)

A0A251TDM5	20	Pyruvate kinase	Carbohydrate metabolic process; generation of precursor metabolites and energy	-	Up
A0A251TJC8	8	Pyruvate kinase	Carbohydrate metabolic process; generation of precursor metabolites and energy	-	Up
A0A251SC35	4	Pyruvate kinase	Carbohydrate metabolic process; generation of precursor metabolites and energy	-	Up
A0A251SX18	19	Malate dehydrogenase	Carbohydrate metabolic process; generation of precursor metabolites and energy	-	Up
A0A251TLI1	9	Malate dehydrogenase	Carbohydrate metabolic process; generation of precursor metabolites and energy	-	Up
A0A251VCJ8	19	Malate dehydrogenase	Carbohydrate metabolic process; generation of precursor metabolites and energy	-	Up
A0A251RMC4	23	Glyceraldehyde-3-phosphate dehydrogenase	Carbohydrate metabolic process; generation of precursor metabolites and energy	-	Up
A0A251RUY3	19	Glyceraldehyde-3-phosphate dehydrogenase	Carbohydrate metabolic process; generation of precursor metabolites and energy	-	Up
A0A251T816	4	Glyceraldehyde-3-phosphate dehydrogenase	Carbohydrate metabolic process; generation of precursor metabolites and energy	-	Up
A0A251VRK6	5	Citrate synthase	Generation of precursor metabolites and energy; tricarboxylic acid cycle	Down	Up
A0A251SQ34	15	ATP-citrate synthase beta chain protein 1	Generation of precursor metabolites and energy; tricarboxylic acid cycle	-	Up
A0A251T189	5	Citrate synthase	Generation of precursor metabolites and energy; tricarboxylic acid cycle	Up	Up
A0A251TWM3	11	Succinate dehydrogenase	Generation of precursor metabolites and energy	-	Up
A0A251S412	9	Succinate dehydrogenase	Generation of precursor metabolites and energy	Up	Up
A0A251TIT5	13	Cysteine synthase	Generation of precursor metabolites and energy	Down	Up
A0A251RZ67	9	Cysteine synthase	Generation of precursor metabolites and energy	-	Up

Table 1 (continued)

A0A251VA91	6	Aconitate hydratase, cytoplasmic	Amino-acid metabolic process; tricarboxylic acid cycle	Up	Up
A0A251UMF5	15	Aconitate hydratase, cytoplasmic	Amino-acid metabolic process; tricarboxylic acid cycle	Up	Up
A0A251SFI7	9	Serine hydroxymethyltransferase	Amino-acid metabolic process	-	Up
A0A251V0T5	3	Starch synthase, chloroplastic/amyloplastic	Carbohydrate metabolic process	Down	Down
A0A251SGT6	2	Fructokinase-6, chloroplastic	Carbohydrate metabolic process; lipid metabolic process	Down	Down
P45738	21	Ribulose bisphosphate carboxylase large chain	Carbohydrate metabolic process; photosynthesis	Down	Down
P85189	4	Oxygen-evolving enhancer protein 2, chloroplastic	Photosynthesis	Down	Down
A0A251TE28	3	Oxygen-evolving enhancer protein 3-2, chloroplastic-like	Photosynthesis	Down	Down
P85194	6	Oxygen-evolving enhancer protein 1, chloroplastic	Photosynthesis	Down	Down
A0A251S8L8	12	Chlorophyll a-b binding protein, chloroplastic	Photosynthesis	Down	Down
A0A251V9V2	11	Chlorophyll a-b binding protein, chloroplastic	Photosynthesis	Down	Down

[a]Proteins were deemed up-regulated if the $\log_2$ value of the fold change (FC) was greater than 0.60 and deemed down-regulated if the $\log_2$ value of the FC was less than -0.60, as determined by Student's T-Test (two-tailed; $P< 0.05$).

DISCUSSION

The use of auxins to promote adventitious roots have been reported as necessary for the *in vitro* propagation of some tree species (De Klerk et al., 1999; Dias et al., 2012). In this work, the results showed that the use of IBA auxin is necessary for root formation (Fig. 2a) during the *in vitro* propagation of *C. legalis*. Auxins has been

considered effective substances in the rooting process, able to start *de novo* organogenesis stimulating initial cell division and acquisition of cell regeneration competency (Sang et al., 2018). Among the auxins, IBA shows better results due to its higher stability in solution and in the tissue, increasing rooting promotion by maintaining its high level for longer than the indole-3-acetic acid (IAA) (Epstein e Ludwig-Müller, 1993; Dewir et al., 2016).

In *in vitro* culture, the exogenous concentration of growth regulators is very important and a dose-dependent experiment is necessary to observe the optimal concentration. For the *C. legalis* species, which show a difficulty for rooting the microcuttings, presenting a recalcitrant response to root formation, the IBA concentrations above 250 µM inhibited root formation (Aragão et al., 2017). In this sense, our results showed that the use of 50 and 100 µM IBA was effective to induce up to 60% of rooting (Fig 2a), which can be considered a positive result for the *C. legalis*.

The auxins added into culture medium may be easily degraded from time of exposition at light,decreasing their period of activity (Drew et al., 1991). PG have been proposed to protect auxins from oxidation in a synergic action, increasing the time of auxin activity and its effect on root induction phase (De Klerk et al., 2011; da Silva et al., 2013). Besides this effect, PG has been seen to act as a root growth promoter (da Silva et al., 2013). The positive effect of PG and IBA was seen in the rooting of *Pterocarpus marsupium*, enhancing the number and length of root (Husain et al., 2008), as well as, in *Carica papaya*, resulting in the best induction, number and length root (Pérez et al., 2016). In our work, the increase in the roots number in the treatments which PG was added with IBA was not statistically significant compared to the other and PG did not influence root induction. In this sense, perhaps other concentrations of PG combined with 50 or 100 of IBA could give a significantly result for the number of roots in *C. legalis*.

Usually, in adventitious rooting, the cells that give rise to root primordia are close to vascular bundles, cambium and procambium cells (Zhou et al., 1992; Liu et al., 2014). Our results showed that in *C. legalis* microcutting tissues, the cells close to the xylem and phloem divided continuously giving rise to callus. From this callus, there was a cellular reorganization and acquisition of competence for formation of *de novo* root

apical meristem, by the establishment of meristems, primordia and then the root development (Fig. 6). This observation can characterize the *in vitro* rooting of *C. legalis* as indirect pattern, i.e., the formation of a callus occurs prior to differentiation of meristems and root primordia, similarly to observed by Altamura (1996) for herbaceous and woody explants.

The tissue organization, as well the time of adventitious roots formation in *C. legalis,* has different pattern of some others species, as *Cedrela odorata*. In *C. odorata* species, the roots began to emerge from the 6th day of incubation with or without IBA, with cell division occurring from to cambial zone and without the callus formation, being considered an easy-rooting species (Millán-Orozco et al., 2011). Besides that, in apple rootstocks variety M26, adventitious rooting was accelerated after treatment with IAA, and the roots were initiated from the cambium cells, which emerged at the surface of stem bases 10 days after treatment. However, for apple rootstocks variety EMLA 9 also treated with IAA, occurs callus formation which delay the root development, and the root emergence was observed after 21 days of the treatment (Zhou et al., 1992). One of the key factors responsible for these differences between species and between varieties, may be the endogenous level and the capacity of basipetally transported auxins from the shoot apex at the cutting base, probably higher in species of easy rooting (Blakesley et al., 1991; Da Costa et al., 2013). Therefore, the time for root development and low induction of roots in *C. legalis* microcuttings and the necessity of IBA supplementation, suggests that this species has difficulties to induce the rooting.

The callus formation at the base of microcuttings is a negative response affecting root formation and can occurs due to IBA use. In addition, wounding at the base of the microcutting, necessary to separate it from the origin explant, can act as a trigger for callus formation (Iwase et al., 2017). In our results, the callus was seen in the microcuttings with or without IBA treatment (Fig. 3), suggesting that the callus formation before root induction becomes paramount for the *in vitro* root development of *C. legalis*, compared to others species easy-to-root, which usually do not produce callus during rooting. Therefore, from our results, IBA was essential for adventitious rooting compared to non-treated microcuttings.

In addition, significant alterations on proteomic analysis were also observed (Fig. 7a-b). Among the identified proteins, peroxidases isoforms (A0A251TG61 and

A0A251U4X4) were found in the two comparisons (Table 1) being up-regulated in 12-days IBA+PG-treated microcuttings compared to 12-day non-treated comparison (Table 1). The peroxidases are seen as a marker of the rooting (Correa et al., 2012). This enzyme have catalytic activity on diverse organic compounds, including oxidation IAA *in vitro*, in order to regulate the cell auxin homeostasis (Zhang et al., 2014). In cell, IBA exogenous is easily converted to IAA, and in the root initiation phase, when meristem and primordia are formed, auxin is no more a key factor for root development, so an increase in peroxidase activity occurs, in order to catabolize the accumulated auxin, which may be inhibitory to root development (Da Costa et al., 2013). This can explain the up regulation of peroxidases in the microcuttings 12-days treated with IBA plus PG, when the formation of the meristems and primordia root occurred in the basis of *C. legalis* microcuttings.

Moreover, the peroxidases also are important antioxidant enzymes related to stress responses, such as wounding (Hiraga et al., 2001) and reactive oxygen species (ROS) (Zhang e Peer, 2017). In addition, the catalase (A0A251U688), which is one type of peroxidase enzyme (Hiraga et al., 2001) and glutamate-cysteine ligase (A0A251RL14) present a similar function to peroxidases as antioxidant enzymes (Zhang e Peer, 2017) and were up-regulated in the IBA+PG-treated microcuttings compared to non-treated (Table 1). A 10 kDa chaperonin (A0A251U2Z0) proteins, which is well known for their role in maintaining cellular homeostasis (Saibil, 2013), was up-regulated in 12-days treated compared to 12-days non-treated microcuttings (Table 1). In this context, different isoforms of HSPs were up-regulated in 12-days treated compared to 12-day non-treated microcuttings (four isoforms) and in 12-days treated compared to 0-day microcuttings (eight isoforms) (Table 1). The HSPs are expressed in response to environmental stress conditions such as heat, but also may increase its activity with the accumulation of toxic compounds in cells, as ROS, in order to ensure maintenance of cellular homeostasis (Timperio et al., 2008). In this context, the IAA catabolism may increase the ROS production resulting in an increase in the levels of proteins related to oxidative stress response (Zhang e Peer, 2017). Therefore, during rooting initiation phase, the auxin catabolism may have led to higher accumulation of these proteins of stress response and cell homeostasis in the microcuttings treated with IBA plus PG in *C. legalis*.

In addition, proteins of the translation signal group, such as the eukaryotic translation initiation factor (A0A251RNJ4) and ribosomal protein S28e (A0A251TVC8) were more accumulated in 12-days treated microcuttings compared to 12-days non-treated (Table 1). These proteins are related to protein metabolism (Heringer et al., 2017; Heringer et al., 2018), indicating that during the adventitious rooting the cells experience an increase in the protein synthesis, as already suggested for Ahkami et al. (2009). In addition, the leucine aminopeptidase (A0A251V5D0), unique in 12-days treated with IBA+ PG compared to 12-days non-treated microcuttings (Table 1), is thought to be involved in the regulation of protein in plants and they can be up-regulated by wounding. In this context, these proteins may hydrolyze proteins in order to supply amino acids for protein synthesis associated with wounding (Chao et al., 1999).

Moreover, some secondary compounds can also be induced by stress conditions, as the lignin (Vanholme et al., 2010). Lignin are polymers deposited in cell wall making them rigid and impervious, and its biosynthesis can occur in response to wounding (Rogers e Campbell, 2004).The phenylpropanoid pathway is the via involved in lignin synthesis and, in our analysis, some proteins of this route were down-regulated in 12-day treated compared to 12-days non-treated microcuttings. Among the down-regulated proteins there are the enzyme phenylalanine ammonia-lyase (A0A251TUG3), that catalyzes the first reaction in the phenylpropanoid pathway (MacDonald e D'Cunha, 2007), and caffeoyl-CoA O-methyltransferase 1 enzyme (A0A251TLQ4), which participate of guaiacyl lignin monomers biosynthesis (Do et al., 2007). Therefore, with the higher accumulation of these proteins in 12–days non-treated with IBA + PG, may there has been an investment in cell wall strengthening in the cells of microcutting, resulting in no root induction.The chalcone synthase (B5KUB7 and A0A0S1M144), down-regulated in the 12-days treated compared to 12-days non-treated microcuttings (Table 1), is another protein from the phenylpropanoid pathway, which plays a key role in the biosynthesis of flavonoids, such as quercetin and kaempferol (Buer et al., 2010).These compounds have been shown to inhibit polar auxin transport by affect the distribution of PIN proteins (Peer et al., 2004; Santelia et al., 2008) and to enhance the localized auxin accumulation in plants (Brown et al., 2001; Peer e Murphy, 2007). Then, chalcone synthase seems to be one of key enzyme to explain the difficulty of rooting in microcuttings without IBA and PG addition. In this

sense, a possible higher content of flavonoids in the non-treated microcuttings, due the higher abundance of the chalcone synthase enzyme, may mean less auxin transport to the base of the microcuttings, limiting *in vitro* root induction of *C. legalis*.

Moreover, in the 12-days treated/0-days microcuttings comparison, isoforms of pyruvate kinase (A0A251TDM5, A0A251TJC8 and A0A251SC35), Glyceraldehyde-3-phosphate dehydrogenase (A0A251RMC4, A0A251RUY3 and A0A251T816), citrate synthase (A0A251VRK6, A0A251SQ34 and A0A251T189), malate dehydrogenase (A0A251SX18,A0A251TLI1 and A0A251VCJ8), succinate dehydrogenase (A0A251TWM3 and A0A251S412), cysteine synthase (A0A251TIT5 and A0A251RZ67), aconitate hydratase (A0A251VA91 andA0A251UMF5) and serine hydroxymethyltransferase (A0A251SFI7) were up-regulated (Table 1). These proteins are either part of the glycolytic process or the tricarboxylic acid cycle (TCA). During rooting cell division and cell enlargement there is a high demand for energy and carbon skeletons (Corrêa et al., 2005; Ahkami et al., 2009). The TCA cycle is the most important process for synthesis these compounds and energy generation being the center of carbohydrate and amino acid metabolism, so the higher accumulation of these proteins may indicate that an increase in levels of stored metabolites and metabolic activities is necessary for promote root initiation (Wang et al., 2019). In this sense, the up-regulation of these proteins in microcuttings at 12-days incubation with IBA+PG compared to initial time (0-day) could be essential to the rooting promotion observed in *C. legalis*.

In the comparison of microcuttings at 12-days treated/12-days non-treated, most of the regulated proteins belonged to the carbohydrate metabolic process and generation of precursor metabolites and energy process, being down-regulated in this comparison (Fig. 6a). Among them, the starch synthase (A0A251V0T5) and fructokinase (A0A251SGT6) enzymes, less accumulated in 12-day-treated microcuttings (Table 1), are involved in the synthesis of starch and sucrose (Geigenberger, 2003), photosynthetic product accumulates in plants (Zeeman et al., 2010). Still, photosynthesis proteins were also more accumulated in 12-days non-treated microcutting compared to 12-days treated. In this context, the higher accumulation of proteins related to the production and storage of energy, belonging to the classes of carbohydrate metabolic, photosynthetic and generation of precursor

metabolites and energy processes, suggests that 12-day non-treated with IBA+PG microcuttings are less competent in organizing the *de novo* rhizogenesis, and thus, invested in proteins that could lead to some temporary development of the aerial part. On other hand, the 12-days *C. legalis* microcuttings treated with IBA plus PG invested in proteins relevant to root development, meristems and primordium root formation, such as the antioxidant proteins, cell homeostasis and protein metabolism.

CONCLUSION

From our results was observed that IBA is necessary for induction of adventitious rooting. The histomorphological analyses revealed the establishment of the *de novo* root meristem from meristematic-type cells presents in the callus, which allowed the root primordia formation and then the root development in microcuttings treated with IBA. The identification of proteins related to carbohydrate and amino-acid metabolic processes in 12-day treated microcuttings compared to 0-day microcuttings could be related to rooting induction. Moreover, the higher accumulation of stress response proteins related to antioxidant process, cell homeostasis and protein metabolism in 12-days IBA plus PG treated microcuttings could be associated to rooting, while accumulation of proteins related to secondary metabolic processes in 12-days non-treated microcuttings could be related to non-root development. This is the first study showing the relationship of IBA and PG on rooting and specific protein regulation related to root formation in *C. legalis*, a non-easy-rooting species.

REFERENCES

Ahkami AH, Lischewski S, Haensch KT, Porfirova S, Hofmann J, Rolletschek H, Melzer M, Franken P, Hause B, Druege U, Hajirezaei MR (2009) Molecular physiology of

adventitious root formation in *Petunia hybrida* cuttings: involvement of wound response and primary metabolism. New Phytol 181:613-625

Altamura M (1996) Root histogenesis in herbaceous and woody explants cultured *in vitro*. A critical review. Agronomie 16:589-602

Aragão VPM, Silveira V, Santa Catarina C (2017) Micropropagation of *Cariniana legalis* (Martius) O. Kuntze, an endangered hardwood tree from the brazilian Atlantic Forest. Plant Cell Cult Micro 13:41-50

Blakesley D, Weston G, Hall J (1991) The role of endogenous auxin in root initiation. Plant Growth Regul 10:341-353

Brown DE, Rashotte AM, Murphy AS, Normanly J, Tague BW, Peer WA, Taiz L, Muday GK (2001) Flavonoids act as negative regulators of auxin transport in vivo in Arabidopsis. Plant Physiol 126:524-535

Buer CS, Imin N, Djordjevic MA (2010) Flavonoids: new roles for old molecules. J Integr Plant Biol 52:98-111

Bunn E, Turner SR, Dixon KW (2011) Biotechnology for saving rare and threatened flora in a biodiversity hotspot. In Vitro Cell Dev Biol Plant 47:188-200

Burrieza HP, Rizzo AJ, Vale EM, Silveira V, Maldonado S (2019) Shotgun proteomic analysis of quinoa seeds reveals novel lysine-rich seed storage globulins. Food chem 293:299-306

Carvalho PER (2005) Jequitibá-rosa. Circular Técnica. Colombo. Embrapa Florestas, Paraná. 10p

Chao WS, Gu Y-Q, Pautot V, Bray EA, Walling LL (1999) Leucine aminopeptidase RNAs, proteins, and activities increase in response to water deficit, salinity, and the wound signals systemin, methyl jasmonate, and abscisic acid. Plant Physiol 120:979-992

Correa L, Stein R, Fett-Neto A (2012) Adventitious rooting of detached *Arabidopsis thaliana* leaves. Biol Plant 56:25-30

Corrêa LdR, Paim DC, Schwambach J, Fett-Neto AG (2005) Carbohydrates as regulatory factors on the rooting of *Eucalyptus saligna* Smith and *Eucalyptus globulus* Labill. Plant Growth Regul 45:63-73

Da Costa CT, De Almeida MR, Ruedell CM, Schwambach J, Maraschin FDS, Fett-Neto AG (2013) When stress and development go hand in hand: main hormonal controls of adventitious rooting in cuttings. Front Plant Sci 4:133

da Silva JAT, Dobránszki J, Ross S (2013) Phloroglucinol in plant tissue culture. In Vitro Cell Dev Biol-Plant 49:1-16

Damerval C, De Vienne D, Zivy M, Thiellement H (1986) Technical improvements in two-dimensional electrophoresis increase the level of genetic variation detected in wheat-seedling proteins. Electrophoresis 7:52-54

De Klerk G-J, Guan H, Huisman P, Marinova S (2011) Effects of phenolic compounds on adventitious root formation and oxidative decarboxylation of applied indoleacetic acid in *Malus* 'Jork 9'. Plant Growth Regul 63:175-185

De Klerk G-J, van der Krieken W, de Jong JC (1999) Review the formation of adventitious roots: new concepts, new possibilities. In Vitro Cell Dev Biol Plant 35:189-199

Dewir YH, Murthy HN, Ammar MH, Alghamdi SS, Al-Suhaibani NA, Alsadon AA, Paek KY (2016) *In vitro* rooting of leguminous plants: Difficulties, alternatives, and strategies for improvement. Hortic Environ Biotechnol 57:311-322

Dias PC, de Oliveira LS, Xavier A, Wendling I (2012) Estaquia e miniestaquia de espécies florestais lenhosas do Brasil. Pesq Flor Bras 32:453-462

Distler U, Kuharev J, Navarro P, Levin Y, Schild H, Tenzer S (2014) Drift time-specific collision energies enable deep-coverage data-independent acquisition proteomics. Nat Methods 11:167-170

Distler U, Kuharev J, Navarro P, Tenzer S (2016) Label-free quantification in ion mobility–enhanced data-independent acquisition proteomics. Nat protocols 11:795

Do C-T, Pollet B, Thévenin J, Sibout R, Denoue D, Barrière Y, Lapierre C, Jouanin L (2007) Both caffeoyl Coenzyme A 3-*O*-methyltransferase 1 and caffeic acid *O*-methyltransferase 1 are involved in redundant functions for lignin, flavonoids and sinapoyl malate biosynthesis in Arabidopsis. Planta 226:1117-1129

Drew RA, Simpson BW, Osborne WJ (1991) Degradation of exogenous indole-3-butyric acid and riboflavin and their influence on rooting response of papaya *in vitro*. Plant Cell Tiss Org Cult 26:29-34

Epstein E, Ludwig-Müller J (1993) Indole-3-butyric acid in plants: occurrence, synthesis, metabolism and transport. Physiol Plant 88:382-389

Geigenberger P (2003) Regulation of sucrose to starch conversion in growing potato tubers. J Exp Bot 54:457-465

Heringer AS, Reis RS, Passamani LZ, de Souza-Filho GA, Santa-Catarina C, Silveira V (2017) Comparative proteomics analysis of the effect of combined red and blue lights on sugarcane somatic embryogenesis. Acta Physiol Plant 39:52

Heringer AS, Santa-Catarina C, Silveira V (2018) Insights from proteomic studies into plant somatic embryogenesis. Proteomics 18:1-9

Hernandez-Valladares M, Aasebø E, Mjaavatten O, Vaudel M, Bruserud Ø, Berven F, Selheim F (2016) Reliable FASP-based procedures for optimal quantitative proteomic and phosphoproteomic analysis on samples from acute myeloid leukemia patients. Biol Proced Online 18:13

Hiraga S, Sasaki K, Ito H, Ohashi Y, Matsui H (2001) A large family of class III plant peroxidases. Plant Cell Physiol 42:462-468

Husain MK, Anis M, Shahzad A (2008) *In vitro* propagation of a multipurpose leguminous tree (*Pterocarpus marsupium* Roxb.) using nodal explants. Acta Physiol Plant 30:353-359

IUCN (2019) The IUCN Red List of Threatened Species. Version 2019-2. http://www.iucnredlist.org. Accessed 8th may 2019

Lerin J, Aragão VPM, Reis RS, Silveira V, Santa-Catarina C (2019) Proteomic profile and polyamine contents are modulated by light source to promote *in vitro* shoot development in *Cariniana legalis* (Martius) O. Kuntze (Lecythidaceae). Plant Cell Tiss Org Cult 137:329–342

Letunic I, Bork P (2016) Interactive tree of life (iTOL) v3: an online tool for the display and annotation of phylogenetic and other trees. Nucleic Acids Res 44:W242-W245

Lipecka J, Chhuon C, Bourderioux M, Bessard MA, van Endert P, Edelman A, Guerrera IC (2016) Sensitivity of mass spectrometry analysis depends on the shape of the filtration unit used for filter aided sample preparation (FASP). Proteomics 16:1852-1857

Liu J, Sheng L, Xu Y, Li J, Yang Z, Huang H, Xu L (2014) *WOX*11 and 12 are involved in the first-step cell fate transition during de novo root organogenesis in *Arabidopsis*. The Plant Cell 26:1081-1093

MacDonald MJ, D'Cunha GB (2007) A modern view of phenylalanine ammonia lyase. Biochem Cell Biol 85:273-282

Millán-Orozco L, Corredoira E, San José MdC (2011) *In vitro* rhizogenesis: histoanatomy of *Cedrela odorata* (Meliaceae) microcuttings. Rev Biol Trop 59:447-453

Murashige T, Skoog F (1962) A revised medium for rapid growth and bio assays with tobacco tissue cultures. Physiol Plant 15:473-497

Nanjo Y, Skultety L, Uváčková Lu, Klubicová Kn, Hajduch M, Komatsu S (2012) Mass spectrometry-based analysis of proteomic changes in the root tips of flooded soybean seedlings. J Prot Res 11:372-385

Oliveira LSd, Dias PC, Brondani GE (2013) Micropropagação de espécies florestais brasileiras. Pes Florest Bras 33:439-453

Pacurar DI, Perrone I, Bellini C (2014) Auxin is a central player in the hormone cross-talks that control adventitious rooting. Physiol Plant 151:83-96

Parveen S, Shahzad A (2010) TDZ-induced high frequency shoot regeneration in *Cassia sophera* Linn. via cotyledonary node explants. Physiol Mol Biol Plant 16:201-206

Parveen S, Shahzad A, Saema S (2010) *In vitro* plant regeneration system for *Cassia siamea* Lam., a leguminous tree of economic importance. Agroforest Syst 80:109-116

Peer WA, Bandyopadhyay A, Blakeslee JJ, Makam SN, Chen RJ, Masson PH, Murphy AS (2004) Variation in expression and protein localization of the PIN family of auxin efflux facilitator proteins in flavonoid mutants with altered auxin transport in *Arabidopsis thaliana*. The Plant Cell 16:1898-1911

Peer WA, Murphy AS (2007) Flavonoids and auxin transport: modulators or regulators? Trends Plant Sci 12:556-563

Pérez LP, Montesinos YP, Olmedo JG, Rodriguez RB, Sánchez RR, Montenegro ON, Escriba RCR, Daniels D, Gómez-Kosky R (2016) Effect of phloroglucinol on rooting and i*n vitro* acclimatization of papaya (*Carica papaya* L. var. Maradol Roja). In Vitro Cell Dev Biol Plant 52:196-203

R core team (2018) R: A Language and Environment for Statistical Computing. R Foundation for Statistical Computing, Vienna, Austria.

Rêgo GM (2002) Jequitibá-rosa (*Cariniana legalis*): espécie em extinção da floresta Atlântica. Circular técnico. Embrapa Tabuleiros Costeiros, Aracaju. 2p

Ribeiro M, Catenacci FS, Smith NP, Cabello NB (2017) *Lecythidaceae* in Flora do Brasil 2020 em construção. Jardim Botânico do Rio de Janeiro. http://floradobrasil.jbrj.gov.br/reflora/floradobrasil/FB8543. Accessed 22 july 2019

Rogers LA, Campbell MM (2004) The genetic control of lignin deposition during plant growth and development. New Phytol 164:17-30

Saibil H (2013) Chaperone machines for protein folding, unfolding and disaggregation. Nat Rev Mol Cell Biol 14:630–642

Sang YL, Cheng ZJ, Zhang XS (2018) Plant stem cells and de novo organogenesis. New Phytol 218:1334-1339

Santelia D, Henrichs S, Vincenzetti V, Sauer M, Bigler L, Klein M, Bailly A, Lee Y, Friml J, Geisler M (2008) Flavonoids redirect PIN-mediated polar auxin fluxes during root gravitropic responses. J Biol Chem 283:31218-31226

Sousa KR, Aragão VPM, Reis RS, Macedo AF, Vieira HD, de Souza CLM, Floh EIS, Silveira V, Santa-Catarina C (2016) Polyamine, amino acid, and carbohydrate

profiles during seed storage of threatened woody species of the Brazilian Atlantic Forest may be associated with seed viability maintenance. Braz J Bot 39:985-995

Stevens ME, Pijut PM (2018) Rapid *in vitro* shoot multiplication of the recalcitrant species *Juglans nigra* L. In Vitro Cell Develop Biol-Plant 54:309-317

Sukumar P, Maloney GS, Muday GK (2013) Localized induction of the ATP-binding cassette B19 auxin transporter enhances adventitious root formation in Arabidopsis. Plant Physiol 162:1392-1405

Tang Z, Du W, Du X, Ban Y, Cheng J (2016) iTRAQ protein profiling of adventitious root formation in mulberry hardwood cuttings. J Plant Grow Regul 35:618-631

Thangjam R, Sahoo L (2012) *In vitro* regeneration and *Agrobacterium tumefaciens*-mediated genetic transformation of *Parkia timoriana* (DC.) Merr.: a multipurpose tree legume. Acta physiol plant 34:1207-1215

Timperio AM, Egidi MG, Zolla L (2008) Proteomics applied on plant abiotic stresses: role of heat shock proteins (HSP). J prot 71:391-411

Vahdati K, Leslie C, Zamani Z, McGranahan G (2004) Rooting and acclimatization of *in vitro*-grown shoots from mature trees of three *Persian walnut* cultivars. HortScience 39:324-327

Vander Mijnsbrugge K, Meyermans H, Van Montagu M, Bauw G, Boerjan W (2000) Wood formation in poplar: identification, characterization, and seasonal variation of xylem proteins. J Planta 210:589-598

Vanholme R, Demedts B, Morreel K, Ralph J, Boerjan W (2010) Lignin biosynthesis and structure. Plant Physiol 153:895-905

Wang Z, Hua J, Yin Y, Gu C, Yu C, Shi Q, Guo J, Xuan L, Yu F (2019) An Integrated Transcriptome and Proteome Analysis Reveals Putative Regulators of Adventitious Root Formation in *Taxodium* ‘Zhongshanshan’. Inter j mol sci 20:1225

Zeeman SC, Kossmann J, Smith AM (2010) Starch: its metabolism, evolution, and biotechnological modification in plants. Annu Rev Plant Biol 61:209-234

Zhang J, Peer WA (2017) Auxin homeostasis: the DAO of catabolism. Jexp bot 68:3145-3154

Zhang S, Wu J, Yuan D, Zhang D, Huang Z, Xiao L, Yang C (2014) Perturbation of auxin homeostasis caused by mitochondrial *FtSH4* gene-mediated peroxidase accumulation regulates *Arabidopsis* architecture. Mol plant 7:856-873

Zhou J, Wu H, Collet G (1992) Histological study of initiation and development *in vitro* of adventitious roots in minicuttings of apple rootstocks of M 26 and EMLA 9. Physiol Plant 84:433-440

3.3. STORAGE ENVIRONMENT ALTERS PHYSIOLOGICAL ASPECTS AND PROTEOMIC PROFILE IN SEEDS OF *CARINIANA LEGALIS* (MARTIUS) O. KUNTZE*

RESUMO

O armazenamento é uma etapa crucial para conservação de sementes, especialmente para espécies ameaçadas de extinção, como *Cariniana legalis*. O objetivo do trabalho foi avaliar a influência da temperatura e do tempo de armazenamento na viabilidade e na alteração do perfil proteômico em sementes de *C. legalis*. Sementes foram armazenadas a 6 e 25°C em embalagem de papel trifoliado por 24 meses. Em intervalos de 4 meses, foram avaliados porcentagem de germinação, comprimento das plântulas, grau de umidade e condutividade elétrica. O perfil proteômico foi avaliado em sementes antes (Tempo 0) e aos 8 meses de armazenamento nas duas temperaturas. As sementes armazenadas a 25°C não apresentaram mais germinação aos 8 meses e exibiram maior grau de umidade e condutividade elétrica, enquanto sementes armazenadas a 6°C mantiveram viabilidade, diminuindo a germinação ao longo dos 24 meses. Na análise proteômica comparando sementes armazenadas a 6°C/sementes não armazenadas; e sementes armazenadas a 25°C/sementes não armazenadas, as proteínas de choque térmico (down-reguladas) e aconitato hidratase (única em não armazenadas), associadas com a manutenção da viabilidade foram

* Os dados deste capítulo serão submetidos para publicação:
Lerin, J; Sousa KR; Vieira HD; Silveira, V; Santa-Catarina, C. (2020). Journal Forestry Research

identificadas sendo negativamente influenciada pelo tempo de armazenamento. Na comparação sementes armazenadas a 25°C/sementes armazenadas a 6°C, a proteína de resposta a estresse, como a álcool desidrogenase (up-regulada), foram afetadas pela temperatura, sendo associada com a rápida perda da viabilidade das sementes. Portanto, o armazenamento a 6°C prolongou a viabilidade das sementes em *C. legalis*, enquanto a 25°C resultou em rápida perda de germinação e no acúmulo de proteínas envolvidas em respostas a estresse e senescência celular.

Palavras-chave: deterioração de sementes, temperatura, acúmulo de proteínas, espécies ameaçadas

ABSTRACT

Storage is a crucial step in seed conservation, especially for endangered species, such as *Cariniana legalis*. The objective of the work was to evaluate the influence of the storage temperature and time on the viability and on the alteration of the proteomic profile in seeds of *C. legalis*. Seeds were stored at 6 and 25°C in trifoliate paper packaging for 24 months. At 4-month intervals, germination percentage, seedling length, moisture content and electrical conductivity were evaluated. The proteomic profile was evaluated in seeds before (Time 0) and at 8 months of storage in the two temperatures. The seeds stored at 25°C showed no more germination at 8 months and showed a higher moisture degree and electrical conductivity. While seeds stored at 6°C maintained viability, reducing germination over 24 months. In the proteomic analysis comparing seeds stored at 6°C/non-stored seeds; and seeds stored at 25°C/non-stored seeds, heat shock proteins (down-regulated) and aconitate hydratase (unique in non-stored) associated with maintaining viability were identified, being negatively influenced by the storage time. In the comparison of seeds stored at 25°C/seeds stored at 6°C, stress response protein such as alcohol dehydrogenase (up-regulated) was affected by temperature, being associated with rapid loss of seeds viability. Therefore, storage at 6°C prolonged seed viability in *C. legalis*, while at 25°C it resulted in a rapid loss of

germination and in the accumulation of proteins involved in stress responses and cellular senescence.

Keywords: seeds deterioration, temperature, proteins accumulation, threatened species

INTRODUCTION

The Brazilian Atlantic Rain Forest is made up of numerous native plant species, including *Cariniana legalis* (Martius) O. Kuntze (Lecythidaceae). Popularly known as jequitibá-rosa (Rêgo, 2002; Carvalho, 2005), this species was intensively exploited and currently, is listed in the red list of threatened species of the International Union for Conservation of Nature (IUCN), classified as vulnerable (IUCN, 2019). Its propagation is commonly made by seeds, which lose viability quickly (Rêgo, 2002), in this sense, the proper storage is essential to prolong the seeds germination capacity and allow the *ex situ* conservation of this species.

Seeds storage is necessary to preserve the physical and physiological qualities, and proper storage can reduce the speed of deterioration, maintaining the availability of viable seeds. After the physiological maturity, the deterioration of seed is inevitable and leads to loss of vigor and viability (Jyoti e Malik, 2013). Temperature and humidity are the two main factors affecting seed storage, and influence the speed of biochemical processes alteration (Roberts, 1973). Therefore, methodologies aiming to reduce the speed of deterioration involve the establishment of better environmental conditions, controlling the temperature and humidity. The ideal storage condition varies according to the feature tolerance of each species. For *Swertia chirayita*, the storage at 4°C during 24 months was the most appropriate temperature compared to -15 and 25°C (Pradhan e Badola, 2012). However, for *Citrullus lanatus*, cv. Crimson Sweet, seeds stored at 10°C and 40-45% relative humidity, was the ideal condition avoiding the loss of physiological quality for 12 months (Torres, 2005).

For *C. legalis,* seeds stored in plastic bags at 4°C, had a reduction from 70 to 20% the seedling emergence in 12 months (Sousa et al., 2016) and presented a decrease in germination from 78 to 44.5% at 12 months when stored in plastic bags at 6°C (Aragão et al. 2019), showing that the seeds lot can also affects the germination during storage. However, no work has been reported using a major time of storage, as 24 months and other types of packaging for this species.

Over storage, physiological and biochemical changes lead to loss of germination capacity. Alteration on the proteomic profile as result of environmental conditions and time of seed storage can occurs. The seed storage proteins (SSPs) have showed a key role in seed longevity such as cruciferins and napins, which are well known for contributing to seed germination and support of early seedling growth (Müntz et al., 2001; Wan et al., 2007). Moreover, the SSPs are already known to act against oxidative stress in seeds during ageing (Nguyen et al., 2015).

For *C. legalis* seeds, comparative analysis using two-dimensional gel electrophoresis (2-DE) method has been done with seeds during 12 months storage, showing a decrease in the acumulation of ferritin and superoxide dismutase proteins, which were related to protection against oxidative stress and damage of cellular components (Aragão et al., 2019). These initial results have improved our understanding of the molecular processes involved in seed storage and germination of *C. legalis*, but a complete analysis using the lable-free comparative proteomics approach can improve a number of identified proteins. The gel-free approach allows the identification of low-abundance proteins that are often missed by gel-based proteomic (Heringer et al., 2018). It is possible increase the knowledgement about the biochemical changes of seeds stored under different environmental conditions.

There is little available knowledge related to seeds storage of native species with ecological and economic relevance as *C. legalis*. In this way, the objective of the work was to evaluate the influence of temperature and time storage on the viability and on the proteomic profile in seeds of *C. legalis*.

MATERIAL AND METHODS

Plant material and storage conditions

Mature seeds, collected soon after its dispersion, were provided by Caiçara nursery located at Brejo Alegre - SP, Brazil (21°10'S and 50°10'W). Analyzes to determine the viability were performed with mature dry seeds before (non-stored, time 0) and after 4, 8, 12, 16, 20 and 24 months of storage under 6 ± 2°C (refrigerator) and 25 ± 2°C (laboratory-room) in trifoliate paper package. During storage, the average of relative humidity was 16 and 60% for 6 and 25°C, respectively.

Germination and seedlings growth

The percentage of germination was analyzed according to Brasil (2013). Four biological replicates (with 50 seeds each) from each treatment, considering the time of incubation and temperature, were distributed upon sheets of germitest® paper (J Prolab, Paraná, Brazil) moistened with sterile distilled water at a ratio of 2.5 times the dry paper mass. Seeds were incubated in a BOD-type germination chamber (Eletrolab, São Paulo, Brazil) at 25°C, with photoperiod of 8 h light/16 h dark, at 40 µmol m^{-2} s^{-1}. The germination was evaluated until the 30^{th} day, when the percentage of germination was obtained. In addition, the length (cm) of normal seedling was determined using a ruler. A normal seedling was considered those with well developed aerial part and root system, showing the ability to continue their development.

Seeds moisture degree determination

The seed moisture degree was determined with four biological samples (2 g FM each sample) of seeds at each time of storage and temperature, adapted from Brasil (2009). To perform it, the samples were weighed to obtain the fresh matter (FM), dried at 105°C for 24 h in a chamber with forced air circulation (Ethik technology, São Paulo, Brazil) and then, weighed again to obtain the dry matter (DM). The results of seed moisture degree were expressed by the formula: seed moisture degree = (water content/FM) x 100 according to Aragão et al. (2019).

Electrical conductivity

Electrical conductivity was determined according to Vieira et al. (1999) with adaptation. Samples of seeds (25 seeds from each sample, in four replicates) from each time of storage and temperature were weighed, soaked in 75 mL of distilled water and kept in a BOD-type germination chamber at 25°C, during 24 h. After this period, the electrical conductivity of imbibition solution was measured using a CD-830 conductivimeter (Instrutherm, São Paulo, SP, Brazil). The results were expressed as $\mu S.cm^{-1}g^{-1}$.

Statistical analysis

The experiment was performed using a completely randomized design. The data were submitted to analysis of variance (ANOVA) ($P<0.05$) followed by a Tukey test in the program R core team (2018) (R Foundation for Statistical Computing, version 3.4.4, 2018, Vienna, Austria).

Comparative proteomic analysis

Protein extraction and digestion

Proteomics analysis was performed with non-stored seeds and seeds stored at 6 and 25°C (in the storage time when there was no more germination in one of the temperatures). Three biological replicates (100 mg FM from each samples) from each treatment were pulverized using a mortar and pestle in liquid nitrogen on ice and macerated with extraction buffer comprising 20 mM Tris-HCl (GE Healthcare, Little Chalfont, UK) pH 6.8, 1% dithiothreitol (DTT; GE Healthcare), 0,1% sodium dodecyl sulfate (SDS; GE Healthcare) and 1 mM phenylmethanesulfonyl fluoride (PMSF; Sigma-Aldrich, St. Louis, USA). Samples were agitated for 30 min and then centrifuged at 16,000 *g* for 10 min at 4°C. The supernatants were collected, and protein concentrations were measured using the 2-D Quant Kit (GE Healthcare, Piscataway, USA).

Before the trypsin digestion step, protein samples were precipitated using the methanol/chloroform methodology to remove any interferent from samples (Nanjo et al., 2012). After protein precipitation, samples were resuspended in 7M urea/2M

thiourea solution for proper resuspension. Protein digestion was performed using the filter-aided sample preparation (FASP) methodology (Burrieza et al., 2019). Before starting the digestion procedure, an integrity test was made to check for damaged filter units (Hernandez-Valladares et al., 2016), thus only the working units were used. After that, 100 µg of protein, from each sample, were added to the Microcon-30 kDa filter units (Millipore) (Lipecka et al., 2016), washed with 200 µL 50 mM ammonium bicarbonate and centrifuged at 12,000 x *g* for 15 min at 25°C (otherwise stated, all centrifugation steps were performed at this condition). This step was repeated once for complete removal of urea before reduction of proteins. Next, 100 µL of 50 mM DTT freshly made in 50 mM ammonium bicarbonate were added, gently vortexed and incubated for 20 min at 60°C (1 min agitation at 650 rpm, and 4 min stopped). Then, 200 µL of 8 M urea in 50 mM ammonium bicarbonate were added and centrifuged for 15 min. For protein alkylation, 100 µL of 50 mM iodoacetamide (GE Healthcare) freshly prepared in 8 M urea in 50 mM ammonium bicarbonate were added, gently vortexed and incubated for 20 min at 25°C in the dark (1 min agitation at 650 rpm, and 19 min stopped). Next, 200 µL of 8 M urea in 50 mM ammonium bicarbonate were added and centrifuged for 15 min. This step was repeated once. Then, 200 µL of 50 mM ammonium bicarbonate were added and centrifuged for 15 min. This step was repeated twice. In the last washing, it should remain approximately 50 µL of sample. For protein digestion, 25 µL of 0.2% (v/v) RapiGest (Waters, Milford, CT, USA) and 20 µL of trypsin solution (50 ng.µL^{-1}, V5111, Promega, Madison, WI, USA) were added, gently vortexed and incubated for 16 h at 37°C (1 min agitation at 650 rpm and 4 min stopped). For peptide elution, the filter units were transferred for new microtubes and centrifuged for 10 min at 12,000 x *g*. Then, 50 µL of 50 mM ammonium bicarbonate were added and centrifuged for 15 min at 12,000 x *g*. This step was repeated once. For RapiGest precipitation and trypsin inhibition, 5 µL of 15% trifluoroacetic acid (TFA, Sigma-Aldrich) were added, gently vortexed and incubated for 30 min at 37°C. Then, samples were centrifuged for 15 min, the supernatants collected and vacuum dried. Peptides were resuspended in 100 µL solution of 95% 50 mM ammonium bicarbonate in 5% acetonitrile and 0.1% formic acid.

Mass spectrometry analysis

Mass spectrometry was performed using a nanoAcquity UPLC connected to a Q-TOF SYNAPT G2-Si instrument (Waters, Manchester, UK). For proper sample normalization, an MSE scouting run approach was used, which consisted of previous MSE runs processed based on the summed intensities of TOP3 matched peptides of all identified proteins for each run. Thus, stoichiometrically injections were performed for HDMSE analysis. Runs consisted of three biological replicates of 1 µg of peptide samples. During separation, samples were loaded onto the nanoAcquity UPLC M-Class Symmetry C18 5 µm trap column (180 µm × 20 mm) at 5 $\mu L.min^{-1}$ during 3 min and then onto the nanoAcquity M-Class HSS T3 1.8 µm analytical reversed phase column (75 µm × 150 mm) at 400 $nL.min^{-1}$, with a column temperature of 45°C. For peptide elution, a binarygradient was used, with mobile phase A consisting of water (Tedia, Fairfield, Ohio, USA) and 0.1% formic acid (Sigma-Aldrich) and mobile phase B consisting of acetonitrile (SigmaAldrich) and 0.1% formic acid. Gradient elution started at 5% B, then ramped from 5 B to 40% B up to 91.12 min, and from 40 B to 99% B until 95.12 min, being maintained at 99% until 99.12 min, then decreasing to 5% B until 101.12 min and kept 5% B until the end of experiment at 117.00 min. The instrument settings were based on that described by Distler et al. (2016) for IMS-enhanced data-independent acquisition (DIA). Briefly, mass spectrometry was performed in positive and resolution mode (V mode), 35,000 FWHM, with ion mobility, and in DIA mode; ion mobility separation (HDMSE) used an IMS wave velocity ramp starting with 800 m/s and ending with 500 m/s, helium and IMS gas flow of 180 and 90 $mL.min^{-1}$, respectively; the transfer collision energy ramped from 25 V to 55 V in high-energy mode; cone and capillary voltages of 30 V and 3000 V, respectively; nano flow gas of 0.5 Bar and purge gas of 150 $L.h^{-1}$; and a source temperature of 100 °C. In TOF parameters, the scan time was set to 0.6 s in continuum mode with a mass range of 50 to 2000 Da. The human [Glu1]-fibrinopeptide B (Sigma-Aldrich) at 100 $fmol.\mu L^{-1}$ was used as an external calibrant and lock mass acquisition was performed every 30 s. Mass spectra acquisition was performed by MassLynx v4.0 software.

Bioinformatics

Spectra processing and database search conditions were performed using ProteinLynx Global SERVER (PLGS) software v.3.02 (Waters). The HDMSE analysis

utilized the following parameters: Apex3D of 150 counts for low-energy threshold, 50 counts for elevated-energy threshold, and 750 counts for intensity threshold; one missed cleavage; minimum fragment ions per peptide equal to three; minimum fragment ions per protein equal to seven; minimum peptides per protein equal to two; fixed modifications of carbamidomethyl (C) and variable modifications of oxidation (M) and phosphoryl (STY); default false discovery rate (FDR) of 1%; automatic peptide and fragment tolerance. For protein identification, we used the *Helianthus annuus* protein databank (ID: UP000215914), which was selected based on the PhyloT phylogenetic tree proximity (Letunic e Bork, 2016) generated from all plant species (http://itol.embl.de), being the database available at UniProtKB (www.uniprot.org). Label-free quantification analyses were performed using ISOQuant software v.1.7(Distler et al., 2014). Briefly, the following parameters were used: peptide and protein FDR 1%, sequence length of at least six amino acid residues, and minimum peptide score equal six. Samples were normalized by a multidimensional normalization process, which corrects peak intensities based on the intensity and retention time domains. The software performed the relative protein quantification based on the TOP3 method. Based on relative abundances of uniquely assigned peptides, the abundances of shared peptides were redistributed to the respective source proteins, followed by the TOP3-based quantification (Distler et al., 2014). To ensure the quality of the results after data processing, only proteins present in the three runs were accepted for differential abundance analysis. Proteins with ANOVA ($P< 0.05$) were deemed up-regulated if the $\log_2$ value of the fold change (FC) was greater than 0.60 and down-regulated if the $\log_2$ value of the FC was less than − 0.60. Functional annotations were performed using OmicsBox software 1.0.34 and UniProtKB (http://www.unipr ot.org).

RESULTS

Effects of storage time and temperature on physiological aspects of seeds

Seeds at the beginning (non-storage seeds) showed 80% of germination, reducing significantly in both temperatures tested during 24 months of storage (Fig. 1). Seeds storage at 6°C decreased significantly the germination from 80 to 48% during the first four months, showing 12% germination after 24 months. On the other hand, seed storage at 25°C decreased significantly the germination on the first four months, with no germination at 8 months of storage (Fig. 1).

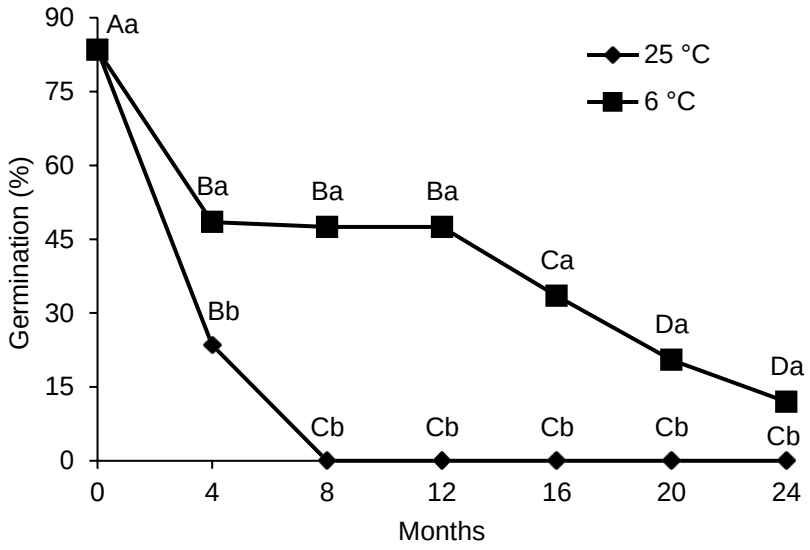

Fig. 1 Germination (%) of *C. legalis* seeds stored at 6 and 25°C temperatures before (non-stored, time 0) and after 4, 8, 12, 16, 20 and 24 months. Uppercase letters indicate significant differences between months of storage. Lowercase letters indicate significant differences between the temperatures of storage. Means followed by the same letter do not differ statistically between them, according to Tukey test ($P < 0.05$). CV = Coefficient of variation (n = 4, CV = 19.32%).

The time of storage and temperature affected the length of seedlings (Fig. 2). Seedlings from seeds stored at 6°C showed significant length higher than those at 25°C. The ausence of seedlings formation was seen at the 8th month at 25°C. Seeds

stored at 6°C showed a significant decrease in seedling length after 20th month of seed storage (Fig. 2).

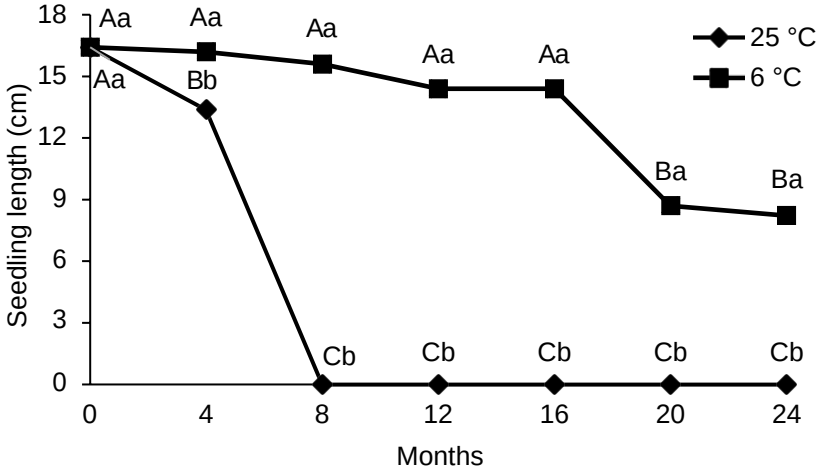

Fig. 2 Seedling length (cm) of *C. legalis* from seeds stored at 6 and 25°C temperatures, before (non-stored, time 0) and after 4, 8, 12, 16, 20 and 24 months. Uppercase letters indicate significant differences between months of storage. Lowercase letters indicate significant differences between the temperatures of storage. Means followed by the same letter do not differ statistically between them, according to Tukey test ($P < 0.05$). CV = Coefficient of variation (n = 4, CV = 13.20%).

On the other hand, the moisture degree of seeds stored at 25°C was significantly higher than those stored at 6°C (Fig. 3). Over time, the moisture degree of seeds stored at 6°C decreased significantly, while for seeds stored at 25°C there was oscillation between the evaluated periods, increasing significantly the value from the initial time (time 0) to 24th month of storage (Fig. 3).

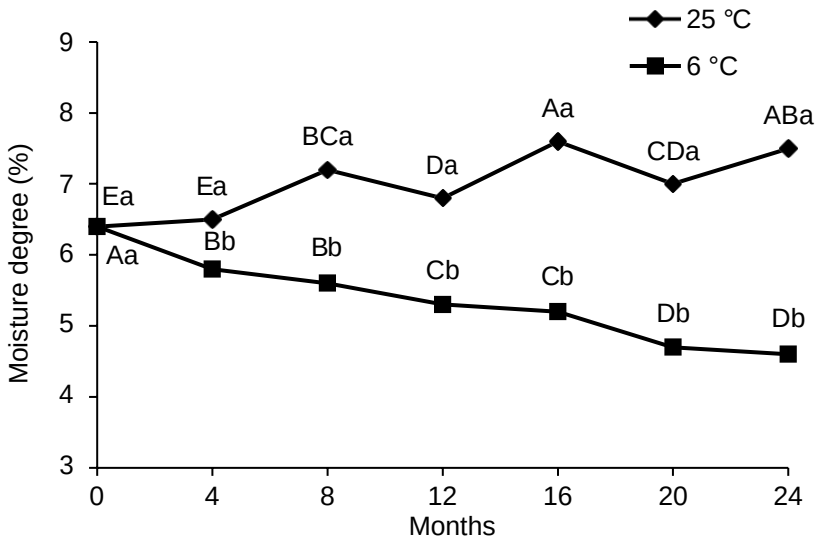

Fig. 3 Moisture degree (%) of *C. legalis* seeds stored at 6 and 25°C temperatures, before (non-stored, time 0) and after 4, 8, 12, 16, 20 and 24 months. Uppercase letters indicate significant differences between months of storage. Lowercase letters indicate significant differences between the temperatures of storage. Means followed by the same letter do not differ statistically between them, according to Tukey test ($P < 0.05$). CV = Coefficient of variation (n = 4, CV = 2.03%).

The electrical conductivity of seeds showed a significant difference between two storage temperatures from the 12th month, being higher to seeds incubated at 25°C. No significant differences between the months of storage in temperature of 6°C was observed, while at 25°C the increase was significant from at 8 months, with some variations, but increasing over time (Fig. 4).

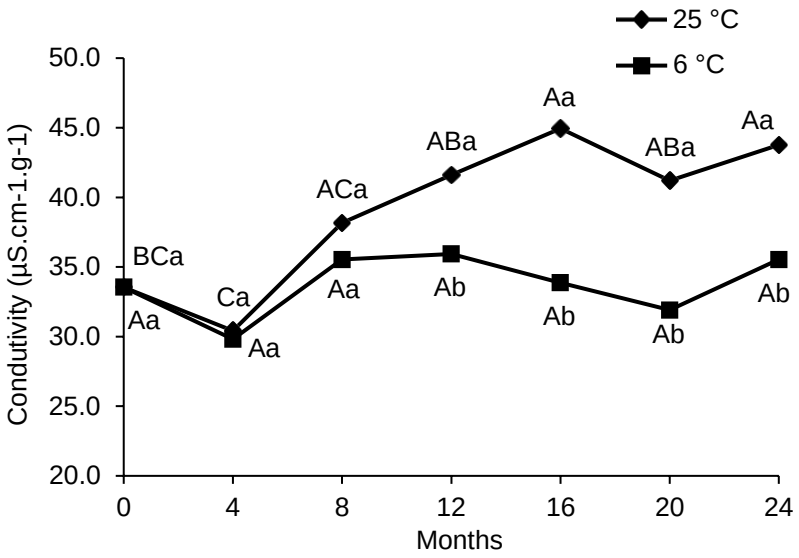

Fig. 4 Electrical conductivity of *C. legalis* seeds stored at 6 and 25°C temperatures, before (non-stored, time 0) and after 4, 8, 12, 16, 20 and 24 months. Uppercase letters indicate significant differences between months of storage. Lowercase letters indicate significant differences between the temperatures of storage. Means followed by the same letter do not differ statistically between them, according to Tukey test ($P < 0.05$). CV = Coefficient of variation (n = 4, CV = 11.11%).

Effects of storage time and temperature on proteomic profile of seeds

The analysis of the proteomic profile was performed using non-stored seeds (time 0, at the beginning of storage) and seeds stored at 6 and 25°C for 8 months (when no germination was seen in seeds stored at 25°C). Thus, three different comparisons were performed and analyzed: seeds stored at 6°C/non-stored seeds; seeds stored at 25°C/non-stored seeds; and seeds stored at 25°C/seeds stored at 6°C.

In this analysis a total of 172 proteins were identified. In the comparison seeds stored at 6°C/non-stored seeds 159 were unchanged and 12 proteins were regulated, being 2 up- and 6 down-regulated, 1unique in seeds stored at 6°C and 3 unique in non-stored seeds (Supplementary table 1). Among the regulated proteins, NADP-dependent glyceraldehyde-3-phosphate dehydrogenase (A0A251V667), and aspartate aminotransferase (A0A251U954) were up-regulated. The heat shock 70 kDa protein (A0A251UNC3, A0A251VA77), heat shock protein 90-2 (A0A251V9N0), Phosphoglycerate kinase (I6LNU0), Ras-related protein RABC1 (A0A251UU95) and tubulin alpha chain-like (A0A251VIL2) were down-regulated. Moreover, 14-3-3-like

protein D (A0A251VGY2), 14-3-3 domain-containing protein (A0A251SG50) and aconitate hydratase 3 (A0A251V7G1), were unique in non-stored seeds, while tubulin alpha-5 chain (A0A251VBZ7) was unique in seeds stored at 6°C (Table 1).

In the comparison of seeds stored at 25°C/non-stored seeds 160 proteins were unchanged and 12 were regulated, being 1up- and 7 down-regulated, 2 proteins were unique in seeds stored at 25°C and 2 were unique in non-stored seeds (Supplementary table 1). Among the regulated proteins, the heat shock 70 kDa protein 4 (A0A251UNC3), tubulin alpha chain-like (A0A251VIL2 and A0A251RP81), phosphoglycerate kinase (I6LNU0), proteasome subunit alpha type (A0A251S3M6), triosephosphate isomerase (A0A251U316) and catalase (A0A251T0Z2), were down-regulated in this comparison (Table 1). The histone H4 (A0A251TVQ0) protein was up-regulated, while, the 14-3-3 domain-containing protein (A0A251SG50) and aconitate hydratase 3 (A0A251V7G1) were unique in non-stored seeds and the tubulin alpha-5 chain (A0A251VBZ7) and aspartic proteinase A1 (A0A251RRT0) were unique in seeds stored at 25°C (Table 1).

In the comparison of seeds stored at 25°C/seeds stored at 6°C 163 proteins were unchanged and 7 were regulated, being 1up- and 4 down-regulated and 2 proteins were unique in seeds stored at 25°C (Supplementary Table 1). The alcohol dehydrogenase 2 (A0A251UTI9) was up-regulated, while, tubulin alpha chain-like (A0A251RP81), proteasome subunit alpha type (A0A251S3M6), triosephosphate isomerase (A0A251U316) and NADP-dependent glyceraldehyde-3-phosphate dehydrogenase (A0A251V667) were down-regulated. The 14-3-3-like (A0A251VGY2) protein D and aspartic proteinase A1 (A0A251RRT0) were unique in seeds stored at 25°C (Table 1).

The differentially regulated proteins were classified according to their biological process (Table 1). Among the regulated proteins, some of them were highlighted and discussed according to their involvement in the maintenance and/or loss of seed viability.

Table 1. Differentially regulated proteins identified in seeds of *C. legalis* during storage at 6 and 25°C.

Accession	Peptide report	Score	Description	Biological Function	Differential abundance regulation[a]		
					Seeds stored at 6°C/non-stored seeds	Seeds stored at 25°C/non-stored seeds	Seeds stored at 25°C/ seeds stored at 6°C
A0A251UTI9	10	7799	Alcohol dehydrogenase 2	Generation of precursor metabolites and energy	-	-	Up
A0A251RP81	6	3897	Tubulin alpha chain-like	Cellular component organization	-	Down	Down
A0A251S3M6	5	4955	Proteasome subunit alpha type	Protein metabolic process	-	Down	Down
A0A251U316	5	5575	Triosephosphate isomerase, cytosolic	Carbohydrate metabolic process	-	Down	Down
A0A251V667	5	461	NADP-dependent glyceraldehyde-3-phosphate dehydrogenase	Carbohydrate metabolic process; generation of precursor metabolites and energy	Up	-	Down
A0A251RRT0	3	1767	Aspartic proteinase A1	Protein metabolic process	-	Unique at 25°C	Unique at 25°C
A0A251V7G1	11	3610	Aconitate hydratase 3	Amino-acid metabolic process; tricarboxylic acid cycle	Unique in non-stored seeds	Unique in non-stored seeds	-
A0A251VGY2	4	1446	14-3-3-like protein D	Stress response; regulation of metabolic process	Unique in non-stored seeds	-	Unique at 25°C
A0A251TVQ0	12	8923	Histone H4	transcription regulation	-	Up	-
A0A251UNC3	20	9985	Heat shock 70 kDa protein 4	Stress response; proteinfolding	Down	Down	-

Table 1 (continued)

A0A251VIL2	7	629	Tubulin alpha chain-like	Cellular component organization	Down	Down	-
I6LNU0	5	4762	Phosphoglycerate kinase	Carbohydrate metabolic process	Down	Down	-
A0A251T0Z2	5	1067	Catalase	Stress response	-	Down	-
A0A251SG50	4	2224	14-3-3 domain-containing protein	Stress response; regulation of metabolic process	Unique in non-stored seeds	Unique in non-stored seeds	-
A0A251VBZ7	7	3918	Tubulin alpha-5 chain	Cellular component organization	Unique at 6°C	Unique at 25°C	-
A0A251U954	9	3113	Aspartate aminotransferase, cytoplasmic-like	Amino acid metabolic process; nitrogen metabolism	Up	-	-
A0A251UU95	4	1147	Ras-related protein RABC1	Signal transduction; intracellular protein transport	Down	-	-
A0A251V9N0	4	1529	Heat shock protein 90-2	Stress response; protein folding	Down	--	-
A0A251VA77	12	4135	Heat shock protein 70 family	Stress response; protein folding	Down	-	-

[a]Proteins were deemed up-regulated if the $\log_2$ value of the fold change (FC) was greater than 0.60 and deemed down-regulated if the $\log_2$ value of the FC was less than -0.60, as determined by Student's T-Test (two-tailed; $P< 0.05$).

DISCUSSION

Loss of seed viability is an important factor that needs to be understood in order to improve the conservation of species with difficulty of propagation and in risk of extinction. In this work, we analyze physiological and biochemical changes in *C. legalis* seeds during 24 months of storage at two temperatures: 25°C (laboratory room) with relative humidity around 60%, as a non-storage condition ambient; and 6°C (refrigerator) with relative humidity around 16%, as a temperature which can minimize seed metabolic activities, and delay seed deterioration.

Our results showed a significant difference on seeds germination between the temperatures conditions tested. Seeds stored at 25°C lost the viability, not germinating at 8 months of storage (Fig. 1), and showed an increase in the moisture degree (Fig. 3) and electrical conductivity (Fig. 4). At higher temperatures, some physiological and biochemical processes are triggered or accelerated, including those leading to seed deterioration. In this context, the sensitivity of the seed to deterioration, at high temperatures, depends on its water content, which may vary depending on the air relative humidity (Shelar et al., 2008; Jyoti e Malik, 2013). Seeds with high moisture degree can increase the respiratory rate, leading consequently, to depletion of reserve substances (Shaban, 2013), contributing for the loss of seed viability. Our data shows the influences of the two factors, temperature and relative humidity, but mainly of the temperature, since the difference in the seeds moisture degree was less than 2% between the two temperatures in the 8^{th} months of storage, when there was no germination of the seeds at 25°C. This highlights the necessity of an adequate environment for *ex situ* seeds storage of tree species after their harvesting, once they are not always readly used and can exhibit rapid loss of viability.

The temperature at 6°C was more efficient to prolong seed viability in *C. legalis* during storage (Fig. 1), besides reduced the moisture degree (Fig. 3) and maintained the electrical conductivity (Fig. 4). Similar result was found by Aragão et al. (2019), the germination of *C. legalis* seeds reduced of 78 to 44.5% and the moisture degree decreased of 6.8 to 5.0% during 12 months of storage at 6°C.These results shows that the moisture degree is an important factor during storage, and the reduction in seed

water content is important to decrease the metabolic activity prolonging its viability (Rosa et al., 2005). In addition, the results of moisture degree observed during *C. legalis* seed storage reveal a level of desiccation tolerance, important characteristic to seed conservation. According to Roberts (1973), seeds can be classified as orthodox or recalcitrant depending of desiccation tolerance. To determine if a specie is orthodox, the seeds needs to be able to germinate after going through a certain cold period with negative temperatures and in this context, seeds called recalcitrant require a high degree of moisture to stay viable and do not tolerate negative temperatures and lost the viability. This classification is not yet known for *C. legalis* and need to be defined aiming to improve the storage conditions to this species.

Moreover, seeds stored at 6°C maintained stable the electrical conductivity index, while seeds at 25°C showed a gradual increase of this parameter over the time of storage (Fig. 4). The electrical conductivity measures the solute leakage from seeds and is associated with dead areas of tissue of the cotyledons (Matthews et al., 2012). According to Shaban (2013), the increase of seed deterioration is associated with an increase in membrane permeability and the leakage of solutes, consequently leading to membrane degradation and viability reductionof seed. The disorganization of membranes and loss of control of their permeability has been considered the first change in a sequence of events leading to seeds deterioration (Matthews et al., 2012; Shaban, 2013). In our work, seeds stored at 25°C intensified this effect compared to the non-stored seeds, with a significant difference in the 12th month, soon after seeds lost germination capacity, suggesting the relationship between the solute leakage analysis and the loss of seed viability in *C. legalis.*

In addition to physiological, biochemical alterations can occurs during seed storage. In this work, significant alterations on proteome profile were observed (Table 1). Among the proteins differentially regulated are the HSPs (A0A251UNC3, A0A251V9N0, A0A251VA77, A0A251UNC3), which were down-regulated in seeds stored at 6 and 25°C compared to non-stored seeds (Table 1). This result is in according to the previous results observed during seeds storage in *C. legalis*, which has been showed a reduction in the accumulation of HSPs (Aragão et al., 2019). In addition, these proteins were observed from 0 to 4 days of seed imbibition, showing the importance of these proteins for early germination in C. *legalis* (Trindade et al.,

2018).To survive from quiescent state, seeds accumulate different stress response-related proteins, such as HSPs, that together with the late embryogenesis abundant (LEA) proteins are referred to as a signature of desiccation tolerance, showing a close relationship between the accumulation of these proteins with seed longevity (Rajjou e Debeaujon, 2008), improving the tolerance to aging (Prieto-Dapena et al., 2006). In this way, the reduction in the accumulation of these proteins influencied by time, from non-stored seeds (time 0) to 8 months of storage seeds in both temperatures may have contributed to the loss of seed viability and germination capacity in *C. legalis*, even at the better temperature (6°C), when a decrease of about 50% of germination occurred at this time (8 month).

The catalase is an enzyme involved in reactive oxygen species (ROS) detoxification. In this work the catalase (A0A251T0Z2) was down-regulated during seed storage at 25°C compared to non-stored seeds (Table 1). Dry seeds have a large number of enzymes involved in oxidative stress, however during seed storage, detoxification potential may decreased and the alteration in enzymes as catalase may lead to a progressive accumulation of ROS. An increase in ROS level may induce cellular dysfunctions, modified activation of proteins, lipids, DNA, and RNA (Oracz et al., 2007; Rajjou e Debeaujon, 2008), leading to a reduction of seed vigor, viability and longevity. In this sense, a reduction in the accumulation of this protein in *C. legalis* seeds during storage at 25 °C suggests the relevance of this protein to the maintenance of seed viability in *C. legalis*.

The aconitate hydratase 3 (A0A251V7G1) was unique in non-stored seeds compared to both temperatures 6 e 25°C (Table 1). This protein is associated to reserve substances mobilization and degradation, such as lipids, used during seed germination (He et al., 2011). In this sense, the lack of this protein during storage time in both temperatures may have affected the metabolization of reserve substances, influencing negatively the germination capacity and viability of seeds storage, even at 6°C, when about 50% of germination potential occurred from the beginning to 8 months.

Moreover, the proteasome subunit alpha type (A0A251S3M6) protein was less accumulated in seeds stored at 25°C in both comparisons, seed stored at 25°C/non-stored seeds and in seed stored at 25°C/seed stored at 6°C (Table 1). The proteasome is involved in degradation of other proteins (Skoda e Malek, 1992) and its activity is

required for germination (Chiu et al., 2016). This proteins group was accumulated in viable quiescent seeds to be requested for degradation of the stocking proteins (He et al., 2011), besides, be helpful to remove some germination inhibitory proteins, as DELLA protein (Wang et al., 2009). Our results suggest that non-adequate seed storage (tested here by 25°C) lead to a reduction in the abundance of this protein and consequently affects germination capacity, being associated to the loss of viability. This protein was affected both storage temperature and time. Besides that, the storage at 6°C is relevant to maintain the abundance of this protein, which could be related to the maintenance of capacity of germination in *C. legalis.*

In addition, proteins involved to carbohydrate metabolic process were down-regulated during storage. Among them, the triosephosphate isomerase (A0A251U316) was down-regulated in seeds stored at 25°C in comparison to 25°C/non-stored seeds and with those 25°C/stored at 6°C (Table 1), showing the effect of 25°C temperature in the loss of seed viability of *C. legalis*. The phosphoglycerate kinase (I6LNU0) was down-regulated in both temperature (6 and 25°C) comparated to non-stored seeds (Table 1), suggesting the effect of the time of storage (independent of temperature) on the reduction of seed germination potential. These two proteins are enzymes involved in glycolysis, one of the primary sources of energy for germination (He e Yang, 2013). The decrease in the accumulation of these proteins can mean the reduction of degradation of carbohydrate reserves for germination of seeds leading to viability loss of *C. legalis* seeds.

On the other hand, an alcohol dehydrogenase (A0A251UTI9) was up-regulated in the comparison of seed stored at 25°C/seed stored at 6°C (Table 1). This protein is part of fermentation way, which is an alternative pathway of glycolysis in stress condition cells. In this case, decarboxylation of pyruvate produces toxic acetaldehyde and the alcohol dehydrogenase acts detoxifying due to the conversion of acetaldehyde to ethanol (Strommer, 2011). Thus, the up-regulation of this protein in the seed stored at 25°C/seed stored at 6°C comparison can be related to a stress condition in which the seeds are subjected during storage at 25°C due to the non ideal condition for seed storage, leding to faster seed deterioration compared to storage at 6°C.

The protein aspartic proteinase (A0A251RRT0) was unique in seeds stored at 25°C in the two comparisons, the seed stored in at 25°C/non-stored seeds and in seed

stored at 25°C/seed stored at 6°C (Table 1). A possible role for aspartic proteinases has been implicated in protein degradation during organ senescence and cell death (Simões e Faro, 2004; Timotijević et al., 2010), as observed in leaves of barley (Kervinen et al., 1990) and senescing flowers of cardoon (Heimgartner et al., 1990). The storage environment at 25°C with high humidity may be considered a stress condition leading to seeds deterioration. Therefore, the increase of this protein in seed *C. legalis* stored to 25°C might be related to seed deterioration, influenced by time and also temperature storage.

CONCLUSION

Our results showed that seed storage at 6°C prolonged seed viability in *C. legalis* compared to 25°C providing physiological characteristics that allowed higher seed viability. The non-adequate condition, tested by the storage at 25°C, results in rapid seed germination reduction, with no germination at 8 months of storage, which could be related to the increase in moisture degree and higher electrical conductivity of seeds. In addition, the acumulation of some proteins, such as HSPs and aconitate hydratase, were affected negativitly by the time of storage, being these proteins relevant to for seed viability. On the other hand, the accumulation of proteins involved with stress condition and senescence of cell, such as alcohol dehydrogenase and aspartic proteinase, were affected by the temperature of storage, as observed in seeds stored at 25°C. This is the first study showing the seed storage during 24 months and comparing different temperatures in *C. legalis*. Further studies testing other temperature conditions and package must be done to increase the seed viability during storage in *C. legalis*.

REFERENCES

Aragão VPM, Trindade BMC, Reis RS, Silveira V, Santa-Catarina C (2019) Storage time affects the germination and proteomic profile of seeds of *Cariniana legalis* (Mart.) O. Kuntze (Lecythidaceae), an endangered tree species native to the Brazilian Atlantic Forest. Braz J Bot 42:407-419

Brasil (2009) Regras para Análise de Sementes. Ministério da Agricultura, Pecuária e Abastecimento. Brasília. Secretaria de Defesa Agropecuária. 395p

Brasil (2013) Instruções para análise de sementes e espécies florestais. Ministério da Agricultura, Pecuária e Abastecimento. Brasília. Secretaria de Defesa Agropecuária. 98p

Burrieza HP, Rizzo AJ, Vale EM, Silveira V, Maldonado S (2019) Shotgun proteomic analysis of quinoa seeds reveals novel lysine-rich seed storage globulins. Food chem 293:299-306

Carvalho PER (2005) Jequitibá-rosa. Circular Técnica. Colombo. Embrapa Florestas, Paraná. 10p

Chiu RS, Pan S, Zhao R, Gazzarrini S (2016) ABA-dependent inhibition of the ubiquitin proteasome system during germination at high temperature in *Arabidopsis*. The Plant J 88:749-761

Distler U, Kuharev J, Navarro P, Levin Y, Schild H, Tenzer S (2014) Drift time-specific collision energies enable deep-coverage data-independent acquisition proteomics. Nat Methods 11:167-170

Distler U, Kuharev J, Navarro P, Tenzer S (2016) Label-free quantification in ion mobility–enhanced data-independent acquisition proteomics. Nat protocols 11:795

Heimgartner U, Pietrzak M, Geertsen R, Brodelius P, da Silva Figueiredo A, Pais M (1990) Purification and partial characterization of milk clotting proteases from flowers of Cynara cardunculus. Phytochemistry 29:1405-1410

Heringer AS, Santa-Catarina C, Silveira V (2018) Insights from proteomic studies into plant somatic embryogenesis. Proteomics 18:1-9

Hernandez-Valladares M, Aasebø E, Mjaavatten O, Vaudel M, Bruserud Ø, Berven F, Selheim F (2016) Reliable FASP-based procedures for optimal quantitative

proteomic and phosphoproteomic analysis on samples from acute myeloid leukemia patients. Biol Proced Online 18:13

IUCN (2019) The IUCN Red List of Threatened Species. Version 2019-2. http://www.iucnredlist.org. Accessed 8th may 2019

Jyoti, Malik CP (2013) Seed deterioration: a review. Int J LifeSc Bt & Pharm Res 2:375-385

Kervinen J, Kontturi M, Mikola J (1990) Changes in the proteinase composition of barley leaves during senescence in field conditions. Cer Res Communic 18:191-197

Letunic I, Bork P (2016) Interactive tree of life (iTOL) v3: an online tool for the display and annotation of phylogenetic and other trees. Nucleic Acids Res 44:W242-W245

Lipecka J, Chhuon C, Bourderioux M, Bessard MA, van Endert P, Edelman A, Guerrera IC (2016) Sensitivity of mass spectrometry analysis depends on the shape of the filtration unit used for filter aided sample preparation (FASP). Proteomics 16:1852-1857

Matthews S, Noli E, Demir I, Khajeh-Hosseini M, Wagner M-H (2012) Evaluation of seed quality: from physiology to international standardization. Seed Sci Res 22:S69-S73

Müntz K, Belozersky MA, Dunaevsky YE, Schlereth A, Tiedemann J (2001) Stored proteinases and the initiation of storage protein mobilization in seeds during germination and seedling growth. J Exp Bot 52:1741-1752

Nanjo Y, Skultety L, Uváčková Lu, Klubicová Kn, Hajduch M, Komatsu S (2012) Mass spectrometry-based analysis of proteomic changes in the root tips of flooded soybean seedlings. J Prot Res 11:372-385

Nguyen T-P, Cueff G, Hegedus DD, Rajjou L, Bentsink L (2015) A role for seed storage proteins in *Arabidopsis* seed longevity. J Exp Bot 66:6399-6413

Oracz K, Bouteau HEM, Farrant JM, Cooper K, Belghazi M, Job C, Job D, Corbineau F, Bailly C (2007) ROS production and protein oxidation as a novel mechanism for seed dormancy alleviation. The Plant J 50:452-465

Pradhan BK, Badola HK (2012) Effect of storage conditions and storage periods on seed germination in eleven populations of *Swertia chirayita*: a critically endangered medicinal herb in Himalaya. The Sci World J 2012:1-9

Prieto-Dapena P, Castaño R, Almoguera C, Jordano J (2006) Improved resistance to controlled deterioration in transgenic seeds. Plant Physiol 142:1102-1112

R core team (2018) R: A Language and Environment for Statistical Computing. R Foundation for Statistical Computing, Vienna, Austria.

Rajjou L, Debeaujon I (2008) Seed longevity: survival and maintenance of high germination ability of dry seeds. C R Biol 331:796-805

Rêgo GM (2002) Jequitibá-rosa (*Cariniana legalis*): espécie em extinção da floresta Atlântica. Circular técnico. Embrapa Tabuleiros Costeiros, Aracaju. 2p

Roberts EH (1973) Predicting the storage life of seeds. Seed Sci Technol 1:499-514

Rosa SDVFD, Pinho ÉVRV, Vieira ESN, Veiga RD, Veiga AD (2005) Enzimas removedoras de radicais livres e proteínas lea associadas à tolerância de sementes milho à alta temperatura de secagem. Rev Bras Sementes 27:91-101

Shaban M (2013) Review on physiological aspects of seed deterioration. Intl J Agri Crop Sci 6:627-631

Shelar V, Shaikh R, Nikam A (2008) Soybean seed quality during storage: a review. J Agric Rev 29:125-131

Simões I, Faro C (2004) Structure and function of plant aspartic proteinases. Eur J Biochem 271:2067-2075

Skoda B, Malek L (1992) Dry pea seed proteasome: purification and enzymic activities. Plant Physiol 99:1515-1519

Sousa KR, Aragão VPM, Reis RS, Macedo AF, Vieira HD, de Souza CLM, Floh EIS, Silveira V, Santa-Catarina C (2016) Polyamine, amino acid, and carbohydrate profiles during seed storage of threatened woody species of the Brazilian Atlantic Forest may be associated with seed viability maintenance. Braz J Bot 39:985-995

Strommer J (2011) The plant ADH gene family. The Plant J 66:128-142

Timotijević GS, Milisavljević MD, Radović SR, Konstantinović MM, Maksimović VR (2010) Ubiquitous aspartic proteinase as an actor in the stress response in buckwheat. J Plant Physiol 167:61-68

Torres SB (2005) Qualidade de sementes de melancia armazenadas em diferentes embalagens e ambientes. Rev Ciên Agro 36:163-168

Trindade BMC, Reis RS, Vale EM, Santa-Catarina C, Silveira V (2018) Proteomics analysis of the germinating seeds of *Cariniana legalis* (Mart.) Kuntze (Meliaceae): an endangered species of the Brazilian Atlantic Rainforest. Braz J Bot 41:117-128

Vieira RD, Krzyzanowski FC, França Neto JDB (1999) Vigor de sementes: conceitos e testes vol 1. ABRATES, Londrina. 26p

Wan L, Ross AR, Yang J, Hegedus DD, Kermode AR (2007) Phosphorylation of the 12 S globulin cruciferin in wild-type and *abi1-1* mutant *Arabidopsis thaliana* (thale cress) seeds. Biochem J 404:247-256

Wang F, Zhu D, Huang X, Li S, Gong Y, Yao Q, Fu X, Fan L-M, Deng XW (2009) Biochemical insights on degradation of *Arabidopsis* DELLA proteins gained from a cell-free assay system. The Plant Cell 21:2378-2390

4. RESUMO E CONCLUSÕES

A *C. legalis* é uma espécie do bioma brasileiro Mata Atlântica que se encontra ameaçada de extinção em decorrência da exploração ao longo dos anos. Além das ações antrópicas, sua propagação é comumente feita por sementes, as quais perdem rapidamente a viabilidade agravando a propagação e preservação da espécie. Portanto, métodos alternativos aos convencionais de propagação, bem como práticas de conservação *ex situ* podem ser importantes aliadas na busca pela preservação dessa espécie.

A propagação *in vitro* tem importante papel na busca pela conservação desta espécie. Nesse sentido, o estudo desenvolvido no primeiro capítulo objetivou avaliar o desenvolvimento de brotações *in vitro* de *C. legalis* a partir do uso de diferentes fontes de luz, sendo elas, lâmpadas de diodo emissor de luz (LED) com diferentes combinações espectrais e a lâmpada fluorescente (controle). Embora sabido a importância do tipo e espectro de luz no crescimento das plantas, estudos ainda não haviam sido desenvolvidos para esta espécie. Assim, verificou-se que o tratamento com lâmpada LED consistindo dos espectros branco, azul baixo e vermelho profundo, apresentou maior alongamento das brotações em explantes nodais cotiledonares por estimular respostas de evitação a sombra. Este tratamento aumentou a concentração de putrescina, espermidina e PAs totais. Adicionalmente, proteínas up-reguladas em brotações cultivadas sob a lâmpada LED foram relacionadas à organização e

composição celular, bem como, processos de regulação biológica, enquanto as proteínas relacionadas aos processos de estresse foram down-reguladas em comparação a lâmpada fluorescente. Esses resultados sugerem a relevância da fonte de luz no desenvolvimento de brotações *in vitro* nessa espécie. Como desafio, destaca-se a necessidade de estudos voltados ao desenvolvimento das brotações oriundas de explantes nodais apicais, os quais não mostraram resultados satisfatórios a partir do uso de lâmpadas LED. Podendo-se, com isso, aumentar o número de brotações e mudas obtidas a partir de uma plântula utilizada como explante inicial.

O objetivo do segundo capítulo foi avaliar o efeito do ácido indol-3-butírico (AIB) e do floroglucinol (PG) no enraizamento *in vitro* e perfil proteômico da microestacas obtidas de brotações cultivadas *in vitro* de *C. legalis.* Estudos iniciais com a indução de enraizamento foram realizados para a espécie, no entanto, a resposta ainda é baixa. Neste sentido, estudos visando aumentar o enraizamento das brotações é fundamental para a produção de mudas. Verificou-se que o AIB é necessário para a indução e o PG aumentou o número de raízes. No tratamento AIB 50 µM mais PG 30 µM, aos 12 dias de incubação, células meristemáticas foram observadas nos calos induzidos na base das microestacas, permitindo o enraizamento. Proteínas relacionadas a processos metabólicos de carboidratos e aminoácidos foram acumuladas em microestacas, induzidas pela presença de AIB com PG comparativamente ao tempo inicial (comparação 12 dias tratadas/ 0 dias). Na comparação 12 dias tratadas/12 dias não tratadas, proteínas relacionadas ao processo metabólico secundário, como a chalcona sintase, foram relacionadas ao não enraizamento, enquanto as proteínas relacionadas à homeostase celular e ao processo metabólico foram associadas ao enraizamento em microestacas tratadas. Os resultados alcançados neste trabalho foram bastante significativos e relevantes para o enraizamento *in vitro*. Porém, em um contexto de produção de mudas, a fase seguinte, de aclimatização, ainda é uma limitação para propagação *in vitro* de *C. legalis* e precisa ser aperfeiçoada.

Em uma outra proposta para preservação de *C. legalis*, o terceiro e último trabalho desta tese teve por objetivo avaliar a influência da temperatura de armazenamento na viabilidade e na alteração do perfil proteômico de sementes de *C. legalis.* Embora estudos iniciais tenham sido desenvolvidos para a espécie, testando

o armazenamento por 12 meses, estudos visando aumentar o tempo de armazenamento e diferentes temperaturas ainda não haviam sido realizados. Verificou-se neste estudo que, aos 8 meses as sementes armazenadas a 25°C não germinaram mais e exibiram maior grau de umidade e condutividade elétrica, enquanto as sementes armazenadas a 6°C apresentaram germinação por mais tempo, proporcionando maior viabilidade das sementes. A análise comparando o proteoma de sementes armazenadas a 6°C/sementes não armazenadas; e sementes armazenadas a 25°C/sementes não armazenadas, possibilitou a identificação de proteínas de choque térmico (down-reguladas) e aconitato hidratase (única em não armazenadas) associadas com a manutenção da viabilidade, sendo negativamente influenciada pelo tempo de armazenamento. Na comparação de sementes armazenadas a 25°C/sementes armazenadas a 6°C, a proteína como a álcool desidrogenase (up-regulada) foi afetada pela temperatura, sendo associada com condição de estresse e rápida perda da viabilidade. Portanto, o armazenamento a 6°C prolongou a viabilidade das sementes em *C. legalis*, enquanto a 25°C resultou em maior redução na germinação e no acúmulo de proteínas envolvidas em condição de estresse e senescência celular. Como perspectivas futuras, é de grande importância compreender as alterações histomorfológicas que levam as sementes à deterioração, além de buscar metodologias que possam reduzir ainda mais a velocidade de deterioração das sementes ao longo de tempo.

Esses estudos forneceram informações inéditas e relevantes sobre eventos fisiológicos e bioquímicos, possibilitando otimizar as condições tanto para a propagação *in vitro*, quanto para a conservação de sementes de *C. legalis*. Os resultados apresentados nesta tese são de grande relevância para a conservação e propagação de *C. legalis,* uma espécie de alto valor econômico e ecológico, que se encontra ameaçada de extinção.

REFERÊNCIAS BIBLIOGRÁFICAS

Ahkami, A.H., Lischewski, S., Haensch, K.T., Porfirova, S., Hofmann, J., Rolletschek, H., Melzer, M., Franken, P., Hause, B., Druege, U., Hajirezaei, M.R. (2009). Molecular physiology of adventitious root formation in *Petunia hybrida* cuttings: involvement of wound response and primary metabolism. *New Phytol. 181*(3):613-625.

Alcázar, R., Altabella, T., Marco, F., Bortolotti, C., Reymond, M., Koncz, C., Carrasco, P., Tiburcio, A.F. (2010). Polyamines: molecules with regulatory functions in plant abiotic stress tolerance. *Planta. 231*(6):1237-1249.

Altamura, M. (1996). Root histogenesis in herbaceous and woody explants cultured *in vitro*. A critical review. *Agronomie. 16*(10):589-602.

Andreadakis, A., Kotzabasis, K. (1996). Changes in the biosynthesis and catabolism of polyamines in isolated plastids during chloroplast photodevelopment. *J. Photochem. Photobiol. B: Biol. 33*(2):163-170.

Aragão, V.P.M., Reis, R.S., Silveira, V., Santa-Catarina, C. (2017b). Putrescine promotes changes in the endogenous polyamine levels and proteomic profiles to regulate organogenesis in *Cedrela fissilis* Vellozo (Meliaceae). *Plant Cell Tiss Org Cult. 130*(3):495–505.

Aragão, V.P.M., Ribeiro, Y.R.d.S., Reis, R.S., Macedo, A.F., Floh, E.I.S., Silveira, V., Santa-Catarina, C. (2016). *In vitro* organogenesis of *Cedrela fissilis* Vell.(Meliaceae): the involvement of endogenous polyamines and carbohydrates on shoot development. *Plant Cell Tiss Org Cult. 124*(3):611-620.

Aragão, V.P.M., Silveira, V., Santa Catarina, C. (2017). Micropropagation of *Cariniana legalis* (Martius) O. Kuntze, An Endangered Hardwood Tree From The Brazilian Atlantic Forest. *Plant Cell Cult Micro. 13*:41-50.

Aragão, V.P.M., Silveira, V., Santa Catarina, C. (2017a). Micropropagation of *Cariniana legalis* (Martius) O. Kuntze, An Endangered Hardwood Tree From The Brazilian Atlantic Forest. *Plant Cell Cult Micro. 13*:41-50.

Aragão, V.P.M., Trindade, B.M.C., Reis, R.S., Silveira, V., Santa-Catarina, C. (2019). Storage time affects the germination and proteomic profile of seeds of *Cariniana legalis* (Mart.) O. Kuntze (Lecythidaceae), an endangered tree species native to the Brazilian Atlantic Forest. *Braz J Bot. 42*(3):407-419.

Beale, S.I. (1999). Enzymes of chlorophyll biosynthesis. *Photosynt Res. 60*(1):43-73.

Blakesley, D., Weston, G., Hall, J. (1991). The role of endogenous auxin in root initiation. *Plant Growth Regul. 10*(4):341-353.

Brasil. (2013). Instruções para análise de sementes e espécies florestais. Brasília. Secretaria de Defesa Agropecuária. 98p

Brown, D.E., Rashotte, A.M., Murphy, A.S., Normanly, J., Tague, B.W., Peer, W.A., Taiz, L., Muday, G.K. (2001). Flavonoids act as negative regulators of auxin transport in vivo in Arabidopsis. *Plant Physiol. 126*(2):524-535.

Budiarto, K. (2010). Spectral quality affects morphogenesis on *Anthurium* plantlet during *in vitro* culture. *Agrivita. 32*(3):234-240.

Buer, C.S., Imin, N., Djordjevic, M.A. (2010). Flavonoids: new roles for old molecules. *J Integr Plant Biol. 52*(1):98-111.

Bunn, E., Turner, S.R., Dixon, K.W. (2011). Biotechnology for saving rare and threatened flora in a biodiversity hotspot. *In Vitro Cell. Dev. Biol. Plant. 47*(1):188-200.

Burrieza, H.P., Rizzo, A.J., Vale, E.M., Silveira, V., Maldonado, S. (2019). Shotgun proteomic analysis of quinoa seeds reveals novel lysine-rich seed storage globulins. *Food chem. 293*:299-306.

Calderan-Rodrigues, M.J., Jamet, E., Bonassi, M.B.C.R., Guidetti-Gonzalez, S., Begossi, A.C., Setem, L.V., Franceschini, L.M., Fonseca, J.G., Labate, C.A. (2014). Cell wall proteomics of sugarcane cell suspension cultures. *Proteomics. 14*(6):738-749.

Carvalho, P.E.R. (1994). Espécies florestais brasileiras: recomendações silviculturais, potencialidades e uso da madeira (Colombo: Embrapa/CNPF ed.). Brasília: Embrapa/SPI. 640p

Carvalho, P.E.R. (2005). Jequitibá-rosa. Paraná: Embrapa Florestas. 10p

Chao, W.S., Gu, Y.-Q., Pautot, V., Bray, E.A., Walling, L.L. (1999). Leucine aminopeptidase RNAs, proteins, and activities increase in response to water deficit, salinity, and the wound signals systemin, methyl jasmonate, and abscisic acid. *Plant Physiol 120*(4):979-992.

Chiu, R.S., Pan, S., Zhao, R., Gazzarrini, S. (2016). ABA-dependent inhibition of the ubiquitin proteasome system during germination at high temperature in *Arabidopsis*. *The Plant J. 88*(5):749-761.

Conesa, A., Götz, S., García-Gómez, J.M., Terol, J., Talón, M., Robles, M. (2005). Blast2GO: a universal tool for annotation, visualization and analysis in functional genomics research. *Bioinformatics. 21*(18):3674-3676.

Correa, L., Stein, R., Fett-Neto, A. (2012). Adventitious rooting of detached *Arabidopsis thaliana* leaves. *Biol. Plant. 56*(1):25-30.

Corrêa, L.d.R., Paim, D.C., Schwambach, J., Fett-Neto, A.G. (2005). Carbohydrates as regulatory factors on the rooting of *Eucalyptus saligna* Smith and *Eucalyptus globulus* Labill. *Plant Growth Regul. 45*(1):63-73.

Cybularz-Urban, T., Hanus-Fajerska, E., Swiderski, A. (2007). Effect of light wavelength on *in vitro* organogenesis of a *Cattleya* hybrid. *Acta Biol Cracov. 49*(1):113-118.

Da Costa, C.T., De Almeida, M.R., Ruedell, C.M., Schwambach, J., Maraschin, F.D.S., Fett-Neto, A.G. (2013). When stress and development go hand in hand: main hormonal controls of adventitious rooting in cuttings. *Front. Plant Sci. 4*:133.

da Silva, J.A.T. (2013). The phloroglucinol conundrum: increase in root growth of hybrid *Cymbidium* (Orchidaceae) with no toxic effect on protocorm-like body formation. *Plant Tiss Cult Biotech. 23*(2):275-282.

da Silva, J.A.T., Dobránszki, J., Ross, S. (2013). Phloroglucinol in plant tissue culture. *In Vitro Cell Dev Biol-Plant. 49*(1):1-16.

Damerval, C., De Vienne, D., Zivy, M., Thiellement, H. (1986). Technical improvements in two-dimensional electrophoresis increase the level of genetic variation detected in wheat-seedling proteins. *Electrophoresis. 7*(1):52-54.

De Klerk, G.-J., Guan, H., Huisman, P., Marinova, S. (2011). Effects of phenolic compounds on adventitious root formation and oxidative decarboxylation of applied indoleacetic acid in *Malus* 'Jork 9'. *Plant Growth Regul. 63*(2):175-185.

De Klerk, G.-J., van der Krieken, W., de Jong, J.C. (1999). Review the formation of adventitious roots: new concepts, new possibilities. *In Vitro Cell. Dev. Biol. Plant. 35*(3):189-199.

Demotes-Mainard, S., Péron, T., Corot, A., Bertheloot, J., Le Gourrierec, J., Pelleschi-Travier, S., Crespel, L., Morel, P., Huché-Thélier, L., Boumaza, R. (2016). Plant responses to red and far-red lights, applications in horticulture. *Environ Exp Bot. 121*:4-21.

Dewir, Y.H., Murthy, H.N., Ammar, M.H., Alghamdi, S.S., Al-Suhaibani, N.A., Alsadon, A.A., Paek, K.Y. (2016). *In vitro* rooting of leguminous plants: Difficulties, alternatives, and strategies for improvement. *Hortic Environ Biotechnol. 57*(4):311-322.

Dias, P.C., de Oliveira, L.S., Xavier, A., Wendling, I. (2012). Estaquia e miniestaquia de espécies florestais lenhosas do Brasil. *Pesq Flor Bras. 32*(72):453-462.

Distler, U., Kuharev, J., Navarro, P., Levin, Y., Schild, H., Tenzer, S. (2014). Drift time-specific collision energies enable deep-coverage data-independent acquisition proteomics. *Nat. Methods. 11*(2):167-170.

Distler, U., Kuharev, J., Navarro, P., Tenzer, S. (2016). Label-free quantification in ion mobility–enhanced data-independent acquisition proteomics. *Nat protocols. 11*(4):795.

Do, C.-T., Pollet, B., Thévenin, J., Sibout, R., Denoue, D., Barrière, Y., Lapierre, C., Jouanin, L. (2007). Both caffeoyl Coenzyme A 3-*O*-methyltransferase 1 and caffeic acid *O*-methyltransferase 1 are involved in redundant functions for lignin, flavonoids and sinapoyl malate biosynthesis in Arabidopsis. *Planta. 226*(5):1117-1129.

Drew, R.A., Simpson, B.W., Osborne, W.J. (1991). Degradation of exogenous indole-3-butyric acid and riboflavin and their influence on rooting response of papaya *in vitro*. *Plant Cell Tiss. Org. Cult. 26*(1):29-34.

Epstein, E., Ludwig-Müller, J. (1993). Indole-3-butyric acid in plants: occurrence, synthesis, metabolism and transport. *Physiol Plant. 88*(2):382-389.

Geigenberger, P. (2003). Regulation of sucrose to starch conversion in growing potato tubers. *J Exp Bot. 54*(382):457-465.

Gillet, B., Beyly, A., Peltier, G., Rey, P. (1998). Molecular characterization of CDSP 34, a chloroplastic protein induced by water deficit in *Solanum tuberosum* L. plants, and regulation of CDSP 34 expression by ABA and high illumination. *The Plant J. 16*(2):257-262.

Gupta, S.D., Jatothu, B. (2013). Fundamentals and applications of light-emitting diodes (LEDs) in *in vitro* plant growth and morphogenesis. *Plant Biotechnol Rep. 7*(3):211-220.

Gupta, S.D., Sahoo, T. (2015). Light emitting diode (LED)-induced alteration of oxidative events during *in vitro* shoot organogenesis of *Curculigo orchioides* Gaertn. *Acta Physiol Plant. 37*(11):233.

Hazarika, B. (2006). Morpho-physiological disorders in *in vitro* culture of plants. *Sci Hortic. 108*(2):105-120.

He, D., Han, C., Yao, J., Shen, S., Yang, P. (2011). Constructing the metabolic and regulatory pathways in germinating rice seeds through proteomic approach. *J Prot. 11*(13):2693-2713.

He, D., Yang, P. (2013). Proteomics of rice seed germination. *Frontiers. 4*:246.

Heimgartner, U., Pietrzak, M., Geertsen, R., Brodelius, P., da Silva Figueiredo, A., Pais, M. (1990). Purification and partial characterization of milk clotting proteases from flowers of Cynara cardunculus. *Phytochemistry. 29*(5):1405-1410.

Heringer, A.S., Reis, R.S., Passamani, L.Z., de Souza-Filho, G.A., Santa-Catarina, C., Silveira, V. (2017). Comparative proteomics analysis of the effect of combined red and blue lights on sugarcane somatic embryogenesis. *Acta Physiol Plant. 39*(2):52.

Heringer, A.S., Santa-Catarina, C., Silveira, V. (2018). Insights from proteomic studies into plant somatic embryogenesis. *Proteomics. 18*(5-6):1-9.

Hernandez-Valladares, M., Aasebø, E., Mjaavatten, O., Vaudel, M., Bruserud, Ø., Berven, F., Selheim, F. (2016). Reliable FASP-based procedures for optimal quantitative proteomic and phosphoproteomic analysis on samples from acute myeloid leukemia patients. *Biol Proced Online 18*(1):13.

Hiraga, S., Sasaki, K., Ito, H., Ohashi, Y., Matsui, H. (2001). A large family of class III plant peroxidases. *Plant Cell Physiol. 42*(5):462-468.

Hunter, D.C., Burritt, D.J. (2005). Light quality influences the polyamine content of lettuce (*Lactuca sativa* L.) cotyledon explants during shoot production *in vitro*. *Plant growth regul. 45*(1):53-61.

Husain, M.K., Anis, M., Shahzad, A. (2008). *In vitro* propagation of a multipurpose leguminous tree (*Pterocarpus marsupium* Roxb.) using nodal explants. *Acta Physiol Plant. 30*(3):353-359.

Ignoul, S., Eggermont, J. (2005). CBS domains: structure, function, and pathology in human proteins. *Am. J. Physiol. Cell Physiol. 289*(6):C1369-C1378.

Ioannidis, N.E., Kotzabasis, K. (2007). Effects of polyamines on the functionality of photosynthetic membrane *in vivo* and *in vitro*. *Biochim Biophy Acta 1767*(12):1372-1382.

IUCN (2018) International Union for Conservation of Nature.The Red List of Threatened species. http://www.iucnredlist.org/about. Accessed 8th july 2018

IUCN (2019) The IUCN Red List of Threatened Species. Version 2019-2. http://www.iucnredlist.org. Accessed 8th may 2019

Jia, X.Y., He, L.H., Jing, R.L., Li, R.Z. (2009). Calreticulin: conserved protein and diverse functions in plants. *Physiol Plant. 136*(2):127-138.

Jin, Z.L., Ryu, S.H., Hong, J.K., Song, C.E., Lim, C.J., Choi, Y.J., Lee, K.O., Chung, W.S., Lee, S.Y., Lim, C.O. (2007). Over-expression of Chinese cabbage calreticulin 1b, BrCRT1b, induces initiation of organogenesis in *Arabidopsis*. *Genes Genom. 29*(3):409-418.

Jyoti, Malik, C.P. (2013). Seed deterioration: a review. *Int J LifeSc Bt & Pharm Res. 2*(3):375-385.

Keller, M.M., Jaillais, Y., Pedmale, U.V., Moreno, J.E., Chory, J., Ballaré, C.L. (2011). Cryptochrome 1 and phytochrome B control shade-avoidance responses in *Arabidopsis* via partially independent hormonal cascades. *The Plant J. 67*(2):195-207.

Kervinen, J., Kontturi, M., Mikola, J. (1990). Changes in the proteinase composition of barley leaves during senescence in field conditions. *Cer Res Communic. 18*:191-197.

Kim, S.-J., Hahn, E.-J., Heo, J.-W., Paek, K.-Y. (2004). Effects of LEDs on net photosynthetic rate, growth and leaf stomata of *chrysanthemum* plantlets *in vitro*. *Sci Horti. 101*(1-2):143-151.

Kirch, H.-H., Bartels, D., Wei, Y., Schnable, P.S., Wood, A.J. (2004). The ALDH gene superfamily of *Arabidopsis*. *Trends Plant Sci. 9*(8):371-377.

Kotzabasis, K., Strasser, B., Navakoudis, E., Senger, H., Dörnemann, D. (1999). The regulatory role of polyamines in structure and functioning of the photosynthetic apparatus during photoadaptation. *J. Photochem. Photobiol. B: Biol. 50*(1):45-52.

Kusano, T., Berberich, T., Tateda, C., Takahashi, Y. (2008). Polyamines: essential factors for growth and survival. *Planta. 228*(3):367-381.

Lazzarini, L.E.S., Bertolucci, S.K.V., Pacheco, F.V., dos Santos, J., Silva, S.T., de Carvalho, A.A., Pinto, J.E.B.P. (2018). Quality and intensity of light affect *Lippia gracilis* Schauer plant growth and volatile compounds *in vitro*. *Plant Cell Tiss Org Cult. 135*:367–379.

Lee, S., Tsai, F. (2005). Molecular chaperones in protein quality control. *J Biochem Mol Biol. 38*(3):259-265.

Leitner-Dagan, Y., Ovadis, M., Shklarman, E., Elad, Y., David, D.R., Vainstein, A. (2006). Expression and functional analyses of the plastid lipid-associated protein CHRC suggest its role in chromoplastogenesis and stress. *Plant Physiol. 142*(1):233-244.

Lerin, J., Aragão, V.P.M., Reis, R.S., Silveira, V., Santa-Catarina, C. (2019). Proteomic profile and polyamine contents are modulated by light source to promote *in vitro* shoot development in *Cariniana legalis* (Martius) O. Kuntze (Lecythidaceae). *Plant Cell Tiss Org Cult. 137*:329–342.

Letunic, I., Bork, P. (2016). Interactive tree of life (iTOL) v3: an online tool for the display and annotation of phylogenetic and other trees. *Nucleic Acids Res. 44*(W1):W242-W245.

Lipecka, J., Chhuon, C., Bourderioux, M., Bessard, M.A., van Endert, P., Edelman, A., Guerrera, I.C. (2016). Sensitivity of mass spectrometry analysis depends on the shape of the filtration unit used for filter aided sample preparation (FASP). *Proteomics. 16*(13):1852-1857.

Liu, J., Sheng, L., Xu, Y., Li, J., Yang, Z., Huang, H., Xu, L. (2014). *WOX*11 and 12 are involved in the first-step cell fate transition during de novo root organogenesis in *Arabidopsis*. *The Plant Cell. 26*(3):1081-1093.

Lloyd, G., McCown, B. (1981). Commercially-feasible micropropagation of mountain laurel, *Kalmia latifolia*, by use of shoot-tip culture. *Int Plant Propag Societ. 30*:421-427.

MacDonald, M.J., D'Cunha, G.B. (2007). A modern view of phenylalanine ammonia lyase. *Biochem. Cell Biol. 85*(3):273-282.

Massa, G.D., Kim, H.-H., Wheeler, R.M., Mitchell, C.A. (2008). Plant productivity in response to LED lighting. *HortScience. 43*(7):1951-1956.

Matta, L.B.V., Scudeller, V.V. (2012). Lecythidaceae Poit. in the Tupé Sustainable Development Reserve, Manaus, Brazil. *Braz J Bot. 35*(2):195-217.

Matthews, S., Noli, E., Demir, I., Khajeh-Hosseini, M., Wagner, M.-H. (2012). Evaluation of seed quality: from physiology to international standardization. *Seed Sci Res. 22*(S1):S69-S73.

Matton, D.P., Constabel, P., Brisson, N. (1990). Alcohol dehydrogenase gene expression in potato following elicitor and stress treatment. *Plant Mol. Biol. 14*(5):775-783.

Mengxi, L., Zhigang, X., Yang, Y., Yijie, F. (2011). Effects of different spectral lights on *Oncidium* PLBs induction, proliferation, and plant regeneration. *Plant Cell Tiss Org Cult. 106*(1):1-10.

Millán-Orozco, L., Corredoira, E., San José, M.d.C. (2011). *In vitro* rhizogenesis: histoanatomy of *Cedrela odorata* (Meliaceae) microcuttings. *Rev. Biol. Trop. 59*(1):447-453.

Muneer, S., Kim, E.J., Park, J.S., Lee, J.H. (2014). Influence of green, red and blue light emitting diodes on multiprotein complex proteins and photosynthetic activity under different light intensities in lettuce leaves (*Lactuca sativa* L.). *Int J Mol Sci. 15*(3):4657-4670.

Müntz, K., Belozersky, M.A., Dunaevsky, Y.E., Schlereth, A., Tiedemann, J. (2001). Stored proteinases and the initiation of storage protein mobilization in seeds during germination and seedling growth. *J Exp Bot. 52*(362):1741-1752.

Murashige, T., Skoog, F. (1962). A revised medium for rapid growth and bio assays with tobacco tissue cultures. *Physiol Plant. 15*(3):473-497.

Nanjo, Y., Skultety, L., Uváčková, L.u., Klubicová, K.n., Hajduch, M., Komatsu, S. (2012). Mass spectrometry-based analysis of proteomic changes in the root tips of flooded soybean seedlings. *J Prot Res. 11*(1):372-385.

Nguyen, T.-P., Cueff, G., Hegedus, D.D., Rajjou, L., Bentsink, L. (2015). A role for seed storage proteins in *Arabidopsis* seed longevity. *J Exp Bot. 66*(20):6399-6413.

Niemi, K., Sarjala, T., Chen, X., Häggman, H. (2002). Spermidine and methylglyoxal bis (guanylhydrazone) affect maturation and endogenous polyamine content of Scots pine embryogenic cultures. *J. Plant Physiol. 159*(10):1155-1158.

Olinares, P.D.B., Kim, J., Van Wijk, K.J. (2011). The Clp protease system; a central component of the chloroplast protease network. *Biochim Biophys Acta Bioenerg. 1807*(8):999-1011.

Oliveira, L.S.d., Dias, P.C., Brondani, G.E. (2013). Micropropagação de espécies florestais brasileiras. *Pes Florest Bras. 33*(76):439-453.

Oracz, K., Bouteau, H.E.M., Farrant, J.M., Cooper, K., Belghazi, M., Job, C., Job, D., Corbineau, F., Bailly, C. (2007). ROS production and protein oxidation as a novel mechanism for seed dormancy alleviation. *The Plant J. 50*(3):452-465.

Pacurar, D.I., Perrone, I., Bellini, C. (2014). Auxin is a central player in the hormone cross-talks that control adventitious rooting. *Physiol Plant. 151*(1):83-96.

Parimalan, R., Giridhar, P., Ravishankar, G. (2011). Enhanced shoot organogenesis in *Bixa orellana* L. in the presence of putrescine and silver nitrate. *Plant Cell Tiss Org Cult. 105*(3):285-290.

Park, J.S., Naing, A.H., Kim, C.K. (2016). Effects of ethylene on shoot initiation, leaf yellowing, and shoot tip necrosis in roses. *Plant Cell Tiss Org Cult. 127*(2):425-431.

Parveen, S., Shahzad, A. (2010). TDZ-induced high frequency shoot regeneration in *Cassia sophera* Linn. via cotyledonary node explants. *Physiol Mol Biol Plant. 16*(2):201-206.

Parveen, S., Shahzad, A., Saema, S. (2010). *In vitro* plant regeneration system for *Cassia siamea* Lam., a leguminous tree of economic importance. *Agroforest Syst. 80*(1):109-116.

Paschalidis, K.A., Roubelakis-Angelakis, K.A. (2005). Spatial and temporal distribution of polyamine levels and polyamine anabolism in different organs/tissues of the tobacco plant. Correlations with age, cell division/expansion, and differentiation. *Plant Physiol. 138*(1):142-152.

Pedmale, U.V., Huang, S.-s.C., Zander, M., Cole, B.J., Hetzel, J., Ljung, K., Reis, P.A., Sridevi, P., Nito, K., Nery, J.R. (2016). Cryptochromes interact directly with PIFs to control plant growth in limiting blue light. *Cell. 164*(1):233-245.

Peer, W.A., Bandyopadhyay, A., Blakeslee, J.J., Makam, S.N., Chen, R.J., Masson, P.H., Murphy, A.S. (2004). Variation in expression and protein localization of the PIN family of auxin efflux facilitator proteins in flavonoid mutants with altered auxin transport in *Arabidopsis thaliana*. *The Plant Cell. 16*(7):1898-1911.

Peer, W.A., Murphy, A.S. (2007). Flavonoids and auxin transport: modulators or regulators? *Trends Plant Sci. 12*(12):556-563.

Pérez, L.P., Montesinos, Y.P., Olmedo, J.G., Rodriguez, R.B., Sánchez, R.R., Montenegro, O.N., Escriba, R.C.R., Daniels, D., Gómez-Kosky, R. (2016). Effect of phloroglucinol on rooting and i*n vitro* acclimatization of papaya (*Carica papaya* L. var. Maradol Roja). *In Vitro Cell. Dev. Biol. Plant. 52*(2):196-203.

Persson, S., Wyatt, S.E., Love, J., Thompson, W.F., Robertson, D., Boss, W.F. (2001). The Ca2+ status of the endoplasmic reticulum is altered by induction of calreticulin expression in transgenic plants. *Plant Physiol. 126*(3):1092-1104.

Plaxton, W.C. (1996). The organization and regulation of plant glycolysis. *Annu Rev Plant biol. 47*(1):185-214.

Pradhan, B.K., Badola, H.K. (2012). Effect of storage conditions and storage periods on seed germination in eleven populations of *Swertia chirayita*: a critically endangered medicinal herb in Himalaya. *The Sci World J. 2012*:1-9.

Prieto-Dapena, P., Castaño, R., Almoguera, C., Jordano, J. (2006). Improved resistance to controlled deterioration in transgenic seeds. *Plant Physiol. 142*(3):1102-1112.

Pua, E.-C., Lee, J.E. (1995). Enhanced de novo shoot morphogenesis *in vitro* by expression of antisense 1-aminocyclopropane-1-carboxylate oxidase gene in transgenic mustard plants. *Planta. 196*(1):69-76.

R core team (2018) R: A Language and Environment for Statistical Computing. R Foundation for Statistical Computing, Vienna, Austria.

Rajjou, L., Debeaujon, I. (2008). Seed longevity: survival and maintenance of high germination ability of dry seeds. *C. R. Biol. 331*(10):796-805.

Ravanel, S., Gakière, B., Job, D., Douce, R. (1998). The specific features of methionine biosynthesis and metabolism in plants. *Proc Natl Acad Sci. 95*(13):7805-7812.

Rêgo, G.M. (2002). Jequitibá-rosa (*Cariniana legalis*): espécie em extinção da floresta Atlântica. Aracaju: Embrapa Tabuleiros Costeiros. 2p

Rego, G.M., Possamai, E. (2006). Efeito do Sombreamento sobre o Teor de Clorofila e Crescimento Inicial do Jequitibá-rosa. *Pesq Fl Bras*(53):179-194.

Reis, R.S., Vale, E.M., Heringer, A.S., Santa-Catarina, C., Silveira, V. (2016). Putrescine induces somatic embryo development and proteomic changes in embryogenic callus of sugarcane. *J Prot. 130*:170-179.

Ribeiro, M., Catenacci, F.S., Smith, N.P., Cabello, N.B. (2017) *Lecythidaceae* in Flora do Brasil 2020 em construção. Jardim Botânico do Rio de Janeiro. http://floradobrasil.jbrj.gov.br/reflora/floradobrasil/FB8543. Accessed 22 july 2019

Roberts, E.H. (1973). Predicting the storage life of seeds. *Seed Sci Technol. 1*:499-514.

Rogers, L.A., Campbell, M.M. (2004). The genetic control of lignin deposition during plant growth and development. *New Phytol. 164*(1):17-30.

Rosa, S.D.V.F.D., Pinho, É.V.R.V., Vieira, E.S.N., Veiga, R.D., Veiga, A.D. (2005). Enzimas removedoras de radicais livres e proteínas lea associadas à tolerância de sementes milho à alta temperatura de secagem. *Rev Bras Sementes. 27*(2):91-101.

Saibil, H. (2013). Chaperone machines for protein folding, unfolding and disaggregation. *Nat. Rev. Mol. Cell Biol. 14*(10):630–642.

Sang, Q., Shan, X., An, Y., Shu, S., Sun, J., Guo, S. (2017). Proteomic analysis reveals the positive effect of exogenous spermidine in tomato seedlings' response to high-temperature stress. *Front Plant Sci. 8*:120.

Sang, Y.L., Cheng, Z.J., Zhang, X.S. (2018). Plant stem cells and de novo organogenesis. *New Phytol. 218*(4):1334-1339.

Santa-Catarina, C., Silveira, V., Balbuena, T.S., Viana, A.M., Estelita, M.E.M., Handro, W., Floh, E.L.S. (2006). IAA, ABA, polyamines and free amino acids associated with zygotic embryo development of *Ocotea catharinensis*. *Plant Growth Regul. 49*(2-3):237-247.

Santelia, D., Henrichs, S., Vincenzetti, V., Sauer, M., Bigler, L., Klein, M., Bailly, A., Lee, Y., Friml, J., Geisler, M. (2008). Flavonoids redirect PIN-mediated polar auxin fluxes during root gravitropic responses. *J. Biol. Chem. 283*(45):31218-31226.

Sarropoulou, V., Maloupa, E. (2017). Effect of the NO donor "sodium nitroprusside"(SNP), the ethylene inhibitor "cobalt chloride"(CoCl 2) and the antioxidant vitamin E "α-tocopherol" on *in vitro* shoot proliferation of *Sideritis raeseri* Boiss. & Heldr. subsp. *raeseri*. *Plant Cell Tiss Org Cult. 128*(3):619-629.

Shaban, M. (2013). Review on physiological aspects of seed deterioration. *Intl J Agri Crop Sci. 6*(11):627-631.

Shelar, V., Shaikh, R., Nikam, A. (2008). Soybean seed quality during storage: a review. *J Agric Rev. 29*(2):125-131.

Simões, I., Faro, C. (2004). Structure and function of plant aspartic proteinases. *Eur. J. Biochem. 271*(11):2067-2075.

Singh, D., Basu, C., Meinhardt-Wollweber, M., Roth, B. (2015). LEDs for energy efficient greenhouse lighting. *Renew Sust Energ Rev. 49*:139-147.

Skoda, B., Malek, L. (1992). Dry pea seed proteasome: purification and enzymic activities. *Plant Physiol. 99*(4):1515-1519.

Smith, H. (1982). Light quality, photoperception, and plant strategy. *Annual Rew Plant Physiol. 33*(1):481-518.

Sokal, R.R., Rohlf, F.J. (1995). *Biometry* (ed.). NY: WH Freeman and Co.

Sousa, K.R., Aragão, V.P.M., Reis, R.S., Macedo, A.F., Vieira, H.D., de Souza, C.L.M., Floh, E.I.S., Silveira, V., Santa-Catarina, C. (2016). Polyamine, amino acid, and carbohydrate profiles during seed storage of threatened woody species of the Brazilian Atlantic Forest may be associated with seed viability maintenance. *Braz J Bot. 39*(4):985-995.

Stevens, M.E., Pijut, P.M. (2018). Rapid *in vitro* shoot multiplication of the recalcitrant species *Juglans nigra* L. *In Vitro Cell Develop Biol-Plant. 54*(3):309-317.

Strommer, J. (2011). The plant ADH gene family. *The Plant J. 66*(1):128-142.

Sukumar, P., Maloney, G.S., Muday, G.K. (2013). Localized induction of the ATP-binding cassette B19 auxin transporter enhances adventitious root formation in Arabidopsis. *Plant Physiol. 162*(3):1392-1405.

Swaine, M.D., Whitmore, T. (1988). On the definition of ecological species groups in tropical rain forests. *Vegetatio. 75*(1-2):81-86.

Tang, Z., Du, W., Du, X., Ban, Y., Cheng, J. (2016). iTRAQ protein profiling of adventitious root formation in mulberry hardwood cuttings. *J Plant Grow Regul. 35*(3):618-631.

Thangjam, R., Sahoo, L. (2012). *In vitro* regeneration and *Agrobacterium tumefaciens*-mediated genetic transformation of *Parkia timoriana* (DC.) Merr.: a multipurpose tree legume. *Acta physiol plant. 34*(3):1207-1215.

Timotijević, G.S., Milisavljević, M.D., Radović, S.R., Konstantinović, M.M., Maksimović, V.R. (2010). Ubiquitous aspartic proteinase as an actor in the stress response in buckwheat. *J. Plant Physiol. 167*(1):61-68.

Timperio, A.M., Egidi, M.G., Zolla, L. (2008). Proteomics applied on plant abiotic stresses: role of heat shock proteins (HSP). *J prot. 71*(4):391-411.

Torres, S.B. (2005). Qualidade de sementes de melancia armazenadas em diferentes embalagens e ambientes. *Rev Ciên Agro. 36*(2):163-168.

Trindade, B.M.C., Reis, R.S., Vale, E.M., Santa-Catarina, C., Silveira, V. (2018). Proteomics analysis of the germinating seeds of *Cariniana legalis* (Mart.) Kuntze (Meliaceae): an endangered species of the Brazilian Atlantic Rainforest. *Braz J Bot. 41*(1):117-128.

Vahdati, K., Leslie, C., Zamani, Z., McGranahan, G. (2004). Rooting and acclimatization of *in vitro*-grown shoots from mature trees of three *Persian walnut* cultivars. *HortScience. 39*(2):324-327.

Vander Mijnsbrugge, K., Meyermans, H., Van Montagu, M., Bauw, G., Boerjan, W. (2000). Wood formation in poplar: identification, characterization, and seasonal variation of xylem proteins. *J Planta. 210*(4):589-598.

Vanholme, R., Demedts, B., Morreel, K., Ralph, J., Boerjan, W. (2010). Lignin biosynthesis and structure. *Plant Physiol. 153*(3):895-905.

Vieira, R.D., Krzyzanowski, F.C., França Neto, J.D.B. (1999). Vigor de sementes: conceitos e testes (Vol. 1). Londrina: ABRATES. 26p

Vieira, T.O., Lage-Pinto, F., Ribeiro, D.R., Alencar, T.d.S., Vitória, A.P. (2012). Estresse luminoso em plântulas de jequitibá-rosa *(Cariniana legalis*, Lecythidaceae): monitoramento da capacidade de aclimatação fotossintética sob duas intensidades de luz. *Vértices. 13*(3):129-142.

Von Wettstein, D., Gough, S., Kannangara, C.G. (1995). Chlorophyll biosynthesis. *The Plant Cell. 7*(7):1039-1057.

Wan, L., Ross, A.R., Yang, J., Hegedus, D.D., Kermode, A.R. (2007). Phosphorylation of the 12 S globulin cruciferin in wild-type and *abi1-1* mutant *Arabidopsis thaliana* (thale cress) seeds. *Biochem. J. 404*(2):247-256.

Wang, F., Zhu, D., Huang, X., Li, S., Gong, Y., Yao, Q., Fu, X., Fan, L.-M., Deng, X.W. (2009). Biochemical insights on degradation of *Arabidopsis* DELLA proteins gained from a cell-free assay system. *The Plant Cell. 21*(8):2378-2390.

Wang, Z., Hua, J., Yin, Y., Gu, C., Yu, C., Shi, Q., Guo, J., Xuan, L., Yu, F. (2019). An Integrated Transcriptome and Proteome Analysis Reveals Putative Regulators of Adventitious Root Formation in *Taxodium* 'Zhongshanshan'. *Inter j mol sci. 20*(5):1225.

Yamashita, T., Nishimura, K., Saiki, R., Okudaira, H., Tome, M., Higashi, K., Nakamura, M., Terui, Y., Fujiwara, K., Kashiwagi, K., Igarashi, K. (2013). Role of polyamines at the G1/S boundary and G2/M phase of the cell cycle. *The Int J Biochem Cell Biol 45*(6):1042-1050.

Yang, Y., Sulpice, R., Himmelbach, A., Meinhard, M., Christmann, A., Grill, E. (2006). Fibrillin expression is regulated by abscisic acid response regulators and is involved in abscisic acid-mediated photoprotection. *Proc Nat Acad Sci. 103*(15):6061-6066.

Yokota, S.-i., Yanagi, H., Yura, T., Kubota, H. (1999). Cytosolic Chaperonin Is Up-regulated during Cell Growth: preferential expression and binding to tubulin at g1/s transition through early s phase. *J Biol Chemis. 274*(52):37070-37078.

Youssef, A., Laizet, Y.h., Block, M.A., Maréchal, E., Alcaraz, J.P., Larson, T.R., Pontier, D., Gaffé, J., Kuntz, M. (2010). Plant lipid-associated fibrillin proteins condition jasmonate production under photosynthetic stress. *The Plant J. 61*(3):436-445.

Zeeman, S.C., Kossmann, J., Smith, A.M. (2010). Starch: its metabolism, evolution, and biotechnological modification in plants. *Annu Rev Plant Biol. 61*:209-234.

Zhang, J., Peer, W.A. (2017). Auxin homeostasis: the DAO of catabolism. *Jexp bot. 68*(12):3145-3154.

Zhang, S., Wu, J., Yuan, D., Zhang, D., Huang, Z., Xiao, L., Yang, C. (2014). Perturbation of auxin homeostasis caused by mitochondrial *FtSH4* gene-mediated peroxidase accumulation regulates *Arabidopsis* architecture. *Mol plant. 7*(5):856-873.

Zhang, S., Zhou, H., Yu, F., Bai, C., Zhao, Q., He, J., Liu, C. (2016). Structural insight into the cooperation of chloroplast chaperonin subunits. *BMC Biol. 14*(1):29.

Zhou, J., Wu, H., Collet, G. (1992). Histological study of initiation and development *in vitro* of adventitious roots in minicuttings of apple rootstocks of M 26 and EMLA 9. *Physiol Plant. 84*(3):433-440.

APÊNDICES

Apêndice A – Capítulo: Proteomic profile and polyamine contents are modulated by light source to promote *in vitro* shoot development in *Cariniana legalis* (Martius) O. Kuntze (lecythidaceae)

Tabela suplementar 1: Lista completa de todas as proteínas idetificadas

accession	description	max score	reported peptides	sequence coverage	FLUORESCENT 1	FLUORESCENT 2	FLUORESCENT 3	LED3 1	LED3 2	LED3 3	AVERAGE FLUORESCENT	AVERAGE LED3	Test-t	Log2 fc - LED/Fluorescente	Differential accumulation
A0A251SX18	Malate dehydrogenase OS=Helianthus annuus GN	11010.45	11	39.55	125306	128367	110150	189283	144543	217294	121274	183707	0.04649	0.60	UP
A0A251V667	Putative NADP-dependent glyceraldehyde-3-phos	1304.85	6	17.14	30029	30114	23613	46005	41940	40546	27919	42830	0.005285	0.62	UP
Q9M504	Catalase OS=Helianthus annuus GN=CATA2 PE=2	2231.62	6	14.84	39561	52092	45496	77458	59942	77822	45716	71741	0.019778	0.65	UP
A0A251VPF5	Putative chaperonin-60alpha OS=Helianthus annu	2186.83	6	11.66	50892	54335	44197	98410	77406	90371	49808	88729	0.004623	0.83	UP
A0A251RV70	Putative biotin carboxylase 2, chloroplastic OS=He	969.03	3	9.80	16201	17755	15625	28129	31756	36420	16527	32102	0.003295	0.96	UP
A0A251RND2	Putative hydroxypyruvate reductase OS=Helianth	530.94	3	7.10	17480	17983	13901	31264	36075	28638	16454	31992	0.003556	0.96	UP
A0A251VPP7	Putative chaperonin 20 OS=Helianthus annuus GN	1236.32	2	11.36	26782	25071	22250	51673	38724	54699	24701	48365	0.009563	0.97	UP
A0A251TPX4	Putative chaperonin 60 beta OS=Helianthus annu	4692.02	15	34.11	91717	104209	78655	178312	217475	148407	91527	181398	0.013518	0.99	UP
A0A251TTN4	Putative ribulose bisphosphate carboxylase/oxyge	14467.90	21	50.73	121002	125851	120568	268881	214922	250950	122473	244917	0.00155	1.00	UP
A0A251V3J4	Putative glutamate synthase 1 OS=Helianthus ann	262.50	5	3.83	16106	18433	13357	29009	30580	43360	15965	34316	0.018415	1.10	UP
A0A251VIG0	Lipoxygenase OS=Helianthus annuus GN=LOXC1 P	377.88	3	3.30	42058	58391	34180	84655	91026	116813	44877	97498	0.01232	1.12	UP
A0A251TN12	Polyadenylate-binding protein OS=Helianthus ann	712.20	3	7.35	15626	17992	19594	42985	31581	44746	17737	39771	0.006777	1.16	UP
A0A251VBK3	Putative chaperonin Cpn60/TCP-1 family OS=Helia	3275.08	12	26.71	13666	14923	13422	66840	49550	58046	14004	58145	0.000918	2.05	UP
A0A251SKJ6	Putative cell division cycle protein OS=Helianthus	4363.94	20	25.03	14385	15026	12806	40400	83988	59719	14072	61369	0.020023	2.12	UP
A0A251TD80	Tubulin alpha chain OS=Helianthus annuus GN=TB	7482.28	15	40.98	5833	5587	6446	59424	75348	58776	5955	64516	0.000418	3.44	UP
A0A251RL41	Tubulin beta chain OS=Helianthus annuus GN=TB	10869.76	11	41.35				9420	18832	10500		12917	_	_	UNIQUE LED
A0A251U6F5	Putative alcohol dehydrogenase superfamily, zinc	10186.94	14	38.42				76452	72832	51852		67045	_	_	UNIQUE LED
A0A251SHB7	Putative pyridoxal phosphate-dependent decarbo	1798.64	3	15.05				9244	11698	9787		10243	_	_	UNIQUE LED
A0A251VIL2	Tubulin alpha chain OS=Helianthus annuus GN=TB	11394.47	19	48.78	98956	91753	110998				100569		_	_	UNIQUE FLU
A0A251UUW2	Putative alcohol dehydrogenase superfamily, zinc	10204.29	14	36.68	3295	3681	3239				3405		_	_	UNIQUE FLU
A0A251UC35	Glutamine synthetase OS=Helianthus annuus GN=	5200.04	3	15.13	854	792	1026				891		_	_	UNIQUE FLU
A0A251UP18	Histone H4 OS=Helianthus annuus GN=HannXRQ_	4763.81	6	42.98	11334	14237	8248				11273		_	_	UNIQUE FLU
A0A251V7Z7	Putative HEAT SHOCK PROTEIN 89.1 OS=Helianth	2960.25	7	11.69	1361	1106	1349				1272		_	_	UNIQUE FLU
A0A251S412	Succinate dehydrogenase [ubiquinone] flavoprote	1981.89	6	14.14	13789	14784	12725				13766		_	_	UNIQUE FLU
A0A251SZA2	Putative AAA-type ATPase family protein OS=Heli	1538.46	3	11.43	13330	15218	25632				18060		_	_	UNIQUE FLU

A0A251SJQ7	Putative aldehyde/histidinol dehydrogenase OS=H	1397.48	4	10.51	64091	80763	117326				87393		_	_	UNIQUE FLU
A0A251SNE7	Tubulin beta chain OS=Helianthus annuus GN=TB	12647.23	18	52.22	25130	18189	57293	2253	1975	3609	33537	2612	0.062306	-3.68	UNCHANG
A0A251TAE7	Putative small GTPase superfamily, Rab type OS=	11400.27	8	49.39	111811	205079	534972	89729	73998	135726	283954	99817	0.228689	-1.51	UNCHANG
A0A251UAE5	Putative NADH-ubiquinone oxidoreductase OS=H	299.83	2	2.69	100876	102151	110760	114019	20164	18650	104596	50944	0.165734	-1.04	UNCHANG
A0A251V7G0	Putative succinyltransferase OS=Helianthus annu	945.01	5	13.78	32774	28793	66436	20307	17848	26206	42668	21454	0.156901	-0.99	UNCHANG
A0A251UBX5	Putative inorganic pyrophosphatase OS=Helianth	1941.84	3	21.33	19915	21262	27362	18516	2964	14390	22847	11957	0.103618	-0.93	UNCHANG
A0A251UGR1	S-(hydroxymethyl)glutathione dehydrogenase OS	3166.55	3	10.08	46016	69421	60153	19062	45806	30657	58530	31842	0.060748	-0.88	UNCHANG
A0A251SAT8	UTP--glucose-1-phosphate uridylyltransferase OS	771.24	3	7.66	59778	54636	75673	47429	18325	39946	63362	35233	0.059475	-0.85	UNCHANG
A0A251V5D4	Putative 26S proteasome AAA-ATPase subunit RP	3460.73	15	51.77	76525	49478	255567	37234	122315	54328	127190	71292	0.467429	-0.84	UNCHANG
A0A251RKM4	Putative luminal-binding protein OS=Helianthus a	17387.72	27	42.55	98576	67585	151336	68112	48319	65768	105832	60733	0.148401	-0.80	UNCHANG
A0A251S3K4	Alpha-mannosidase OS=Helianthus annuus GN=H	264.53	2	1.50	51781	42132	32541	26625	10684	35704	42151	24338	0.124385	-0.79	UNCHANG
A0A251SFI7	Serine hydroxymethyltransferase OS=Helianthus	825.85	5	13.38	26234	20712	34570	14447	18898	14293	27172	15879	0.058481	-0.77	UNCHANG
A0A251SL31	Putative ATPase, AAA-type, core OS=Helianthus a	6954.87	21	30.93	36614	33668	35221	5727	23343	32627	35168	20566	0.139549	-0.77	UNCHANG
A0A251V9X3	Phosphoribulokinase OS=Helianthus annuus GN=	732.79	6	17.28	4052	3658	4168	1273	3678	2119	3959	2356	0.090344	-0.75	UNCHANG
A0A251RS16	Putative ATPase, AAA-type, core OS=Helianthus a	1350.27	11	24.25	60848	47115	80923	37017	26625	50831	62962	38158	0.108917	-0.72	UNCHANG
P85194	Oxygen-evolving enhancer protein 1, chloroplasti	13591.83	12	41.67	338669	355635	424297	277623	123549	283467	372867	228213	0.068866	-0.71	UNCHANG
A0A251UFA4	Putative nucleotide-binding alpha-beta plait doma	3043.42	3	13.26	147500	89910	141077	92533	36414	103841	126162	77596	0.154289	-0.70	UNCHANG
A0A251SFZ4	Putative aldo/keto reductase/potassium channel	2914.12	4	17.46	10523	8665	9936	3242	1464	13368	9708	6024	0.381334	-0.69	UNCHANG
A0A251UVM5	Phospholipase D OS=Helianthus annuus GN=PLDA	205.35	2	2.26	15753	17715	13138	5933	3677	19315	15535	9642	0.308637	-0.69	UNCHANG
A0A251V047	Chlorophyll a-b binding protein, chloroplastic OS=	18412.96	6	43.35	231565	225519	337595	184474	120974	187807	264893	164418	0.076816	-0.69	UNCHANG
A1Y2J9	Phosphoglycerate kinase OS=Helianthus annuus G	7687.09	12	30.17	75740	60349	107649	49428	36252	66016	81246	50565	0.134283	-0.68	UNCHANG
A0A251S8W7	Glyceraldehyde-3-phosphate dehydrogenase OS=	16108.83	10	33.63	79632	77064	67471	64053	19419	58274	74722	47248	0.130929	-0.66	UNCHANG
A0A251SDV8	Putative triosephosphate isomerase, Aldolase-typ	7089.03	5	27.09	120641	121728	119151	84646	29571	115249	120507	76489	0.154076	-0.66	UNCHANG
A0A251UCL5	6-phosphogluconate dehydrogenase, decarboxyla	978.01	3	8.28	33856	33383	33024	27313	4875	32924	33421	21704	0.243469	-0.62	UNCHANG
A0A251VH41	Malate dehydrogenase OS=Helianthus annuus GN	1635.45	6	20.11	51664	43191	69619	28229	47473	32051	54824	35918	0.124839	-0.61	UNCHANG
A0A251VP43	Putative nascent polypeptide-associated complex	1846.27	3	20.40	43325	34768	47759	38526	5296	39046	41951	27623	0.29135	-0.60	UNCHANG
A0A251RZ67	Putative cysteine synthase OS=Helianthus annuus	3754.35	5	25.96	71143	60924	103032	42483	32347	80425	78366	51752	0.241249	-0.60	UNCHANG
A0A251SM18	Putative calcium-binding EF-hand family protein C	2200.62	2	14.47	24216	26902	16681	15641	12337	17594	22600	15191	0.09635	-0.57	UNCHANG
A0A251S3M6	Proteasome subunit alpha type OS=Helianthus an	1210.49	4	23.39	24828	25067	24491	16138	8368	25882	24795	16796	0.189702	-0.56	UNCHANG
A0A251TIG3	Tubulin beta chain OS=Helianthus annuus GN=TB	10945.10	17	42.00	23630	24080	32019	23121	12781	18448	26576	18117	0.104644	-0.55	UNCHANG
A0A251T314	Putative 26S protease regulatory subunit 10B OS=	1232.05	3	11.78	12607	8811	18532	9822	6162	11302	13316	9096	0.259444	-0.55	UNCHANG
A0A251RW81	Putative DEAD/DEAH box RNA helicase family pro	2105.11	9	39.44	25853	29384	32493	16199	26720	17095	29243	20005	0.075664	-0.55	UNCHANG
A0A251T3E2	Proteasome subunit beta type OS=Helianthus anr	2479.08	2	7.64	25110	23708	28513	18080	15568	19276	25777	17641	0.010596	-0.55	UNCHANG
A0A251T8X7	Chlorophyll a-b binding protein, chloroplastic OS=	2653.26	3	7.44	153800	134231	184400	123007	74110	126529	157477	107882	0.090663	-0.55	UNCHANG
A0A251U871	Putative 31 kDa ribonucleoprotein OS=Helianthus	3619.12	2	8.14	57116	34150	68980	58841	7179	45017	53415	37012	0.42579	-0.53	UNCHANG
A0A251T8N9	Serine hydroxymethyltransferase OS=Helianthus	1744.54	7	17.79	83827	68753	103034	56326	36394	84786	85205	59169	0.204489	-0.53	UNCHANG
A0A251UU89	Proteasome subunit alpha type OS=Helianthus an	1298.77	3	13.01	31006	25268	33055	17166	12404	32740	29776	20770	0.242207	-0.52	UNCHANG
A0A251TK20	Putative photosystem II PsbH, phosphoprotein OS	1236.56	2	11.60	44808	53463	39287	30256	20978	44728	45853	31988	0.160032	-0.52	UNCHANG
A0A251U7G3	Peptidyl-prolyl cis-trans isomerase OS=Helianthus	5198.51	3	16.67	104248	114928	78763	71101	65960	71134	99313	69399	0.051197	-0.52	UNCHANG

A0A251UAH6	Putative isocitrate dehydrogenase [NAD] regulato	735.11	2	8.95	29040	26955	47425	22116	29450	22721	34473	24762	0.232942	-0.48	UNCHANG
A0A251SDE9	Putative ribulose bisphosphate carboxylase/oxyge	14622.52	27	62.40	339767	348530	330377	263986	201240	277731	339558	247652	0.018933	-0.46	UNCHANG
A0A251RL35	Putative photosystem I reaction center subunit II	13848.99	6	42.44	144753	173724	98720	95067	89230	120946	139066	101748	0.193656	-0.45	UNCHANG
A0A251V0F8	Sucrose synthase OS=Helianthus annuus GN=SUS	448.08	5	5.60	28635	30364	33815	22653	20704	25208	30938	22855	0.015711	-0.44	UNCHANG
A0A251VCJ8	Malate dehydrogenase OS=Helianthus annuus GN	10229.14	9	27.71	222974	230025	178782	161956	132622	172206	210594	155595	0.050984	-0.44	UNCHANG
A0A251TLQ4	Putative caffeoyl-CoA O-methyltransferase OS=He	1767.80	3	17.62	20995	19155	19925	8352	20332	15723	20025	14802	0.213013	-0.44	UNCHANG
A0A251V9V2	Chlorophyll a-b binding protein, chloroplastic OS=	14908.76	7	41.89	280000	324941	372188	302594	101020	320031	325709	241219	0.32377	-0.43	UNCHANG
A0A251U205	Purple acid phosphatase OS=Helianthus annuus G	981.10	3	4.87	64180	64659	65488	53774	49378	40884	64776	48012	0.011613	-0.43	UNCHANG
A0A251SP12	Putative triosephosphate isomerase, Aldolase-typ	1683.62	2	6.77	72800	64619	70987	67508	30409	57059	69469	51657	0.190717	-0.43	UNCHANG
A0A251UJ06	Putative transaldolase/Fructose-6-phosphate aldo	637.84	5	11.98	44249	48063	45063	39711	25266	38087	45792	34354	0.072254	-0.41	UNCHANG
A0A251TUX6	Isocitrate dehydrogenase [NADP] OS=Helianthus	669.42	4	8.26	45642	48728	46287	43126	17152	45517	46886	35265	0.272089	-0.41	UNCHANG
A0A251VJF8	Putative 2,3-bisphosphoglycerate-independent ph	1212.76	6	14.16	67489	67337	64994	41068	53262	57171	66607	50500	0.030606	-0.40	UNCHANG
A0A251THW2	Putative SPFH/Band 7/PHB domain-containing me	3129.66	7	32.52	132044	127128	114966	79548	70823	133953	124712	94779	0.215989	-0.40	UNCHANG
A0A251VHR4	Aspartate aminotransferase OS=Helianthus annuu	512.06	4	7.60	32897	32507	29268	21908	20567	29750	31557	24075	0.072407	-0.39	UNCHANG
A0A251U736	Histone H2B OS=Helianthus annuus GN=HannXRQ	13697.66	5	39.10	203970	220275	287302	176019	143092	228774	237182	182628	0.200974	-0.38	UNCHANG
A0A251TNI0	40S ribosomal protein SA OS=Helianthus annuus	9881.03	10	45.61	133095	146355	116682	101242	97066	107039	132044	101782	0.028793	-0.38	UNCHANG
A0A251SEI5	Putative guanine nucleotide-binding protein subu	706.76	4	13.76	55694	56339	52562	57385	34215	35779	54865	42459	0.176455	-0.37	UNCHANG
A0A251RMS7	Putative ribosomal protein S3, eukaryotic/archae	4051.45	6	23.67	81485	87366	70021	68046	42547	74726	79624	61773	0.181455	-0.37	UNCHANG
A0A251S9G8	Putative photosystem I subunit K OS=Helianthus a	5157.66	3	35.11	73744	65036	70481	97085	14182	51219	69754	54162	0.553089	-0.36	UNCHANG
A0A251TIU9	Cysteine synthase OS=Helianthus annuus GN=CYS	2964.47	8	28.92	37238	31572	39140	28113	11948	44314	35983	28125	0.459667	-0.36	UNCHANG
A0A251S612	Aminomethyltransferase OS=Helianthus annuus G	2901.22	8	28.65	345183	352856	375711	316566	82710	444213	357916	281163	0.510011	-0.35	UNCHANG
A0A251VRZ2	Putative fructokinase-2 OS=Helianthus annuus GN	2002.73	4	13.68	60200	43143	56409	64891	12576	48817	53251	42095	0.531599	-0.34	UNCHANG
A0A172W418	Photosystem I iron-sulfur center OS=Helianthus a	36270.49	8	81.48	267544	265905	303088	229427	225521	206693	278846	220547	0.014146	-0.34	UNCHANG
A0A251T3T1	Malate dehydrogenase OS=Helianthus annuus GN	2435.07	5	20.95	35978	33775	42127	15989	43402	29186	37293	29525	0.40234	-0.34	UNCHANG
A0A251T3D2	Glyceraldehyde-3-phosphate dehydrogenase OS=	20128.51	9	26.76	222804	222169	217758	198081	110110	219287	220910	175826	0.249122	-0.33	UNCHANG
A0A251UTE2	Putative alcohol dehydrogenase 1 OS=Helianthus	12212.77	19	48.92	432984	434983	355845	373523	228322	374307	407937	325384	0.208312	-0.33	UNCHANG
A0A251RQT3	Putative peptidyl-prolyl cis-trans isomerase prote	1104.53	3	8.82	145118	141916	147191	125296	89422	132328	144742	115682	0.095513	-0.32	UNCHANG
A0A251TQC4	Putative leucine aminopeptidase 2, chloroplastic	1289.28	8	15.98	54704	51665	56041	43418	41863	45021	54137	43434	0.002499	-0.32	UNCHANG
A0A251SGR2	Putative 14-3-3-like protein OS=Helianthus annuu	3452.91	10	38.22	87495	83679	109644	85670	63308	76793	93606	75257	0.151898	-0.31	UNCHANG
A0A251U2V1	Putative gamma aminobutyrate transaminase 3 p	783.17	4	12.37	30412	46074	68501	41086	24059	51460	48329	38867	0.525982	-0.31	UNCHANG
A0A251SM99	Putative heat shock protein Hsp90 family OS=Heli	3165.66	21	18.05	90171	99567	129846	75005	81542	100619	106528	85722	0.217375	-0.31	UNCHANG
A0A251VJB1	Putative peroxisomal 3-ketoacyl-CoA thiolase 3 O	1087.64	4	12.47	52778	50459	53662	39757	35506	51310	52300	42191	0.103853	-0.31	UNCHANG
A0A251T8A4	Glucose-1-phosphate adenylyltransferase OS=Hel	928.28	4	12.74	28068	29741	27443	25552	10171	33234	28417	22986	0.470071	-0.31	UNCHANG
A0A251SVC1	Glycine cleavage system P protein OS=Helianthus	1585.96	8	15.36	11257	10249	13393	4902	14146	9270	11633	9440	0.480955	-0.30	UNCHANG
A0A251VCR5	Malic enzyme OS=Helianthus annuus GN=MAOC P	324.27	2	5.40	31206	34856	38577	24126	28350	32943	34880	28473	0.125703	-0.29	UNCHANG
A0A251U031	Putative aldehyde dehydrogenase OS=Helianthus	1263.68	7	10.97	42313	41748	57891	38789	32561	44533	47318	38628	0.241051	-0.29	UNCHANG
A0A251TYG9	ATP synthase subunit beta OS=Helianthus annuus	16500.30	19	44.36	205339	169696	194767	152607	166494	147310	189934	155470	0.045571	-0.29	UNCHANG
A0A251RXQ5	Putative nucleotide-binding alpha-beta plait doma	4378.06	2	12.33	136660	137544	144122	104308	137866	100955	139442	114376	0.105333	-0.29	UNCHANG
A0A251S3U7	Glucose-1-phosphate adenylyltransferase OS=Hel	870.72	5	10.47	15266	18236	16231	17523	5997	17314	16578	13611	0.489968	-0.28	UNCHANG

A0A251UJB3	Proteasome endopeptidase complex OS=Helianth	1835.77	2	11.56	43088	43378	71957	46252	28480	56788	52808	43840	0.517375	-0.27	UNCHANG
A0A251TT89	Putative peptidase M17, leucine aminopeptidase/	1292.52	4	7.88	41433	46279	45692	40233	31187	39581	44468	37000	0.085674	-0.27	UNCHANG
A0A251S2E6	Putative aldolase-type TIM barrel family protein O	9502.52	6	25.29	41430	37448	63534	39369	22012	57226	47471	39535	0.574751	-0.26	UNCHANG
F2VYC9	Beta-hydroxyacyl-ACP dehydratase OS=Helianthu	2252.46	3	15.86	49187	30229	67877	44502	40876	37373	49098	40917	0.500595	-0.26	UNCHANG
A0A251SZ13	Aspartate aminotransferase OS=Helianthus annuu	593.70	2	6.21	48833	11604	13297	20494	21386	19811	24578	20564	0.757609	-0.26	UNCHANG
A0A251VIE1	Putative alpha-1,4-glucan-protein synthase [UDP-	2530.00	3	11.86	40376	36362	51868	25275	36105	46303	42869	35894	0.413241	-0.26	UNCHANG
A0A251S4I0	Thioredoxin reductase OS=Helianthus annuus GN	486.20	2	9.19	24389	28463	24629	18479	28443	18176	25827	21699	0.318046	-0.25	UNCHANG
A0A251T841	Putative protochlorophyllide oxidoreductase OS=	1050.38	2	9.55	72004	77630	71331	45519	55353	86309	73655	62394	0.416911	-0.24	UNCHANG
A0A251VHX8	GTP-binding nuclear protein OS=Helianthus annu	6330.59	9	42.99	75032	73599	76108	75179	44679	70696	74913	63518	0.298092	-0.24	UNCHANG
A0A251S7I3	Pyruvate dehydrogenase E1 component subunit a	796.17	4	11.45	31149	31633	38835	28786	26967	30570	33873	28774	0.131397	-0.24	UNCHANG
A0A251SWL4	Histone H2A OS=Helianthus annuus GN=HannXRO	2026.72	2	12.12	82498	100004	65987	70985	59210	81083	82829	70426	0.348096	-0.23	UNCHANG
A0A251SYY4	Putative mitochondrial-processing peptidase subu	741.35	4	8.35	32712	32225	41666	32506	30839	27846	35535	30397	0.200799	-0.23	UNCHANG
A0A251RNE8	Peroxidase OS=Helianthus annuus GN=HannXRQ_	2901.50	4	22.53	170293	160778	159735	157758	148443	114673	163602	140291	0.159589	-0.22	UNCHANG
A0A251S377	Putative phosphoglucomutase/phosphomannom	771.20	6	11.47	35000	32888	37712	30941	22185	37550	35200	30225	0.346226	-0.22	UNCHANG
A0A251T9C0	Putative RNA-binding (RRM/RBD/RNP motifs) fam	516.54	2	5.25	42269	46768	40692	33162	37705	41426	43243	37431	0.125132	-0.21	UNCHANG
A0A251UPU8	Putative chloroplastic drought-induced stress pro	497.35	2	5.20	31474	30923	28912	24447	19113	36197	30436	26586	0.492715	-0.20	UNCHANG
P69313	Ubiquitin OS=Helianthus annuus PE=3 SV=2	20287.55	7	84.42	239373	280566	225036	216029	182428	254400	248325	217619	0.313148	-0.19	UNCHANG
A0A251UK46	Putative 26S protease regulatory subunit 6B OS=H	1259.71	7	31.42	21485	21045	26086	17301	19624	23239	22872	20054	0.299016	-0.19	UNCHANG
A0A251VR46	Putative thioredoxin-like fold protein OS=Helianth	6279.73	4	18.46	85089	75204	104821	40015	138561	54007	88371	77528	0.751686	-0.19	UNCHANG
A0A251UH15	Putative translationally-controlled tumor protein	5987.86	2	17.86	48403	41225	90237	58800	46182	52991	59955	52657	0.666447	-0.19	UNCHANG
A0A251SYL1	Proteasome subunit beta type OS=Helianthus ann	910.20	2	10.76	33386	33903	31050	30379	17378	38812	32779	28856	0.566941	-0.18	UNCHANG
A0A251TG61	Peroxidase OS=Helianthus annuus GN=HannXRQ_	948.36	3	8.73	43917	43497	58378	43004	44298	41316	48597	42873	0.31332	-0.18	UNCHANG
A0A251SVS3	Fructose-bisphosphate aldolase OS=Helianthus an	19278.36	13	41.46	51790	47295	42569	48751	24892	51439	47218	41694	0.566224	-0.18	UNCHANG
A0A251UXL3	Formate dehydrogenase, mitochondrial OS=Helia	1443.95	5	16.06	85161	94009	80594	68876	69419	91176	86588	76490	0.292313	-0.18	UNCHANG
A0A251VFN4	Putative aldehyde dehydrogenase 12A1 OS=Helia	467.09	3	6.37	23990	29075	22867	22046	23049	22689	25311	22595	0.232515	-0.16	UNCHANG
A0A251VAN6	Putative aldehyde dehydrogenase 11A3 OS=Helia	2492.61	8	21.93	52652	47516	50181	35015	59338	40431	50116	44928	0.528208	-0.16	UNCHANG
A0A1Y3BX41	Putative photosynthetic reaction centre, L/M OS=	27656.00	8	29.94	187463	216328	156514	194964	132062	178169	186768	168398	0.511629	-0.15	UNCHANG
A0A251VHI2	Photosystem II CP47 reaction center protein OS=	7643.91	11	29.07	126094	144276	116833	111767	105930	131958	129068	116552	0.329247	-0.15	UNCHANG
A0A251RY43	D-3-phosphoglycerate dehydrogenase OS=Heliant	339.79	3	5.01	31189	26965	31014	27105	26392	27415	29723	26970	0.12316	-0.14	UNCHANG
A0A251T2Q2	Putative ubiquitin-conjugating enzyme/RWD-like	1695.35	2	22.22	32404	32688	25877	30446	21737	30713	30323	27632	0.506651	-0.13	UNCHANG
A0A251SQ34	Putative ATP-citrate synthase beta chain protein 1	1418.25	9	17.55	33426	35412	33123	34336	24517	34062	33987	30971	0.413438	-0.13	UNCHANG
A0A251RL14	Putative glutamate--cysteine ligase protein OS=He	778.29	4	13.65	18752	17706	22878	15524	23982	14690	19779	18065	0.63712	-0.13	UNCHANG
A0A251V987	Aconitate hydratase OS=Helianthus annuus GN=A	17952.48	19	29.80	81348	78936	109883	78605	83237	85304	90056	82382	0.491049	-0.13	UNCHANG
A0A251V3V8	Aconitate hydratase OS=Helianthus annuus GN=A	17404.37	16	22.55	69581	65176	100477	68995	68625	78299	78411	71973	0.606903	-0.12	UNCHANG
A0A251SZB9	Glutamine synthetase OS=Helianthus annuus GN=	1252.91	5	15.34	24276	29397	25401	24767	23836	24022	26358	24208	0.245156	-0.12	UNCHANG
A0A251VPD5	Putative late embryogenesis abundant protein, gr	652.02	3	12.74	38717	36097	43816	38163	38328	32531	39543	36340	0.340179	-0.12	UNCHANG
A0A251SFM3	Putative aldo/keto reductase/potassium channel	2952.65	4	13.78	12275	12326	11546	12325	6332	14721	12049	11126	0.731411	-0.11	UNCHANG
A0A251SG14	Putative ruBisCO large subunit-binding protein su	3255.14	18	35.37	142534	153608	122075	126880	87622	171758	139406	128754	0.703036	-0.11	UNCHANG
A0A251TE31	Putative chaperonin Cpn60/TCP-1 family OS=Helia	1985.65	4	8.15	25075	22426	26428	22666	19176	27289	24643	23044	0.575481	-0.10	UNCHANG

A0A251TQG2	Sucrose synthase OS=Helianthus annuus GN=Han	1685.37	8	11.81	61732	64341	72527	61977	58040	65757	66200	61925	0.339094	-0.10	UNCHANG
A0A251SI61	Putative actin family OS=Helianthus annuus GN=H	15915.19	23	65.83	115701	113382	101308	101858	104489	103052	110130	103132	0.196931	-0.09	UNCHANG
A0A251TMX6	Glutamine synthetase OS=Helianthus annuus GN=	5783.63	8	25.84	137097	143663	131231	151216	85474	149627	137330	128772	0.716492	-0.09	UNCHANG
A0A251T4H2	Tubulin alpha chain OS=Helianthus annuus GN=H	15349.58	21	48.67	116948	110745	124827	104885	124080	102547	117507	110504	0.42794	-0.09	UNCHANG
A0A251T9L1	Putative ribosomal protein S5/Elongation factor G	1166.74	12	15.07	78052	81566	89618	92244	56182	86037	83079	78154	0.69415	-0.09	UNCHANG
A0A251SWI0	40S ribosomal protein S3a OS=Helianthus annuus	1809.39	2	9.23	20527	28546	16263	17579	9600	34340	21778	20506	0.88325	-0.09	UNCHANG
A0A251RLS7	Putative glycosyl hydrolase family protein OS=Hel	636.57	2	3.11	72981	74737	74481	76180	80497	54229	74066	70302	0.668229	-0.08	UNCHANG
A0A251SAA5	Adenosylhomocysteinase OS=Helianthus annuus	2730.19	12	30.93	65809	64324	61468	57200	52154	73933	63867	61096	0.700546	-0.06	UNCHANG
A0A251SGX7	Proteasome subunit alpha type OS=Helianthus an	1541.97	8	43.88	24882	38813	39399	31402	30288	36961	34365	32883	0.788883	-0.06	UNCHANG
A0A251UH30	Succinate--CoA ligase [ADP-forming] subunit alph	703.87	2	8.43	36081	36373	27556	33871	26901	35177	33336	31983	0.743988	-0.06	UNCHANG
A0A251TC63	Putative photosystem II cytochrome b559, alpha	12550.97	3	27.27	232538	241150	144902	232540	145514	216054	206197	198036	0.850913	-0.06	UNCHANG
A0A251STQ6	Putative actin OS=Helianthus annuus GN=ACT1 PE	10467.86	24	48.95	14331	13213	17613	12959	18696	11749	15053	14468	0.827699	-0.06	UNCHANG
A0A251TLI1	Malate dehydrogenase OS=Helianthus annuus GN	5581.77	8	26.74	81819	85621	90800	88235	78839	81232	86080	82769	0.436776	-0.06	UNCHANG
A0A251U4X4	Peroxidase OS=Helianthus annuus GN=PER4 PE=3	566.01	2	8.31	77210	74824	84426	73312	76058	77999	78820	75790	0.396021	-0.06	UNCHANG
A0A251SXU2	Putative bifunctional polymyxin resistance protein	9927.39	10	42.31	155847	159103	142217	159469	116503	163746	152389	146573	0.73379	-0.06	UNCHANG
A0A251U0S0	Glyceraldehyde-3-phosphate dehydrogenase OS=	30295.55	11	46.45	212304	202208	233829	214093	190102	221493	216114	208563	0.600398	-0.05	UNCHANG
A0A251UFT5	Putative ribulose bisphosphate carboxylase OS=H	54198.46	22	42.98	890108	829371	1072899	844938	897258	962200	930793	901466	0.734572	-0.05	UNCHANG
A0A251TLM3	Putative chloroplast heat shock protein 70-1 OS=	3950.11	13	19.51	149354	139617	157126	155044	126638	151103	148699	144262	0.686777	-0.04	UNCHANG
A0A251SC90	Fructose-bisphosphate aldolase OS=Helianthus an	2679.08	4	16.81	26091	31338	25592	26427	24560	29648	27674	26878	0.753446	-0.04	UNCHANG
A0A251SSA0	Putative elongation factor 1-beta OS=Helianthus a	2167.40	5	26.87	40359	45362	37093	36659	37768	45535	40938	39987	0.80918	-0.03	UNCHANG
A0A251T8H1	Putative RAB GTPase OS=Helianthus annuus GN=	1636.83	5	26.07	53410	51556	51104	53101	52421	47797	52023	51106	0.639011	-0.03	UNCHANG
A0A251T1H4	Putative photosystem I reaction center subunit III	5197.76	6	35.65	191667	149841	208782	195007	148033	197736	183430	180259	0.900451	-0.03	UNCHANG
A0A251RMQ6	Putative ketol-acid reductoisomerase, UDP-glucos	1834.04	5	12.02	76142	73644	72831	67642	51964	99369	74206	72992	0.934982	-0.02	UNCHANG
A0A251TCL9	Putative aldo/keto reductase/potassium channel	5731.19	5	21.21	2741	3113	2619	2676	3526	2134	2825	2779	0.920159	-0.02	UNCHANG
A0A251RMF3	40S ribosomal protein S27 OS=Helianthus annuus	7112.65	2	24.42	76635	65360	53985	73325	51467	69868	65326	64886	0.964991	-0.01	UNCHANG
A0A251ST32	Putative heat shock protein 81-2 OS=Helianthus a	10951.31	33	45.91	142370	147130	155111	144205	129013	168433	148204	147217	0.938758	-0.01	UNCHANG
A0A251RQX9	Peptidyl-prolyl cis-trans isomerase OS=Helianthus	10772.10	5	39.53	149994	156632	132493	157559	156237	122803	146373	145533	0.953221	-0.01	UNCHANG
A0A251ST38	Putative heat shock protein 81-3 OS=Helianthus a	10358.47	32	49.79	78283	80976	83790	88076	64968	89077	81016	80707	0.971116	-0.01	UNCHANG
A0A251RP88	Carbonic anhydrase OS=Helianthus annuus GN=C	5722.10	7	31.38	185167	192272	160771	147096	227781	161687	179403	178854	0.984519	0.00	UNCHANG
A0A251UL77	Putative oxygen-evolving enhancer protein 2 prot	3377.17	2	5.91	213147	259511	149169	169697	254237	203856	207275	209263	0.963047	0.01	UNCHANG
A0A251UN61	Putative heat shock 70 kDa protein OS=Helianthu	2212.30	13	24.34	161392	169238	133091	163792	201291	103113	154574	156065	0.963505	0.01	UNCHANG
A0A251TLI6	Putative phosphoenolpyruvate carboxylase OS=H	434.48	2	4.38	18438	18924	15262	10111	30953	12092	17541	17718	0.980271	0.01	UNCHANG
A0A251U5B9	Putative 26S proteasome non-ATPase regulatory	2541.45	2	8.06	58987	57174	51043	73149	54479	43108	55735	56912	0.903103	0.03	UNCHANG
A0A251U4W4	Putative small GTPase superfamily, Ran GTPase, P	833.41	3	15.12	18357	21908	20230	20911	21732	19411	20165	20685	0.694337	0.04	UNCHANG
A0A251V1J0	Putative transketolase protein OS=Helianthus ann	2148.47	6	12.38	80953	66643	96886	87057	76041	87950	81494	83683	0.829749	0.04	UNCHANG
U3RF21	S-adenosylmethionine synthase OS=Helianthus an	1373.09	4	14.36	59867	66966	56078	68581	73307	46088	60970	62659	0.860075	0.04	UNCHANG
A0A251S227	Putative ribosomal protein L5 OS=Helianthus ann	4518.92	4	21.98	66332	70537	55785	70299	32186	95627	64218	66037	0.928155	0.04	UNCHANG
A0A251S633	Putative ATP synthase gamma chain protein OS=H	1846.29	3	13.37	55602	50929	45939	52144	33947	71148	50823	52413	0.89302	0.04	UNCHANG
A0A251SGT6	Putative pfkB-like carbohydrate kinase family prot	531.26	2	5.28	52113	53205	46562	52842	61613	43230	50627	52562	0.751058	0.05	UNCHANG

A0A251SA85	Ferredoxin--NADP reductase OS=Helianthus annu	638.10	3	5.45	26211	23761	20261	20628	20906	31473	23411	24336	0.826972	0.06	UNCHANG
A0A251SL49	Putative elongation factor 1-alpha OS=Helianthus	3955.97	15	38.57	179704	200566	192192	175769	218972	201329	190821	198689	0.602343	0.06	UNCHANG
A0A251UD92	Putative sedoheptulose-bisphosphataseOS=Helia	7743.85	7	17.86	92121	109434	109228	100019	106108	118694	103594	108274	0.587604	0.06	UNCHANG
A0A251SFD5	Fructose-bisphosphate aldolase OS=Helianthus an	6044.29	10	34.45	130192	131420	108723	136139	120840	131186	123445	129388	0.529281	0.07	UNCHANG
A0A251RVY3	Proteasome subunit alpha type OS=Helianthus an	1703.51	5	22.26	30798	30318	28312	33726	26422	33757	29809	31302	0.590584	0.07	UNCHANG
A0A251UM81	Putative ATPase, AAA-type, core, P-loopcontainin	13612.45	20	51.48	431592	443076	387499	433552	383894	508619	420723	442022	0.622726	0.07	UNCHANG
A0A251SNA8	Putative chaperone protein htpG family protein O	1504.62	13	16.36	109141	116926	110186	127919	110187	115984	112084	118030	0.360403	0.07	UNCHANG
A0A251RYB8	Putative helicase Cas3, CRISPR-associated, core O	2453.00	9	35.20	30641	29095	37180	26851	46882	28335	32306	34023	0.815819	0.07	UNCHANG
A0A251RZF8	Putative enolase OS=Helianthus annuus GN=ENO	10675.99	19	54.16	191113	188573	187078	186833	176957	233478	188921	199089	0.591757	0.08	UNCHANG
A0A251UQC2	Putative V-type proton ATPase subunit B 2 OS=He	6393.42	15	50.42	95832	100867	88932	87730	111329	102600	95210	100553	0.5264	0.08	UNCHANG
A0A251T4P8	Putative alanine:glyoxylate aminotransferase OS=	1993.56	7	19.46	189153	190832	183170	198560	176735	221088	187718	198794	0.442664	0.08	UNCHANG
A0A251RN63	Pyruvate kinase OS=Helianthus annuus GN=Hann	1956.89	11	36.29	34805	36970	33742	35452	37657	38807	35172	37306	0.193913	0.08	UNCHANG
A0A251RX31	Putative aldehyde dehydrogenase 2B4 OS=Helian	1189.81	5	6.92	80186	78257	87550	93837	79676	87600	81998	87038	0.368823	0.09	UNCHANG
A0A251V7E7	Putative flavodoxin-like quinone reductase 1 OS=	1647.00	2	13.30	42331	28465	41358	38810	38468	42019	37384	39766	0.632656	0.09	UNCHANG
A0A251V4I2	Lactoylglutathione lyase OS=Helianthus annuus G	1850.81	9	26.14	63277	64881	68007	74701	69359	64796	65389	69617	0.254561	0.09	UNCHANG
A0A251UNC3	Putative heat shock protein OS=Helianthus annuu	21789.43	34	51.08	140989	143240	137098	166154	132036	152953	140442	150381	0.380535	0.10	UNCHANG
A0A251U5Z0	Putative heat shock protein 70 family OS=Heliant	18705.09	26	42.46	161560	164836	149700	166041	156950	187568	158699	170186	0.322078	0.10	UNCHANG
A0A251TBB1	Putative ras-related small GTP-binding family prot	2376.74	4	30.05	30954	31026	24357	32042	22779	37886	28779	30902	0.688482	0.10	UNCHANG
A0A251UYK6	Succinate--CoA ligase [ADP-forming] subunit beta	565.79	3	10.40	26986	32585	16877	35762	25634	20734	25482	27377	0.781315	0.10	UNCHANG
A0A251T3E7	Chlorophyll a-b binding protein, chloroplastic OS=	3203.33	4	13.01	68518	61591	80681	62012	99651	64921	70263	75528	0.71277	0.10	UNCHANG
A0A251U6R5	Putative heat shock protein Hsp90 family OS=Heli	3762.43	9	14.84	62019	62382	63088	57219	69453	75069	62497	67246	0.419071	0.11	UNCHANG
A0A251TK47	Putative translation elongation factor EF1B, gamn	2195.84	2	9.03	81818	88891	71382	77668	69892	113284	80697	86948	0.684449	0.11	UNCHANG
A0A251VB88	Nucleoside diphosphate kinase OS=Helianthus an	13604.53	3	34.21	100317	98517	109878	115139	116202	102023	102904	111121	0.227077	0.11	UNCHANG
A0A251TGF0	Putative chaperonin Cpn60/TCP-1 family OS=Helia	2891.28	13	19.82	52190	55165	48069	55107	44181	68774	51808	56021	0.599892	0.11	UNCHANG
P93171	Calmodulin OS=Helianthus annuus GN=CAM PE=2	3228.32	3	40.94	44559	49154	44407	32837	18671	98580	46040	50029	0.879359	0.12	UNCHANG
A0A251TFL2	Putative 30S ribosomal protein S1 protein OS=Hel	701.89	2	5.53	33205	34680	34342	36672	28123	46472	34076	37089	0.601381	0.12	UNCHANG
Q1KXW3	Photosystem II CP43 reaction center protein OS=	30228.76	17	33.83	269902	274911	249360	315959	289180	259888	264724	288342	0.259265	0.12	UNCHANG
A0A251SCB2	Chlorophyll a-b binding protein, chloroplastic OS=	2086.95	3	9.56	124167	120176	140310	157015	119075	143398	128217	139829	0.411916	0.13	UNCHANG
A0A251TZ13	Malate dehydrogenase OS=Helianthus annuus GN	1080.44	4	18.90	26570	27102	28280	30742	27465	31292	27317	29833	0.124403	0.13	UNCHANG
A0A251U960	Tubulin beta chain OS=Helianthus annuus GN=Ha	19947.86	22	60.13	207380	212769	204177	245861	243888	195614	208109	228454	0.28807	0.13	UNCHANG
A0A251VQU0	Putative ribosomal protein L11/L12 OS=Helianthu	2206.29	6	52.41	66899	69869	63119	80400	83511	55571	66629	73161	0.510557	0.13	UNCHANG
A0A251TBW8	Putative aldo/keto reductase/potassium channel	6888.20	7	20.65	266275	244107	247795	263812	281239	289194	252726	278082	0.067063	0.14	UNCHANG
Q1KXW0	Photosystem I P700 chlorophyll a apoprotein A2 O	18588.06	12	23.57	109493	127270	144908	143910	113684	162934	127224	140176	0.50285	0.14	UNCHANG
A0A251USB3	Putative chaperone protein dnaK2 OS=Helianthus	3557.96	9	15.03	156514	162499	149961	162542	164916	190888	156325	172782	0.16752	0.14	UNCHANG
A0A251VLR1	T-complex protein 1 subunit delta OS=Helianthus	496.97	5	10.84	13793	11621	11814	12174	14306	14928	12409	13803	0.268276	0.15	UNCHANG
A0A251TVR1	Putative 40S ribosomal protein S14 OS=Helianthu	1329.28	2	21.33	24565	30942	19292	29824	22462	31536	24933	27940	0.529099	0.16	UNCHANG
A0A142K3L6	Cytoplasmic enolase OS=Helianthus annuus GN=E	5965.29	10	26.74	40517	39846	40985	44698	45112	46294	40450	45368	0.00107	0.17	UNCHANG
A0A1Y3BXH9	Putative ATPase, F1 complex, delta/epsilon subun	36438.95	29	54.65	318715	303675	332797	329175	365513	377627	318396	357439	0.080925	0.17	UNCHANG
A0A251T4T6	Putative alpha-hydroxy acid dehydrogenase, FMN	12642.08	10	32.52	106740	110005	129517	144352	84116	162092	115421	130187	0.581367	0.17	UNCHANG

A0A251VK45	Glutamate decarboxylase OS=Helianthus annuus	2121.19	5	17.00	25047	31840	16887	31016	20621	31577	24592	27738	0.604265	0.17	UNCHANG
A0A251S1C6	Putative arginase OS=Helianthus annuus GN=Han	1975.85	2	6.21	48594	49999	38787	52015	50672	51483	45793	51390	0.189866	0.17	UNCHANG
A0A251S456	Putative gamma carbonic anhydrase 2 OS=Heliant	704.93	2	8.09	11288	9687	13210	14113	13829	10713	11395	12885	0.37424	0.18	UNCHANG
A0A251UIN6	Glycine cleavage system P protein OS=Helianthus	1905.18	9	14.40	61611	70514	82110	67701	82223	93117	71412	81013	0.367331	0.18	UNCHANG
A0A251S1X1	Ribulose bisphosphate carboxylase small chain OS	1294.19	2	10.29	196046	280282	7899	253282	113068	180742	161409	182364	0.827543	0.18	UNCHANG
A0A251RTS5	Putative NAD(P)-binding Rossmann-fold superfam	914.13	3	8.97	48605	47651	51750	54475	60849	52795	49335	56040	0.071207	0.18	UNCHANG
A0A251TDM5	Pyruvate kinase OS=Helianthus annuus GN=Hann	3064.02	10	26.94	61994	59126	77020	80319	64640	80396	66047	75118	0.300304	0.19	UNCHANG
A0A251T0L1	Putative V-type proton ATPase catalytic subunit A	5193.45	23	49.12	117465	104374	132435	138596	114337	152395	118091	135109	0.283957	0.19	UNCHANG
A0A251V8Z9	Pectin acetylesterase OS=Helianthus annuus GN=	1157.61	3	8.18	83760	85655	80706	93686	113664	80207	83374	95852	0.272917	0.20	UNCHANG
A0A251VE03	Putative glutamate-1-semialdehyde 2,1-aminomu	1123.87	5	14.35	142226	138272	146200	183381	89589	218370	142232	163780	0.605688	0.20	UNCHANG
Q1KXU6	Cytochrome f OS=Helianthus annuus GN=petA PE	3806.91	4	11.88	63725	69158	58961	83258	65886	72926	63948	74023	0.159671	0.21	UNCHANG
A0A251UPH3	Putative citrate synthase OS=Helianthus annuus G	1705.63	9	19.38	28587	32983	24214	34968	29002	35371	28595	33114	0.238316	0.21	UNCHANG
A0A251TP29	Phospholipase D OS=Helianthus annuus GN=PLDA	574.12	2	3.73	38762	47402	29844	46920	36494	51886	38669	45100	0.39794	0.22	UNCHANG
A0A251SRS2	Putative thioredoxin-like fold protein OS=Helianth	8462.42	2	11.74	142742	163272	144147	151875	180525	196790	150054	176397	0.147688	0.23	UNCHANG
A0A251T725	Putative heat shock protein 70 family OS=Heliant	509.01	3	5.86	17738	18178	20288	12129	40186	13834	18734	22050	0.734498	0.24	UNCHANG
A0A251UA02	ATP-dependent 6-phosphofructokinase OS=Helian	280.32	2	4.93	20351	27905	16928	28053	22562	26244	21728	25620	0.343218	0.24	UNCHANG
A0A251T350	Putative heat shock protein 70 family OS=Heliant	528.71	6	8.70	31695	35200	33157	41595	47293	29634	33351	39507	0.310138	0.24	UNCHANG
A0A251T1X6	Putative actin OS=Helianthus annuus GN=ACT1 PE	13278.61	22	56.94	202649	206229	206105	258652	246659	230306	204994	245206	0.008365	0.26	UNCHANG
A0A251UC74	Putative carrier protein OS=Helianthus annuus GN	361.92	3	10.17	51565	40375	50871	65872	45392	60267	47604	57177	0.248967	0.26	UNCHANG
A0A251U202	Putative alanine-2-oxoglutarate aminotransferase	1595.14	4	9.77	61182	58321	55064	72069	43061	95636	58189	70255	0.474616	0.27	UNCHANG
A0A251U0L3	Putative aldehyde/histidinol dehydrogenase OS=H	612.03	3	5.64	60406	52112	75683	79160	49706	99409	62734	76092	0.450649	0.28	UNCHANG
A0A251UBL4	Ribulose-phosphate 3-epimerase OS=Helianthus a	1180.29	2	9.26	44981	57402	48195	45248	63384	74059	50193	60897	0.30913	0.28	UNCHANG
I6LNU0	Phosphoglycerate kinase OS=Helianthus annuus G	12725.13	19	52.81	273029	262439	259834	308148	340639	319484	265101	322757	0.005072	0.28	UNCHANG
A0A251TWM3	Succinate dehydrogenase [ubiquinone] flavoprote	2051.73	6	13.51	95554	109816	79676	124870	105735	117352	95016	115986	0.112266	0.29	UNCHANG
A0A251VLM0	Putative chloroplast RNA binding protein OS=Heli	559.47	2	7.85	40415	42245	51109	44053	54109	64839	44589	54334	0.227938	0.29	UNCHANG
Q1KXW5	ATP synthase subunit alpha, chloroplastic OS=Hel	27427.78	15	34.45	291470	289169	276645	398157	305299	345689	285761	349719	0.078951	0.29	UNCHANG
A0A172W3U6	Photosystem II D2 protein OS=Helianthus annuus	13333.35	7	27.20	183587	200713	165824	246928	187807	238652	183375	224462	0.122676	0.29	UNCHANG
A0A251RX12	Elongation factor Tu OS=Helianthus annuus GN=E	5055.91	11	28.84	126066	140956	104355	149785	131769	173694	123792	151749	0.158199	0.29	UNCHANG
A0A251V6W1	Proteasome subunit beta type OS=Helianthus ann	2222.95	4	19.23	48617	65523	53617	69951	63514	72299	55919	68588	0.088802	0.29	UNCHANG
A0A251STV6	Putative DEAD-box ATP-dependent RNA helicase	409.56	2	4.17	15559	29636	11715	21808	29338	19202	18970	23449	0.512367	0.31	UNCHANG
A0A251S481	Fructose-bisphosphate aldolase OS=Helianthus an	35397.34	12	29.29	239661	242436	217012	284128	270221	310112	233036	288154	0.017797	0.31	UNCHANG
A0A251TJC8	Pyruvate kinase OS=Helianthus annuus GN=Hann	2316.55	9	28.30	38543	42401	39605	55501	46259	48236	40183	49998	0.031888	0.32	UNCHANG
A0A251RVM7	Fructose-bisphosphate aldolase OS=Helianthus an	4117.72	6	19.39	68939	66115	68761	97253	80247	77477	67938	84992	0.052503	0.32	UNCHANG
A0A251V954	Putative thioredoxin OS=Helianthus annuus GN=H	869.53	2	9.91	17883	19799	16412	20839	21449	25447	18031	22578	0.059789	0.32	UNCHANG
A0A251SWE6	Putative heat shock protein 70 family OS=Heliant	11217.29	9	19.07	95588	92950	92072	128252	114713	109968	93537	117644	0.012435	0.33	UNCHANG
A0A251UJW5	Putative ATP-dependent zinc metalloprotease FTS	600.43	7	15.20	25894	25212	27735	37970	14751	47115	26280	33279	0.508975	0.34	UNCHANG
A0A251VJH6	Putative chlorophyll A-B binding protein OS=Helia	4511.45	2	9.16	125128	140748	108664	175947	113601	187015	124846	158854	0.239923	0.35	UNCHANG
A0A251TI46	Tubulin alpha chain OS=Helianthus annuus GN=H	18578.85	8	46.12	145746	155332	126570	173780	192496	179681	142549	181986	0.017474	0.35	UNCHANG
A0A251VHG5	Putative glycoside hydrolase family 3 C-terminal d	544.41	3	5.73	35923	25545	38662	33017	32412	62786	33377	42738	0.43464	0.36	UNCHANG

A0A251V082	Histone H3 OS=Helianthus annuus GN=HannXRQ_	1252.61	2	10.29	36357	40901	29169	41683	35428	59760	35475	45624	0.276216	0.36	UNCHANG
P18260	ATP synthase subunit alpha, mitochondrial OS=He	14690.34	20	43.33	166163	186597	149680	238064	201843	215809	167480	218572	0.02717	0.38	UNCHANG
A0A251SBQ9	Glyceraldehyde-3-phosphate dehydrogenase OS=	14110.89	12	37.44	120052	134056	95595	142969	153290	160310	116568	152190	0.04445	0.38	UNCHANG
A0A251RR99	Mg-protoporphyrin IX chelatase OS=Helianthus a	585.75	3	10.61	22577	16214	24667	19587	32730	30977	21152	27765	0.243726	0.39	UNCHANG
A0A251TR27	Putative eukaryotic initiation factor 4A-8 OS=Helia	2703.41	8	27.41	90548	100393	83238	130794	116358	113164	91393	120105	0.017495	0.39	UNCHANG
A0A251U5D0	ATP synthase subunit beta OS=Helianthus annuus	16564.83	24	63.22	189752	160454	184322	247598	246287	208896	178176	234261	0.022646	0.39	UNCHANG
A0A251UU16	Putative photosystem I reaction center subunit V	3868.67	4	25.00	86908	85982	79829	96738	143614	92930	84240	111094	0.17787	0.40	UNCHANG
P45739	Catalase OS=Helianthus annuus PE=2 SV=1	2409.66	6	17.68	92663	109427	80016	128445	113724	130003	94035	124058	0.039529	0.40	UNCHANG
A0A251RV69	Putative clpA/B family OS=Helianthus annuus GN=	764.03	9	12.94	34427	39052	38027	51000	40419	55706	37169	49042	0.066157	0.40	UNCHANG
A0A251UD22	Glutamate decarboxylase OS=Helianthus annuus	1926.39	6	13.13	71599	66154	32528	93883	23719	109753	56760	75785	0.549198	0.42	UNCHANG
A0A251SJZ7	Putative delta l-pyrroline-5-carboxylate synthetas	1722.15	4	8.58	21961	32710	22080	31765	32111	39366	25584	34414	0.111637	0.43	UNCHANG
A0A251SIP5	UDP-glucose 6-dehydrogenase OS=Helianthus an	682.50	4	10.13	17441	16451	17180	24406	25144	19315	17024	22955	0.033051	0.43	UNCHANG
A0A251T0H8	Putative heat shock protein OS=Helianthus annuu	11446.66	19	30.69	396406	415946	398327	604079	310151	726288	403560	546839	0.311012	0.44	UNCHANG
A0A251TZB3	Putative 26S proteasome non-ATPase regulatory	743.70	3	16.99	31494	29932	33102	47456	42818	37977	31509	42750	0.017605	0.44	UNCHANG
A0A251SNX0	Putative RAB GTPase OS=Helianthus annuus GN=	2080.41	3	12.96	28299	34600	29001	41341	44382	39017	30633	41580	0.012335	0.44	UNCHANG
A0A251VJD3	Phosphoribulokinase OS=Helianthus annuus GN=	2241.45	7	22.64	86315	80076	91144	101074	157975	92255	85845	117102	0.208079	0.45	UNCHANG
A0A251UJ12	Putative ADP/ATP carrier 1 OS=Helianthus annuus	982.50	6	17.14	89733	105093	92492	141465	153915	102294	95773	132558	0.086402	0.47	UNCHANG
Q1KXV9	Photosystem I P700 chlorophyll a apoprotein A1 O	1467.37	6	6.67	42366	45347	37393	59126	50235	64129	41702	57830	0.026125	0.47	UNCHANG
A0A251RS68	Delta-aminolevulinic acid dehydratase OS=Heliant	828.67	5	14.32	14591	18817	18701	26493	19581	26436	17369	24170	0.064329	0.48	UNCHANG
A0A251TW23	Putative ruBisCO large subunit-binding protein su	3733.89	11	23.05	112411	117313	107960	156915	108066	206442	112561	157141	0.193154	0.48	UNCHANG
A0A251SSF6	Putative substrate carrier protein OS=Helianthus	817.03	2	6.69	28010	30920	21299	35611	42101	36189	26743	37967	0.03336	0.51	UNCHANG
A0A251S450	Ferredoxin--NADP reductase OS=Helianthus annu	4267.80	4	16.12	19713	17459	28410	30965	28554	34221	21861	31247	0.065179	0.52	UNCHANG
A0A251VIR5	Putative thioredoxin-like fold protein OS=Helianth	1620.94	6	13.96	45083	46343	37243	70820	49733	64416	42890	61657	0.052143	0.52	UNCHANG
A0A251SC94	Thiamine thiazole synthase, chloroplastic OS=Heli	1000.03	2	7.54	84668	89657	66631	113911	115398	117128	80319	115479	0.007578	0.52	UNCHANG
A0A251S4L0	Putative transketolase, bacterial-like protein OS=	749.51	5	9.24	23706	19647	23725	34287	28818	33703	22359	32269	0.010804	0.53	UNCHANG
A0A251SR24	Putative bifunctional polymyxin resistance protein	425.88	2	7.01	8299	10090	7775	11401	12851	13614	8721	12622	0.015056	0.53	UNCHANG
A0A251VMX3	Putative pyridoxal 5'-phosphate synthase subunit	517.53	4	15.91	18536	22030	16633	30357	23307	30102	19067	27922	0.034024	0.55	UNCHANG
A0A251VNF4	Putative ribosomal protein L14b/L23e OS=Heliant	1930.69	2	20.71	24116	31699	16288	38928	30954	38427	24034	36103	0.078774	0.59	UNCHANG
A0A251SJU5	Putative 4-hydroxy-3-methylbut-2-en-1-yl diphos	455.95	3	5.41	12672	10222	15090	14903	29883	13076	12661	19287	0.295175	0.61	UNCHANG
A0A251S999	Putative chaperonin Cpn60/TCP-1 family OS=Helia	579.68	3	6.92	18475	18440	17913	35615	22096	27029	18276	28247	0.065233	0.63	UNCHANG
A0A251V3R3	Putative cytochrome b6/f complex, subunit IV OS	1252.96	3	7.13	13865	16064	10187	24980	14512	30985	13372	23492	0.118705	0.81	UNCHANG
A0A251ST28	Tubulin beta chain OS=Helianthus annuus GN=Ha	14184.16	19	60.67	17376	18071	20656	19639	54630	26642	18701	33637	0.236549	0.85	UNCHANG
A0A251T7W6	Putative 14-3-3-like protein GF14-BOS=Helianthu	1146.13	2	7.53	21039	21643	23489	35798	53876	31033	22057	40236	0.060159	0.87	UNCHANG
A0A251UPM4	Putative small GTPase superfamily, ARF/SAR type,	4482.91	2	19.80	10600	11024	8589	19225	10671	31953	10071	20616	0.165677	1.03	UNCHANG
A0A251SQM5	T-complex protein 1 subunit gamma OS=Helianth	406.61	3	9.53	16652	9045	10403	16863	46634	24517	12033	29338	0.134019	1.29	UNCHANG
A0A251SRK1	Uncharacterized protein OS=Helianthus annuus G	1186.69	3	8.80	24265	22293	22805	99066	61497	26633	23121	62398	0.133706	1.43	UNCHANG
A0A251VGX8	Putative ATPase, F1 complex, gamma subunit, AT	1714.49	2	8.85	7665	6252	7977	36881	11885	34629	7298	27798	0.062489	1.93	UNCHANG
A0A251TQ78	Putative ribulose bisphosphate carboxylase/oxyge	12844.37	22	58.96	26681	27659	26893	3502	2261	3499	27078	3087	1.21E-06	-3.13	DOWN
A0A251TDI1	Putative ATPase, AAA-type, core OS=Helianthus a	5804.79	21	29.33	20190	19769	27165	1022	3391	5971	22375	3461	0.002478	-2.69	DOWN

A0A251VI84	Putative heat shock protein 70 family OS=Heliant	870.92	2	6.27	107276	81050	129901	12410	26202	21314	106075	19975	0.00422	-2.41	DOWN
A0A251VCX7	Purple acid phosphatase OS=Helianthus annuus G	350.19	2	3.16	84479	59413	95516	17048	11821	24375	79803	17748	0.005331	-2.17	DOWN
A0A251U9Y1	Tubulin beta chain OS=Helianthus annuus GN=TB	17788.95	21	65.85	76498	78427	94574	17416	34287	17120	83166	22941	0.001718	-1.86	DOWN
A0A251UKC4	Peptidyl-prolyl cis-trans isomerase OS=Helianthus	5318.89	3	16.13	141215	117608	223383	47136	69509	44593	160735	53746	0.031668	-1.58	DOWN
A0A251TCD2	Putative aldo/keto reductase/potassium channel	4498.06	5	15.09	142770	176429	140144	31461	97514	52448	153114	60474	0.015128	-1.34	DOWN
A0A251RU22	Putative UV excision repair protein Rad23, UBA-lik	679.67	3	9.76	68137	60028	88955	40588	30379	19684	72373	30217	0.016025	-1.26	DOWN
A0A251VIV4	Elongation factor 1-alpha OS=Helianthus annuus	3708.39	13	34.41	55112	57312	64010	23771	20837	29789	58811	24799	0.000824	-1.25	DOWN
A0A251SRB9	Putative ribosomal protein S7 domain protein OS=	9112.62	5	28.80	104836	110528	110649	51164	27730	61561	108671	46818	0.003717	-1.21	DOWN
A0A251U316	Putative triosephosphate isomerase OS=Helianth	4931.58	8	31.89	33285	33096	30642	11422	9530	21299	32341	14084	0.008202	-1.20	DOWN
I3RXT3	Glyceraldehyde-3-phosphate dehydrogenase (Fra	16971.10	9	50.00	260462	241321	351122	88081	195859	95193	284302	126377	0.031308	-1.17	DOWN
A0A251UDZ3	Putative oxygen-evolving enhancer protein 1 prot	8096.83	5	17.93	143680	128949	133514	62693	34217	87595	135381	61502	0.00995	-1.14	DOWN
A0A251TQ58	Putative photosynthesis system II assembly factor	922.64	2	25.97	21368	21338	26836	9480	13643	8503	23181	10542	0.006353	-1.14	DOWN
A0A251TJP2	ATP-dependent Clp protease proteolytic subunit	1456.60	3	8.97	25209	27348	44537	13141	14954	16672	32365	14922	0.048196	-1.12	DOWN
A0A251RUV1	Carbonic anhydrase OS=Helianthus annuus GN=C	5045.40	4	20.79	113203	107941	130757	32351	93340	41517	117300	55736	0.038122	-1.07	DOWN
A0A251TAV7	Phosphoglycerate kinase OS=Helianthus annuus G	8306.11	12	37.54	50206	42139	73320	23028	24819	30929	55222	26258	0.03983	-1.07	DOWN
A0A251TPA8	Putative regulatory particle triple-A 1A OS=Helian	2070.75	8	27.46	30431	28529	36058	13934	9509	22047	31673	15163	0.018629	-1.06	DOWN
O65352	14-3-3-like protein OS=Helianthus annuus PE=2 S	3219.31	9	36.29	22013	21096	29174	12145	11027	11827	24094	11666	0.008486	-1.05	DOWN
A0A251T0E7	Putative photosystem I PsaH, reaction centre sub	4665.66	2	7.06	75037	96629	77793	46855	24251	55200	83153	42102	0.023171	-0.98	DOWN
A0A251SRU1	Phenylalanine ammonia-lyase OS=Helianthus ann	2153.59	6	17.13	23892	28152	29153	12057	16602	12954	27066	13871	0.003448	-0.96	DOWN
A0A251SL53	Putative actin family OS=Helianthus annuus GN=H	13772.62	23	60.28	123269	115476	96708	58218	44189	70676	111818	57695	0.00789	-0.95	DOWN
A0A251RNJ4	Eukaryotic translation initiation factor 5A OS=Heli	2258.27	5	45.28	91887	94481	96963	62821	32788	51082	94444	48897	0.006789	-0.95	DOWN
A0A251TU95	Putative calreticulin OS=Helianthus annuus GN=C	2866.14	10	37.16	85997	79072	89817	49203	35623	47572	84962	44133	0.001541	-0.94	DOWN
A0A251S9S9	Alpha-mannosidase OS=Helianthus annuus GN=M	204.81	2	2.21	46620	36889	51263	23450	19441	28014	44924	23635	0.012261	-0.93	DOWN
A0A251RY75	Proteasome endopeptidase complex OS=Helianth	609.99	3	11.53	26521	28765	36050	18904	11880	19137	30445	16640	0.020885	-0.87	DOWN
A0A251S6A3	Putative chaperonin Cpn60/TCP-1 family OS=Helia	4548.28	16	32.33	69069	74120	74865	37363	29164	53751	72685	40093	0.011941	-0.86	DOWN
A0A251RVN2	Alpha-mannosidase OS=Helianthus annuus GN=H	245.60	2	2.51	33903	34713	37907	17019	20583	23710	35508	20437	0.002746	-0.80	DOWN
A0A251UD42	Putative cobalamin-independent methioninesynt	2755.18	8	12.85	91019	86020	111178	52879	51405	61683	96072	55322	0.008098	-0.80	DOWN
A0A251VAJ5	Putative B-S glucosidase 44 OS=Helianthus annuu	721.55	2	4.55	59514	65190	55403	27538	39117	37502	60036	34719	0.005315	-0.79	DOWN
A0A251VAW4	Putative oxygen-dependent coproporphyrinogen-	1425.87	3	10.58	39065	38223	40364	15160	21602	31612	39218	22791	0.027197	-0.78	DOWN
A0A251SF43	Putative plastid lipid-associated protein/fibrillin c	2966.52	3	11.68	73433	73410	87174	51637	26901	60444	78006	46327	0.045462	-0.75	DOWN
A0A251U157	Putative elongation factor 1-delta OS=Helianthus	1962.24	6	20.68	72814	78538	76151	39444	48094	48721	75834	45420	0.000886	-0.74	DOWN
A0A251RV88	Nucleoside diphosphate kinase OS=Helianthus an	1323.91	3	11.45	28152	22919	34600	16055	14577	21445	28557	17359	0.047828	-0.72	DOWN
A0A251S5H6	Putative regulatory particle AAA-ATPase 2A OS=H	892.17	4	13.29	19367	17094	13110	9508	10044	11474	16524	10342	0.032309	-0.68	DOWN
A0A251RRT4	Glyceraldehyde-3-phosphate dehydrogenase OS=	15281.42	15	45.25	156743	165195	177002	111876	75202	127731	166313	104936	0.020997	-0.66	DOWN
A0A251SMP9	Putative outer plastidial membrane protein porin	1776.65	4	11.96	221005	220781	203780	100410	178139	132531	215189	137027	0.028299	-0.65	DOWN
A0A251VS82	Tubulin alpha chain OS=Helianthus annuus GN=H	13578.90	15	46.65	39427	38257	38576	24118	27091	23086	38753	24765	0.000363	-0.65	DOWN
A0A251TCM9	Putative NAD(P)-linked oxidoreductase superfami	2200.04	3	12.09	76950	74945	59914	37589	45444	52915	70603	45316	0.022123	-0.64	DOWN
A0A251TDZ2	Putative cell division cycle protein OS=Helianthus	4373.76	19	28.50	284230	283853	260825	127830	218421	193297	276303	179849	0.026442	-0.62	DOWN
A0A251VNA4	Putative CBS domain-containing protein OS=Helia	6635.17	6	38.99	50677	55153	71092	36907	36416	42338	58974	38553	0.034462	-0.61	DOWN

Apêndice B – Capítulo: Differentially regulated proteins could be related to difficulties for *in vitro* rooting of micropropagated shoots in *Cariniana legalis* (Martius) O. Kuntze

Tabela Suplementar 1: Lista completa de todas as proteínas identificadas

Accession	Reported Peptide	Max score	Description	Normalized Total Ion Count (Tic)									Average			t-Test		Log2 Fold Change		Differential accumulation	
				T0_1	T0_2	T0_3	T12 - Control_1	T12 - Control_2	T12 - Control_3	T12 - IBA_1	T12 - IBA_2	T12 - IBA_3	T0	T12 - Control	T12 - IBA	T12 - IBA/ T0	T12 - IBA/ T12 - Control	T12 - IBA/ T0	T12 - IBA/ T12 - Control	T12 - IBA/ T0	T12 - IBA/ T12 - Control
A0A251VKC7	2	660.0	Putative enoyl-[acyl-carrier-protein] reductase [NA	43133	48922	46234	32616	31691	0	38263	43532	24221	46096	32153	35339	0.1475	-	-0.38	-	UNCHANGE	-
A0A251TTN4	9	3306.2	Putative ribulose bisphosphate carboxylase/oxyge	3843	3734	3951	0	0	0	0	0	0	3843	0	0	-	-	-	-	Unique T0	-
A0A251SA89	4	1023.2	Putative GTP-binding 2	2178	2842	2441	0	0	0	0	0	0	2487	0	0	-	-	-	-	Unique T0	-
A0A251TBJ2	35	17424.5	Tubulin beta chain	97022	107652	97584	65728	60240	51315	30086	31013	34882	100752	59094	31994	0.0001	0.0037	-1.65	-0.89	DOWN	DOWN
A0A251SIH1	11	16582.2	Fructose-bisphosphate aldolase	172905	186450	182245	90310	88968	64978	50642	53967	54497	180533	81419	53039	0.0000	0.0270	-1.77	-0.62	DOWN	DOWN
A0A251SBQ9	11	11516.6	Glyceraldehyde-3-phosphate dehydrogenase	49407	53738	59208	18664	25623	29478	14582	14803	16078	54118	24588	15154	0.0002	0.0420	-1.84	-0.70	DOWN	DOWN
A0A1Y3BWX5	11	9619.4	ATP synthase subunit alpha	20347	20621	20771	4811	4452	4593	2262	2265	2661	20580	4619	2396	0.0000	0.0002	-3.10	-0.95	DOWN	DOWN
A0A251UWA2	16	8513.0	Phosphoglycerate kinase	45500	53800	46960	31691	33590	26837	16954	14050	17663	48753	30706	16222	0.0003	0.0032	-1.59	-0.92	DOWN	DOWN
P85189	4	5396.5	Oxygen-evolving enhancer protein 2, chloroplastic	132756	162357	125496	62638	108881	92131	40707	42129	41967	140203	87883	41601	0.0009	0.0267	-1.75	-1.08	DOWN	DOWN
A0A251TE28	3	4656.6	oxygen-evolving enhancer protein 3-2, chloroplast	144440	222326	219061	80958	86333	90046	49199	48177	46086	195276	85779	47821	0.0044	0.0002	-2.03	-0.84	DOWN	DOWN
A0A251SIN0	12	3250.6	Putative 14-3-3-like protein 16R	170607	163965	162143	80574	77922	72363	41740	51134	44346	165572	76953	45740	0.0000	0.0011	-1.86	-0.75	DOWN	DOWN
A0A251RX31	3	2270.9	Putative aldehyde dehydrogenase 2B4	125878	149027	143511	85514	84919	74153	23590	15357	15179	139472	81529	18042	0.0001	0.0002	-2.95	-2.18	DOWN	DOWN
A0A251TDZ2	15	2073.9	Putative cell division cycle protein	77000	89962	74146	43652	39299	50049	22738	21310	29647	80369	44333	24569	0.0005	0.0081	-1.71	-0.85	DOWN	DOWN
A0A251UM81	4	1807.1	Putative ATPase, AAA-type, core, P-loop containi	44963	42581	40251	18498	10193	8471	1228	802	1625	42598	12388	1218	0.0000	0.0228	-5.13	-3.35	DOWN	DOWN
A0A251RP81	24	37408.2	Tubulin alpha chain	247591	254836	272857	250032	300419	258374	43246	42555	44793	258428	269609	43533	0.0000	0.0001	-2.57	-2.63	DOWN	DOWN
A0A251TLR2	35	20722.8	Tubulin beta chain	84894	80376	80966	80159	62483	46146	22128	22031	23270	82078	62929	22476	0.0000	0.0147	-1.87	-1.49	DOWN	DOWN
A0A251S8L8	12	20593.7	Chlorophyll a-b binding protein, chloroplastic	285464	295621	290161	280457	268356	303686	187518	180926	170945	290415	284166	179797	0.0000	0.0008	-0.69	-0.66	DOWN	DOWN
P45738	21	16599.2	Ribulose bisphosphate carboxylase large chain	362051	410228	437250	418562	384031	316168	207049	219891	223956	403176	372920	216966	0.0012	0.0069	-0.89	-0.78	DOWN	DOWN
A0A251VIL2	29	10397.5	Tubulin alpha chain	160848	185368	182408	154568	155228	153779	80987	80831	79823	176208	154525	80547	0.0002	0.0000	-1.13	-0.94	DOWN	DOWN
A0A251V9V2	11	8947.2	Chlorophyll a-b binding protein, chloroplastic	242158	280082	253947	167850	155626	192450	76157	88395	65795	258729	171975	76782	0.0001	0.0017	-1.75	-1.16	DOWN	DOWN
A0A251UTI9	20	7365.2	Putative alcohol dehydrogenase superfamily, zinc-	32537	36131	37252	39500	49804	57553	10804	11767	12253	35307	48952	11608	0.0001	0.0021	-1.60	-2.08	DOWN	DOWN
A0A1Y3BU36	19	7204.3	Putative ATP synthase subunit beta protein	129951	138055	137414	83442	104158	104824	32221	33035	33192	135140	97475	32816	0.0000	0.0008	-2.04	-1.57	DOWN	DOWN
A0A251S0H1	3	3936.0	Malate dehydrogenase	137603	195567	174330	116932	109234	111333	59336	66863	61227	169167	112500	62475	0.0033	0.0001	-1.44	-0.85	DOWN	DOWN
F2VYC9	3	3918.0	Beta-hydroxyacyl-ACP dehydratase	53227	77887	52859	36720	55965	43100	13974	14576	12858	61324	45262	13803	0.0046	0.0052	-2.15	-1.71	DOWN	DOWN
A0A251TLQ4	5	3775.8	Putative caffeoyl-CoA O-methyltransferase	48118	59322	55009	42350	45111	46037	11345	13031	12325	54150	44499	12233	0.0002	0.0000	-2.15	-1.86	DOWN	DOWN
A0A251SNP4	14	3565.8	Putative 5-methyltetrahydropteroyltriglutamate--ho	70806	81561	77916	114773	115281	97817	39622	40912	39904	76761	109290	40146	0.0003	0.0003	-0.94	-1.44	DOWN	DOWN
P85194	6	3555.4	Oxygen-evolving enhancer protein 1, chloroplastic	157958	158116	135802	157432	120964	98041	66125	64148	60664	150625	125479	63645	0.0003	0.0236	-1.24	-0.98	DOWN	DOWN
A0A251SLN4	4	2349.5	Malate dehydrogenase	162506	157084	173525	172474	191326	213021	42137	39419	46151	164371	192274	42569	0.0000	0.0002	-1.95	-2.18	DOWN	DOWN
A0A251RRR8	12	2158.0	UDP-glucose 6-dehydrogenase	24916	28984	21671	27679	41532	28115	10048	11269	11376	25190	32442	10897	0.0027	0.0092	-1.21	-1.57	DOWN	DOWN
A0A251V0T5	3	2051.0	Starch synthase, chloroplastic/amyloplastic	93172	105376	109736	93495	91266	104431	31941	29042	43181	102761	96397	34721	0.0005	0.0005	-1.57	-1.47	DOWN	DOWN
A0A251VE03	4	940.0	Putative glutamate-1-semialdehyde 2,1-aminomut	35511	44121	42809	38187	40672	34319	20223	21803	24201	40814	37726	22075	0.0030	0.0020	-0.89	-0.77	DOWN	DOWN
A0A251SGT6	2	803.1	Fructokinase-6, chloroplastic	35558	34078	32039	28325	25003	22326	12806	13299	12124	33892	25218	12743	0.0000	0.0021	-1.41	-0.98	DOWN	DOWN

A0A251SJZ7	2	536.0	Putative delta l-pyrroline-5-carboxylate synthetase	76337	97264	68334	60530	79678	79121	33118	36218	35057	80645	73109	34798	0.0061	0.0038	-1.21	-1.07	DOWN	DOWN
A0A251VIH6	29	17580.9	Putative actin family	41665	45850	33014	59459	58848	53593	29156	28612	30723	40176	57300	29497	0.0495	0.0001	-0.45	-0.96	UNCHANGED	DOWN
A0A251VS40	19	6343.7	Fructose-bisphosphate aldolase	97434	122797	105965	180694	172129	134350	73467	72095	76738	108732	162391	74100	0.0103	0.0035	-0.55	-1.13	UNCHANGED	DOWN
A0A251RKM4	16	4581.9	Putative luminal-binding protein	46663	53697	47730	71791	65033	79199	35715	35957	35253	49363	72008	35642	0.0034	0.0009	-0.47	-1.01	UNCHANGED	DOWN
A0A251TNB0	30	4244.3	Putative V-type proton ATPase catalytic subunit A	137045	162395	146360	170483	185700	204268	102713	104759	98346	148600	186817	101939	0.0036	0.0010	-0.54	-0.87	UNCHANGED	DOWN
A0A251UJB3	3	3855.1	Proteasome endopeptidase complex	23203	31968	24332	42838	38396	27324	20453	21806	22713	26501	36186	21657	0.1621	0.0356	-0.29	-0.74	UNCHANGED	DOWN
A0A251VNA4	4	3431.7	Putative CBS domain-containing protein	36397	36306	35824	47212	46912	45191	27462	26253	31330	36176	46438	28348	0.0071	0.0004	-0.35	-0.71	UNCHANGED	DOWN
A0A251SQV9	2	1957.2	Putative 60S acidic ribosomal protein family	30071	68288	15018	71118	78968	82723	17757	22229	15788	37792	77603	18591	0.2955	0.0001	-1.02	-2.06	UNCHANGED	DOWN
A0A251T146	2	1050.6	Putative SKU5-similar 6	19788	64797	19629	63041	55557	121342	15991	18752	13153	34738	79980	15965	0.2821	0.0373	-1.12	-2.32	UNCHANGED	DOWN
A0A251RYE8	3	1004.3	Malic enzyme	21875	21908	27623	26972	28257	34372	16782	19327	19397	23802	29867	18502	0.0647	0.0096	-0.36	-0.69	UNCHANGED	DOWN
A0A251UYK6	3	790.5	Succinate--CoA ligase [ADP-forming] subunit beta	43154	34088	43442	38296	45559	51012	30996	28619	28552	40228	44955	29389	0.0269	0.0145	-0.45	-0.61	UNCHANGED	DOWN
A0A251SL53	28	16351.8	Putative actin family	128457	156656	106816	258380	243049	253681	70714	66606	68667	130643	251704	68662	0.0128	0.0000	-0.93	-1.87	DOWN	DOWN
A0A251TUG3	6	3040.4	Phenylalanine ammonia-lyase	12472	14376	14851	19508	23363	31554	6719	7127	7188	13900	24808	7011	0.0007	0.0075	-0.99	-1.82	DOWN	DOWN
A0A251UJ12	2	1305.6	Putative ADP/ATP carrier 1	24674	25604	29895	66981	82358	72140	16852	18224	15236	26725	73826	16770	0.0055	0.0002	-0.67	-2.14	DOWN	DOWN
A0A251T8A4	3	926.8	Glucose-1-phosphate adenylyltransferase	28028	30069	31232	54742	58719	71495	9949	9351	8751	29776	61652	9350	0.0000	0.0005	-1.67	-2.72	DOWN	DOWN
A0A251UPV3	4	864.2	UDP-glucose 6-dehydrogenase	0	0	0	27188	22622	13229	5422	5949	6348	0	21013	5906	-	0.0214	-	-1.83	Unique T12-IB	DOWN
A0A251TDQ3	27	16378.0	Putative enolase	61660	63519	66277	140379	159297	161754	58848	55323	58763	63819	153810	57645	0.0253	0.0001	-0.15	-1.42	UNCHANGED	DOWN
A0A251U6F5	17	5775.8	Putative alcohol dehydrogenase superfamily, zinc-	16682	18566	17967	64651	69870	107618	21975	26024	25352	17738	80713	24450	0.0081	0.0144	0.46	-1.72	UNCHANGED	DOWN
A0A251UGR1	5	4878.7	S-(hydroxymethyl)glutathione dehydrogenase	27400	31766	32881	124291	134601	93440	28834	33293	38887	30682	117444	33671	0.4233	0.0027	0.13	-1.80	UNCHANGED	DOWN
A0A251RN63	8	2914.5	Pyruvate kinase	60776	68739	57379	160770	151600	139770	79944	77030	74209	62298	150713	77061	0.0170	0.0003	0.31	-0.97	UNCHANGED	DOWN
A0A251UHT4	5	2367.1	Ketol-acid reductoisomerase	61119	73208	66218	107813	117711	106741	71571	68581	65447	66848	110755	68533	0.6898	0.0004	0.04	-0.69	UNCHANGED	DOWN
B5KUB7	6	2104.1	Chalcone synthase (Fragment)	31466	34766	33803	76101	82825	64859	31838	31965	29492	33345	74595	31098	0.1509	0.0012	-0.10	-1.26	UNCHANGED	DOWN
A0A251TQC4	5	2064.0	Putative leucine aminopeptidase 2, chloroplastic	45501	49272	44096	90375	87432	75961	48880	49341	51604	46289	84589	49942	0.1066	0.0015	0.11	-0.76	UNCHANGED	DOWN
A0A0S1M144	7	1995.0	Chalcone synthase 2	8329	8507	5216	38773	39442	38521	3524	3522	7873	7351	38912	4973	0.2573	0.0000	-0.56	-2.97	UNCHANGED	DOWN
A0A251VFS0	5	1853.7	6-phosphogluconate dehydrogenase, decarboxyla	22476	30495	22762	43689	64240	64436	20535	21742	20061	25244	57455	20779	0.1703	0.0060	-0.28	-1.47	UNCHANGED	DOWN
A0A251VH41	6	1488.3	Malate dehydrogenase	45487	30146	30233	149109	164534	164209	42156	76221	40234	35289	159284	52871	0.2401	0.0011	0.58	-1.59	UNCHANGED	DOWN
A0A251TTU2	2	373.3	Glucose-6-phosphate isomerase	25344	28764	25531	46867	43266	45354	19585	20070	19042	26546	45162	19565	0.0037	0.0000	-0.44	-1.21	UNCHANGED	DOWN
A0A251TAV7	14	9912.3	Phosphoglycerate kinase	86860	99708	88075	248708	268125	222237	147499	134864	150707	91547	246357	144357	0.0011	0.0020	0.66	-0.77	UP	DOWN
A0A251TIT5	13	7390.8	Cysteine synthase	37192	41940	41795	112750	94492	153115	60641	68280	71835	40309	120119	66918	0.0019	0.0393	0.73	-0.84	UP	DOWN
A0A251TNF0	4	3733.7	Putative pyridoxal phosphate-dependent transfera	3679	3457	3060	25942	27394	24747	10886	10293	9549	3399	26028	10242	0.0001	0.0001	1.59	-1.35	UP	DOWN
A0A251SRB9	3	2734.5	Putative ribosomal protein S7 domain protein	17098	17180	16692	57052	66475	71893	29847	33784	33789	16990	65140	32474	0.0003	0.0020	0.93	-1.00	UP	DOWN
A0A251VHR4	10	1851.8	Aspartate aminotransferase	15224	24599	18129	128122	140324	144351	66049	70656	61709	19318	137599	66138	0.0002	0.0002	1.78	-1.06	UP	DOWN
A0A251UN61	11	1634.4	Putative heat shock 70 kDa protein	3966	3621	3767	14405	15941	18280	10432	10885	9694	3785	16209	10337	0.0001	0.0076	1.45	-0.65	UP	DOWN
A0A251S4I0	3	967.9	Thioredoxin reductase	11420	10982	13326	50877	47606	44366	24100	29450	26541	11909	47616	26697	0.0010	0.0010	1.16	-0.83	UP	DOWN
A0A251VRK6	5	966.2	Citrate synthase	7806	11795	8868	47264	54638	49987	25176	32755	26672	9490	50630	28201	0.0020	0.0021	1.57	-0.84	UP	DOWN
A0A172W418	6	42487.3	Photosystem I iron-sulfur center	281908	318438	251682	93676	81554	92166	88511	76201	77177	284009	89132	80630	0.0005	0.1965	-1.82	-0.14	DOWN	UNCHANGED
A0A251U960	38	23429.5	Tubulin beta chain	385247	390651	438095	236957	239181	207786	224405	219773	205792	404664	227975	216657	0.0004	0.3829	-0.90	-0.07	DOWN	UNCHANGED
A0A251TWK4	5	15283.5	Putative photosynthetic reaction centre, L/M	142482	165553	168254	35339	40551	53782	28221	32755	26982	158763	43224	29319	0.0001	0.0733	-2.44	-0.56	DOWN	UNCHANGED
A0A251RL35	9	13119.6	Putative photosystem I reaction center subunit II p	165828	161747	187538	102651	78108	50057	38761	44616	41571	171704	76938	41649	0.0001	0.0822	-2.04	-0.89	DOWN	UNCHANGED
A0A251SNE7	28	13078.3	Tubulin beta chain	120079	76267	104408	57297	40963	30543	58672	45428	64791	100251	42934	56297	0.0351	0.2387	-0.83	0.39	DOWN	UNCHANGED
B5KUG0	5	11154.4	Glyceraldehyde-3-phosphate dehydrogenase (Fra	88834	103918	91870	13636	21740	25902	14613	8339	9422	94874	20426	10791	0.0001	0.0780	-3.14	-0.92	DOWN	UNCHANGED
I6LNU0	19	10383.8	Phosphoglycerate kinase	189543	196444	206412	88147	88491	76933	119247	119362	116140	197466	84523	118250	0.0001	0.0010	-0.74	0.48	DOWN	UNCHANGED

A0A251VA77	18	9493.4	Putative heat shock protein 70 family	95921	111117	93364	24103	21328	30469	25874	24148	23676	100134	25300	24566	0.0002	0.8052	-2.03	-0.04	DOWN	UNCHANGED
Q1KXV2	25	9145.9	ATP synthase subunit beta, chloroplastic	77458	82663	84449	40500	32811	25417	32406	35399	31858	81523	32909	33221	0.0000	0.9480	-1.30	0.01	DOWN	UNCHANGED
A0A251SG50	10	8164.7	Putative 14-3-3 domain-containing protein	104799	90299	86416	31254	32527	33454	38909	34571	38901	93838	32412	37460	0.0006	0.0330	-1.32	0.21	DOWN	UNCHANGED
A0A161I435	6	6680.7	Photosystem II D2 protein	171173	143812	187147	86691	77973	63492	83923	78100	81550	167377	76052	81191	0.0025	0.5021	-1.04	0.09	DOWN	UNCHANGED
A0A170R5H4	3	5376.9	Photosystem I P700 chlorophyll a apoprotein A2	36199	39008	46492	8619	9957	15279	16102	16131	15137	40566	11285	15790	0.0013	0.0940	-1.36	0.48	DOWN	UNCHANGED
A0A251TBY3	4	5303.6	Putative ribosomal protein L11/L12	35989	42444	38768	23476	22777	24470	26385	26090	23590	39067	23574	25359	0.0027	0.1537	-0.62	0.11	DOWN	UNCHANGED
A0A251RNE8	7	4967.2	Peroxidase	193378	192497	179192	74059	63605	64036	46732	46653	45954	188356	67233	46446	0.0000	0.0037	-2.02	-0.53	DOWN	UNCHANGED
A0A251U7U6	5	4758.0	Photosystem II CP47 reaction center protein	64736	81882	104875	14775	17995	27400	22016	17969	21909	83831	20057	20631	0.0057	0.8931	-2.02	0.04	DOWN	UNCHANGED
A0A251T3T1	8	3860.8	Malate dehydrogenase	198601	194767	209035	85600	91907	91805	109690	106869	122394	200801	89771	112985	0.0002	0.0112	-0.83	0.33	DOWN	UNCHANGED
A0A251VGX1	5	3679.1	Putative 14-3-3-like protein A	72086	71861	64093	44497	36502	21657	20846	20935	17737	69347	34219	19839	0.0001	0.1010	-1.81	-0.79	DOWN	UNCHANGED
A0A251SDE9	10	3299.5	Putative ribulose bisphosphate carboxylase/oxyge	82159	78328	81394	26619	22007	16824	22886	22275	21935	80627	21817	22369	0.0000	0.8564	-1.85	0.04	DOWN	UNCHANGED
A0A251THW2	6	2753.5	Putative SPFH/Band 7/PHB domain-containing m	53314	34191	40462	10259	12637	18248	11185	12744	12462	42656	13715	12130	0.0057	0.5479	-1.81	-0.18	DOWN	UNCHANGED
A0A251TQ78	9	2344.1	Putative ribulose bisphosphate carboxylase/oxyge	59151	57935	52508	15166	12527	10559	10554	9601	10172	56531	12751	10109	0.0000	0.1247	-2.48	-0.33	DOWN	UNCHANGED
A0A251VEV1	9	1941.8	UDP-glucose 6-dehydrogenase	154455	146908	168094	55751	90162	77353	60106	29589	46649	156486	74422	45449	0.0005	0.0961	-1.78	-0.71	DOWN	UNCHANGED
A0A251RSN9	3	1905.3	Putative small GTPase superfamily	143797	131865	101936	20833	18774	21946	31008	31898	29124	125866	20518	30677	0.0016	0.0012	-2.04	0.58	DOWN	UNCHANGED
A0A251SCF6	4	1883.9	Putative 14-3-3 domain-containing protein	50845	46738	38475	31427	22790	18730	15441	15674	14936	45353	24315	15351	0.0012	0.0751	-1.56	-0.66	DOWN	UNCHANGED
A0A251SRW3	10	1762.2	Aspartate aminotransferase	110457	164441	134868	37681	38167	38903	50586	54115	47263	136589	38250	50659	0.0055	0.0035	-1.43	0.41	DOWN	UNCHANGED
A0A251VAN6	3	1333.3	Putative aldehyde dehydrogenase 11A3	58879	49084	52283	26182	27461	23765	32032	24318	20298	53415	25803	25549	0.0034	0.9473	-1.06	-0.01	DOWN	UNCHANGED
A0A251VHG5	2	1229.6	Putative glycoside hydrolase family 3 C-terminal d	48074	48025	43706	27700	27356	26540	18956	18250	25783	46602	27198	20996	0.0008	0.0629	-1.15	-0.37	DOWN	UNCHANGED
A0A251SLT1	3	1032.4	Putative regulatory particle non-ATPase 12A	30275	25200	29065	18900	15205	9308	8146	20705	19317	28180	14471	16056	0.0466	0.7606	-0.81	0.15	DOWN	UNCHANGED
A0A251V4I2	3	916.4	Lactoylglutathione lyase	52423	54793	60802	28790	28505	21420	23256	24582	23310	56006	26238	23716	0.0002	0.3613	-1.24	-0.15	DOWN	UNCHANGED
A0A251V667	2	365.1	Putative NADP-dependent glyceraldehyde-3-phos	16410	9562	11952	5814	5815	5526	5616	3929	3468	12641	5718	4337	0.0170	0.1046	-1.54	-0.40	DOWN	UNCHANGED
A0A251S9S9	2	341.7	Alpha-mannosidase	71069	89093	76034	21659	26966	29554	18397	18428	16692	78732	26059	17839	0.0004	0.0264	-2.14	-0.55	DOWN	UNCHANGED
A0A251TW66	39	23710.1	Tubulin beta chain	119386	109934	110967	79350	61796	51207	82029	81235	85643	113429	64118	82969	0.0008	0.0861	-0.45	0.37	UNCHANGED	UNCHANGED
A0A251V3V8	37	14318.7	Aconitate hydratase	229399	213637	232501	164232	126161	126258	185782	164821	185105	225179	138884	178569	0.0067	0.0513	-0.33	0.36	UNCHANGED	UNCHANGED
A0A251RL41	25	12307.0	Tubulin beta chain	45668	50240	49474	39098	30215	21177	32964	35683	34830	48461	30163	34492	0.0010	0.4548	-0.49	0.19	UNCHANGED	UNCHANGED
A0A251SRZ8	6	4346.2	S-adenosylmethionine synthase	18733	20659	12487	10132	8958	7922	11402	11246	10914	17293	9004	11187	0.0689	0.0290	-0.63	0.31	UNCHANGED	UNCHANGED
A0A251RUV1	6	3526.6	Carbonic anhydrase	107049	108597	102528	82138	56347	52000	74083	70924	68536	106058	63495	71181	0.0001	0.4657	-0.58	0.16	UNCHANGED	UNCHANGED
A0A251UIA5	3	3159.3	Putative small GTPase superfamily	16727	16721	12885	9855	9297	5354	10565	8186	12387	15444	8169	10379	0.0455	0.3020	-0.57	0.35	UNCHANGED	UNCHANGED
A0A251T841	2	882.3	NADPH-protochlorophyllide oxidoreductase	49581	58041	50871	26987	28309	29901	41379	41252	41945	52831	28399	41525	0.0128	0.0001	-0.35	0.55	UNCHANGED	UNCHANGED
A0A251T0H8	31	9132.6	Putative heat shock protein	249024	308435	308313	244205	187209	155321	128114	129083	142610	288591	195578	133269	0.0016	0.0778	-1.11	-0.55	DOWN	UNCHANGED
A0A251V7E7	3	4595.2	Putative flavodoxin-like quinone reductase 1	46393	68338	50938	47785	43504	35956	34638	32492	32486	55223	42415	33205	0.0307	0.0595	-0.73	-0.35	DOWN	UNCHANGED
A0A251S006	6	3886.2	Putative O-methyltransferase, family 3, S-adenos	28272	29496	31637	24612	18467	17775	15402	17371	16375	29802	20285	16383	0.0003	0.1573	-0.86	-0.31	DOWN	UNCHANGED
A0A251U5M3	6	3345.4	Putative small GTPase superfamily	66538	58796	66592	73564	62581	38009	36769	30069	26815	63975	58051	31218	0.0011	0.0697	-1.04	-0.89	DOWN	UNCHANGED
A0A251VRZ2	5	2687.5	Putative fructokinase-2	72959	65984	55386	107712	81499	43214	32826	38180	33513	64776	77475	34840	0.0051	0.0860	-0.89	-1.15	DOWN	UNCHANGED
A0A251TW23	10	2579.2	Putative ruBisCO large subunit-binding protein su	117481	120807	111292	111499	88693	61490	61833	60456	59759	116527	87227	60683	0.0000	0.1404	-0.94	-0.52	DOWN	UNCHANGED
A0A251UXE6	7	1599.0	UDP-glucose 6-dehydrogenase	6179	9075	7356	3077	5750	4851	3209	2719	2760	7536	4559	2896	0.0056	0.1064	-1.38	-0.65	DOWN	UNCHANGED
A0A251TNR9	3	585.2	Putative ras-related protein	38154	39800	38942	25489	27587	26067	22328	23587	21280	38965	26381	22398	0.0000	0.0121	-0.80	-0.24	DOWN	UNCHANGED
A0A251ULU4	3	528.2	Putative UDP-XYL synthase 6	37748	40670	45018	35442	33444	17892	24157	22475	20527	41145	28926	22386	0.0014	0.3111	-0.88	-0.37	DOWN	UNCHANGED
A0A251V4A5	29	26752.3	Tubulin alpha chain	167222	184517	187270	110396	134401	120674	131161	129061	135834	179669	121824	132019	0.0019	0.2316	-0.44	0.12	UNCHANGED	UNCHANGED
A0A1Y3BXK7	7	22724.0	Multifunctional fusion protein	14309	25811	19173	31224	29893	17470	25532	23032	25997	19764	26196	24854	0.2151	0.7792	0.33	-0.08	UNCHANGED	UNCHANGED

P18260	22	22014.7	ATP synthase subunit alpha, mitochondrial	271312	249648	271421	243539	219039	203707	284929	278181	281530	264127	222095	281547	0.0808	0.0072	0.09	0.34	UNCHANGED	UNCHANGED
A0A251T3D2	14	21533.5	Glyceraldehyde-3-phosphate dehydrogenase	229874	218742	230234	272492	298978	320464	281608	282318	311635	226283	297311	291854	0.0035	0.7648	0.37	-0.03	UNCHANGED	UNCHANGED
A0A251T1X6	26	17816.6	Putative actin	420450	437152	355183	400353	411827	340627	333724	348770	357072	404262	384269	346522	0.0899	0.1777	-0.22	-0.15	UNCHANGED	UNCHANGED
A0A251VS82	14	16084.9	Tubulin alpha chain	14359	18100	15246	18641	19023	16235	20080	20353	22149	15902	17966	20861	0.0190	0.0563	0.39	0.22	UNCHANGED	UNCHANGED
A0A251RU72	28	15251.5	ATP synthase subunit beta	369578	450120	369554	419932	355222	395166	413918	409438	419161	396417	390107	414172	0.5467	0.2753	0.06	0.09	UNCHANGED	UNCHANGED
A0A251STQ6	28	13822.8	Putative actin	30815	36690	25710	28973	26493	23784	24184	25366	28110	31071	26416	25886	0.1997	0.7937	-0.26	-0.03	UNCHANGED	UNCHANGED
A0A142K3L6	25	12730.9	Cytoplasmic enolase	89286	86871	85716	71346	73464	59406	98726	97007	93296	87291	68072	96343	0.0092	0.0037	0.14	0.50	UNCHANGED	UNCHANGED
A0A251TYG9	25	12709.1	ATP synthase subunit beta	122345	156954	117974	154354	128905	138332	147708	138250	144199	132424	140530	143386	0.4346	0.7368	0.11	0.03	UNCHANGED	UNCHANGED
A0A251T7V8	26	12390.0	Tubulin beta chain	21191	74880	64224	89060	103274	96960	78520	67066	78657	53432	96431	74748	0.2746	0.0182	0.48	-0.37	UNCHANGED	UNCHANGED
Q1KXW5	12	9620.9	ATP synthase subunit alpha, chloroplastic	180991	178699	191699	120462	140876	124953	173068	162651	165407	183796	128764	167042	0.0299	0.0053	-0.14	0.38	UNCHANGED	UNCHANGED
A0A251UTE2	25	9085.9	Putative alcohol dehydrogenase 1	891710	985655	822260	839181	729711	932943	568440	617079	608105	899875	833945	597875	0.0037	0.0176	-0.59	-0.48	UNCHANGED	UNCHANGED
Q1KXW3	11	8673.2	Photosystem II CP43 reaction center protein	119966	146029	162637	190433	117047	74371	197375	209901	309774	142877	127284	239017	0.0632	0.0853	0.74	0.91	UNCHANGED	UNCHANGED
A0A251TCM9	8	6613.7	Putative NAD(P)-linked oxidoreductase superfami	131779	139267	156584	171359	169040	109278	161613	145005	142474	142543	149892	149697	0.4927	0.9931	0.07	0.00	UNCHANGED	UNCHANGED
A0A251UQC2	28	5858.7	Putative V-type proton ATPase subunit B 2	324846	352192	352134	357853	206219	224059	390203	379740	376492	343057	262710	382145	0.0174	0.0677	0.16	0.54	UNCHANGED	UNCHANGED
A0A251VJ15	9	5641.6	Phenylalanine ammonia-lyase	6300	6889	6925	5129	5609	5336	7539	7122	7015	6704	5358	7226	0.1136	0.0009	0.11	0.43	UNCHANGED	UNCHANGED
A0A251SRU1	13	5632.4	Phenylalanine ammonia-lyase	29794	29154	27779	22112	23425	31788	8485	8450	25266	28909	25775	14067	0.0578	0.1398	-1.04	-0.87	UNCHANGED	UNCHANGED
A0A251TPX4	22	5380.2	Putative chaperonin 60 beta	129195	110150	118216	106076	75462	58312	90855	93184	86216	119187	79950	90085	0.0078	0.5125	-0.40	0.17	UNCHANGED	UNCHANGED
A0A251UL91	18	5221.5	Putative ATP-dependent RNA helicase DEAD-bo	122461	126458	134847	154527	146639	160831	147021	155769	155127	127922	153999	152639	0.0058	0.7982	0.25	-0.01	UNCHANGED	UNCHANGED
A0A251RVM7	15	5201.2	Fructose-bisphosphate aldolase	184304	174675	192307	139341	125157	100854	157984	158486	137708	183762	121784	151393	0.0192	0.0876	-0.28	0.31	UNCHANGED	UNCHANGED
A0A251TAE7	12	4798.6	Putative small GTPase superfamily, Rab type	231106	249023	267526	267996	243267	135181	165959	168751	184527	249218	215481	173079	0.0032	0.3614	-0.53	-0.32	UNCHANGED	UNCHANGED
U3RF21	8	4750.5	S-adenosylmethionine synthase	121723	125128	92076	105993	102890	99961	110156	104948	101217	112976	102948	105440	0.5242	0.4695	-0.10	0.03	UNCHANGED	UNCHANGED
A0A251SG14	12	4293.2	Putative ruBisCO large subunit-binding protein su	146208	143340	125475	117534	112399	110767	95937	92775	93998	138341	113567	94237	0.0025	0.0010	-0.55	-0.27	UNCHANGED	UNCHANGED
A0A251SGX7	12	4058.6	Proteasome subunit alpha type	132042	241321	223540	326266	530985	274539	318074	480210	224118	198968	377263	340801	0.1591	0.7532	0.78	-0.15	UNCHANGED	UNCHANGED
A0A251VK45	8	3859.8	Glutamate decarboxylase	23518	12611	22968	35498	29647	15640	18565	24330	22230	19699	26928	21708	0.6359	0.4423	0.14	-0.31	UNCHANGED	UNCHANGED
A0A251RXL3	3	3461.4	Putative nucleotide-binding alpha-beta plait domai	103979	102932	105249	153688	132780	115766	135225	121917	128167	104053	134078	128436	0.0033	0.6527	0.30	-0.06	UNCHANGED	UNCHANGED
A0A251VIX3	2	3282.7	Putative ribosomal protein S7 domain protein	22332	78450	72650	37654	54494	76018	37854	70470	44537	57811	56055	50954	0.7537	0.7494	-0.18	-0.14	UNCHANGED	UNCHANGED
A0A251UPH3	15	3156.5	Putative citrate synthase	64114	60831	78671	61633	76537	63673	79688	88798	83958	67872	67281	84148	0.0554	0.0346	0.31	0.32	UNCHANGED	UNCHANGED
A0A251USB3	14	3156.3	Putative chaperone protein dnaK2	176385	191917	199829	146440	151872	123067	126466	141658	130362	189377	140459	132829	0.0024	0.4856	-0.51	-0.08	UNCHANGED	UNCHANGED
A0A251VJF8	15	2890.9	Putative 2,3-bisphosphoglycerate-independent ph	74349	94199	96329	118234	118370	124024	101793	98053	125308	88291	120209	108384	0.1427	0.2475	0.30	-0.15	UNCHANGED	UNCHANGED
A0A251S3M6	6	2830.5	Proteasome subunit alpha type	46710	48588	46457	54952	76538	71097	49376	51899	49164	47252	67529	50146	0.0590	0.0565	0.09	-0.43	UNCHANGED	UNCHANGED
A0A251V6W1	3	2738.0	Proteasome subunit beta	62829	61701	64160	56385	62342	61716	71875	69230	67508	62897	60148	69538	0.0103	0.0146	0.14	0.21	UNCHANGED	UNCHANGED
A0A251RMC1	8	2496.5	Putative aldolase-type TIM barrel family protein	116568	112742	98025	116077	115324	127327	93024	85173	78683	109112	119576	85626	0.0286	0.0039	-0.35	-0.48	UNCHANGED	UNCHANGED
A0A251UKC4	3	2461.2	Peptidyl-prolyl cis-trans isomerase	82415	90414	95548	201378	304530	114211	118621	126175	81708	89459	206706	108834	0.2458	0.1594	0.28	-0.93	UNCHANGED	UNCHANGED
A0A251T2Q2	2	2265.0	Putative ubiquitin-conjugating enzyme/RWD-like p	28452	23188	31968	38839	29467	29194	33900	34104	41337	27869	32500	36447	0.0722	0.3801	0.39	0.17	UNCHANGED	UNCHANGED
A0A251TGF0	13	2073.7	Putative chaperonin Cpn60/TCP-1 family	46485	47254	44950	61296	59994	42094	39244	40606	37736	46230	54461	39195	0.0028	0.0710	-0.24	-0.47	UNCHANGED	UNCHANGED
A0A251SP87	5	1963.8	Putative alpha-hydroxy acid dehydrogenase, FMN	25037	28247	30663	26522	26922	17878	25809	29135	28951	27982	23774	27965	0.9935	0.2530	0.00	0.23	UNCHANGED	UNCHANGED
A0A251SPX5	5	1946.2	Putative small GTPase superfamily, Ran GTPase	33138	36403	38820	36329	39875	36059	37722	44874	41948	36120	37421	41515	0.1115	0.1650	0.20	0.15	UNCHANGED	UNCHANGED
A0A251TJF3	2	1846.6	Putative fumarylacetoacetase, putative	67762	80294	79660	51986	58758	46394	41436	77510	68281	75905	52379	62409	0.3079	0.4284	-0.28	0.25	UNCHANGED	UNCHANGED
A0A251VLW1	9	1756.6	Putative chaperonin CPN60-2	43430	44426	40515	45140	46136	33276	42459	39756	42849	42790	41517	41688	0.5094	0.9699	-0.04	0.01	UNCHANGED	UNCHANGED
A0A251U5B9	5	1738.3	Putative 26S proteasome non-ATPase regulatory	43125	47809	50214	61498	57195	59252	53493	56418	56378	47049	59315	55430	0.0218	0.0692	0.24	-0.10	UNCHANGED	UNCHANGED
A0A251TBG5	3	1639.1	Putative aldo/keto reductase/potassium channel s	26964	23688	25225	25716	23394	15368	25052	23369	26436	25292	21493	24952	0.8062	0.3481	-0.02	0.22	UNCHANGED	UNCHANGED
A0A251TWQ3	11	1598.1	Putative stromal 70 kDa heat	48277	43243	44845	63581	49392	44438	33305	37306	33535	45455	52470	34715	0.0055	0.0392	-0.39	-0.60	UNCHANGED	UNCHANGED

			shock-related protei																	
A0A251VPF5	5	1562.7	Putative chaperonin-60alpha	19877	18269	17677	25532	19319	19469	23150	22603	23579	18608	21440	23111	0.0033	0.4640	0.31	0.11	UNCHANGED	UNCHANGED
A0A251RVY3	5	1408.5	Proteasome subunit alpha type	44771	47814	54010	50724	40037	38520	49267	48250	45839	48865	43094	47786	0.7287	0.3030	-0.03	0.15	UNCHANGED	UNCHANGED
A0A251U2V1	2	1403.2	Putative gamma aminobutyrate transaminase 3 pr	28166	31010	45091	40415	47891	62184	69204	79114	38837	34756	50163	62389	0.1044	0.4226	0.84	0.31	UNCHANGED	UNCHANGED
A0A251TE31	4	1394.9	Putative chaperonin Cpn60/TCP-1 family	3314	3046	2958	3006	2364	2281	2487	2454	2561	3106	2551	2501	0.0056	0.8395	-0.31	-0.03	UNCHANGED	UNCHANGED
A0A251S377	6	1328.5	Putative phosphoglucomutase/phosphomannomu	40408	48381	43016	58565	69566	64028	52941	53748	51679	43935	64053	52789	0.0217	0.0252	0.26	-0.28	UNCHANGED	UNCHANGED
A0A251SYY4	4	1321.2	Putative mitochondrial-processing peptidase subu	40211	41909	40404	59133	51922	54274	45077	48155	48372	40841	55109	47201	0.0059	0.0291	0.21	-0.22	UNCHANGED	UNCHANGED
A0A251TZ13	4	1288.6	Malate dehydrogenase	36041	34521	34411	47272	43366	39270	35901	34891	35983	34991	43303	35592	0.3958	0.0299	0.02	-0.28	UNCHANGED	UNCHANGED
A0A251V5D4	13	1214.8	Putative 26S proteasome AAA-ATPase subunit R	36868	33343	37799	50631	44050	41524	43858	42489	42591	36003	45402	42979	0.0081	0.4281	0.26	-0.08	UNCHANGED	UNCHANGED
A0A251S5T4	3	1095.2	T-complex protein 1 subunit eta	24581	26795	28024	31274	33261	32180	39270	41886	37324	26466	32238	39493	0.0014	0.0073	0.58	0.29	UNCHANGED	UNCHANGED
A0A251TZB3	3	938.4	Putative 26S proteasome non-ATPase regulatory	31353	30009	34408	43946	45107	43468	42274	41856	41452	31923	44174	41861	0.0017	0.0129	0.39	-0.08	UNCHANGED	UNCHANGED
A0A251RX12	5	909.1	Elongation factor Tu	32107	36653	44175	33616	36381	35815	25684	24321	26201	37645	35271	25402	0.0264	0.0006	-0.57	-0.47	UNCHANGED	UNCHANGED
A0A251U205	4	870.1	Purple acid phosphatase	40679	44133	39047	66952	52721	26296	55439	55904	48338	41286	48656	53227	0.0142	0.7261	0.37	0.13	UNCHANGED	UNCHANGED
A0A251SSF6	3	783.1	Putative substrate carrier protein	27262	32473	31061	48231	44908	24611	35940	39172	59734	30265	39250	44949	0.1260	0.6158	0.57	0.20	UNCHANGED	UNCHANGED
A0A251UY42	2	772.3	Putative pfkB-like carbohydrate kinase family prot	37969	35512	35901	36490	32010	29938	35183	34211	29697	36461	32813	33031	0.1380	0.9364	-0.14	0.01	UNCHANGED	UNCHANGED
A0A251TDC7	2	764.7	Putative RNA-binding protein 45A	31394	36672	52407	62472	50792	49953	55786	53304	51217	40158	54406	53436	0.1085	0.8307	0.41	-0.03	UNCHANGED	UNCHANGED
A0A251TTA4	2	754.6	Proteasome subunit alpha type	116136	75207	75260	120357	95596	78995	112661	86106	105483	88868	98316	101417	0.4708	0.8400	0.19	0.04	UNCHANGED	UNCHANGED
A0A251VA80	2	750.3	Guanosine nucleotide diphosphate dissociation in	34438	40381	41298	43785	52947	47904	50488	54291	49362	38705	48212	51380	0.0084	0.3562	0.41	0.09	UNCHANGED	UNCHANGED
A0A251TN70	2	738.7	Peroxidase	34863	39898	41093	50730	55889	54039	42364	41592	38915	38618	53553	40957	0.3430	0.0024	0.08	-0.39	UNCHANGED	UNCHANGED
A0A251RLS7	2	717.0	Putative glycosyl hydrolase family protein	59849	65798	45795	48033	40630	46441	69076	70590	62935	57147	45035	67534	0.1786	0.0023	0.24	0.58	UNCHANGED	UNCHANGED
A0A251V9F6	2	675.3	Putative heat shock cognate protein 80	40345	44653	52458	25295	27394	49570	53142	62800	38389	45816	34086	51444	0.5175	0.1743	0.17	0.59	UNCHANGED	UNCHANGED
A0A251UQE5	3	632.3	Putative target of Myb protein 1	17794	16496	14229	18091	13690	12170	20017	21474	20764	16173	14650	20751	0.0152	0.0287	0.36	0.50	UNCHANGED	UNCHANGED
A0A251VCR5	2	607.5	Malic enzyme	42362	42305	56422	32419	31479	34950	37295	42413	39843	47030	32949	39850	0.2185	0.0187	-0.24	0.27	UNCHANGED	UNCHANGED
A0A251TE75	4	535.0	Importin subunit alpha	16610	17698	19654	16143	18779	20861	19105	18697	19147	17987	18594	18983	0.3314	0.7911	0.08	0.03	UNCHANGED	UNCHANGED
A0A251TU31	5	524.7	Clathrin heavy chain	17306	26298	32452	21754	22218	31537	32078	32796	38541	25352	25170	34473	0.1332	0.0699	0.44	0.45	UNCHANGED	UNCHANGED
A0A251TU05	2	521.5	Dihydrolipoyl dehydrogenase	22130	23649	42188	30215	24487	23663	38224	25535	67633	29322	26121	43798	0.3606	0.2344	0.58	0.75	UNCHANGED	UNCHANGED
A0A251UU89	2	449.5	Proteasome subunit alpha type	22331	25833	23355	28654	35504	28899	29871	29304	24562	23839	31019	27912	0.1086	0.3301	0.23	-0.15	UNCHANGED	UNCHANGED
A0A251VAW4	2	445.0	Putative oxygen-dependent coproporphyrinogen-II	19584	16579	22239	25295	23590	10589	19522	18687	19294	19467	19824	19167	0.8649	0.8945	-0.02	-0.05	UNCHANGED	UNCHANGED
A0A251UNG6	2	440.5	Putative pyridoxal phosphate (PLP)-dependent tra	27382	14526	13881	21072	17219	11719	18385	18856	17200	18596	16670	18147	0.9240	0.6207	-0.04	0.12	UNCHANGED	UNCHANGED
A0A251RNZ2	2	362.6	Serine hydroxymethyltransferase	10152	14058	9360	17898	19093	13504	13631	15811	13908	11190	16831	14450	0.1122	0.2635	0.37	-0.22	UNCHANGED	UNCHANGED
A0A251UTA4	16	1354.0	Putative translation elongation factor EFG/EF2	0	0	0	12645	12130	14821	18057	18340	17842	0	13199	18080	-	0.0043	-	0.45	Unique T12-IB	UNCHANGED
A0A251UV16	6	814.5	Putative phosphoenolpyruvate carboxykinase 1	0	0	0	53143	55393	29125	28151	28655	30034	0	45887	28947	-	0.1147	-	-0.66	Unique T12-IB	UNCHANGED
A0A251RMC4	23	32691.5	Glyceraldehyde-3-phosphate dehydrogenase	238391	230230	245861	702299	884387	335488	476483	519805	505755	238161	640725	500681	0.0000	0.4359	1.07	-0.36	UP	UNCHANGED
A0A251SX18	19	17923.1	Malate dehydrogenase	130069	146523	141490	168894	159488	138838	205359	229652	211282	139361	155740	215431	0.0010	0.0066	0.63	0.47	UP	UNCHANGED
A0A251U5Z0	35	10606.3	Putative heat shock protein 70 family	115617	124425	135024	196571	193992	156231	192367	229831	217221	125022	182264	213139	0.0020	0.1446	0.77	0.23	UP	UNCHANGED
A0A251TDM5	20	7697.8	Pyruvate kinase	105309	103207	108242	115774	104215	104983	162914	159800	158513	105586	108324	160409	0.0000	0.0002	0.60	0.57	UP	UNCHANGED
A0A251TLI1	9	6663.7	Malate dehydrogenase	89062	100845	89991	129197	126906	107929	144859	153501	146861	93299	121344	148407	0.0003	0.0201	0.67	0.29	UP	UNCHANGED
A0A251VIE1	14	5747.9	Putative alpha-1,4-glucan-protein synthase [UDP-	70759	66989	68276	102537	108949	85277	147578	144992	139568	68675	98921	144046	0.0000	0.0038	1.07	0.54	UP	UNCHANGED
A0A251TBW8	10	5039.0	Putative aldo/keto reductase/potassium channel s	58431	47001	56390	98920	92122	61680	82669	79866	90456	53941	84241	84330	0.0030	0.9944	0.64	0.00	UP	UNCHANGED
A0A251UCP2	9	3595.6	Phenylalanine ammonia-lyase	55389	49950	47431	138633	130778	67324	97775	104832	93317	50923	112245	98641	0.0003	0.5832	0.95	-0.19	UP	UNCHANGED
A0A251UD42	16	3586.5	Putative cobalamin-independent methionine synth	103249	118016	113343	125971	126070	105469	165028	178311	173736	111536	119170	172358	0.0005	0.0025	0.63	0.53	UP	UNCHANGED
A0A251SKA0	6	3550.3	Phenylalanine ammonia-lyase	75520	65120	74430	123033	106812	54216	114049	137925	123172	71690	94687	125049	0.0023	0.2380	0.80	0.40	UP	UNCHANGED

A0A251RMS7	3	3311.8	Putative ribosomal protein S3, eukaryotic/archaea	32541	21772	24158	32892	50929	58121	63658	61986	71129	26157	47314	65591	0.0008	0.0847	1.33	0.47	UP	UNCHANGED
A0A251UVM0	8	3116.8	Putative 14-3-3-like protein C	12353	11450	12056	20153	15882	12239	18992	18777	16634	11953	16091	18134	0.0015	0.4439	0.60	0.17	UP	UNCHANGED
A0A251TU95	11	2165.8	Putative calreticulin	91543	84055	74627	120127	109803	96850	141363	133436	136397	83408	108927	137069	0.0006	0.0168	0.72	0.33	UP	UNCHANGED
A0A251S3U4	7	1999.0	UTP--glucose-1-phosphate uridylyltransferase	848	821	1050	1567	1568	485	2143	1802	2241	906	1207	2062	0.0016	0.0901	1.19	0.77	UP	UNCHANGED
A0A251TI04	11	1785.2	Putative heat shock protein 70 family	63623	68426	73333	97631	104089	85557	110094	112612	109632	68461	95759	110779	0.0001	0.0526	0.69	0.21	UP	UNCHANGED
A0A251UK46	8	1173.6	Putative 26S protease regulatory subunit 6B	30949	31128	33727	40479	43237	46067	52592	51996	57090	31935	43261	53892	0.0003	0.0095	0.75	0.32	UP	UNCHANGED
A0A251VJB1	5	1154.5	Putative peroxisomal 3-ketoacyl-CoA thiolase 3	68048	75123	76300	77969	86737	71768	117972	118411	118178	73157	78825	118187	0.0001	0.0008	0.69	0.58	UP	UNCHANGED
A0A251TM90	6	1047.9	D-3-phosphoglycerate dehydrogenase	50107	43317	40029	67903	55360	36303	68752	69073	65765	44485	53189	67863	0.0018	0.1877	0.61	0.35	UP	UNCHANGED
A0A251UAH6	2	868.3	Putative isocitrate dehydrogenase [NAD] regulator	13236	13818	13738	30120	20522	14051	31762	33155	27074	13597	21564	30664	0.0008	0.1439	1.17	0.51	UP	UNCHANGED
A0A251U157	3	822.8	Putative elongation factor 1-delta	30686	31702	24703	98157	76065	37017	48802	58441	58012	29030	70413	55085	0.0024	0.4459	0.92	-0.35	UP	UNCHANGED
A0A251SQM5	2	438.1	T-complex protein 1 subunit gamma	40414	39523	29874	45427	45959	39254	49828	62802	59085	36604	43547	57238	0.0158	0.0362	0.64	0.39	UP	UNCHANGED
A0A251UXA6	2	339.4	Polyadenylate-binding protein	28677	29508	24270	41880	44650	36684	41579	43213	42410	27485	41071	42400	0.0009	0.6065	0.63	0.05	UP	UNCHANGED
A0A251VB88	5	20777.1	Nucleoside diphosphate kinase	103972	87286	84544	162755	139414	119122	131087	122121	111133	91934	140430	121447	0.0244	0.2428	0.40	-0.21	UNCHANGED	UNCHANGED
P69313	9	16797.2	Ubiquitin	125108	108526	112084	209360	152597	175152	169248	161632	150903	115239	179036	160594	0.0035	0.3474	0.48	-0.16	UNCHANGED	UNCHANGED
A0A251V987	42	15102.3	Aconitate hydratase	108140	142627	131307	194558	234155	182038	158635	163930	144195	127358	203584	155587	0.0740	0.0459	0.29	-0.39	UNCHANGED	UNCHANGED
A0A251V7G1	32	14155.3	Aconitate hydratase	113680	110824	122380	184827	185903	178782	118814	119970	132270	115628	183170	123685	0.2191	0.0003	0.10	-0.57	UNCHANGED	UNCHANGED
A0A251SDV8	9	11900.1	Putative triosephosphate isomerase, Aldolase-typ	133335	125961	126028	216129	239199	178070	153453	147513	142215	128441	211133	147727	0.0090	0.0249	0.20	-0.52	UNCHANGED	UNCHANGED
A0A251UVM9	12	9881.5	40S ribosomal protein SA	194500	213111	191477	289161	365340	372135	254544	235214	219379	199696	342212	236379	0.0398	0.0205	0.24	-0.53	UNCHANGED	UNCHANGED
A0A251S6A3	13	2277.7	Putative chaperonin Cpn60/TCP-1 family	30851	27851	26511	59220	57604	38107	32225	30435	35425	28404	51644	32695	0.0918	0.0524	0.20	-0.66	UNCHANGED	UNCHANGED
A0A251T3E2	3	1535.0	Proteasome subunit beta	10866	18235	18460	38255	33982	24581	20858	17195	23306	15854	32273	20453	0.2075	0.0553	0.37	-0.66	UNCHANGED	UNCHANGED
A0A251UC74	3	782.8	Putative carrier protein	29548	26164	38224	50104	69817	47954	37444	39642	48962	31312	55958	42016	0.1007	0.1485	0.42	-0.41	UNCHANGED	UNCHANGED
A0A251V1J0	3	542.1	Putative transketolase protein	35909	38842	37157	88318	65524	57798	48667	48614	50728	37302	70547	49336	0.0004	0.0822	0.40	-0.52	UNCHANGED	UNCHANGED
A0A251RUY3	19	27536.2	Glyceraldehyde-3-phosphate dehydrogenase	42658	43389	44495	101554	110544	56916	90437	95313	93712	43514	89672	93154	0.0000	0.8445	1.10	0.05	UP	UNCHANGED
A0A251RZF8	32	22689.5	Putative enolase	229562	231668	235592	546069	470402	378788	589439	553089	528341	232274	465086	556956	0.0001	0.1491	1.26	0.26	UP	UNCHANGED
A0A251VCJ8	19	17682.7	Malate dehydrogenase	147064	169139	164618	305794	301594	345948	232265	257519	243376	160274	317779	244387	0.0011	0.0099	0.61	-0.38	UP	UNCHANGED
A0A251UZB2	32	12405.1	Putative heat shock protein 70 family	79273	74440	82214	123620	120016	141682	179813	179523	165380	78642	128440	174906	0.0001	0.0048	1.15	0.45	UP	UNCHANGED
A0A251SFD5	19	11471.1	Fructose-bisphosphate aldolase	130551	147994	132669	372151	393086	313661	326693	325509	342549	137071	359633	331584	0.0000	0.3143	1.27	-0.12	UP	UNCHANGED
A0A251RZ67	9	9550.4	Putative cysteine synthase	103844	108368	128159	372030	457307	496206	371106	332859	339494	113457	441848	347820	0.0001	0.0711	1.62	-0.35	UP	UNCHANGED
A0A251VQU0	12	8690.5	Putative ribosomal protein L11/L12	29235	29141	29552	118774	111016	111508	159533	161540	158852	29310	113766	159975	0.0000	0.0001	2.45	0.49	UP	UNCHANGED
A0A251SHB7	6	6864.5	Putative pyridoxal phosphate-dependent decarbox	24205	24120	25999	100127	81344	52806	56822	55672	63794	24775	78093	58763	0.0002	0.2392	1.25	-0.41	UP	UNCHANGED
A0A251SFZ4	6	6355.4	Putative aldo/keto reductase/potassium channel s	37185	36734	36885	101569	97590	81253	118340	106490	135504	36934	93471	120111	0.0006	0.0636	1.70	0.36	UP	UNCHANGED
A0A251UIF7	12	6333.2	Putative aldo/keto reductase/potassium channel s	19386	20096	22313	48257	43637	45775	43076	36322	39552	20598	45890	39650	0.0009	0.0576	0.94	-0.21	UP	UNCHANGED
A0A251VHX8	13	6048.4	GTP-binding nuclear protein	46264	56808	55992	126470	132820	130845	125907	124445	138564	53021	130045	129639	0.0002	0.9374	1.29	0.00	UP	UNCHANGED
A0A251SVS3	9	5840.7	Fructose-bisphosphate aldolase	30111	31049	29424	62260	58598	44336	44315	46546	49527	30195	55065	46796	0.0005	0.2186	0.63	-0.23	UP	UNCHANGED
O04058	14	5666.3	Phenylalanine ammonia-lyase	18714	20660	20091	35814	37017	37423	37803	34018	37262	19822	36751	36361	0.0002	0.7750	0.88	-0.02	UP	UNCHANGED
A0A251SXU2	7	5578.2	Putative bifunctional polymyxin resistance protein,	44715	39842	53610	83193	71144	74459	84284	81987	86255	46056	76265	84175	0.0008	0.1058	0.87	0.14	UP	UNCHANGED
A0A251S4H3	6	4940.5	Glutamine synthetase	52750	62243	63096	106299	112350	95383	107491	101439	104027	59363	104677	104319	0.0003	0.9490	0.81	0.00	UP	UNCHANGED
A6XIG5	2	4825.2	Superoxide dismutase	54796	60279	61057	146924	143906	94876	92232	86866	90389	58711	128569	89829	0.0002	0.0842	0.61	-0.52	UP	UNCHANGED
A0A251RVT5	6	4450.2	Putative pyridoxal phosphate-dependent transfera	30541	22006	29884	95961	108813	86906	79834	75725	73442	27477	97227	76334	0.0001	0.0344	1.47	-0.35	UP	UNCHANGED
A0A251SC90	5	4087.8	Fructose-bisphosphate aldolase	30092	37333	27598	50874	56500	44191	64301	62740	64983	31674	50521	64008	0.0004	0.0204	1.01	0.34	UP	UNCHANGED
A0A251RM91	11	3870.7	Putative UDP-arabinopyranose mutase	14803	14093	15856	36365	30010	20919	23450	22513	23193	14917	29098	23052	0.0002	0.2494	0.63	-0.34	UP	UNCHANGED
A0A251VNF4	2	3746.2	Putative ribosomal protein L14b/L23e	16499	16293	24468	58559	73477	82277	99523	111586	113105	19086	71436	108071	0.0001	0.0109	2.50	0.60	UP	UNCHANGED

A0A251RWQ6	10	3744.9	Putative reversibly glycosylated polypeptide 1	22843	19966	23814	65630	61504	49452	42659	39197	36849	22208	58862	39568	0.0011	0.0199	0.83	-0.57	UP	UNCHANGED
A0A251S9P3	9	3639.9	Putative alcohol dehydrogenase 1	16666	15103	19063	98861	98944	80743	85650	82699	82268	16944	92849	83539	0.0000	0.2044	2.30	-0.15	UP	UNCHANGED
A0A251RMF3	2	3372.0	40S ribosomal protein S27	22634	26728	30566	46840	44701	34723	58367	60625	60866	26643	42088	59952	0.0002	0.0095	1.17	0.51	UP	UNCHANGED
A0A251SL49	14	3321.9	Putative elongation factor 1-alpha	74200	101236	92022	181027	195243	283633	271089	254696	323956	89153	219968	283247	0.0010	0.1738	1.67	0.36	UP	UNCHANGED
A0A251S5A3	7	3250.0	Putative naringenin,2-oxoglutarate 3-dioxygenase	30756	36253	34399	92557	99184	102755	71930	69488	69839	33803	98165	70419	0.0000	0.0008	1.06	-0.48	UP	UNCHANGED
A0A251SAT8	8	3092.9	UTP--glucose-1-phosphate uridylyltransferase	71532	79178	68913	153709	149928	107953	115546	116726	111612	73208	137197	114628	0.0003	0.2006	0.65	-0.26	UP	UNCHANGED
A0A251UXL3	9	3064.3	Formate dehydrogenase, mitochondrial	42619	44783	55286	261443	469947	366382	232057	205333	213683	47563	365924	217024	0.0000	0.0702	2.19	-0.75	UP	UNCHANGED
A0A251SIP5	10	2913.9	UDP-glucose 6-dehydrogenase	26778	28858	30752	106464	121780	109407	88859	83971	80367	28796	112551	84398	0.0000	0.0060	1.55	-0.42	UP	UNCHANGED
A0A251TJH9	10	2894.3	Putative guanine nucleotide-binding protein subun	11168	21282	13705	50096	42770	33582	42791	43052	41537	15385	42149	42460	0.0009	0.9515	1.46	0.01	UP	UNCHANGED
A0A251SZ13	8	2873.5	Aspartate aminotransferase	24568	24852	28246	92246	109603	53133	110908	112742	118480	25889	84994	114043	0.0000	0.1599	2.14	0.42	UP	UNCHANGED
A0A251T6A5	5	2748.1	Carbonic anhydrase	2452	2546	2426	6952	6007	4185	8551	7682	7922	2475	5715	8052	0.0000	0.0518	1.70	0.49	UP	UNCHANGED
A0A251SQ34	15	2594.0	Putative ATP-citrate synthase beta chain protein 1	36274	42565	41308	54651	77363	92014	90064	87328	104172	40049	74676	93855	0.0006	0.1869	1.23	0.33	UP	UNCHANGED
A0A251SFI7	9	2370.2	Serine hydroxymethyltransferase	36985	45185	46842	90145	90579	74478	66267	65315	67225	43004	85067	66269	0.0017	0.0242	0.62	-0.36	UP	UNCHANGED
A0A251S4G9	11	2326.6	Putative phosphoglycerate mutase, 2,3-bisphosph	22357	25071	23776	70568	66874	74700	69071	65359	80111	23734	70714	71514	0.0004	0.8801	1.59	0.02	UP	UNCHANGED
A0A251U954	8	2281.4	Aspartate aminotransferase	51735	52449	49767	151913	136073	88700	138738	145026	156840	51317	125562	146868	0.0001	0.3407	1.52	0.23	UP	UNCHANGED
A0A251SC86	5	2046.6	Putative adenine nucleotide alpha hydrolases-like	42762	52366	39736	88644	75945	80261	82601	83624	78907	44955	81617	81711	0.0008	0.9823	0.86	0.00	UP	UNCHANGED
A0A251TWM3	11	2043.2	Succinate dehydrogenase [ubiquinone] flavoprotei	15578	16202	17124	46531	50288	40213	41600	39888	41256	16301	45677	40915	0.0000	0.1859	1.33	-0.16	UP	UNCHANGED
A0A251STB4	21	1976.8	Putative translation elongation factor EFG/EF2, ar	59188	59162	64297	183667	176706	228756	168755	172353	178918	60882	196377	173342	0.0000	0.2372	1.51	-0.18	UP	UNCHANGED
A0A251T816	4	1932.7	Glyceraldehyde-3-phosphate dehydrogenase	13559	6213	16612	52167	66723	41880	40637	35797	39092	12128	53590	38509	0.0015	0.1093	1.67	-0.48	UP	UNCHANGED
A0A251U6R5	7	1737.3	Putative heat shock protein Hsp90 family	11775	14676	11732	22446	19663	24875	19886	20829	22861	12727	22328	21192	0.0030	0.5500	0.74	-0.08	UP	UNCHANGED
A0A251U6Q5	4	1663.6	ATP-dependent 6-phosphofructokinase	19569	17545	19768	52650	48563	37073	57450	56004	56708	18961	46096	56721	0.0000	0.0858	1.58	0.30	UP	UNCHANGED
A0A251T3K3	4	1614.1	Eukaryotic translation initiation factor 5A	16687	16922	9904	117805	61829	49405	57068	58960	53230	14504	76346	56419	0.0001	0.3985	1.96	-0.44	UP	UNCHANGED
A0A251TJC8	8	1606.3	Pyruvate kinase	28704	26323	29905	38572	44699	46388	49072	48380	48769	28311	43220	48740	0.0000	0.0814	0.78	0.17	UP	UNCHANGED
A0A251SM90	2	1461.8	Eukaryotic translation initiation factor 3 subunit F	23004	20172	20398	46277	43220	38018	40479	40434	46332	21191	42505	42415	0.0006	0.9783	1.00	0.00	UP	UNCHANGED
A0A251RY43	8	1423.9	D-3-phosphoglycerate dehydrogenase	20323	19836	19534	46384	45276	43801	45071	44082	45093	19898	45153	44749	0.0000	0.6473	1.17	-0.01	UP	UNCHANGED
A0A251TYV0	2	1388.7	Putative porin domain, Eukaryotic porin/Tom40	75139	71108	86477	146848	140938	132811	177466	155860	150914	77574	140199	161413	0.0009	0.0804	1.06	0.20	UP	UNCHANGED
A0A251S4C1	3	1294.0	Isocitrate dehydrogenase [NADP]	2632	3394	2345	16780	35795	58724	20152	18949	35542	2790	37100	24881	0.0145	0.4086	3.16	-0.58	UP	UNCHANGED
A0A251TPA8	8	1269.6	Putative regulatory particle triple-A 1A	22874	20863	21014	63403	63137	48728	52905	53244	58110	21584	58423	54753	0.0001	0.5140	1.34	-0.09	UP	UNCHANGED
A0A251SC35	4	1224.4	Pyruvate kinase	18096	22071	21134	51442	49699	52621	42434	43341	43260	20434	51254	43012	0.0001	0.0008	1.07	-0.25	UP	UNCHANGED
A0A251RW81	5	1086.8	Putative DEAD/DEAH box RNA helicase family p	10634	9190	11185	17654	17295	14681	20177	20555	22514	10337	16543	21082	0.0003	0.0186	1.03	0.35	UP	UNCHANGED
A0A251UCL5	5	1048.2	6-phosphogluconate dehydrogenase, decarboxyla	14041	14397	14031	40840	31145	35355	26418	26238	24714	14156	35780	25790	0.0000	0.0250	0.87	-0.47	UP	UNCHANGED
A0A251SET7	6	940.4	Ferredoxin--NADP reductase, chloroplastic	5320	9346	4952	73730	60858	41310	58950	58295	57866	6539	58633	58370	0.0000	0.9791	3.16	-0.01	UP	UNCHANGED
A0A251V6Y9	5	846.9	Putative rhamnose biosynthesis 1	5266	5766	5939	26005	31752	37465	19507	26268	25474	5657	31741	23749	0.0011	0.1122	2.07	-0.42	UP	UNCHANGED
A0A251S7I3	2	818.9	Pyruvate dehydrogenase E1 component subunit a	4416	5392	5553	26547	27204	32883	30519	29918	34196	5120	28878	31544	0.0000	0.3315	2.62	0.13	UP	UNCHANGED
A0A251UVK3	3	719.9	Putative enolase 1	10381	11787	9256	24767	22390	21225	24700	26675	23714	10474	22794	25030	0.0002	0.1750	1.26	0.13	UP	UNCHANGED
A0A251S999	2	551.5	Putative chaperonin Cpn60/TCP-1 family	15808	13924	17312	28485	30582	33440	33807	33495	33258	15681	30835	33520	0.0001	0.1368	1.10	0.12	UP	UNCHANGED
A0A251TNS0	3	456.2	Putative heat shock protein 70 family	16528	14721	19526	30681	30607	20648	31297	30478	36500	16925	27312	32758	0.0025	0.2280	0.95	0.26	UP	UNCHANGED
A0A251UZF1	2	408.2	Putative FUMARASE 2	14419	16758	17067	33465	39733	28892	36573	34680	32819	16081	34030	34690	0.0002	0.8521	1.11	0.03	UP	UNCHANGED
A0A251SSL2	3	395.9	Putative NAD(P)-linked oxidoreductase superfami	11310	11560	11582	24546	22287	22280	25275	26194	23613	11484	23038	25027	0.0001	0.1358	1.12	0.12	UP	UNCHANGED
A0A251RZ00	2	393.5	Pyrophosphate--fructose 6-phosphate 1-phosphot	9654	7366	9074	37492	29199	14928	15820	15885	17482	8698	27206	16396	0.0009	0.1774	0.91	-0.73	UP	UNCHANGED
A0A251TK70	2	348.7	Importin subunit alpha	15280	12476	13044	25534	22869	22733	25862	29422	26927	13600	23712	27404	0.0005	0.0572	1.01	0.21	UP	UNCHANGED

A0A251S450	2	1748.0	Ferredoxin--NADP reductase, chloroplastic	41143	41596	45714	21400	29526	26331	0	0	0	42818	25752	0	-	-	-	-	Unique T0	nique T12-Contr
A0A251TWM2	4	1104.3	Putative alpha-hydroxy acid dehydrogenase, FMN	19631	23571	24191	8246	8981	5671	0	0	0	22464	7632	0	-	-	-	-	Unique T0	nique T12-Contr
A0A251SWE6	3	5204.8	Putative heat shock protein 70 family	2026	2579	2954	1230	1655	2006	0	0	0	2520	1630	0	-	-	-	-	Unique T0	nique T12-Contr
Q94EN1	4	2092.1	Tubulin alpha chain	14084	17906	15202	17946	17423	12832	0	0	0	15731	16067	0	-	-	-	-	Unique T0	nique T12-Contr
A0A251U0S0	11	29880.4	Glyceraldehyde-3-phosphate dehydrogenase	0	0	0	214893	266205	205409	0	0	0	0	228836	0	-	-	-	-	-	nique T12-Contr
A0A251TIG3	23	14433.2	Tubulin beta chain	0	0	0	51257	68745	64484	0	0	0	0	61496	0	-	-	-	-	-	nique T12-Contr
A0A251UUW2	20	6466.4	Putative alcohol dehydrogenase superfamily, zinc-	0	0	0	18789	25780	28111	0	0	0	0	24227	0	-	-	-	-	-	nique T12-Contr
A0A251SRH7	11	2871.3	Putative cobalamin-independent methionine synth	0	0	0	6143	6401	5574	0	0	0	0	6039	0	-	-	-	-	-	nique T12-Contr
A0A251UC35	2	1845.4	Glutamine synthetase	0	0	0	2642	3006	2714	0	0	0	0	2787	0	-	-	-	-	-	nique T12-Contr
A0A251UXN7	2	2778.3	S-(hydroxymethyl)glutathione dehydrogenase	53402	60848	63088	0	0	0	20181	31174	38959	59113	0	30109	0.0094	-	-0.97	-	DOWN	Unique T12-IBA
A0A251T4H2	28	28572.5	Tubulin alpha chain	0	0	0	0	0	0	2665	2722	2758	0	0	2719	-	-	-	-	Unique T12-IB	Unique T12-IBA
A0A251UI91	4	1200.0	Putative metalloenzyme, LuxS/M16 peptidase-like	0	0	0	0	0	0	4535	5180	4730	0	0	4819	-	-	-	-	Unique T12-IB	Unique T12-IBA
A0A251UBI4	2	1129.6	Putative glycoside hydrolase family 3 C-terminal d	11440	10392	10698	0	0	0	13073	11971	11719	10843	0	12259	0.0531	-	0.18	-	UNCHANGE	Unique T12-IBA
A0A251V3B5	2	917.8	Putative cupredoxin	4828	7937	14237	0	0	0	15991	18752	13153	9001	0	15969	0.0955	-	0.83	-	UNCHANGE	Unique T12-IBA
A0A251V5D0	3	1151.0	Putative leucine aminopeptidase 2, chloroplastic	22510	12986	20265	0	0	0	34335	33866	31174	18587	0	33129	0.0087	-	0.83	-	UP	Unique T12-IBA
A0A251SIJ8	6	944.9	Putative phosphoenolpyruvate carboxykinase 2	0	2334	1576	43958	39081	12744	61861	63265	69109	1955	31928	64745	-	0.0299	-	1.02	-	UP
A0A251U9A3	25	12203.1	Tubulin beta chain	34639	38514	35730	12363	9487	6815	16017	16599	15920	36294	9555	16179	0.0001	0.0149	-1.17	0.76	DOWN	UP
A0A251TYC2	4	1444.9	Putative band 7 domain, Stomatin family	30341	24619	23559	2843	3654	3505	15395	13755	13783	26173	3334	14311	0.0055	0.0001	-0.87	2.10	DOWN	UP
I3RXT3	7	17218.4	Glyceraldehyde-3-phosphate dehydrogenase (Fra	40641	40567	42538	3356	3291	2501	45499	49103	50040	41248	3049	48214	0.0103	0.0000	0.23	3.98	UNCHANGE	UP
A0A251TC36	8	11645.8	Putative ubiquitin	58574	59381	58171	38567	28952	31342	53029	55111	49971	58709	32954	52704	0.0173	0.0037	-0.16	0.68	UNCHANGE	UP
A0A251S3K3	7	1786.7	Putative heat shock protein Hsp90 family, DNA m	0	0	0	7494	6565	8306	18150	18123	19243	0	7455	18509	-	0.0001	-	1.31	Unique T12-IB	UP
A0A251TVR1	2	779.2	Putative 40S ribosomal protein S14	0	0	0	12095	12589	18558	40115	43245	47793	0	14414	43718	-	0.0007	-	1.60	Unique T12-IB	UP
A0A251TI46	13	30420.8	Tubulin alpha chain	117682	114841	125558	30085	28218	26425	329432	330319	402969	119360	28243	35424	0.0007	0.0002	1.57	3.65	UP	UP
A0A251VA91	6	12717.7	aconitate hydratase, cytoplasmic	9030	8967	10448	2521	2418	1852	34998	35181	33978	9482	2264	34719	0.0000	0.0000	1.87	3.94	UP	UP
A0A251UD22	7	4577.0	Glutamate decarboxylase	152574	139701	156735	105370	93419	47863	411373	419756	429739	149670	82218	420289	0.0000	0.0001	1.49	2.35	UP	UP
A0A251TVC8	4	3480.6	Putative ribosomal protein S28e	47899	29215	42617	27541	23014	18354	39244	37811	33857	39910	22970	36971	0.6384	0.0107	-0.11	0.69	UNCHANGE	UP
A0A251RNJ4	4	1566.7	Eukaryotic translation initiation factor 5A	61856	65659	55647	66463	52429	35459	91338	90412	82165	61054	51450	87971	0.0028	0.0179	0.53	0.77	UNCHANGE	UP
A0A251UWT5	3	874.1	Putative mov34/MPN/PAD-1 family protein	4445	3904	4717	2811	4013	4188	6611	5327	6347	4356	3671	6095	0.0192	0.0142	0.48	0.73	UNCHANGE	UP
A0A251U4X4	3	761.0	Peroxidase	101440	121868	135372	77208	91041	85859	191893	146008	177735	119560	84703	171879	0.0355	0.0035	0.52	1.02	UNCHANGE	UP
A0A251U688	3	680.8	Catalase	59934	64433	66605	54134	60786	68380	88430	88150	104487	63657	61100	93689	0.0064	0.0086	0.56	0.62	UNCHANGE	UP
Q9LKG3	33	15232.9	Actin	284903	249421	271876	307435	296220	290659	521204	496771	511877	268733	298105	509951	0.0000	0.0000	0.92	0.77	UP	UP
A0A251VHZ2	37	13949.8	Putative heat shock protein 70 (Hs 70) family pro	134226	140004	150983	165461	182996	211046	287109	287983	276881	141738	186501	283991	0.0000	0.0021	1.00	0.61	UP	UP
A0A251U8U5	19	9666.5	Adenosylhomocysteinase	63204	70333	76360	82259	96738	132193	252264	247960	226529	69966	103730	242251	0.0000	0.0012	1.79	1.22	UP	UP
A0A251U2Z0	4	8599.0	10 kDa chaperonin, mitochondrial-like	32765	26455	29937	42128	32614	18824	56217	56754	45876	29719	31189	52949	0.0043	0.0464	0.83	0.76	UP	UP
A0A251SEI5	10	3076.3	Putative guanine nucleotide-binding protein subun	59029	65257	61863	115989	88084	57935	152275	146518	152564	62050	87336	150452	0.0000	0.0201	1.28	0.78	UP	UP
A0A251SL31	18	2539.4	Putative ATPase, AAA-type, core	13076	14832	14017	14643	19756	25139	42932	39429	55961	13975	19846	46107	0.0031	0.0111	1.72	1.22	UP	UP
A0A251TG61	5	2417.4	Peroxidase	58477	50952	54991	88476	75726	60473	123012	121955	118341	54806	74892	121103	0.0000	0.0049	1.14	0.69	UP	UP
A0A251STZ1	3	2260.0	Putative band 7 domain, Stomatin family	6950	6163	6719	8893	7612	7156	18841	18469	18408	6611	7887	18573	0.0000	0.0000	1.49	1.24	UP	UP
A0A251S412	9	2169.8	Succinate dehydrogenase [ubiquinone] flavoprotei	23620	22534	26485	29772	32553	25954	62263	59826	62548	24213	29426	61546	0.0000	0.0001	1.35	1.06	UP	UP
A0A251RL14	5	1813.1	Putative glutamate--cysteine ligase protein	40364	34276	47942	45767	34168	36705	100341	104831	107533	40861	38880	104239	0.0001	0.0001	1.35	1.42	UP	UP
A0A251SVK6	2	1349.9	Putative hydrolyase LeuD/HacB/DmdB, Aconitase	12396	19703	10883	22113	17013	20708	32437	31724	29833	14327	19945	31331	0.0039	0.0026	1.13	0.65	UP	UP

A0A251RYB8	6	1163.0	Putative helicase Cas3, CRISPR-associated, core	21485	14434	21580	30500	29537	26259	52628	55432	66385	19166	28765	58149	0.0013	0.0026	1.60	1.02	UP	UP
A0A251TK47	2	1142.3	Putative translation elongation factor EF1B, gamm	48790	46203	58336	52940	54746	50784	165659	157103	160732	51110	52823	161164	0.0000	0.0000	1.66	1.61	UP	UP
A0A251RV70	4	874.5	Putative biotin carboxylase 2, chloroplastic	16304	13613	17920	18255	16730	18459	28856	28846	27117	15946	17814	28273	0.0009	0.0002	0.83	0.67	UP	UP
A0A251VGM2	3	743.6	Putative UDP-XYL synthase 5	29951	27999	35803	40858	42718	32941	57549	57183	63675	31251	38839	59469	0.0009	0.0049	0.93	0.61	UP	UP
A0A251RY75	4	678.3	Proteasome endopeptidase complex	16021	14084	15590	14085	12704	4109	26604	24542	22292	15232	10299	24479	0.0026	0.0135	0.68	1.25	UP	UP
A0A251TQG2	2	572.6	Sucrose synthase	18796	21672	24432	29889	23492	22194	44411	48257	77621	21633	25192	56763	0.0297	0.0426	1.39	1.17	UP	UP
A0A251SKI7	4	533.6	Putative heat shock protein 70 family	31889	31061	24834	40752	43102	33019	74293	69034	74093	29262	38958	72473	0.0001	0.0007	1.31	0.90	UP	UP
A0A251UM84	3	5529.6	Putative heat shock protein 70 family	15589	15946	18909	37053	35770	36193	70891	70746	74251	16814	36338	71963	0.0000	0.0000	2.10	0.99	UP	UP
A0A251T0P6	7	4404.5	Putative alanine aminotransferase 2	5702	3818	4759	98044	106993	95791	163612	160516	148081	4760	100276	157403	0.0000	0.0006	5.05	0.65	UP	UP
A0A251TDI1	15	2600.6	Putative ATPase, AAA-type, core	10521	10926	11044	24649	19263	24377	71855	63409	86863	10830	22763	74042	0.0008	0.0019	2.77	1.70	UP	UP
A0A251UMF5	15	1718.1	Aconitate hydratase	3003	3709	3456	6197	7262	6199	14529	15975	15915	3389	6552	15473	0.0000	0.0001	2.19	1.24	UP	UP
A0A251T189	5	1599.8	Citrate synthase	21082	20095	26212	44431	52199	48084	72686	75503	77816	22463	48238	75339	0.0000	0.0005	1.75	0.64	UP	UP
A0A251TUX6	3	1120.9	Isocitrate dehydrogenase [NADP]	5729	9159	10703	24242	30055	42768	71764	69485	70089	8530	32355	70446	0.0000	0.0023	3.05	1.12	UP	UP
A0A251S029	2	560.8	Eukaryotic translation initiation factor 3 subunit D	5267	4101	6650	9556	9006	9913	15250	16334	14439	5339	9491	15341	0.0004	0.0007	1.52	0.69	UP	UP
A0A251U744	2	500.2	Acyl-coenzyme A oxidase	3442	3919	5370	17541	21030	17131	37975	38869	37872	4244	18567	38238	0.0000	0.0001	3.17	1.04	UP	UP

Apêndice C – Capítulo: Storage environment alters physiological aspects and proteomic profile in seeds of Cariniana legalis (Martius) O. Kuntze

Tabela Suplementar 1: Lista completa de todas as proteínas identificadas

				Nermalized Total Ion Cout (Tic)									AVERAGE			t-Test			Log2 of fold change			Differncial accumulation		
accession	reported peptides	max score	description	T0 1	T0 2	T0 3	T8_6 1	T8_6 2	T8_6 3	T8_25 1	T8_25 2	T8_25 3	AVERAGE T0	VERAGE T8_	VERAGE T8_	6°CxT0	25°Cx T0	25°Cx6°C	6°CxT0	25°Cx T0	25°Cx6°C	6°CxT0	25°Cx T0	25°Cx6°C
A0A251V667	5	461	Putative NADP-dependent glyceralde	2947	1812	1653	3220	3197	3831	1136	1492	1779	2137	3416	1469	0.0489	0.2100	0.002	0.67	-0.54	-1.21	UP	UNCHANG	Down
A0A251U954	9	3113	Aspartate aminotransferase	34000	61265	44074	144711	101939	93682	67343	88752	67795	46447	113444	74630	0.0194	0.0571	0.088	1.28	0.68	-0.60	UP	UNCHANG	UNCHANGED
A0A251UNC3	20	9985	Putative heat shock protein	32832	45033	48162	28717	27882	17040	19969	13772	21678	42009	24547	18473	0.0437	0.0110	0.245	-0.77	-1.18	-0.41	Down	Down	UNCHANGED
A0A251VIL2	7	629	Tubulin alpha chain	25725	28268	26784	14651	18496	20036	13821	17477	15574	26926	17728	15624	0.0064	0.0009	0.334	-0.60	-0.78	-0.18	Down	Down	UNCHANGED
I6LNU0	5	4762	Phosphoglycerate kinase	4113	4687	4704	2819	3007	3072	2490	2481	2210	4501	2966	2394	0.0018	0.0006	0.008	-0.60	-0.91	-0.30	Down	Down	UNCHANGED
A0A251UU95	4	1147	Putative RAB GTPase	26374	26405	28228	14002	18979	18940	18939	21600	22748	27003	17307	21096	0.0053	0.0100	0.131	-0.64	-0.35	0.28	Down	UNCHANG	UNCHANGED
A0A251V9N0	4	1529	Heat shock protein 90-2	32064	31357	29037	18377	21538	15728	22436	28257	31819	30819	18548	27504	0.0030	0.3143	0.049	-0.73	-0.16	0.56	Down	UNCHANG	UNCHANGED
A0A251VA77	12	4135	heat shock protein 70 family; Lumina	33655	43007	34852	22018	23236	28269	20106	26703	27028	37171	24508	24612	0.0225	0.0275	0.973	-0.60	-0.59	0.00	Down	UNCHANG	UNCHANGED
A0A251VGY2	4	1446	14-3-3-like protein D	18245	20251	16946	0	0	0	17562	16889	17738	18481	0	17396	-	0.3373	-	-	-0.08	-	ÚNICA T0	UNCHANG	ÚNICA 25°
A0A251SG50	4	2224	14-3-3 domain-containing protein	5777	6412	5369	0	0	0	0	0	0	5851	0	0	-	-	-	-	-	-	ÚNICA T0	ÚNICA T0	-
A0A251V7G1	11	3610	Aconitate hydratase	34577	33425	31630	0	0	0	0	0	0	33210	0	0	-	-	-	-	-	-	ÚNICA T0	ÚNICA T0	-
A0A251VBZ7	7	3918	Tubulin alpha chain	0	0	0	2208	3813	4069	4093	5795	4353	0	3363	4747	-	-	0.153	-	-	0.49	ÚNICA 6°C	ÚNICA 25°	UNCHANGED
A0A251UKK8	7	13519	PutChr04g0120111 PE=4 SV=1	270004	299543	303624	145267	257399	327465	260710	308706	245382	291057	243377	271599	0.4280	0.4229	0.643	-0.25	-0.10	0.15	UNCHANG	UNCHANG	UNCHANGED
A0A251RP81	6	3897	Tubulin alpha chain	31623	31381	34140	25539	32473	33353	16449	18209	16263	32381	30455	16973	0.5037	0.0001	0.006	-0.08	-0.93	-0.84	UNCHANG	Down	Down
A0A251S3M6	5	4955	Proteasome subunit alpha type	32556	36011	38466	32258	33769	39941	18631	23151	20245	35678	35323	20676	0.9088	0.0023	0.005	-0.01	-0.78	-0.77	UNCHANG	Down	Down
A0A251U316	5	5575	Putative triosephosphate isomerase	41266	48446	35436	51655	51769	74004	26091	28131	22922	41716	59143	25715	0.1046	0.0169	0.011	0.50	-0.69	-1.20	UNCHANG	Down	Down
A0A251UTI9	10	7799	Alcohol dehydrogenase 2	132262	124652	127581	39870	109332	115705	170646	174801	202761	128165	88303	182736	0.1775	0.0061	0.022	-0.53	0.51	1.04	UNCHANG	UNCHANG	UP
A0A251RRT0	3	1767	Putative aspartic proteinase	0	0	0	0	0	0	38968	43095	48467	0	0	43509	-	-	-	-	-	-	-	UNICA 25°	UNICA 25°
A0A251T0Z2	5	1067	Catalase	26485	23482	18683	12572	12820	18694	14006	12269	16861	22883	14695	14378	0.0538	0.0321	0.901	-0.63	-0.67	-0.03	UNCHANG	Down	UNCHANGED
A0A1Y3BTI5	13	11686	Putative ribulose bisphosphat carbo	235274	193335	187093	198606	237382	234456	220169	216376	237929	205234	223481	224825	0.4046	0.3013	0.928	0.12	0.13	0.00	UNCHANG	UNCHANG	UNCHANGED
A0A251RKM4	12	3783	Putative luminal-binding protein	27453	29608	26186	19668	24073	24708	20937	23395	23143	27749	22816	22492	0.0580	0.0143	0.863	-0.28	-0.30	-0.02	UNCHANG	UNCHANG	UNCHANGED
A0A251RL83	3	1118	40S ribosomal protein S3a	36430	31679	30146	28163	26870	29204	21442	27555	38405	32751	28079	29134	0.0806	0.5330	0.843	-0.22	-0.16	0.05	UNCHANG	UNCHANG	UNCHANGED
A0A251RM91	6	1281	PutChr17g0538791 PE=4 SV=1	27870	22908	24146	7238	15943	19635	13150	19115	22802	24974	14272	18355	0.0542	0.1061	0.427	-0.80	-0.44	0.36	UNCHANG	UNCHANG	UNCHANGED
A0A251RMC4	14	10535	Glyceraldehyde-3-phosphate dehydr	275998	267362	268087	268547	292515	313575	257814	281202	253902	270482	291546	264306	0.1884	0.5286	0.154	0.10	-0.03	-0.14	UNCHANG	UNCHANG	UNCHANGED
A0A251RMF3	2	4797	40S ribosomChr12g0362521 PE=3 S	41527	45090	44342	38392	34366	52003	42672	33637	35747	43653	41587	37352	0.7237	0.0985	0.518	-0.07	-0.22	-0.15	UNCHANG	UNCHANG	UNCHANGED
A0A251RMQ6	2	1094	PutChr17g0541211 PE=3 SV=1	55623	63255	68461	61710	68946	68426	58845	30154	71199	62446	66361	53399	0.4236	0.5161	0.354	0.08	-0.22	-0.31	UNCHANG	UNCHANG	UNCHANGED
A0A251RMS7	2	530	PutChr17g0543661 PE=3 SV=1	33769	18237	16420	30917	17027	14438	16700	15854	29770	22808	20794	20775	0.8019	0.7891	0.997	-0.13	-0.13	-0.00	UNCHANG	UNCHANG	UNCHANGED
A0A251RNJ4	2	2222	EukChr17g0545401 PE=3 SV=1	20793	15590	19061	6897	22130	30612	6705	17258	16763	18481	19880	13575	0.8535	0.2623	0.461	0.10	-0.44	-0.55	UNCHANG	UNCHANG	UNCHANGED
A0A251RNK6	6	2884	PutChr17g0539461 PE=3 SV=1	122724	139767	132797	107057	142755	129818	118629	135148	132841	131763	126543	128873	0.6747	0.7068	0.851	-0.05	-0.03	0.02	UNCHANG	UNCHANG	UNCHANGED
A0A251RQX9	3	5340	Peptidyl-prolyl cis-trans isomerase	81874	101621	101336	62292	87433	104784	80810	78054	93532	94944	84836	84132	0.5091	0.2523	0.960	-0.16	-0.17	-0.01	UNCHANG	UNCHANG	UNCHANGED
A0A251RU22	2	495	PutChr17g0567641 PE=4 SV=1	35193	47938	47200	34004	42965	40782	38562	37000	39400	43444	39250	38321	0.4432	0.2886	0.755	-0.14	-0.18	-0.03	UNCHANG	UNCHANG	UNCHANGED

A0A251RUY3	12	8311	Glyceraldehyde-3-phosphate dehydr	98898	106435	121036	79387	93705	104097	83574	117019	115821	108790	92396	105471	0.1653	0.8073	0.374	-0.23	-0.04	0.19	UNCHANG	UNCHANG	UNCHANGED
A0A251RV70	2	729	Putative biotin carboxylase 2, chloro	30163	23505	17946	30238	28008	20603	34997	26827	27866	23871	26283	29897	0.6262	0.2397	0.404	0.13	0.32	0.18	UNCHANG	UNCHANG	UNCHANGED
A0A251RVM7	8	3197	Fructose-bisphosphChr17g0567101	105688	96101	97104	150892	96120	90299	87179	94176	96280	99631	112437	92545	0.5480	0.1591	0.365	0.17	-0.10	-0.28	UNCHANG	UNCHANG	UNCHANGED
A0A251RVY3	5	1646	Proteasome subunit alpha type	36345	33400	62938	36123	33114	41478	27670	48133	35080	44228	36905	36961	0.4926	0.5497	0.993	-0.26	-0.25	0.00	UNCHANG	UNCHANG	UNCHANGED
A0A251RWQ6	7	2151	Putative reversibly glycosylated poly	43969	40828	54671	54570	58994	41566	66883	52822	59683	46489	51710	59796	0.4795	0.0847	0.289	0.15	0.36	0.21	UNCHANG	UNCHANG	UNCHANGED
A0A251RX31	2	437	Putative aldehyde dehydrogenase 2B	18338	20188	21987	16363	24166	25463	16013	21577	24942	20171	21997	20844	0.5792	0.8224	0.779	0.12	0.04	-0.07	UNCHANG	UNCHANG	UNCHANGED
A0A251RXQ5	2	1406	PutChr16g0505641 PE=4 SV=1	44571	48938	36668	50768	47470	52232	41196	35221	47052	43392	50157	41156	0.1543	0.6752	0.071	0.20	-0.07	-0.28	UNCHANG	UNCHANG	UNCHANGED
A0A251RY75	4	1787	ProteChr16g0510391 PE=3 SV=1	61994	56066	65721	50087	59160	65505	50068	62983	60731	61260	58251	57927	0.5994	0.5318	0.959	-0.07	-0.08	-0.00	UNCHANG	UNCHANG	UNCHANGED
A0A251RZ67	4	1832	PutChr16g0513741 PE=4 SV=1	123971	110378	110502	104458	114150	105718	108483	120301	118203	114950	108108	115662	0.2770	0.9082	0.186	-0.08	0.00	0.09	UNCHANG	UNCHANG	UNCHANGED
A0A251RZF8	22	11126	Putative enolase	202635	249226	241998	192646	245630	266955	209163	217682	212721	231286	235077	213189	0.8928	0.2853	0.380	0.02	-0.11	-0.14	UNCHANG	UNCHANG	UNCHANGED
A0A251S0H1	3	3565	MChr16g0519291 PE=3 SV=1	4023	4756	4470	2958	2851	3064	3858	2780	4336	4417	2957	3658	0.0028	0.2091	0.205	-0.57	-0.27	0.30	UNCHANG	UNCHANG	UNCHANGED
A0A251S220	3	1344	PutChr16g0525281 PE=4 SV=1	15566	39166	39684	34700	35227	37788	34959	49389	49089	31472	35905	44479	0.6095	0.2332	0.152	0.19	0.49	0.30	UNCHANG	UNCHANG	UNCHANGED
A0A251S227	4	2283	PutChr10g0295381 PE=3 SV=1	52840	51732	47520	47608	46108	45448	43448	45259	45707	50697	46388	44805	0.0687	0.0287	0.167	-0.12	-0.17	-0.05	UNCHANG	UNCHANG	UNCHANGED
A0A251S4C1	2	1169	IsocitrChr16g0532251 PE=3 SV=1	44167	57478	55027	51312	50286	44164	38345	48364	45833	52224	48587	44181	0.4787	0.1883	0.304	-0.10	-0.24	-0.13	UNCHANG	UNCHANG	UNCHANGED
A0A251S4G9	2	301	PutChr15g0464621 PE=4 SV=1	20274	26789	24666	40289	30511	34309	24030	23221	25230	23909	35036	24160	0.0316	0.9065	0.020	0.55	0.01	-0.53	UNCHANG	UNCHANG	UNCHANGED
A0A251S512	3	1880	40S ribosomChr15g0466781 PE=3 S	25125	45432	32198	42619	40901	26120	30490	52047	31296	34252	36547	37944	0.7866	0.7096	0.881	0.09	0.14	0.05	UNCHANG	UNCHANG	UNCHANGED
A0A251S8W7	12	4140	GlycerChr15g0475141 PE=3 SV=1	14837	18292	18002	18652	19104	20769	15125	20651	18447	17044	19508	18074	0.1265	0.6252	0.453	0.19	0.08	-0.11	UNCHANG	UNCHANG	UNCHANGED
A0A251S9P3	4	1741	Putative alcohol dehydrogenase 1	3550	3401	3086	2246	4160	4027	3375	3538	2506	3346	3478	3140	0.8445	0.5862	0.652	0.05	-0.09	-0.14	UNCHANG	UNCHANG	UNCHANGED
A0A251SAA5	11	2031	Adenosylhomocysteinase	31911	36256	34403	26338	35273	40284	26882	31560	31594	34190	33965	30012	0.9604	0.1060	0.416	-0.01	-0.18	-0.17	UNCHANG	UNCHANG	UNCHANGED
A0A251SAT8	4	624	UTP--glucose-1-phosphate uridylyltr	65039	40147	37831	52998	55826	66753	44482	62554	68700	47672	58526	58579	0.3243	0.3908	0.995	0.29	0.29	0.00	UNCHANG	UNCHANG	UNCHANGED
A0A251SDV8	8	7309	PutChr14g0428971 PE=3 SV=1	151713	144368	134787	109893	117022	137838	114471	139919	164399	143623	121584	139596	0.0858	0.8045	0.340	-0.24	-0.04	0.19	UNCHANG	UNCHANG	UNCHANGED
A0A251SFD5	8	7454	Fructose-bisphosphChr14g0432581	211166	248467	239208	139061	232394	224723	178007	128707	226051	232947	198726	177589	0.3444	0.1413	0.633	-0.22	-0.39	-0.16	UNCHANG	UNCHANG	UNCHANGED
A0A251SFI7	3	488	Serine hydroxymethyltransferase	17335	19372	16119	18872	16083	16003	16388	16604	19681	17609	16986	17558	0.6659	0.9732	0.708	-0.05	-0.00	0.04	UNCHANG	UNCHANG	UNCHANGED
A0A251SGX5	2	473	PutChr14g0441661 PE=4 SV=1	51139	78409	69119	61578	56284	51926	62912	85580	62938	66222	56596	70476	0.3195	0.7188	0.159	-0.22	0.09	0.31	UNCHANG	UNCHANG	UNCHANGED
A0A251SGX7	12	5461	Proteasome subunit alpha type	276064	265726	278861	369831	284569	284103	272568	279895	306471	273551	312834	286311	0.2440	0.3123	0.430	0.19	0.06	-0.12	UNCHANG	UNCHANG	UNCHANGED
A0A251SI55	3	639	40S ribosomChr14g0445451 PE=3 S	39231	51632	46859	41271	52113	42752	30818	48110	45468	45907	45379	41465	0.9202	0.5306	0.571	-0.01	-0.14	-0.13	UNCHANG	UNCHANG	UNCHANGED
A0A251SI61	13	5637	PutChr14g0446641 PE=3 SV=1	134410	151711	153502	93134	129716	146996	102722	140065	106081	146541	123282	116290	0.2432	0.0868	0.742	-0.24	-0.33	-0.08	UNCHANG	UNCHANG	UNCHANGED
A0A251SIN0	5	2222	PutChr14g0445101 PE=3 SV=1	51771	53187	44507	58344	59136	60239	45294	43558	50939	49822	59240	46597	0.0265	0.4079	0.005	0.25	-0.09	-0.34	UNCHANG	UNCHANG	UNCHANGED
A0A251SKJ5	3	402	CChr14g0455731 PE=3 SV=1	36252	42033	37627	37136	37509	44363	35237	32662	43714	38637	39669	37204	0.7421	0.7229	0.578	0.03	-0.05	-0.09	UNCHANG	UNCHANG	UNCHANGED
A0A251SKR1	3	677	PutChr14g0456851 PE=4 SV=1	31352	39834	38511	20562	31555	34379	22464	30812	35568	36566	28832	29615	0.1947	0.2092	0.897	-0.34	-0.30	0.03	UNCHANG	UNCHANG	UNCHANGED
A0A251SL31	12	788	PutChr14g0454481 PE=4 SV=1	10348	11282	10926	7397	8573	8030	6329	8577	8825	10852	8000	7909	0.0028	0.0249	0.921	-0.44	-0.45	-0.01	UNCHANG	UNCHANG	UNCHANGED
A0A251SL49	15	6147	Putative elongation factor 1-alpha	293116	342477	264657	293280	350424	290272	344904	375204	409347	300083	311326	376485	0.7268	0.0600	0.073	0.05	0.32	0.27	UNCHANG	UNCHANG	UNCHANGED
A0A251SM99	25	3531	PutChr14g0462551 PE=3 SV=1	241919	155194	122545	82164	112851	106248	69448	102096	112643	173219	100421	94729	0.1192	0.1072	0.740	-0.78	-0.87	-0.08	UNCHANG	UNCHANG	UNCHANGED
A0A251SMR0	2	1872	PutChr14g0449471 PE=4 SV=1	63968	76678	74290	120388	68342	54109	60782	59165	66299	71645	80946	62082	0.6738	0.0985	0.404	0.17	-0.20	-0.38	UNCHANG	UNCHANG	UNCHANGED
A0A251SPR1	3	2901	PutChr13g0395301 PE=4 SV=1	29051	45103	38727	49495	33313	36278	30210	36561	36138	37627	39695	34303	0.7768	0.5499	0.372	0.07	-0.13	-0.21	UNCHANG	UNCHANG	UNCHANGED
A0A251SPZ1	5	567	Pyruvate kinase	24643	24770	27786	20901	25941	26540	17998	24183	27821	25733	24461	23334	0.5706	0.4749	0.755	-0.07	-0.14	-0.06	UNCHANG	UNCHANG	UNCHANGED
A0A251SQ90	3	4639	Ferritin	50966	44090	47929	38864	58826	59404	29634	63291	52280	47662	52365	48402	0.5406	0.9452	0.757	0.13	0.02	-0.11	UNCHANG	UNCHANG	UNCHANGED
A0A251SRB9	2	1506	PutChr13g0397821 PE=3 SV=1	37412	37046	16726	29763	30356	27693	34482	36753	38458	30394	29271	36564	0.8782	0.4237	0.006	-0.05	0.26	0.32	UNCHANG	UNCHANG	UNCHANGED
A0A251SRM4	6	2050	GTP-binding nuclear protein	55347	61377	59969	62364	62161	62306	53072	31215	59801	58898	62277	48029	0.1373	0.2853	0.174	0.08	-0.29	-0.37	UNCHANG	UNCHANG	UNCHANGED

A0A251SRW3	2	557	Chr13g0403701 PE=4 SV=1	673434	621483	617258	650398	674147	547473	702842	632063	681810	637392	624006	672239	0.7704	0.2766	0.336	-0.03	0.07	0.10	UNCHANG	UNCHANG	UNCHANGED
A0A251ST32	22	4560	Putative heat shock protein 81-2	275487	140360	119875	63469	79904	72263	64992	66519	71705	178574	71879	67739	0.0952	0.0859	0.467	-1.31	-1.39	-0.08	UNCHANG	UNCHANG	UNCHANGED
A0A251ST38	22	4560	Putative heat shock protein 81-3	94226	49629	29912	23651	27800	27786	32109	30546	31312	57922	26412	31322	0.1739	0.2347	0.027	-1.13	-0.88	0.24	UNCHANG	UNCHANG	UNCHANGED
A0A251STQ6	12	3098	Putative actin	23997	21562	23605	20321	25075	25494	24794	29283	25469	23055	23630	26515	0.7682	0.0949	0.254	0.03	0.20	0.16	UNCHANG	UNCHANG	UNCHANGED
A0A251SVF6	3	1806	PutChr13g0417551 PE=4 SV=1	43714	55966	55063	37696	44382	55323	36362	35939	52759	51581	45801	41685	0.4225	0.2191	0.614	-0.17	-0.30	-0.13	UNCHANG	UNCHANG	UNCHANGED
A0A251SX18	6	5639	MChr13g0421951 PE=3 SV=1	626817	739419	755505	421934	681102	821867	668980	731611	650162	707247	641634	683585	0.6245	0.6437	0.743	-0.14	-0.04	0.09	UNCHANG	UNCHANG	UNCHANGED
A0A251SY27	5	1029	PutChr12g0354681 PE=3 SV=1	37357	27613	33853	25791	29410	33811	26498	28368	28582	32941	29671	27816	0.4237	0.1547	0.484	-0.15	-0.24	-0.09	UNCHANG	UNCHANG	UNCHANGED
A0A251SYL1	2	623	Proteasome subunit beta	24116	31262	32866	30215	27125	24836	28342	24681	23709	29414	27392	25577	0.5507	0.2751	0.436	-0.10	-0.20	-0.09	UNCHANG	UNCHANG	UNCHANGED
A0A251SZ13	6	3918	Chr12g0355551 PE=4 SV=1	101115	127094	131187	94384	113046	119864	127580	117482	130245	119798	109098	125102	0.4269	0.6301	0.134	-0.13	0.06	0.19	UNCHANG	UNCHANG	UNCHANGED
A0A251SZA2	5	785	PutChr12g0356501 PE=3 SV=1	17010	16450	20675	16856	17401	17030	14974	17872	17903	18045	17096	16916	0.5160	0.5298	0.864	-0.07	-0.09	-0.01	UNCHANG	UNCHANG	UNCHANGED
A0A251SZF3	2	3090	PutChr12g0359671 PE=4 SV=1	205436	196219	214358	164224	203131	203530	185913	191552	203038	205337	190295	193500	0.3446	0.1786	0.829	-0.11	-0.08	0.02	UNCHANG	UNCHANG	UNCHANGED
A0A251SZN4	2	437	ATP-dependent (S)-NAD(P)H-hydrate	25957	28442	25354	25419	26009	25608	23421	21813	24430	26584	25678	23221	0.3992	0.0503	0.034	-0.05	-0.19	-0.14	UNCHANG	UNCHANG	UNCHANGED
A0A251T0H8	13	5319	Putative heat shock protein	75909	83043	81788	47426	61664	69092	57920	70722	73895	80247	59394	67512	0.0362	0.0762	0.368	-0.43	-0.24	0.18	UNCHANG	UNCHANG	UNCHANGED
A0A251T0P6	3	525	Putative alanine aminotransferase 2	29919	49092	46056	36859	33549	37591	30801	36061	39125	41689	36000	35329	0.4023	0.3784	0.818	-0.21	-0.23	-0.02	UNCHANG	UNCHANG	UNCHANGED
A0A251T1X6	12	5124	Putative actin	59544	56993	62377	46580	49006	54622	47242	54957	52394	59638	50069	51531	0.0282	0.0421	0.679	-0.25	-0.21	0.04	UNCHANG	UNCHANG	UNCHANGED
A0A251T2W0	4	8075	PutChr12g0359591 PE=4 SV=1	257012	246041	249991	170729	246095	284115	209033	271145	257597	251014	233646	245925	0.6312	0.8033	0.764	-0.10	-0.03	0.07	UNCHANG	UNCHANG	UNCHANGED
A0A251T314	4	682	Putative 26S protease regulatory sub	8085	8463	9137	6066	7883	7436	5788	8569	7902	8562	7128	7420	0.0843	0.2702	0.785	-0.26	-0.20	0.05	UNCHANG	UNCHANG	UNCHANGED
A0A251T3D2	11	5973	Glyceraldehyde-3-phosphate dehydr	236605	209579	223071	102337	200443	192471	182492	211426	203652	223085	165084	199190	0.1480	0.1095	0.354	-0.43	-0.16	0.27	UNCHANG	UNCHANG	UNCHANGED
A0A251T3J8	2	1281	PutChr06g0163851 PE=3 SV=1	28082	33475	27763	30623	27527	26498	28486	30293	25576	29773	28216	28118	0.5234	0.5128	0.960	-0.07	-0.08	-0.00	UNCHANG	UNCHANG	UNCHANGED
A0A251T3T1	4	983	Malate dehydrogenase	20956	24068	26501	23045	22985	24041	26229	25198	27782	23842	23357	26403	0.7825	0.2218	0.021	-0.03	0.14	0.17	UNCHANG	UNCHANG	UNCHANGED
A0A251T4T6	2	872	PutChr12g0374381 PE=3 SV=1	45787	37416	29722	26912	32602	29280	44400	31122	38212	37641	29598	37911	0.1777	0.9664	0.117	-0.34	0.01	0.35	UNCHANG	UNCHANG	UNCHANGED
A0A251T9L1	4	504	Putative ribosomal protein S5/Elong	55287	41146	48676	24481	37581	47996	19773	36585	39074	48369	36686	31810	0.2149	0.0862	0.620	-0.39	-0.60	-0.20	UNCHANG	UNCHANG	UNCHANGED
A0A251TAV7	7	5349	PhosphoglycerChr11g0335611 PE=3	70804	74484	68446	79097	73560	69833	72300	72052	84644	71245	74164	76332	0.4152	0.3227	0.684	0.05	0.09	0.04	UNCHANG	UNCHANG	UNCHANGED
A0A251TBB1	4	1422	PutChr11g0340891 PE=3 SV=1	27981	27053	30799	24367	27665	23932	25577	30403	25462	28611	25321	27147	0.1138	0.5008	0.415	-0.17	-0.07	0.10	UNCHANG	UNCHANG	UNCHANGED
A0A251TBJ2	9	825	Tubulin betChr11g0337991 PE=3 SV	7390	9341	9892	8766	10105	9165	6788	8869	7725	8874	9345	7794	0.6116	0.3272	0.097	0.07	-0.18	-0.26	UNCHANG	UNCHANG	UNCHANGED
A0A251TDI1	13	1015	PutChr11g0350361 PE=4 SV=1	14229	14243	13909	12743	16444	14630	9056	13474	13470	14127	14606	12000	0.6788	0.2230	0.225	0.04	-0.23	-0.28	UNCHANG	UNCHANG	UNCHANGED
A0A251TDQ3	15	7210	Putative enolase	303598	411897	338343	244962	317069	396541	189566	257739	292054	351279	319524	246453	0.5893	0.0753	0.241	-0.13	-0.51	-0.37	UNCHANG	UNCHANG	UNCHANGED
A0A251TFV1	7	1812	Putative DEAD-box ATP-dependent R	20405	20073	17018	22083	21837	19572	15397	13823	20364	19165	21164	16528	0.2105	0.3055	0.094	0.14	-0.21	-0.35	UNCHANG	UNCHANG	UNCHANGED
A0A251TG16	10	7342	Putative ribulose bisphosphat carbo	112302	141919	125988	83646	97725	120847	76987	105557	113768	126737	100739	98771	0.1330	0.1175	0.905	-0.33	-0.36	-0.02	UNCHANG	UNCHANG	UNCHANGED
A0A251TGF0	3	551	PutChr10g0280521 PE=3 SV=1	15451	14785	15931	7816	15252	14965	14216	14513	15823	15389	12678	14851	0.3314	0.4172	0.430	-0.28	-0.05	0.22	UNCHANG	UNCHANG	UNCHANGED
A0A251THF9	2	784	PutChr10g0284761 PE=4 SV=1	13314	15998	14119	15433	17986	16758	16445	16009	16825	14476	16726	16426	0.1067	0.0784	0.718	0.20	0.18	-0.02	UNCHANG	UNCHANG	UNCHANGED
A0A251TIU9	4	2545	Cysteine synthase	72140	70809	70607	67506	75806	68085	61638	68411	68283	71185	70466	66111	0.8043	0.0908	0.279	-0.01	-0.10	-0.09	UNCHANG	UNCHANG	UNCHANGED
A0A251TJC8	2	449	PyruvChr10g0296281 PE=3 SV=1	9664	13988	13897	9555	10699	10733	11631	12369	12214	12516	10329	12071	0.2130	0.7734	0.017	-0.27	-0.05	0.22	UNCHANG	UNCHANG	UNCHANGED
A0A251TLI1	6	3436	MChr10g0304821 PE=3 SV=1	64249	81017	73191	74344	89131	80864	69848	77753	88464	72819	81446	78689	0.2528	0.4636	0.709	0.16	0.11	-0.05	UNCHANG	UNCHANG	UNCHANGED
A0A251TLM9	2	712	Uncharacterized protein	39012	26826	23421	21625	26187	38268	22113	19121	40748	29753	28693	27327	0.8847	0.7836	0.878	-0.05	-0.12	-0.07	UNCHANG	UNCHANG	UNCHANGED
A0A251TNI0	9	2644	40S ribosomChr10g0311931 PE=3 S	43236	45810	44795	35829	39926	43191	37829	34331	41825	44614	39649	37995	0.0927	0.0446	0.614	-0.17	-0.23	-0.06	UNCHANG	UNCHANG	UNCHANGED
A0A251TNY8	8	6978	Ribulose bisphosphate carboxylase s	119802	126480	131152	98480	142862	161634	130293	119839	145389	125811	134325	131840	0.6775	0.4988	0.907	0.09	0.06	-0.02	UNCHANG	UNCHANG	UNCHANGED
A0A251TST3	11	6050	ElongChr09g0246511 PE=3 SV=1	35394	37518	40516	34308	30277	31209	23951	28714	33682	37809	31932	28782	0.0377	0.0468	0.361	-0.24	-0.39	-0.15	UNCHANG	UNCHANG	UNCHANGED
A0A251TU95	6	930	Putative calreticulin	156435	157255	149770	142277	163610	158198	145786	167395	169331	154487	154695	160837	0.9771	0.4670	0.568	0.00	0.05	0.05	UNCHANG	UNCHANG	UNCHANGED
A0A251TVF7	5	4935	ProteChr09g0256741 PE=3 SV=1	21177	18829	23073	17240	23285	23952	26006	32315	28259	21026	21493	28860	0.8590	0.0241	0.059	0.03	0.45	0.42	UNCHANG	UNCHANG	UNCHANGED

A0A251TYG9	12	4074	Chr09g0262451 PE=3 SV=1	5108	5903	5238	5006	6609	6329	5738	5415	3718	5416	5981	4957	0.3641	0.5328	0.268	0.14	-0.12	-0.27	UNCHANG	UNCHANG	UNCHANGED
A0A251TZ13	7	2693	Malate dehydrogenase	50671	35061	42074	39633	56064	42197	32875	49236	52254	42602	45965	44788	0.6475	0.7856	0.888	0.11	0.07	-0.03	UNCHANG	UNCHANG	UNCHANGED
A0A251U4W4	2	420	PutChr08g0216651 PE=4 SV=1	19458	16426	17690	12003	14743	15131	16225	19018	16961	17858	13959	17401	0.0418	0.7255	0.056	-0.35	-0.03	0.31	UNCHANG	UNCHANG	UNCHANGED
A0A251U4W7	3	991	Putative senescence associated prot	28208	25957	28828	23706	29635	26976	17508	28065	23843	27664	26772	23139	0.6669	0.2289	0.359	-0.04	-0.25	-0.21	UNCHANG	UNCHANG	UNCHANGED
A0A251U5D0	13	4762	Chr08g0212971 PE=3 SV=1	121859	129668	114838	107418	123839	120501	120753	112632	90347	122122	117253	107911	0.5011	0.2302	0.419	-0.05	-0.17	-0.12	UNCHANG	UNCHANG	UNCHANGED
A0A251U5Z0	26	9277	PutChr08g0220411 PE=3 SV=1	160852	177200	173089	162600	179622	164890	111048	167069	162923	170380	169037	147014	0.8620	0.2791	0.306	-0.01	-0.21	-0.20	UNCHANG	UNCHANG	UNCHANGED
A0A251U688	4	1894	Catalase	135496	133472	111675	104678	114268	130216	117013	109941	126115	126881	116387	117690	0.3806	0.3624	0.889	-0.12	-0.10	0.01	UNCHANG	UNCHANG	UNCHANGED
A0A251U736	4	9350	Histone H2B	184871	193553	185259	183799	185058	172741	130966	179946	164718	187894	180533	158543	0.2021	0.1174	0.216	-0.05	-0.24	-0.18	UNCHANG	UNCHANG	UNCHANGED
A0A251U8U5	11	3567	Chr07g0185591 PE=3 SV=1	54504	62780	60207	36096	49996	53033	48234	56090	56149	59163	46375	53491	0.0905	0.1893	0.289	-0.35	-0.14	0.20	UNCHANG	UNCHANG	UNCHANGED
A0A251U960	13	1586	Tubulin betChr07g0187021 PE=3 SV	34472	36364	37795	30349	31855	29725	26676	29136	26674	36210	30643	27495	0.0084	0.0023	0.038	-0.24	-0.39	-0.15	UNCHANG	UNCHANG	UNCHANGED
A0A251UB30	5	6624	Putative 1-Cys peroxiredoxin PER1	177778	202938	200201	142832	185484	189291	171200	179262	167935	193639	172536	172799	0.2796	0.0736	0.987	-0.16	-0.16	0.00	UNCHANG	UNCHANG	UNCHANGED
A0A251UBC5	2	1512	PutChr02g0051941 PE=3 SV=1	18299	24191	15722	22918	17961	39775	14184	33125	20816	19404	26884	22708	0.3492	0.6162	0.653	0.47	0.22	-0.24	UNCHANG	UNCHANG	UNCHANGED
A0A251UC65	2	2128	Histone H2Chr07g0196031 PE=3 SV=	31556	112591	98097	119416	113585	119513	87514	100610	14504	80748	117505	67543	0.2158	0.7365	0.136	0.54	-0.25	-0.79	UNCHANG	UNCHANG	UNCHANGED
A0A251UD42	5	1774	PutChr07g0197131 PE=3 SV=1	81184	97194	97522	68140	84316	89398	71186	94064	104037	91966	80618	89762	0.2469	0.8525	0.476	-0.19	-0.03	0.15	UNCHANG	UNCHANG	UNCHANGED
A0A251UIY6	2	911	PutChr06g0174951 PE=3 SV=1	17202	21825	22238	11267	15014	16411	13539	13554	17103	20421	14231	14732	0.0499	0.0468	0.808	-0.52	-0.47	0.05	UNCHANG	UNCHANG	UNCHANGED
A0A251UJB3	3	1560	ProteChr06g0182251 PE=3 SV=1	97264	90135	94673	90694	88077	96974	85600	93982	99394	94024	91915	92992	0.5646	0.8306	0.833	-0.03	-0.01	0.01	UNCHANG	UNCHANG	UNCHANGED
A0A251UK46	3	757	Putative 26S protease regulatory sub	4630	4799	5271	3845	3840	4043	3677	3935	4243	4902	3909	3952	0.0084	0.0199	0.822	-0.32	-0.31	0.01	UNCHANG	UNCHANG	UNCHANGED
A0A251UL57	4	3795	LChr05g0129471 PE=3 SV=1	59479	20250	18845	12919	33427	40428	15236	19919	27276	32858	28924	20810	0.8141	0.4310	0.416	-0.18	-0.65	-0.47	UNCHANG	UNCHANG	UNCHANGED
A0A251UN40	22	8021	Putative heat shock cognate 70 kDa	96159	126503	117855	103645	110923	88723	120749	114264	126082	113506	101097	120365	0.3278	0.5165	0.059	-0.16	0.08	0.25	UNCHANG	UNCHANG	UNCHANGED
A0A251UN61	5	555	PutChr05g0136881 PE=3 SV=1	20754	18017	20001	13212	19683	18208	19348	16794	19785	19591	17034	18642	0.2945	0.4868	0.499	-0.20	-0.07	0.13	UNCHANG	UNCHANG	UNCHANGED
A0A251UQ28	4	438	Xylose isomerChr05g0136751 PE=3	33598	43717	43452	33850	43510	41848	30088	33822	34895	40255	39736	32935	0.9131	0.1143	0.109	-0.01	-0.29	-0.27	UNCHANG	UNCHANG	UNCHANGED
A0A251UQC2	3	526	Vacuolar proton pump subunit B	12121	11933	12320	9735	10068	10184	9305	9803	11268	12125	9995	10125	0.0003	0.0290	0.840	-0.27	-0.26	0.01	UNCHANG	UNCHANG	UNCHANGED
A0A251UQF6	4	2145	Putative general regulatory factor 2	35070	38925	32572	34477	34945	35597	33136	31866	33468	35522	35006	32824	0.7968	0.2307	0.020	-0.02	-0.11	-0.09	UNCHANG	UNCHANG	UNCHANGED
A0A251UQM2	2	3677	Proteasome subunit beta	69678	64746	66468	50151	59442	59328	42154	62894	58970	66964	56307	54672	0.0351	0.1326	0.828	-0.25	-0.29	-0.04	UNCHANG	UNCHANG	UNCHANGED
A0A251UQZ4	2	519	Dihydrolipoyl dehydrogenase	32964	32402	36138	25423	33760	32526	54924	30785	32479	33834	30569	39396	0.3153	0.5186	0.342	-0.14	0.22	0.36	UNCHANG	UNCHANG	UNCHANGED
A0A251USB3	2	574	Putative chaperone protein dnaK2	24988	35997	36328	27425	34578	32707	44133	31161	59235	32438	31570	44843	0.8498	0.2370	0.188	-0.03	0.46	0.50	UNCHANG	UNCHANG	UNCHANGED
A0A251USI0	5	702	Malate synthase	36666	59816	52831	41069	35945	40239	35006	43841	42023	49771	39084	40290	0.2035	0.2675	0.719	-0.34	-0.30	0.04	UNCHANG	UNCHANG	UNCHANGED
A0A251USZ4	3	1947	PutChr05g0159361 PE=4 SV=1	68461	59473	65645	51676	54866	61968	57869	45838	57431	64526	56170	53713	0.1072	0.0851	0.647	-0.20	-0.26	-0.06	UNCHANG	UNCHANG	UNCHANGED
A0A251UTE2	14	8458	Putative alcohol dehydrogenase 1	396154	363516	382133	134207	394758	419799	270138	281488	323071	380601	316255	291566	0.5220	0.0088	0.803	-0.26	-0.38	-0.11	UNCHANG	UNCHANG	UNCHANGED
A0A251UU89	3	1910	Proteasome subunit alpha type	30126	28052	37782	30056	26974	25777	26004	23766	23621	31986	27602	24464	0.2452	0.0697	0.102	-0.21	-0.38	-0.17	UNCHANG	UNCHANG	UNCHANGED
A0A251UV16	2	369	Putative phosphoenolpyruvate carb	6401	9710	7301	11864	8826	6644	7977	6396	8352	7804	9111	7575	0.5096	0.8524	0.398	0.22	-0.04	-0.26	UNCHANG	UNCHANG	UNCHANGED
A0A251UVK3	3	466	Putative enolase 1	18675	16522	17098	10941	17270	17653	14167	18102	19591	17432	15288	17286	0.3984	0.9376	0.502	-0.18	-0.01	0.17	UNCHANG	UNCHANG	UNCHANGED
A0A251UWA2	6	4769	Phosphoglycerate kinase	212510	233559	218656	195372	231025	222270	214716	182508	214454	221575	216222	203893	0.6886	0.2266	0.461	-0.03	-0.12	-0.08	UNCHANG	UNCHANG	UNCHANGED
A0A251UWB5	3	2986	PutChr04g0102451 PE=3 SV=1	55618	46881	26981	26286	37809	18792	13738	31872	31356	43160	27629	25655	0.1996	0.1664	0.820	-0.64	-0.75	-0.10	UNCHANG	UNCHANG	UNCHANGED
A0A251UYG3	3	730	PutChr04g0106961 PE=3 SV=1	26782	30028	28581	24809	24651	21775	21473	22384	24242	28464	23745	22700	0.0257	0.0098	0.459	-0.26	-0.32	-0.06	UNCHANG	UNCHANG	UNCHANGED
A0A251UZB2	19	10170	PutChr04g0107061 PE=3 SV=1	101247	106667	94344	98090	86794	91756	87555	84876	96413	100752	92214	89615	0.1523	0.0893	0.615	-0.12	-0.16	-0.04	UNCHANG	UNCHANG	UNCHANGED
A0A251UZG1	2	2248	PutChr04g0114801 PE=4 SV=1	50539	61166	53424	57987	49407	47161	41360	50752	46345	55043	51518	46152	0.4842	0.1002	0.277	-0.09	-0.25	-0.15	UNCHANG	UNCHANG	UNCHANGED
A0A251UZU7	4	750	Isocitrate lyase	98020	98444	91652	87849	70020	100568	71563	72650	88128	96039	86145	77447	0.3394	0.0324	0.447	-0.15	-0.31	-0.15	UNCHANG	UNCHANG	UNCHANGED
A0A251V3F8	9	3669	Chr04g0127591 PE=3 SV=1	38349	40169	40776	31780	35375	38265	25685	25461	29096	39765	35140	26747	0.0831	0.0007	0.019	-0.17	-0.57	-0.39	UNCHANG	UNCHANG	UNCHANGED
A0A251V5D4	4	670	Putative 26S proteasome AAA-ATPas	27518	24580	24478	22963	26931	24363	24962	26899	27369	25525	24752	26410	0.6400	0.5148	0.294	-0.04	0.04	0.09	UNCHANG	UNCHANG	UNCHANGED
A0A251V6N7	10	6664	Putative aspartic proteinase A1	232272	251527	236638	227641	250370	201779	270997	182083	208124	240146	226597	220401	0.4231	0.5056	0.845	-0.08	-0.12	-0.04	UNCHANG	UNCHANG	UNCHANGED

A0A251V6W1	4	2842	Proteasome subunit beta	26532	28579	30714	23771	25752	24404	20032	11027	26530	28609	24642	19197	0.0417	0.1132	0.295	-0.21	-0.57	-0.36	UNCHANG	UNCHANG	UNCHANGED
A0A251V6Y0	2	913	PutChr03g0069281 PE=4 SV=1	40650	39047	38177	24668	29862	33226	27848	34220	37272	39291	29252	33113	0.0180	0.0976	0.358	-0.42	-0.24	0.17	UNCHANG	UNCHANG	UNCHANGED
A0A251V8J6	2	2274	Proteasome subunit beta	46635	48945	59285	48475	59387	55597	42350	42695	51009	51622	54486	45351	0.5999	0.2624	0.099	0.07	-0.18	-0.26	UNCHANG	UNCHANG	UNCHANGED
A0A251V987	11	3451	Aconitate hydratase	32485	35746	36286	41943	45516	51369	44664	43390	47826	34839	46276	45294	0.0188	0.0041	0.763	0.41	0.37	-0.03	UNCHANG	UNCHANG	UNCHANGED
A0A251VAN6	8	1669	Putative aldehyde dehydrogenase 11	47366	58375	48857	44297	45433	43858	43866	41144	49460	51533	44530	44823	0.1145	0.1878	0.911	-0.21	-0.20	0.00	UNCHANG	UNCHANG	UNCHANGED
A0A251VB59	2	3356	Putative translationally-controlled tu	38773	37863	38552	29507	42241	38238	33753	32720	42494	38396	36662	36322	0.6694	0.5417	0.947	-0.06	-0.08	-0.01	UNCHANG	UNCHANG	UNCHANGED
A0A251VH41	3	1585	MChr02g0043601 PE=3 SV=1	53278	50117	42856	37065	52909	53312	26059	39279	37834	48750	47762	34391	0.8806	0.0508	0.120	-0.03	-0.50	-0.47	UNCHANG	UNCHANG	UNCHANGED
A0A251VIE1	8	2266	Putative alpha-1,4-glucan-protein sy	19349	18971	19344	22076	22753	18237	15565	14391	14712	19221	21022	14889	0.2712	0.0003	0.013	0.12	-0.36	-0.49	UNCHANG	UNCHANG	UNCHANGED
A0A251VJB1	4	1635	Putative peroxisomal 3-ketoacyl-CoA	74523	78117	60965	57797	73700	72894	53932	55107	68058	71201	68130	59032	0.6975	0.1530	0.256	-0.06	-0.27	-0.20	UNCHANG	UNCHANG	UNCHANGED
A0A251VKC7	5	1423	Putative enoyl-[acyl-carrier-protein]	77667	57807	294393	63405	333136	304909	60709	32119	67651	143289	233817	53493	0.4727	0.3058	0.104	0.70	-1.42	-2.12	UNCHANG	UNCHANG	UNCHANGED
A0A251VNA4	2	940	PutChr01g0013431 PE=4 SV=1	18243	21696	24933	18890	23877	17268	15971	24137	18157	21624	20012	19422	0.5920	0.5182	0.860	-0.11	-0.15	-0.04	UNCHANG	UNCHANG	UNCHANGED
A0A251VQU0	6	1518	PutChr01g0019411 PE=3 SV=1	43610	46814	23566	19582	16007	19272	17914	19516	22063	37997	18287	19831	0.0554	0.0694	0.405	-1.05	-0.93	0.11	UNCHANG	UNCHANG	UNCHANGED
A0A251VRZ2	3	592	Putative fructokinase-2	52886	64026	47001	43586	58803	49591	47214	57764	52792	54637	50660	52590	0.5831	0.7439	0.737	-0.10	-0.05	0.05	UNCHANG	UNCHANG	UNCHANGED
A0A251VS40	8	3602	Fructose-bisphosphChr01g0028911	19932	16318	15104	24069	32170	53399	18518	18606	26576	17118	36546	21234	0.0935	0.2472	0.169	1.09	0.31	-0.78	UNCHANG	UNCHANG	UNCHANGED
A0A251VSG2	4	874	PyruvChr01g0028101 PE=3 SV=1	16754	16572	16574	11486	15738	16704	12028	17176	17777	16634	14643	15661	0.2823	0.6222	0.696	-0.18	-0.08	0.09	UNCHANG	UNCHANG	UNCHANGED
A0A251VTA7	13	5173	Putative enolase 2	1682	1921	2153	1395	1865	1993	2033	2414	2279	1919	1751	2242	0.5008	0.1398	0.082	-0.13	0.22	0.35	UNCHANG	UNCHANG	UNCHANGED
A6XIG5	3	2783	Superoxide dismutChr08g0221521 P	47034	40039	43403	49682	48250	63376	33770	33274	53631	43492	53769	40225	0.1207	0.6651	0.176	0.30	-0.11	-0.41	UNCHANG	UNCHANG	UNCHANGED
F2VYC9	4	5117	F2VYC9_ Beta-hydroxyacyl-ACP dehy	130687	112341	112162	102665	101537	86744	96773	117211	138325	118396	96982	117436	0.0555	0.9466	0.192	-0.28	-0.01	0.27	UNCHANG	UNCHANG	UNCHANGED
O24498	2	850	O24498_ Acyl-[acyl-carrier-protein] d	5923	13080	13682	12533	11716	6103	8337	11327	9282	10895	10117	9649	0.8204	0.6619	0.842	-0.10	-0.17	-0.06	UNCHANG	UNCHANG	UNCHANGED
W0FGD1	9	2471	W0FGD1_ ATP synthase subunit alph	36455	38298	34717	27362	30725	27025	40354	37496	46497	36490	28371	41449	0.0066	0.1568	0.010	-0.36	0.18	0.54	UNCHANG	UNCHANG	UNCHANGED
A0A251TVQ0	12	8923	Histone H4	779961	1067953	239088	1128545	1612594	214906	1558265	1668976	1582020	695667	985348	1603087	0.5760	0.0208	0.207	0.50	1.20	0.70	UNCHANG	UP	UNCHANGED